Fall 8-31-2022

Telomerase Reverse Transcriptase Marks a Novel Population of Adult Stem Cells in the Mouse Brain That Respond to Metabolic Interventions by Modulating Adult Brain Plasticity

Gabriel S. Jensen
University of Maine, gabriel.jensen@maine.edu

TELOMERASE REVERSE TRANSCRIPTASE MARKS A NOVEL POPULATION OF ADULT STEM CELLS IN THE MOUSE BRAIN THAT RESPOND TO METABOLIC INTERVENTIONS BY MODULATING ADULT BRAIN PLASTICITY

By

Gabriel Sheinbach Jensen

B.A. St. Mary's College of Maryland, 2015

A DISSERTATION

Submitted in Partial Fulfillment of the

Requirements for the Degree of

Doctor of Philosophy

(in Biomedical Science)

The Graduate School

The University of Maine

August 2022

Advisory Committee:

Kristy Townsend, Associate Professor, The Ohio State University, Advisor

Ashley Webb, Assistant Professor, Brown University

Katherine Motyl, Faculty Scientist, Maine Medical Center Research Institute

Thane Fremouw, Associate Professor, The University of Maine

Martin Pera, Professor, The Jackson Laboratory

TELOMERASE REVERSE TRANSCRIPTASE MARKS A NOVEL POPULATION OF ADULT STEM CELLS IN THE MOUSE BRAIN THAT RESPOND TO METABOLIC INTERVENTIONS BY MODULATING ADULT BRAIN PLASTICITY

By Gabriel Jensen

Dissertation Advisor: Dr. Kristy Townsend

An Abstract of the Dissertation Presented
in Partial Fulfillment of the Requirements for the
Degree of Doctor of Philosophy
(in Biomedical Science)
August 2022

Telomerase reverse transcriptase (TERT) is expressed by quiescent adult stem cells (qASC) in numerous adult murine and human tissues but has never been explored in the adult brain. Here, these data demonstrate that TERT+ cells in the adult mouse brain represent a novel population of multipotent qASCs. TERT+ cells were localized to numerous classical neuro/gliogenic niches including the ventricular-subventricular zone, hypothalamus and olfactory bulb, as well as newly discovered regions of adult tissue plasticity such as the meninges and choroid plexus. TERT+ cells expressed neural stem cell markers such as Nestin and Sox2, but not markers of activated stem/progenitor cells, nor markers of mature neuronal or glial cells. TERT+ qASCs also rarely expressed the proliferation marker Ki67, further confirming a quiescent phenotype. When cultured, TERT+ cells behaved like brain stem cells by forming proliferative neurospheres. Lineage tracing of TERT+ cells in adult transgenic mice revealed large-scale expansion of TERT+ progeny and differentiation in multiple brain regions to diverse cell types. Lineage-traced cells expressed markers of mature neurons, oligodendrocytes, astrocytes, ependymal cells, microglia, and choroid epithelial cells, thus demonstrating the striking multipotency of this stem cell population in basal tissue turnover. Finally, the neurogenic treatment of caloric restriction (CR) in lineage tracing animals revealed a decrease in TERT-traced cell

signal within the median eminence (ME) of the hypothalamus, with no change in the arcuate nucleus (ARC), when compared to unrestricted diet (UR)-treated animals. Single-cell RNA sequencing of TERT-traced cells in mice administered CR treatment also revealed an increase in the neuroprotective gene brain lipid binding protein (BLBP) in TERT-traced cells after 1 month of CR. As neuroprotection is a classical response to inflammation, we then studied the role of TERT+ cells in the inflammatory process of aging. TERT+ cell numbers varied with aging across neurogenic niches but remained a similar percentage of the full brain. However, TERT-traced cell signal increased significantly with aging, although label retention decreased. Together, these data demonstrate that TERT+ cells represent a new population of multipotent stem cells that contribute to basal brain plasticity and regeneration.

DEDICATION

To my wife, family, friends, and dogs.

No weaving of words can thank you enough for everything.

ACKNOWLEDGEMENTS

I would like to extend thanks to the Graduate School of Biomedical Science and Engineering at the University of Maine for the opportunity to work alongside many amazing people and beautiful souls.

Thank you as well to the students and staff at both the University of Maine and the Ohio State University. I have learned so much from you. The energy and dedication that you have all brought to the lab never fails to reinvigorate me, even on my most down days.

Thanks to my committee, who have always guided my growth and progress in ways that have molded me into (in my opinion) a thoughtful, scientifically minded person.

Nothing that I have accomplished could have been done without my lab-mates who mentored, trained, and worked with me throughout my years. Thanks to everyone who has played a part in the research that I have been a part of. The academic collaborations and real-life friendships have been invaluable.

Finally, I would not be where I am today without the mentoring and teachings of my advisor, Kristy Townsend, who has pushed me to be the best version of myself.

TABLE OF CONTENTS

LIST OF TABLES

LIST OF FIGURES

CHAPTER 1

REVIEW OF THE LITERATURE

This dissertation will describe the role of adult stem cells (ASCs) in the adult mammalian brain and their role in the maintenance of neurons, glia, and other brain cell types. Section 1.1 will cover niches of the adult brain that contain ASCs, the process by which ASCs produce adult-born cell types, and the current methods of studying ASCs and their progeny. Section 1.2 will compare the processes of adult neurogenesis and gliogenesis in humans and rodents and will explain the current discrepancies in the field regarding the translation of mouse studies to humans. Section 1.3 will detail the importance of quiescence signaling pathways in the brain and their roles in the processes of ASC activation and differentiation. Section 1.4 will describe the identification of telomerase reverse transcriptase (TERT) as a stem cell marker in multiple adult mammalian tissues and the possibility of TERT as an ASC marker in the adult brain. Finally, Section 1.5 will isolate the hypothalamus as a brain region of interest to the field of adult metabolism and energy balance and provide reasoning for why the identification of a specific and unique marker of ASCs in this brain region may provide insight into metabolic dysfunction during dietary interventions such as caloric restriction (CR).

In Chapter 2 we will identify TERT+ cells in the adult mouse brain as quiescent ASCs (qASCs) and detail their quiescence and multipotency throughout the adult brain. In Chapter 3 we will study the role of TERT+ cells in the process of hypothalamic plasticity with both CR and aging to learn more about these cells in the context of energy balance and metabolism. Further information regarding the studies performed in this dissertation and signaling pathways of relevance to both adult plasticity and metabolism are covered in the Appendices.

1.1. Adult Brain Plasticity – Significance and Function

The creation of adult-born cells in the adult brain allows for the maintenance of neural pathways involved in learning, motor function, and metabolism, the upkeep of glial cell types which are instrumental in proper brain function, and the replenishing of non-neuronal tissues required for the proper transport of nutrients and growth factors. While the adult human brain was not believed to generate adult-born neurons until the late 1990's, numerous studies have since provided evidence for neurogenic plasticity throughout our lifetimes (Section 1.2). Similarly, the production of adult-born oligodendrocytes and astrocytes in the adult human brain has been identified in recent years as well [1-3]. Together, adult brain plasticity encompasses the generation of adult-born neurons and glia, as well as the integration of these newborn cells into existing circuitry. In addition, the production of adult-born epithelial, ependymal, and endothelial cells has also been observed in the mammalian brain (Section 1.1.5). These processes allow for us to respond to various forms of learning, stress, exercise, olfactory cues, dietary changes, as well as traumatic injury. Indeed, changes in the production of adult-born cells in the brain are observed in various neurodegenerative and neurological diseases (Section 1.2.4) This section will review previous research on adult neurogenesis, adult gliogenesis, and the turnover of tissues in the adult brain made up of other cell types.

In the brain, adult neurogenesis, the process by which adult neurons are created, encompasses one aspect of adult neural plasticity. The field of adult neurogenesis is still conflicted regarding whether adult humans rely on quiescent adult stem cells (qASCs) to create newborn neurons in the brain or if newborn adult neurons are birthed from a population of proliferative neuronal precursors known as neuroblasts. In fact, debates are still ongoing regarding whether adult humans can create fully integrating newborn neurons at all. Our incomplete understanding of adult mammalian neurogenesis is linked to the limited time in which of the field of adult neurogenesis has been studied. It was not until 1965 that the production of newborn neurons in higher order vertebrates was discovered. Here, a pioneering study in rats

showed incorporation of the molecule ^{3}H-thymidine into cells within the adult rat brain, specifically within the dentate gyrus (DG) of the hippocampus [4]. ^{3}H-thymidine is a radioactive nucleoside that is incorporated into newly created strands of DNA. As DNA is naturally replicated during cell division, the incorporation of ^{3}H-thymidine into newly formed DNA indicates a cell that has divided or resulted from a division. After ^{3}H-thymidine treatment in adult humans, cells containing ^{3}H-thymidine were found within a population of hippocampal neurons in the DG and it was believed that these cells were proliferative after ^{3}H-thymidine administration. This formed the argument for the existence of adult neurogenesis in the mammalian brain. A second study was performed in 1977, replicating these results [5].

However, a study in 1985 slowed the field of adult neurogenesis. In this study, adult rhesus monkeys were injected with ^{3}H-thymidine and no newborn cells were found in the brain. It was concluded that few to none of the adult rhesus monkey brain cells were formed following early postnatal development [6]. The re-emergence of the study of adult neurogenesis occurred following influential studies regarding the newborn production of neurons in adult songbird brains [7]. Furthermore, additional evidence for adult neurogenesis as a process that not only produced adult-born neurons but allowed for the integration of adult-born neurons into existing mossy fiber tracts within the hippocampus of rat brains was established [8]. Functional studies also discovered the rate of adult neurogenesis responded to levels of adrenal steroids in rats [9] and N-methyl-D-aspartate (NMDA) signaling in tree shrews [10]. However, at that point in time we as a scientific community had never observed adult neurogenesis in the human brain.

Finally, in 1998, a study examining brains from deceased humans treated with bromodeoxyuridine (BrdU) prior to death identified cells in the human ventricular-subventricular zone (V-SVZ) of the lateral ventricles and subgranular zone (SGZ) of the DG that contained BrdU-labeled cells [11]. This ingenious study provided evidence for the existence of adult neurogenesis in the human brain by identifying cells in the brain that contained this thymine analog that could only be taken up by cells that were replicating their DNA, which was correlated with the process

of mitosis. Indeed, activated stem cells and various intermediate neural and glial progenitor cell types in the brain retain their proliferative capacity (as shown in Figure 1.1). BrdU has since been a valuable utilized across the discipline to identify proliferating cells and their progeny. In the years that have followed, much has been discovered regarding the processes of adult neurogenesis and adult plasticity. We now understand much more about the stem cells that give rise to newborn neurons and glia, the pathways that activate these processes, and the role of these adult-born cells in responding to external stimuli that, as it turns out, are shaping our brains as a result.

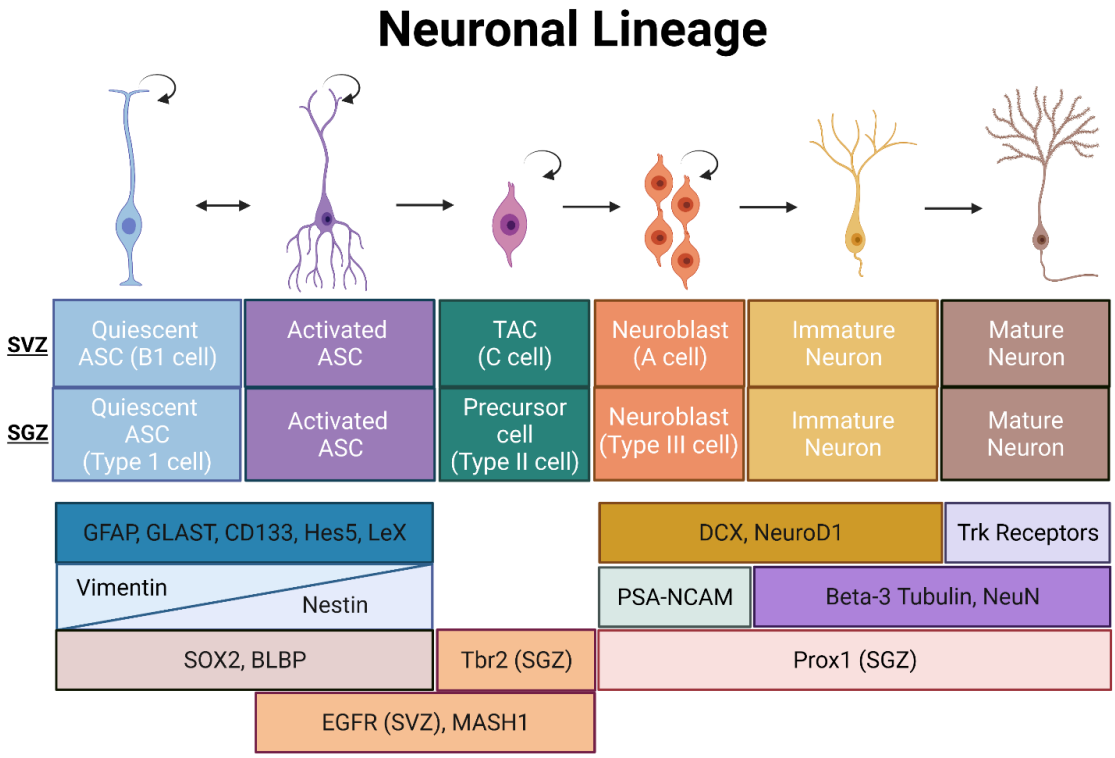

Figure 1.1. Markers of adult neurogenesis in the mouse brain. Brain-region specific markers are identified as SGZ or SVZ, indicating the regions where these markers are expressed. Rounded arrows identify self-replicating cell types. Straight arrows indicate progression of differentiation to mature neuron. Abbreviations: ASC (adult stem cell), TAC (transit amplifying cell), SVZ (subventricular zone), SGZ (subgranular zone).

However, while ^{3}H-thymidine and BrdU allow for the marking of proliferative cells and their progeny in brain regions where stem cells are poorly understood, these studies were hindered by

the downsides of the tools. ^{3}H-thymidine induces cell-cycle arrest, apoptosis, and dose-dependent DNA synthesis inhibition [12], while BrdU marks cells at varying levels depending on the route of administration [13] and is taken up by cells during repair or apoptosis, as well as during cell division [14]. More efficient labeling methods have been utilized recently, such as labeling with 5-ethynyl-2'-deoxyuridine (EdU), but this molecule has many of the same issues as BrdU [15]. This dissertation will propose a novel stem cell marker that can be utilized to mark ASCs in the adult brain, which will not rely on proliferation or mark various other cell types.

1.1.1. Classical Neurogenic Niches of the Adult Mammalian Brain

Adult neurogenesis in the mammalian brain has been studied most thoroughly in the V-SVZ and the DG of the hippocampus. These two areas of the brain were identified as areas of proliferation and label retention in early studies of rats [4], mice [16], and tree shrews [10], before they were identified in humans [11]. Additional mammalian species have since shown similar patterns of neurogenesis, including sheep [17]. While expression of proliferation markers such as Ki67 as well as BrdU label retention occurs in various other brain regions, the vastly heightened amount of proliferation in these two regions and the neuronal identity of newborn cells, quickly led to them being regarded as the only two neurogenic niches of the adult brain. Other niches have more recently been identified, and for that reason the V-SVZ and DG will be denoted as 'classical' neurogenic niches. These two classical neurogenic niches contain quiescent adult neural stem cells (qANSC), which undergo a combination of proliferation and differentiation to create neuronal progenitors that will differentiate into adult-born mature neurons [18, 19]. Both the V-SVZ and DG retain their neurogenic potential due to the presence of qANSCs.

1.1.1.1. The V-SVZ/OB Neurogenic Axis

In the V-SVZ, qANSCs are termed B cells (Figure 1.1) [19]. B cells express the astrocyte markers glial fibrillary protein (GFAP) and glutamate aspartate transporter 1 (GLAST), proliferate

slowly, and give rise to all intermediate neurogenic cell types in the V-SVZ after mitotic inhibition [19]. In a landmark study by Doetsch et al., the administration of the mitotic inhibitor cytosine arabinoside (Ara-C) caused ablation of the proliferative C cells (proliferative transit amplifying cells (also known as TACs)) and A cells (proliferative and migratory cells (also known as neuroblasts)), leaving behind only B cells. After a few days however, the C cells began to return, and A cells after that. Altogether, it was concluded that slowly cycling B cells must be creating C cells, which in turn differentiate into A cells (Figure 1.1) [19].

While B cells are hypothesized to be qANSCs, the activation pathways wherein activated ANSCs (aANSCs) are created, as well as the identity of these aANSCs remains unknown. B cells differentiate via asymmetric mitosis into epidermal growth factor receptor (EGFR)-expressing TACs, also known as C cells [20]. C cells then differentiate into the migratory intermediate cell type of the V-SVZ known as neuroblasts or A cells which travel through the rostral migratory stream (RMS) to the olfactory bulb (OB; Figure 1.2). The RMS is made up of migratory neuroblasts and astrocytes, creating a niche wherein neuroblasts can travel and proliferate through large swathes of neural tissue to the destination of the OB [21]. Within the granule cell layer (GCL) of the OB, neuroblasts begin to lose expression of neuroblast markers and features and begin to resemble immature neurons [19]. While many adult-born immature neurons will die before maturation, most adult-born immature neurons will differentiate into mature neurons in the GCL and integrate into existing neural circuitry [22, 23]. A small number of immature neurons will become mature periglomerular neurons in the glomerular layer of the OB [24].

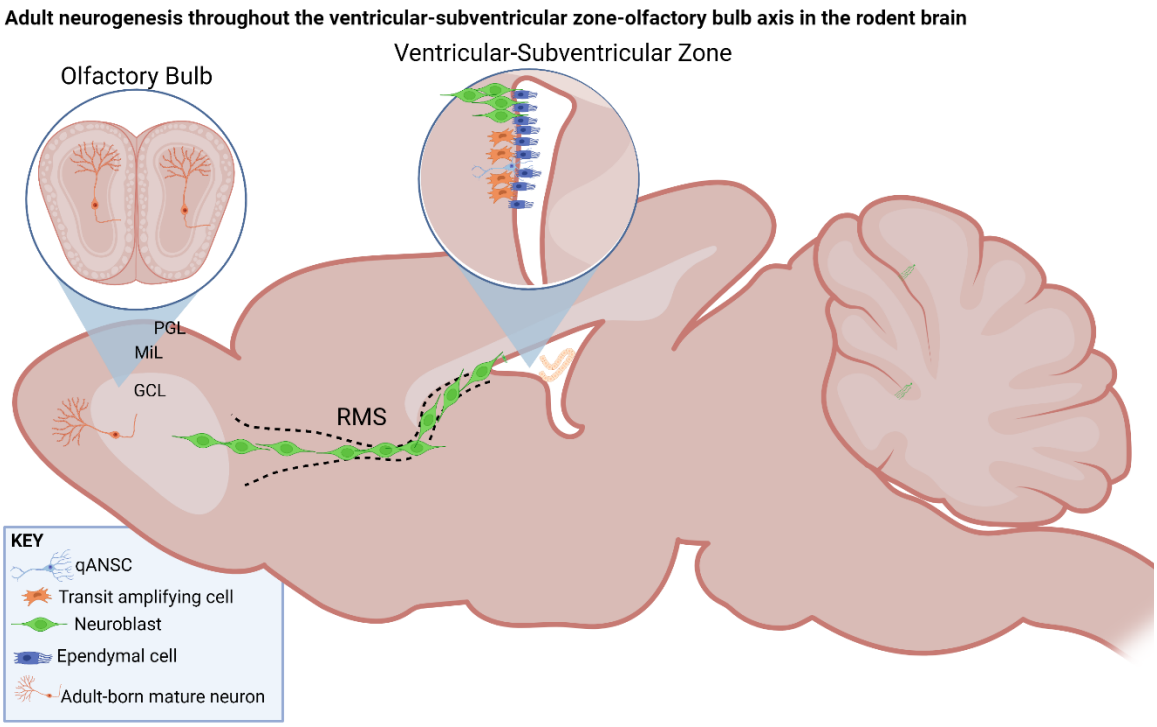

Figure 1.2. The process of adult neurogenesis from the V-SVZ into the OB. GFAP-expressing qANSCs in the V-SVZ give rise to transit amplifying cells, which divide and differentiate to form neuroblasts. Neuroblasts travel through the RMS until they reach the OB, where they differentiate into immature neurons, and finally mature neurons.

While the ANSCs that generate mature adult-born neurons in the V-SVZ/OB axis are in the V-SVZ, mature neurons resulting from adult neurogenesis are incorporated into the OB. The OB functions to collect and relay messages from the olfactory epithelium (OE) regarding smell [24]. One may then infer that the generation of newborn neurons in the OB allows for these neuronal pathways to undergo upkeep throughout life. Indeed, adult neurogenesis in the V-SVZ/OB axis allows for functional integration of adult-born OB neurons [24]. Accordingly, after a 4-week “pulse” of BrdU in adult mice, where BrdU was administered via the drinking water to label proliferating or repairing cells, followed by a 3-week “chase” where BrdU+ cells and their progeny could proliferate, migrate, and differentiate, exposure to odorants induced c-Fos expression in BrdU+ periglomerular neurons [25]. In fact, approximately 17% of c-Fos+ cells were also BrdU+,

indicating large-scale generation of functional neurons in the adult mouse OB [25]. Adult-born neurons in the OB exhibited spontaneous synaptic activity and spiking activity only after maturation, although throughout V-SVZ/OB neuronal maturation, each cell type exhibits electrophysiologically distinguishable differences [26]. Mature adult-born neurons in the OB exhibited electrophysiological properties of previously defined periglomerular cells and granule cells, which were functionally affected by both GABA and glutamate [23]. Retrograde viral tracing from the piriform cortex, where OB projection neuron axons reside, supports that these adult-born neurons are integrated into the neuronal circuitry [25].

The functionality of adult neurogenesis in the olfactory system can be analyzed by the abilities of 1) adult-born neurons to respond to olfactory cues and 2) the response of the adult brain to produce differential levels of adult-born olfactory neurons based on the input from the external environment. Odor deprivation studies where rats underwent naris occlusion showed that reduced odor sensitivity decreased the complexity of newborn OB cells, while at the same time increasing their excitability, indicating an activity-dependent system [27]. Similar findings from mice housed in odor-enriched environments revealed that enrichment increased the number of BrdU+ cells in the OB [28]. These newborn cells were found to express the mature neuron marker Neuronal Nuclear protein (NeuN) at the same rate as mice without enrichment (~80%). The increase in adult-born olfactory neurons was correlated with significantly longer olfactory memory and odor recognition. This intervention did not affect neurogenesis in the SGZ or hippocampal memory tasks. Similarly, other interventions that affect hippocampal neurogenesis such as exercise did not affect neurogenesis in the OB [29].

1.1.1.2. The Dentate Gyrus of the Hippocampus

The DG of the hippocampus is the other major classical niche of adult neurogenesis in the mammalian brain. The presence of proliferating cells in the adult DG was first discovered in adult rats in 1965 with ^{3}H-Thymidine [4]. These results were replicated in 1977, with electron

microscopy analysis demonstrating that the newborn cells in this area were neurons [5]. By 1988 the neuronal integration of these newborn granule neurons (a mature neuronal population in the hippocampus) could be traced with retrograde tracers to determine that adult neurogenesis in the DG produced adult-born neurons that integrated within the existing mossy fiber tracts in the hippocampus [8]. We now understand that within this niche, qANSCs within the SGZ produce mature neurons through various steps of neuronal differentiation. Similar to the V-SVZ, radial glia-like qANSCs begin the process of neurogenesis [18]. Also known as Type 1 cells, these qANSCs sit within the SGZ of the DG and will remain quiescent until activated [18]. Upon activation, Type 1 cells will begin to differentiate into neuronal progenitor cells known as Type 2 cells. At this point, the qANSC marker GFAP is no longer expressed [30]. Type 2 cells can then differentiate into neuroblasts (Type 3 cells), which will further differentiate into immature neurons, and finally mature neurons [31].

The hippocampus plays an integral role in learning and memory, mood, stress response, and anxiety [32]. Unsurprisingly, the creation of new adult-born neurons within this brain region therefore allows for the brain to respond to new instances of learning and memory and mood-related stressors. The first example of the ability of the brain to respond to external stimuli such as stress through changes in neurogenesis was in 1997, when Gould et al. measured label retention in the tree shrew hippocampus after psychosocial stress [10]. This group determined that stress decreased BrdU-labeled cells in the DG, indicating reduced adult hippocampal neurogenesis [10]. In the time since, studies have shown that adult hippocampal neurogenesis can also be increased via environmental enrichment, exercise, and learning [10, 33-39].

Integration of adult-born neurons in the hippocampus for functional response to external stimuli requires newborn neurons to connect to the current synaptic framework. Two separate groups determined that new adult-born granule cells in the DG integrated axons within existing mossy fiber tracts in 1999 by utilizing retrograde tracers [40]. As adult-born neurons matured, they were found to extend long axons throughout the hippocampus from the DG to field A3 [40].

Injection of a retrograde tracer into the field A3 region resulted in labeling of BrdU+ adult-born mature granule neurons, indicating that newborn neurons integrated into the hippocampal synaptic pathways [40]. Furthermore, neurons in the cerebral cortex infected with pseudorabies virus, another retrograde tracer, showed synaptic connection between neurons in the cortex, DG, and CA3 [25]. Electrophysiological studies of retrograde marker-traced newborn hippocampal neurons identified that mature adult-born neurons in this region respond to glutamatergic and GABAergic inputs [41, 42], elicit similar electrophysiological signatures to mature granule neurons in this region [43, 44], and produce c-Fos in response to external stimuli [45].

While adult-born neuronal electrophysiology and synaptic connectivity are well understood, the relationship between adult neurogenesis and hippocampal functions such as memory and cognition are only starting to be uncovered. For example, we understand that stimuli such as exercise increases adult-born neuron generation, but what do these newborn neurons do to support an environment where exercise was necessary? Is the process of neurogenesis important to hippocampal function in times of increased exercise? This was first examined in 2001, when mitotic inhibition decreased hippocampal-dependent conditioning, examined via the eyeblink memory test, wherein puffs of air are associated with additional stimuli and can blinking can become trained through associated memory [46]. Mitotic inhibition did not have an effect on the ability to navigate a Morris water maze [47], although there is a correlation between the spatial memory performance in this test and the levels of hippocampal neurogenesis [48]. While there is clear evidence that adult neurogenesis is impacted by neurogenic stimuli, we still do not fully understand the role of adult hippocampal neurogenesis in cognition.

1.1.2. Non-Classical Niches of Adult Neurogenesis in the Mammalian Brain

Newly identified neurogenic niches have recently been discovered in addition to the two classical neurogenic niches of the adult brain. These neurogenic niches are much less completely understood than the V-SVZ and SGZ, due in part to the lack of a well characterized stem cell

population in these niches. While lineage tracing studies and label retention studies have identified the presence of proliferative and newly formed cell types, the stem cells that give rise to these newborn cells are not well understood. These novel niches include the hypothalamus, striatum, cortex, and OE. While the OE is not a part of the brain, the newborn neurons within this neural tissue reach directly into the OB and integrate into the neural circuitry in this neurogenic brain region. For that reason, the OE will be discussed in this section.

1.1.2.1. The Hypothalamus

The hypothalamus is a more recently identified neuro/gliogenic niche of the adult brain. This niche contains two populations of stem cell-like cells, parenchymal oligodendrocyte progenitor cells (OPCs) and tanycytes, radial glial-like cells that line the ventral third ventricle. NG2+ and Olig2+ OPCs make up most of the proliferative cells within the hypothalamus, as identified via EdU immunofluorescence [49]. These OPCs are located within the hypothalamic parenchyma, including the arcuate nucleus (ARC) and median eminence (ME) [49]. ME OPCs form self-renewing and multipotent clusters of stem-like cells known as neurospheres, with a higher tendency to form oligodendrocytes than other mature cell types *in vitro* [50]. Transplantation of ME-derived OPC neurospheres into myelin basic protein (MBP)-null *Shi* mice revealed expansion of these cells and the regenerative capacity of ME-derived OPCs in periods of demyelination [50]. cells require additional study in the adult hypothalamus, as these neuro/gliogenic cells may reveal themselves as the true quiescent stem cell population of the basal hypothalamus and could shed light on the changes occurring during neurogenic and gliogenic interventions.

Tanycytes, radial glial-like cells that act as stem cells and can receive signals from the cerebrospinal fluid (CSF) and traffic them into the hypothalamic parenchyma [51]. Tanycytes line the floor and ventro-lateral portion of the ventral third ventricle (V3V) and utilize extensions that extend laterally to transport signaling molecules to neurons within the hypothalamus. These cells

can be divided into four major subtypes - alpha 1 tanycytes (a1), alpha 2 tanycytes (a2), beta 1 tanycytes (B1), and beta 2 tanycytes (B2). Each of these occupies a specific area of the hypothalamus and plays a unique role in the process of hypothalamic plasticity [52]. Alpha tanycytes reside below ependymal cells at the dorsal portion of the V3V (Figure 1.1), with a1 tanycytes more dorsal than their a2 counterparts. Beta tanycytes reside on the floor of the V3V (B2), and along the ventral portion of the V3V (B1). Importantly, the localization of tanycytes changes from a rostro-caudal perspective, with fewer tanycytes in the rostral portion of the hypothalamic V3V, and greater numbers near the caudal end [51]. The organization of hypothalamic tanycytes allows for these subsets of tanycytes to play distinct roles in the process of hypothalamic plasticity. For example, while both alpha and beta tanycytes are exposed to the milieu of factors and nutrients within the CSF, only beta tanycytes are positioned to receive input from the fenestrated capillaries within the median eminence [53]. As with B cells in the V-SVZ, these cells are exposed to factors within the CSF and blood.

Tanycytes are currently hypothesized as a qANSC population in the hypothalamus, as the proliferation and differentiation of tanycytes into adult-born neurons and glia appears in many ways similar to the processes undergone by qANSCs in the SGZ and V-SVZ. In fact, hypothalamic progenitors in culture act identically to hippocampal progenitor populations [54]. Tanycytes express common markers of adult stem cells, such as Nestin [52], Sox2, and Vimentin [55] and beta tanycytes will proliferate *in vivo* [55]. BrdU studies identified label-retaining tanycytes within the V3V which expanded upon treatment with EGF and bFGF [56]. Additional studies on the neurosphere formation properties of tanycytes reveal the ability to form multipotent and self-renewing neurospheres in adult mice and rats [56]. Lineage tracing of Nestin-expressing cells in the young adult (P35) mouse reveal BrdU+ traced cells nearby to these beta tanycytes [55]. However, due to the expression of Nestin by various adult brain cell types, the localization of these newborn cells in proximity to the tanycyte layer has been required to identify them as tanycyte-derived cell types [55, 57]. Metabolic dysfunction resulting from decreased production of

newborn cells in the tanycyte-enriched ME has also identified beta tanycytes as a stem cell niche important for metabolic function (Section 1.6.2).

It is important to note that while tanycytes have long been hypothesized as the major stem-cell population of the adult hypothalamus, more recent data support the hypothesis that these cells are largely quiescent and respond to injury but do not contribute to basal turnover. All tanycytes utilize the unique identifying promoter, retina and anterior neural fold homeobox transcription factor (Rax), which is only expressed within the brain in tanycytes [49] and can thus be followed during lineage tracing experiments. Recently, Rax-traced cells in the adult hypothalamus were found to be largely quiescent and not produce the proliferation effects within the hypothalamus. While Rax+ tanycytes respond to neural injury in the form of a needle jab in the ME, they were not found to give rise to any significant number of cells in the basal brain [49]. Intriguingly, another study by Chaker et al. identified insulin-like growth factor 1 (IGF-1) signaling as a major pathway responsible for the continued neurogenic effects in the hypothalamus, as decreased IGF-1 signaling increased the age at which hypothalamic neurogenesis declined [57]. Alpha tanycytes were especially reliant on IGF-1 signaling, as adult mice not treated with IGF-1 revealed decreased proliferation in the alpha tanycytes of the V3V and reduced numbers of alpha tanycytes as well [57]. Together, these studies shed light on IGF-1 signaling as a possible neurogenic modulation pathway required for basal turnover and utilized to prevent heightened levels of proliferation from reducing the stem cell pool early in life.

Indeed, it was discovered that nearly all the mitotic cells in this niche were NG2+ OPCs and Olig2+ OPCs, identified within the hypothalamic parenchyma and not in the ventricular lining [49]. Single-cell RNA sequencing revealed that Igf1r signaling is necessary for tanycyte-led tissue repair [49]. For these reasons, there remains controversy regarding whether tanycytes or a currently undescribed subset of ASCs in the hypothalamus produce adult-born mature neurons and glia in this niche. While newborn neurons continue to be produced in the adult hypothalamus into adulthood and old age [57], tanycyte-derived ‘adult’ neurogenesis has mostly been studied

in young adult mice (postnatal neurogenesis), where neurogenesis is higher in all brain regions when compared to adulthood (~12 weeks).

Adult hypothalamic neurogenesis is hypothesized to respond to an adapting metabolic and nutritional environment, allowing for newborn neurons to modulate feeding behavior. Appetite is modulated by actions of orexigenic (hunger-inducing) and anorexigenic (appetite suppressing) neurons that reside within the hypothalamus. Two major appetite modulating neuronal populations in the hypothalamus are orexigenic Agouti-related peptide (AgRP) and Neuropeptide Y (NPY) expressing neurons, and anorexigenic pro-opiomelanocortin (POMC)-expressing neurons. These neurons are found in the ARC of the hypothalamus, where they are exposed to metabolic signals including leptin and ghrelin through the blood stream or CSF. Activation of AgRP neurons and subsequent NPY release to POMC neurons will stimulate hunger while inhibiting appetite suppressing signaling.

Importantly, a combination of high fat diet (HFD) and central administration of ciliary neurotrophic factor (CNTF), which can induce weight loss in obese rodents and humans, stimulated cell proliferation within the feeding centers of the hypothalamus of adult mice as identified via BrdU incorporation in adult animals [58]. Resulting newborn cells expressed neuronal markers and following leptin injections also expressed phosphorylated Signal Transducer and Activator of Transcription 3 (pSTAT3), signifying that these newborn neuronal cells can respond to appetite-suppressing leptin. Furthermore, these newborn cells were also characterized by expression of NPY or POMC, supporting their role as appetite-regulating neurons. Co-administration of the mitotic inhibitor Ara-C blocked the effects of CNTF on hypothalamic neurogenesis and long-term weight loss, highlighting the importance of adult neurogenesis and cellular turnover in body weight regulation [58].

Overall, hypothalamic neurogenesis is thought to be constitutive in action which may contribute to the neural flexibility of the hypothalamus to respond to HFD and other metabolic interventions [59]. This is supported by research which revealed that progressive degeneration of

AgRP neurons in adult mice due to the deletion of the mitochondrial transcription factor A (Tfam) gene, does not affect food intake, due to a compensatory increase in newly generated cells [59]. These adult-born cells were able to differentiate into leptin-responsive AgRP+ neurons. Importantly, while the progressive degeneration of AgRP neurons could be reversed through neurogenesis in the hypothalamus, acute ablation of these cells through the anti-proliferation drug Ara-C induced significant weight loss and anorexia, which could not be saved through basal neurogenesis of AgRP neurons [58].

Hypothalamic neurogenesis is also be affected by various neurotrophic factors, a family of signaling molecules that protect neuronal populations during survival and differentiation [60]. Brain-derived neurotrophic factor (BDNF) is one such neurotrophic factor which increases neuronal survival in the adult canary [61] and rodent brain [62]. BDNF works to improve dendritic branching and synaptic plasticity [63] throughout the adult brain. In the hypothalamus, BDNF regulates both central energy balance via effects on hypothalamic pathways and adult neurogenesis in the hypothalamus [64]. The ability of BDNF signaling in the hypothalamus to regulate appetite [65], as well as energy expenditure via sympathetic innervation of adipose tissue [66] may be dependent on changes in hypothalamic neurogenesis.

Taken together, hypothalamic neurogenesis plays a critical role in the upkeep of proper energy balance and metabolism through adulthood. While the suite of factors that mediate hypothalamic neurogenesis, the physiological stimuli for promoting hypothalamic plasticity, and the exact markers of the ANSCs in this brain region have not been identified, the role of niche stem cells and neurogenesis within this niche cannot be overstated.

1.1.2.2. The Striatum

The striatum is a principal component of the basal ganglia and plays an important role in voluntary movement. The striatum also plays a critical role in the reward system and is activated by social behavior and addictive drugs. The wide range of inputs that are available to

the striatum support the possibility of a plastic niche, due to the brain's ability to learn and unlearn reward pathways. Indeed, there is evidence that human neuroblasts from the V-SVZ may migrate to the nearby striatum instead of the olfactory bulb. Cells expressing typical neuroblast markers such as doublecortin (DCX) and polysialylated-neural cell adhesion molecule (PSA-NCAM) have been identified in the striatum [67]. Analysis of lipofuscin accumulation, an indicator of cell aging, revealed that some immature cell types expressed low levels of lipofuscin which indicated newborn cell types within the striatum [67]. Adult-born striatal neurons are transient, as demonstrated by one study in the adult guinea pig which found that BrdU label retention in newborn neurons born from a population of qANSCs residing in the striatum decreased in number from 13 to 23 days, and could no longer be seen after 65 days *in vivo* [68]. Much remains to be learned regarding plasticity within this niche, but the striatum retains plastic abilities into adulthood.

1.1.2.3. The Cortex

The neurogenic potential of the SVZ and SGZ are highlighted by the distinct expression patterns of proliferation markers in the adult mammalian brain. In these niches, expression of Ki67 and uptake of BrdU and EdU are markedly higher than any other brain region in the basal state [69]. However, adult neural plasticity allows for response to various stimuli as well and understanding the role of plasticity throughout brain regions where injury or disease are common is important if we are to understand the full story of adult neural plasticity. The cerebral cortex is composed of layers of neurons that are associated with higher level processes such as consciousness, emotion, and memory [70]. In the songbird, cortical neuronal death results in neuron replacement from slowly cycling endogenous neural precursors [71]. In the adult mouse, selective degeneration of layer II/III pyramidal neurons followed by transplantation of multipotent neural precursor C17.2 cells resulted in integration and differentiation into pyramidal neurons, indicative of a regenerative potential in this brain region [72]. While this study indicated the

potential for transplantation for neural regeneration, the role of endogenous stem cells in the adult mouse brain in cortical neurogenesis remained unknown.

To analyze the potential of endogenous stem cells in cortical neurogenesis, apoptotic degeneration of adult murine cortical neurons nearby to the neurogenic V-SVZ was performed in adult mice. This experiment resulted in adult-born mature and immature neurons in the cortex [73]. These cells expressed the migratory marker DCX, early neuronal marker Hu, and mature neuronal markers such as NeuN after a 28 week study [73]. These cells appeared to migrate to the cortex from the V-SVZ through the corpus callosum, as trails of BrdU+DCX+ cells were found between the V-SVZ and cortex after only 2 weeks [73]. These newly created cortical neurons in the adult mouse brain were able to integrate with thalamic cell types, as retrovirus injected into the thalamus was identified in the adult-born cell types [73]. While there appears to be a regenerative response made possible by the neurogenic V-SVZ, there is also evidence of endogenous stem cells throughout the brain that may play a role in regeneration. While most proliferative and label retaining cells in the mouse brain are found in specific areas, it appears as though various brain regions, including the cortex, are not outside the influence of adult neural plasticity and neurogenesis. The characterization of cortical stem cells will be further discussed in section 1.1.4.

1.1.2.4. The Olfactory Epithelium

The OE is a neural organ within the nasal cavity that is directly connected to the OB via the axons of olfactory sensory neurons (OSNs). OSN axons synapse with periglomerular neurons and allow for the transfer of information regarding odorants to the central nervous system (CNS) [74]. Adult neurogenesis is well-characterized in the OE, as OSNs are produced at high numbers throughout adult life, and can regenerate following injury [75]. The relatively robust regenerative ability of the OE lends credence to the neurogenic potential of this tissue, as the destruction of all OSNs as well as other cell types within the OE often results in a complete regeneration of the

tissue [76]. Two stem cell populations reside within the OE, globose basal cells (GBCs), and horizontal basal cells (HBCs). GBCs are multipotent and can give rise to both OSNs and glial cell types within the OE under basal conditions as well as following injury [77-79]. The production of OSNs occurs via the differentiation of GBCs into transit amplifying cells (Ascl1+) to immediate neuronal progenitors (Neurog1+) to late neuronal progenitors (NeuroD1+). These cells are highly proliferative and give rise to a constant supply of adult born OSNs throughout adult mammalian life, and are therefore easier to study than their counterparts, HBCs. This population of ASCs, the HBCs, are a potentially quiescent population, as they proliferate rarely and regenerate only small numbers of OE cells following injury [80]. Additionally, while these cells were found to proliferate 2 weeks post-injury, tracing of these cells via X-gal showed no additional proliferation of these HBC-derived cell types after 5 months [80]. In fact, mice treated with methyl bromide to induce OE lesions showed 5-fold higher numbers of GBCs labeled with BrdU when compared to BrdU+ HBCs [79]. However, although HBCs give rise to few cells following injury, they are able to differentiate into all OE cell types, indicating multipotency supportive of an ASC cell type [80].

Uncertainty remains regarding the ability of GBCs to differentiate into HBCs, as conflicting results have been observed. Schwabb et al. reported the differentiation of GBCs into both HBCs and OSNs following injury although the process was not determined and due to the lack of any protein markers separating these cell types, morphological analysis was required [81]. Contradicting these findings, a study wherein GBCs were grafted into injured OEs *in vivo* concluded that GBCs did not give rise to HBCs [82]. These studies indicate GBCs and HBCs may be two separate ASC types within the OE with similar but separate functions. The creation of newborn OSNs throughout adult life, while not directly within the brain, affects the olfactory bulb directly, and is of great importance to brain function and neural control of full-body processes [83].

1.1.3. Gliogenesis in the Adult Mammalian Brain

Gliogenesis, the production of newborn glial cells such as astrocytes and oligodendrocytes, is a prevalent process that occurs throughout the adult mammalian brain. This contrasts with neurogenesis, which is restricted to a few specific niches after birth. Gliogenesis encompasses both astrogliogenesis and oligodendrogenesis, the formation of newborn astrocytes and oligodendrocytes, respectively. Adult astrogliogenesis occurs in the cortex, where mature astrocytes divide to produce newborn astrocytes [84]. NSCs also produce newborn adult astrocytes in the SGZ and V-SVZ [85, 86]. Unlike astrocytes, mature oligodendrocytes are unable to divide. Oligodendrogenesis relies on OPCs to proliferate and differentiate into mature cell types. Chondroitin Sulfate Proteoglycan NG2 (NG2)-positive cells in the adult CNS are a population of oligodendrocyte precursor cells. NG2+ glial precursor cells (GPCs) can be found throughout the adult mouse brain and provide evidence for the wide-spread process of gliogenesis when compared to the niche-specific process of neurogenesis [87]. While the word glia comes from the Greek word for “glue”, indicating that glial cells were merely the scaffold by which neurons could operate, we now understand that glia are vital to all processes within the brain.

1.1.3.1. Astrogliogenesis

Astrocytes are specialized glial cells characterized by several branched processes, which contact blood vessels, synapses, nodes of Ranvier, and other astrocytes [88]. These cells are found throughout the brain and outnumber neurons five to one, highlighting their importance in adult brain function [89]. Astrocytes have various functions, including the transport of glucose-derived lactate to neurons, which allow neurons access to increased energy supplies [90]. Although separate from neuronal excitability, astrocytes can also perform gliotransmission, wherein they can be excited and release gliotransmitters such as glutamate [91]. Astrocytes also serve as a vessel for the uptake of neurotransmitters glutamate, gamma aminobutyric acid

(GABA), and more [92]. While neurons and oligodendrocytes cannot undergo mitosis, astrocytes can be produced in the brain via mitosis of mature astrocytes or through the activation and differentiation of qNSCs and GPCs [93, 94]. Further confounding the study of gliogenesis is the fact that qNSCs in the adult mammalian brain are astrocytic in nature. These qNSCs, which have been characterized most completely in the V-SVZ and SGZ, express most markers of astrocytes, including GFAP, brain lipid binding protein (BLBP), and achaete-scute homolog 1 (ASCL1), also known as MASH1 (mammalian Ascl1 homolog). This has complicated efforts to characterize qNSCs and hinders our understanding of astrogliogenesis and neurogenesis. Much remains to be discovered regarding astrocyte function in the adult brain and thus the role that astrocytes play in the process of adult neurogenesis, as well as the importance of astrocyte production through astrogliogenesis, cannot be understated (Figure 1.3).

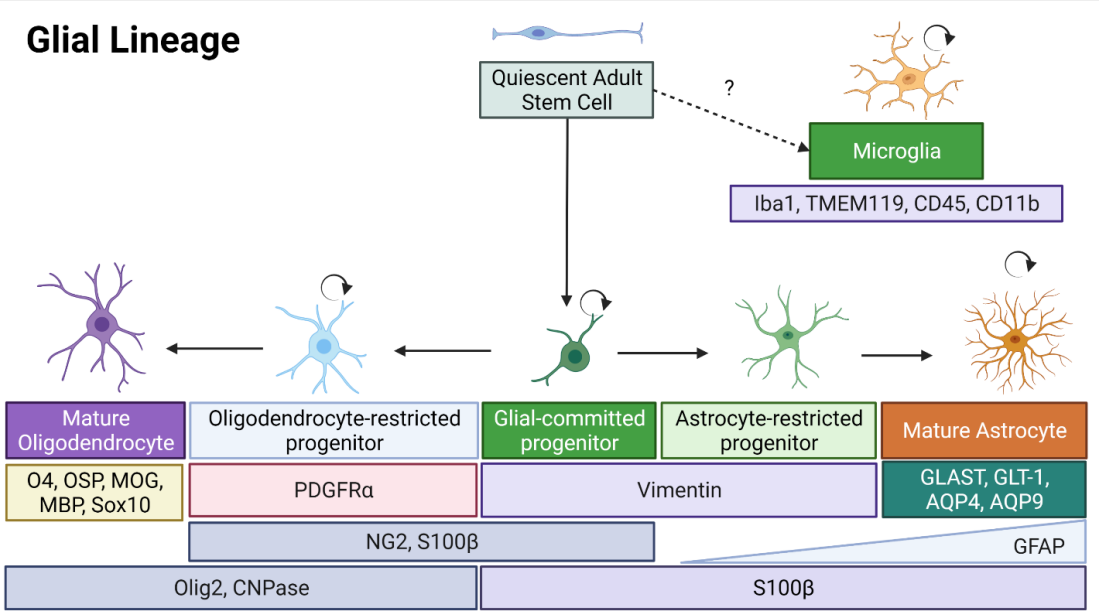

Figure 1.3. Adult gliogenesis in the mammalian brain. All glial cell types are able to regenerate within the adult brain, through stem/progenitor activation or mitosis.

Astrogliogenesis in the adult brain occurs via the division of mature astrocytes in the cerebral cortex [84]. This process is restricted to times of stress, such as following brain injury [95, 96]. In one study, lineage tracing of GLAST-CreERT2 x R26R-Bgal astrocytes in adult mice following stab wound lesion in the adult mouse neocortex identified astrocyte-driven reactive

gliosis and proliferation of astrocytes [95]. While these cells were proliferative and multipotent *in vitro*, they only formed newborn astrocytes *in vivo*, indicating a restricted astroglial lineage of these GLAST+ astrocytes within the cortex. For information on astrogliogenesis in the V-SVZ, DG, and hypothalamus, see section 1.1.3.4.

1.1.3.2. Oligodendrogenesis

Oligodendrocytes are specialized glia cells which wrap myelin sheaths around the axons of neurons to improve the conduction of action potentials [97, 98]. During development, myelination of neuronal axons is accomplished by oligodendrocytes, but throughout life, it is necessary to remyelinate axons through the regeneration of oligodendrocytes [99]. These oligodendrocytes can be lost via natural degradation, injury, or numerous diseases. The brain will therefore create adult-born oligodendrocytes through the differentiation of OPCs. OPCs are able to proliferate, migrate, and differentiate, and unlike qNSCs which reside within specific niches, OPCs can be found throughout the optic nerve [100] motor cortex, corpus callosum [101], and cerebellum [102]. These cells can be identified via their expression of NG2 and PDGFRa [103]. A small population of B-cell derived OPCs also exist within the V-SVZ [104]. These cells retain the ability to divide during basal states, although they proliferate at higher rates following injury [100].

Interestingly, for proper oligodendrogenesis from OPCs, the functionality of adult oligodendrogenesis was demonstrated in a study performed by Mckenzie et al, when the inhibition of oligodendrogenesis via the deletion of myelin regulatory factor (Myrf) in OPCs in healthy adult mice resulted in an inability to learn new motor skills [105]. Other groups have identified that the loss of NG2 glia in adult mouse brains results in improper function of both neurons and glia and can cause depressive behavior [106]. While these cells are clearly critical for proper functioning of oligodendrocyte turnover and neuronal function, it was previously determined that NG2+ glia account for 5-8% of the cells in the CNS [107]. These numbers suggest a huge role for OPCs, but other studies have determined that yearly oligodendrocyte turnover to be 0.3% [108]. This

raises questions regarding the identity and role of NG2+ cells in the adult mammalian CNS and highlights current needs in the field.

1.1.3.3. Microgliogenesis

Glial cell types can be separated roughly into macroglia, which include astrocytes and oligodendrocytes, and microglia (Figure 1.3). Microglia are derived from myeloid tissue in the yolk sac, although the specifics are unknown, and are a population of specialized immune cells [109, 110]. Microglia move into the brain during development, where they remain throughout adult life as the major cell type of the CNS-specific immune system [111]. Indeed, the brain has been described as immune-privileged for this reason. While we now understand that the brain requires extensive immunological pathways to regulate both immune health and neural plasticity, the importance of microglia, which make up about 10% of the cells in the brain and 80% of immune cells within the CNS, cannot be overstated [112, 113]. Microglia maintain surveillance throughout the CNS and can become actuated to an inflammatory state by signals of infection and viral DNA and RNA (reviewed in [114]). Additionally, these cells are required for spatial memory [115], neuroprotection [116], proper synaptic activity [117], and neural plasticity and learning [118].

Microglia regenerate entirely via self-renewal and are not created through the actions of any adult stem cells within the brain or myeloid progenitors from the periphery [119]. At a basal state, microglia enter the cell cycle each day at about 1% in adult mice [120], 2.35% in adult macaque [121], and 0.2% in adult humans [122]. After chemical ablation of 90% of microglia in the brain via the CSF receptor 1 inhibitor PLX5622 or diphtheria toxin, the microglial population was restored after 7 days of removal of the treatment. Most of these newborn Iba1+ microglia were EdU+ and found in pairs, indicating that they had undergone mitosis to repopulate [123].

1.1.3.4. Gliogenesis in the V-SVZ, SGZ, and Hypothalamus of the Adult Mammalian Brain

Adult gliogenesis occurs throughout the brain in a less restricted manner than adult neurogenesis (see sections 1.1.3.1 and 1.1.3.2). However, the classical neurogenic niches of the SGZ and V-SVZ have also been identified as major gliogenic areas. Within the V-SVZ, the anterior SVZ (aSVZ) contains qANSCs that give rise to mature neurons in the OB [19], while the posterior SVZ (pSVZ) serves to produce adult-born glia [124]. Retroviral tracing of cells within the postnatal rat SVZ identified progeny within the cortex and striatum with distinct astroglial and oligodendrocytic morphology. In this study, the cells within the SVZ with the potential to differentiate into mature glia, termed glioblasts, migrated into parenchyma where they then differentiated into astrocytes or oligodendrocytes [124]. Interestingly, *in vitro* analysis of the postnatal dorsolateral SVZ revealed the ability of these cells to differentiate into both neurons and glia [125].

Recent research has identified the cell types within the V-SVZ that have the ability to produce adult-born glia, namely, platelet-derived growth factor beta (PDGFRB)-expressing, GFAP+ qNSCs [93]. When traced over 30 and 120 days, these cells were observed differentiating into neuroblasts, mature neurons, and oligodendrocytes. Additionally, deletion of PDGFRB from GFAP+ cells in the V-SVZ increased activation of these cell types, as well as more mature neurons in the OB and oligodendrocytes in the corpus callosum. Platelet-derived growth factor D, which binds PDGFRB and is present within the CSF in basal conditions, prevented mitosis and differentiation of PDGFRB+ progenitors, indicating that under normal conditions these cells are largely held in quiescence. These studies also identified astrocytic progenitors in the septal side of the SVZ, distinguishing niche-specific differences in the V-SVZ regarding gliogenesis [93]. For additional information regarding gliogenic reprogramming due to signaling pathways, see Appendix A.

The hippocampal DG also contains GFAP+ qNSCs which allow for the production of adult-born neurons and glia throughout life. Initially believed to be a rare process within the DG [126],

adult gliogenesis is understood to occur at a similar rate to neurogenesis in the SGZ [127]. Here, the number of asymmetric and symmetric divisions from qNSC to mature cell type differs between neurons and astrocytes, which confounds lineage tracing and label retention studies [127]. Astrogliogenesis can be stimulated in the DG by running, which also increases neurogenesis in this niche, indicating that both processes are dynamic [126]. In rhesus monkeys, labeling of proliferation via ^{3}H-thymidine identified astrogliogenesis in young, juvenile, and adult ages, with an increase in the ratio of astrogliogenesis in adults when compared to neurogenesis [128]. It is important to note that the marked decrease in adult neurogenesis in rhesus monkeys into adulthood may overstate the amount of adult gliogenesis. Additionally, 3H-thymidine may have marked dividing mature astrocytes in the brains of these animals. However, it is clear that adult gliogenesis in the SGZ is an important process that cannot be overlooked.

The hypothalamus contains adult stem and progenitor cells that give rise to both newborn neurons and glia. Adult gliogenesis has been understudied in the adult hypothalamus, yet new evidence for the role of adult gliogenesis in this niche offer clues into the role of this process in this niche. For example, lineage tracing studies with tanycytes identified traced astrocytes within the hypothalamus [129]. After treatment with FGF2, newborn BrdU+GFAP+ cells were identified as well [129]. Of note, the mouse line used for the basal state experiments in this study traced GLAST+ cells in the adult mouse brain, and while tanycytes express GLAST, it is also a marker of astrocytes. It is possible, therefore, that the traced GFAP+ cells were astrocytes from the start. Further, BrdU+GFAP+ cells were identified within the tanycytic layer of the 3V, raising questions regarding the astrocytic vs. tanycytic nature of these newborn GFAP+ cells [129]. Newborn oligodendrocytes and microglia have been observed in the adult hypothalamus as well. NG2+ glia in the adult mouse hypothalamus give rise to oligodendrocytes and neurons [130], and are required for hypothalamic leptin sensing and body weight control (Section 1.5) [131]. Metabolic interventions can induce proliferation of microglia as well, as HFD-fed adult mice show increased microglia in the ARC [132]. Mitotic inhibition during HFD treatment prevented this microglial

expansion and in addition, weight gain [132]. These studies indicate a role for gliogenesis in energy balance in the adult mammalian brain.

Additional evidence of adult gliogenesis within the hypothalamus can be gleaned from the amount of EdU+ cells that did not express NeuN, Hu, or other neuronal markers in studies where gliogenesis was not specifically studied. In one study where 16-week mice were treated with BrdU via intracerebroventricular (*i.c.v.*) injections for 7 days, the percentage of Hu+BrdU+ cells to total BrdU+ cells in the hypothalamus were about 60% after 4 weeks [133]. Clearly, 40% of the newborn cells in the hypothalamus were non-neuronal, indicating a stem, glial, endothelial, or infiltrating cell type. Due to the astrogliogenesis, oligodendrogenesis, and microgliogenesis observed in previously discussed research, it is highly probable that a number of these label retaining cells were glia [49].

1.1.4. Identification and Analysis of Stem Cells in the Adult Brain

Stem cells differ from all other cell types in that they: 1) have the ability to produce multiple mature cell types, and 2) retain the ability to divide and renew tissues for long periods of time. There are two major denominations of stem cells, embryonic stem cells (ESCs), which are present during development, and ASCs. Adult stem cells are often found within developed tissues and give rise to mature cell types required for the long-term regeneration of that tissue. For example, ANSCs are located in the brain and give rise to mature neurons and glia. ANSCs produce adult-born mature cells through the processes of activation, proliferation, differentiation, and migration. ANSCs, naturally in a quiescent state, can become activated by cues from the CSF, blood stream, or nearby cells. They will then divide either asymmetrically into one ANSC and one more differentiated cell type or symmetrically into two ANSCs or two differentiated cells. These more differentiated cells are no longer stem cells, as they are no longer multipotent, and will continue differentiating to a specific mature cell type unless they de-differentiate.

There are multiple populations of qANSCs in the adult brain. These cells serve to replenish neurons, astrocytes, and oligodendrocytes. These cells are astrocytic in nature, and express the astrocyte markers GFAP, BLBP, and GLAST (Figure 1.4). The identification of qANSCs in the V-SVZ utilized the mitotic inhibitor Ara-C to identify quiescent cells that could produce newborn TACs, neuroblasts, and neurons after destruction of these mitotic cell types. GFAP+ qANSCs in the V-SVZ are radial glial-like cells, with extensions that contact both the CSF and vasculature [134]. These cells are therefore able to respond to quiescent and activating signaling effectors within these environments. Indeed, qANSCs will proliferate more often when treated with CSF taken from young mice compared to aged mice [135]. GFAP-expressing qANSCs reside within the DG as well. These cells give rise to intermediate and neuronal cell types distinct from those within the V-SVZ, although they share many similarities between these qANSCs and the cells within the V-SVZ. These cells were identified through ^{3}H-Thymidine label retention studies. Here, short experiments with ^{3}H-Thymidine identified that this thymidine analog was incorporated into GFAP+ qANSCs only, while longer studies led to label retention in intermediate Type D cells as well [18]. Further studies of GFAP+ qANSCs within the DG have supported these findings and identified cell types and cell markers that have expanded our understanding of qANSCs in the adult mammalian brain [30, 136].

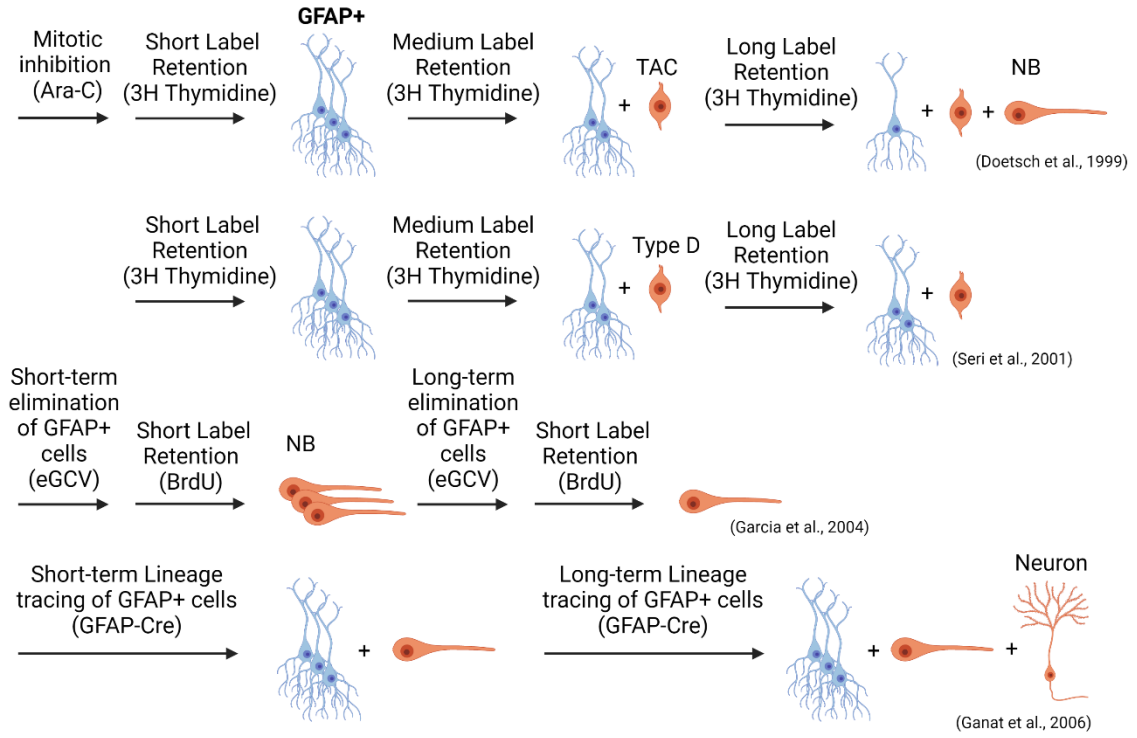

Figure 1.4. Evidence for GFAP+ cells in the adult brain as a population of qANSCs. Experimental outline of studies from landmark papers reporting the presence of GFAP+ astrocyte-like cells in the adult mouse brain which are quiescent and give rise to intermediate progenitor and mature neuronal cell types in the V-SVZ/OB axis and SGZ.

Other markers such as Nestin and Sox2 are also expressed by ANSCs. These markers are not specific to ANSCs and are expressed by various other cell types throughout the brain. EGFR, which is expressed by aANSCs in the V-SVZ, is also expressed by more differentiated cell types, such as transit amplifying cells. These ANSCs, as well as the intermediate cell types and mature cell types generated during neuro/gliogenesis depends on their localization within the brain. In the DG, the process of neurogenesis occurs when ANSCs give rise to type II cells, type III neuroblasts, immature neurons, and then mature neurons within the hippocampus. Comparatively in the V-SVZ, ANSCs give rise to type C TACs, which differentiate into migratory type A neuroblasts, which then migrate through the RMS to the OB, wherein they mature into

mature neurons. V-SVZ ANSCs also differ from DG ANSCs in that they are exposed to the CSF in addition to the bloodstream. The CSF contains a milieu of growth factors that serve to activate or hold ANSCs in quiescence. Signaling factors in the process of adult neuro/gliogenesis will be covered in section 1.2.

The study of qANSCs *in vitro* has illuminated the abilities of these cells to proliferate and differentiate. When cultured with the growth factors EGF and FGF, qANSCs will proliferate and form floating neurospheres [137]. Primary neurospheres can be formed from single cells or from the plating of multiple cells per well [138, 139]. These studies elucidate the stem-like nature of the cells used for neurosphere formation, as the ability to self-renew and to differentiate into multiple mature cell types and are thus indicative of a stem cell like population. Self-renewal is measured via neurosphere growth, which can be divided into neurosphere size and clonal secondary neurosphere growth from isolated cells derived from primary neurospheres [140]. The size of individual neurospheres indicates the proliferative ability of the cells within neurospheres, as each neurosphere will grow only when the cells within that 3D cell structure are proliferating [140]. Individual neurospheres are composed of NSCs and differentiated cell types, as well as an extracellular matrix (ECM) [140]. For that reason, growth within individual neurospheres can be attributed solely to the cells within each sphere. Secondary neurospheres are formed after dissociation of primary neurospheres and indicate that the cells derived from primary neurospheres still retain the ability to replicate. Interestingly, both primary and secondary neurosphere formation relies upon unknown factors supplied by the cells in culture, as single NSCs and neurosphere-derived NSCs plated at a low density will often not form neurospheres [141-144]. Additionally, the low proliferative capacity of qANSCs is a major drawback when attempting to analyze the growth or label retention of these cells (see section 1.1).

The differentiation of neurospheres into mature astrocytes, oligodendrocytes, and neurons is key to understanding the multipotent potential of neurosphere-forming cells. Importantly, even before these cells are treated with differentiation factors, neurospheres are differentiating into

various proliferative non-mature cell types [145]. While there is high variability between neurospheres formed depending on cell types, growth factors, surface adhesion, and more, most often differentiated cells reside within the core of the neurosphere and undifferentiated GFAP+, SOX2+, and/or Nestin+ cells reside in the outer layers of the sphere [146, 147]. It is clear that these cells are differentiating constantly, even before differentiation is induced via factor administration. Therefore, we as a community must take care to understand the role of factors coming from neurospheres and their role in differentiation versus the factors administered to induce differentiation. Ultimately however, the ability of a small number of cells to generate large numbers of proliferative and differentiation-capable cells points to the stem-cell like nature of neurosphere forming cell types.

The identification of a cell type as a stem cell in the adult brain is often supported by the ability of that cell/ cell type to form neurospheres in culture. However, it is important to recognize the caveats intrinsic to neurosphere studies. It can be difficult to isolate a stem cell population of interest due to the lack of a specific and unique marker for qASNCs in the adult brain. The first step of any neurosphere study begins with the identification and isolation of a population of cells wherein identification of neurosphere potential is required. Often, cells will be labeled via antibody and isolated through FACS sorting. However, even through a combination of markers designed to isolate only qANSCs (GFAP+/EGFR-/CD133-), it remains highly likely that additional populations of cells, especially GFAP+ astrocytes may be within these populations. Indeed, astrocytes or oligodendrocyte progenitors cultured with EGF and FGF can form neurospheres *in vitro*, requiring extreme care when isolating and culturing cells believed to be qANSCs [148, 149]. Questions also surround the state of qANSCs exposed to the factors within neurosphere media. This is because the gene expression changes in cells that make up neurospheres are more ESC-like in nature than gene expression patterns of cells from the *in vivo* V-SVZ [150]. While improvements are being made to neurosphere culture, including the production of *in vivo* structures such as pinwheel structures in culture [151], it is important that we work to uncover the

implications of neurosphere studies in the adult brain to verify that these experiments are applicable to the adult brain.

1.1.5. Plasticity of Non-Neuronal and Non-Glial Cell Types in the Adult Brain

In addition to neurons and glia, the adult brain retains plastic abilities of cell types such as epithelial cells, endothelial vasculature and associated pericytes, non-microglial immune cells, and meningeal cells. The choroid plexus (CP) is a circumventricular organ composed of choroid epithelial cells (CPECs) connected by tight junctions. CPECs surround large blood vessels and meningeal cell types and separate the blood from the CSF within the ventricles. Together, these tissues form the blood-CSF-barrier (BCSFB), which feeds the brain's ventricles with water, growth factors, and necessary nutrients, allowing for the production of CSF. Breakdown of the CP across all layers occurs with disease or aging and leads to unwanted factors entering the CSF. To prevent breakdown of the BCSFB, the adult CP regenerates under a basal state through the use of proliferation [69, 152]. This may occur through the use of stem cells that reside within the CP, as isolation and culture of CP cells leads to neurosphere formation and differentiation to neurons, astrocytes, and oligodendrocytes [153]. *In vivo* experiments with EGF and FGF2 infusion result in increased numbers of label-retaining BrdU+ cells in the CP. Additionally, implantation into injured spinal cords of adult rats, CP-derived cells differentiate into GFAP+/GLT-1+ astrocytes [153].

The meninges, which is contained within and around the brain, is not composed of neurons or glia. Instead, the meninges contain blood vessels, lymphatic vessels, fibroblasts, and additional unknown cell types. Stem-like cells are found in this organ as well, as identified through the expression of Ki67, Nestin, DCX, and Sox2 [154]. Cells isolated from the leptomeninges, made up of the arachnoid mater and pia mater also form neurospheres and can be subsequently differentiated into neurons *in vitro* [155].

The CP and meninges both facilitate the infiltration of immune cells from the bloodstream into the adult brain. In addition, CNS-associated macrophages reside at parenchymal borders within the adult brain [156]. While many immune cells in the blood are mature hematopoietic cell types, there also exist hematopoietic stem cells (HSCs), multipotent stem cells that can be found throughout bone marrow and peripheral blood [157]. Indeed, in adult mice which cannot develop myeloid cells (PU.1-/- mutant mice), transplantation of HSCs revealed the differentiation of these cells into NeuN+ neurons in the brain [158]. Additionally, HSCs can differentiate into epithelial and endothelial cell types across numerous adult organs, including the liver, lung, and skin [159]. Due to the ability of these cells to infiltrate within the brain, it remains possible that stem cells from both the brain and the periphery can lead to adult-born reconstitution of the adult brain. Taken together, it is clear that ASCs reside within the brain to give rise to mature cell types other than neurons and glia.

1.2. Adult Neural Plasticity in Humans and Rodents – Similarities and Differences

The field of adult neurogenesis has exploded since the discovery of adult-born neurons in the adult rodent. We now know that adult neurogenesis occurs in cows [160], dogs [161], lemurs [162], and many more species [163]. The study of neurogenesis in rodent models has revealed much about the inner workings of the mammalian brain. However, stark contrasts exist between rodent and human brain development and adult neurogenesis. Adult mice and rats produce newborn intermediate progenitor cells in the thousands each day in both of the V-SVZ and SGZ, while human SGZ neurogenesis is still hotly debated, and the human RMS has not yet been identified to produce OB neurons [164]. While there is much to be learned about human neurogenesis from model organisms in the lab, measures must be taken to validate that research allows for accurate and representative translational results from rodent models.

1.2.1. Prenatal and Postnatal Plasticity

The first stage of brain development in both humans and mice is the formation of the neural tube [165]. In humans the neural tube forms within the first tenth of the prenatal development period (3-4 weeks into gestation), while in rodents neural tube formation occurs near the mid-gestation point (9-10 days into gestation) [165, 166]. Neural development sees the differentiation of the spinal cord and brain from this organ, a highly conserved process across humans and rodents [167, 168]. While the process of neural development is highly conserved, the ages at which these processes occur differs drastically at times between humans and mice. Mice and rats have short gestation periods and have brains that continue to develop postnatally in ways that occur in human brains while in the womb [169]. For example, the rodent brain peaks in gliogenesis at postnatal day 7, while in humans this process occurs at 36wks gestation [169]. It is for these reasons that the age at which neurogenesis is studied must be taken into account when comparing this process between humans and rodents. Studies that examine postnatal animal brains must be sure to use animals at an age where they can be comparable to humans at the same stage of human development. Indeed, various murine studies which utilize animals under postnatal day 60 yet claim to have implications for adult human neurogenesis should be analyzed with care and should be replicated with animals at an age of mature adult brain behavior [55].

1.2.2. Differences in Ventricular-Subventricular Zone Plasticity

Under normal conditions in the mouse V-SVZ, the role of stem and intermediate cells is to produce newborn neurons in the olfactory bulb. Due to the large size of the OBs and the role of smell in the lifestyle of rodents, the importance of neurogenesis within this niche is clear [170]. In fact, in the mouse brain, newborn neurons enter the OB daily [171]. The human olfactory bulbs in contrast, are quite small. We humans rely on smell to determine if the oven is burning or whether the milk in our refrigerator has gone bad, which pales in comparison to the reliance on smell that

mice have, which include: finding food, locating mates, and avoiding predators [172]. It stands to reason that the role of olfactory neurogenesis would be enhanced in mice when compared to humans. In fact, it is still unclear whether olfactory bulb neurogenesis occurs in humans.

The human V-SVZ was identified to contain neuron-producing cells *in vitro* in the mid-1990s [173]. After this, BrdU administered to humans revealed BrdU+ cells within the V-SVZ in the adult brain [11]. Indeed, neurosphere culture of human V-SVZ cells mimicked the ability of V-SVZ qANSCs to produce self-renewing, multipotent cells in adult humans [174]. The human V-SVZ is unique in that the structural layout of this niche is less dense than in the mouse, with layers that differentiate it from the mouse V-SVZ. Here, the astrocytic layer, where astrocytes and qANSCs reside is lateral to the ependymal cells (layer I) that contact the CSF and the hypocellular gap (layer II) where extensions from the astrocyte layer (layer III) and ependymal layer are spread [175]. In mice (as in dogs and other primates), B-cells reside directly behind ependymal cells and have shorter extensions that contact the CSF [175]. Interestingly, this hypocellular gap is also present in cows [175]. These cells produce C cells lateral to the ventricle. In humans, the final layer of the V-SVZ is identified as the transitional layer (layer IV), which separates the V-SVZ from the brain parenchyma.

While similarities in the neurogenic potential of the V-SVZ exist between humans and mice, questions remain regarding the human RMS, which feeds the OB with chains of neuroblasts. Initial studies revealed proliferating cells between the V-SVZ and OB that expressed neuroblast markers. While this study could not confirm the maturation of adult neurons in the OB, they observed the human RMS, pointing to a human V-SVZ/OB axis [176]. However, subsequent studies were unable to identify any human RMS after 18 months of age [177] or neurogenesis in the OB of significant proportion to the DG [178, 179]. In fact, it is hypothesized that human OB neurogenesis may occur in the OB, without the presence of the RMS [24].

1.2.3. Differences in Hippocampal Plasticity

In the adult mouse hippocampus GFAP+ radial glial-like Type I cells, qANSCs, in the SGZ give rise to mature neurons in the CA1 region [18]. These qANSCs differentiate and proliferate to form Type II precursor cells, which in turn differentiate into Type III neuroblast cells [18]. Adult hippocampal neurogenesis (AHN) concludes with the differentiation of neuroblasts into immature neurons and finally mature neurons. This process decreases with age in both rodents and humans [179], but can be increased with exercise, environmental enrichment, and learning [35, 38, 39]. These newborn neurons impact mood regulation and learning and memory [180].

AHN in the aged human brain (67-72 years) was discovered via the incorporation of the thymine analog BrdU into cells within the hippocampus [11]. Because these cells were identified as mature neurons via immunohistochemistry with the marker NeuN, it was concluded that adult-born mature neurons were located in the dentate gyrus [11]. Additional evidence for AHN in humans is supported by studies showing the presence of Ki67+ cells [181, 182] as well as DCX+ neuroblasts [183-185]. Additional support for the presence and functional importance of AHN were found when comparing disease-state and control brains. Brains from epileptic patients, patients with Alzheimer's disease, and brains following hypoxic-ischemic encephalopathy showed heightened AHN [181, 184].

1.2.4. Hippocampal Neurogenesis – Controversy in Mouse/Human Data

The current methods of analyzing AHN have been called to the forefront recently, due to marked differences in the amount of AHN identified by different groups and techniques. For example, in direct contrast to the studies described above, decreased AHN was associated with depression, schizophrenia, and alcoholism [186-188]. While these conclusions have significant implications for human health, subsequent studies have shown the opposite effects of Alzheimer's disease [189, 190], epilepsy [191, 192], and depression [193] in AHN. In fact, a variety of prominent researchers in the field have argued that AHN in humans does not occur in any

meaningful amount in adulthood [194-196]. An initial study of adult human neurogenesis showed BrdU incorporation in the adult human brain in the neurogenic V-SVZ and DG after a number of months [11]. Further experimentation with neuronal uptake of ^{14}C, identified that in humans born before nuclear testing had begun, neurons showed uptake of this carbon isotype, indicating these cells had arisen from cellular division after development [179].

More recent experimentation, which has relied heavily on immunostaining of proteins in fixed human brain tissue, has yielded conflicting results. Evidence for the presence of adult human neurogenesis was identified in 17-53-year-old control brains with the use of antibodies for the stem cell markers Nestin and GFAP, proliferation marker Ki67, and neuronal marker NeuN. Furthermore, the number of stem-like cells was decreased with aging, showing similarities to adult neurogenesis in rodents [182]. Additional studies on postmortem human brains showed similar features of adult human neurogenesis [189, 197]. However, other groups report that during childhood, cells that express markers of adult neurogenesis are absent, when compared to young postnatal brains [194, 195, 198, 199]. Additionally, the morphology and location of DCX+ neuroblasts was changed with aging, as the cells had less complex extensions and were found outside of the traditional SGZ. These studies are in direct contrast to other groups who show expression of markers of adult hippocampal neurogenesis into adulthood [190, 200]. Due to these conflicting studies, the field of neurogenesis is currently at an impasse, with prominent researchers on each side of the spectrum.

There remain major limitations to the study of AHN in humans. Notably, the tissues utilized to study this process come with a myriad of issues. In mice and rats, perfusion with a fixative allows for the tissues to be fixed at death, keeping the tissues well-preserved and in their natural state. Not only this, but the tissues are able to be fixed for well-defined periods of time. Additionally, due to the large number of antibodies for rodent tissue neurogenic studies, the process of tissue preparation for antibody usage has been well-documented. In human research,

brains must be fixed and collected post-mortem, potentially hours after death. Tissues are then processed and disseminated via biobanks, which may take long periods of time and may result in tissues being fixed differently across studies. Fixation technique affects the markers that can be identified via immunohistochemical or immunofluorescent studies, further complicating the matter [190, 201]. Finally, it must be mentioned that human lifestyles are largely heterogeneous. Unlike that of a lab mouse that is provided with the same food, water, enrichment, and social life throughout its lifetime, humans have a plethora of other stimuli and external factors that may influence differences in AHN. These differences may produce changes that can be difficult or impossible to attribute to the study of AHN.

Finally, due to the intrinsically fleeting nature of type II and III cells, as their presence is due only to type I cell differentiation, it has been common for studies to correlate the number of DCX+, PSA-NCAM+, or NeuroD1+ cells in the adult hippocampus to the amount of adult neurogenesis occurring within this niche. Label retention studies in the hippocampus will often quantify BrdU-positive or EdU-positive neuroblasts, immature neurons, and mature neurons to identify patterns of adult neurogenesis within this niche. There are additional questions that cannot be answered through these methods. One question that pertains to both mice and humans is: is the increase in neuroblast/ newborn neuron number due to proliferation of intermediate cell types, qANSCs, or both? To study adult neurogenesis, we require knowledge of the intermediate cells as well as the qANSCs that supply them. Additionally, while the expression of DCX has classically been used as a marker of neuroblasts in the V-SVZ and SGZ in both humans and rodents [190], there is recent evidence for the possibility that DCX is a promiscuous marker that is expressed by various human neuron populations, but not immature neurons [202].

Taken together it is clear that work must be done to bring the field of AHN to a point where human brain studies can be consistently compared, be that through tissue processing, staining techniques, and marker utilization.

1.3. Signaling Pathways Involved in Adult Plasticity

The adult brain has access to important circulating factors from the CSF and blood such as growth factors and neurotrophic factors, which govern a variety of processes, including adult neuro/gliogenesis. Growth factors such as EGF, FGF, and nerve growth factor (NGF) can activate qANSCs and intermediate cell types or hold them in quiescence and are directly associated with proliferation, growth, and regeneration of tissues [137, 203, 204]. Neurotrophic factors, such as BDNF are essential for the survival and differentiation of neuronal cell types [205]. In brain regions exposed to the ventricular system, such as the V-SVZ and hypothalamus, CSF from young animals can induce neural plasticity, even in cells from aged mice [135]. Therefore, it stands to reason that the changes observed in adult plasticity with aging, with various metabolic interventions, or during certain disease states, may not be due to changes in the stem/ intermediate progenitor cells themselves, but rather the signals acting upon them. This section will provide evidence for the importance of signaling pathways involved in adult plasticity.

1.3.1. Niches Involved in Secreting Neurotrophic Signals: The Blood Cerebrospinal Fluid Barrier and the Blood Brain Barrier

The BCSFB is created by the choroid plexus, a circumventricular organ present in all four of the brain's ventricles. This organ is composed of an outer layer of epithelial cells, which are joined by tight junctions, so that any movement between the CP and the CSF requires transport mechanisms in the cell membrane of these CPECs. Within the CP are fenestrated blood vessels, which supply blood to CPECs to supply their intense supplies of mitochondria, as well as the nutrients, water, and factors required for production of the CSF by the CPECs [206]. While still poorly understood, there also exists an inner layer of meningeal tissue that forms within the choroid plexus and may serve to protect the brain during infection [207].

An elegant study conducted by Silva-Vargas et al. outlined the natural interplay between factors within the CSF on qANSCs in the V-SVZ and highlighted the significance of circulating

factors on neurogenesis [135]. In this study, qNSCs, aNSCs, and TACs were grown separately and exposed to the growth factor EGF or the lateral ventricle choroid plexus secretome (LVCPsec). It was observed that exposure to the LVCPsec induced proliferation and sphere formation in qNSCs and aNSCs at significantly higher levels than control or EGF-containing media. This was not the case for TACs, which had similar levels of growth when exposed to EGF or the LVCPsec, indicating that TACS, more differentiated than qNSCs or aNSCs, had lost the ability to respond to a variety of stimuli. Furthermore, exposure of aNSCs, but not qNSCs or TACS isolated from aged mice to the LVCPsec of young mice increased cell proliferation when compared to the LVCPsec of aged mice. A huge number of factors are found in the LVCPsec, which still need to be fully understood. However, it is clear that of these factors there lies a fine balance of activation and proliferation of stem and intermediate progenitor cells [135]. This study identified bone morphogenetic proteins (BMPs) within the CSF that modulated the growth of NSCs *in vitro*. BMPs play a role in adult neural plasticity throughout the adult brain and are important for quiescence and activation signaling in both ventricular niches and niches without direct access to the CSF. The role of BMPs in neural plasticity is discussed in Appendix A.

The blood brain barrier (BBB) consists of continuous nonfenestrated blood vessels connected with tight junctions, and the associated neural cells that form the neurovascular unit (NVU) [208]. The NVU is composed of smooth muscle cells, pericytes and astrocytes. Together, the NVU works to keep transcytosis levels low and prevent molecules from the blood from infiltrating into the brain [209-212]. Similarly to the contact between qANSCs and the CSF in the V-SVZ, qANSCs in the V-SVZ and SGZ utilize extensions to contact and interact with the blood supply through the BBB [213]. These connections allow for factors such as pigment epithelium-derived factor to upregulate Notch signaling in qANSCs [214]. As with the effects of aging on the LVCPsec, BBB breakdown with aging in the SGZ [215] and V-SVZ [216], consisting of decreased flow rate and leaky blood vessels, occurs in tandem with decreased neurogenesis [217, 218].

1.3.2. Activation and Quiescence

The first stage of adult neuro/gliogenesis begins with the activation of a quiescent stem cell. Quiescence is characterized by cell cycle arrest, commonly at the G0 cycle checkpoint [219]. The quiescence of classical qANSCs is supported by the survival of GFAP+ qANSCs during treatment with the anti-mitotic drug Ara-C [19]. While quiescent cells are held in cell cycle arrest, it is not for a lack of cellular activity. qANSCs utilize glycolysis at high levels when compared to more differentiated neuronal cell types, which require oxidative phosphorylation to fuel action potentials and synaptic vesicle recycling [220]. Quiescent cells also overexpress transcriptional repressor genes such as REST to suppress ribosome biogenesis [221]. qANSCs additionally repress the expression of Sox2, Pax6, and Ascl1, activation and fate-determining factors associated with more differentiated cell types [219, 222]. In fact, ingenious methods of inactivation of these activating molecules include competitive binding of DNA, as is the case with FOXO3, which outcompetes ASCL1 and induces quiescence [223]. Activation also occurs in conjunction with the downregulation of inhibitory proteins like REST or ID4, allowing for transcription of Sox2 and Pax6. then leads to the generation of more differentiated progenitor cells through asymmetric or symmetric proliferation and differentiation. This results in intermediate progenitor populations, which will differentiate along a predetermined circuit, resulting in a newborn mature cell type. Moreover, quiescent stem cells may also be acted on by quiescent factors, which work to keep them quiescent. These signals are often found together, highlighting that the interplay between factors that induce activation or quiescence is critical for proper adult brain upkeep and tissue turnover.

Importantly, and in support of the idea that the qANSCs in the adult V-SVZ and SGZ are highly similar, many signaling morphogens and growth factors induce neurogenesis (or prevent it) in both niches. In cells derived from the adult mammalian brain, the neurotrophic factor BDNF increases neurogenesis within the DG and V-SVZ [224, 225]. The morphogen sonic hedgehog (Shh) also acts on the SGZ and V-SVZ in similar ways, with decreased neurogenesis occurring

when Shh signaling was interrupted in the DG [226]. Shh was found to act on both qANSCs and neuroblasts in these niches [227, 228]. Notch signaling works to prevent aberrant neurogenesis, causing the exit from the cell cycle by NSCs in the adult SGZ [229, 230]. Finally, the Wnt signaling pathway is critical for neurogenesis in the DG [231] and V-SVZ [232]. Taken together, a variety of signaling molecular and pathways are required for the proper functioning of adult neurogenesis in the adult brain.

1.4. Telomerase Reverse Transcriptase (TERT)

The ribonucleoprotein telomerase synthesizes repeats of telomeric DNA to prevent chromosomal damage in replicating cells [233]. Telomeres are structures at the ends of linear chromosomes made up of telomeric DNA and proteins [234]. Telomeric DNA is made up of multiple tandem repeats (5'-(TTAGGG)n-3', followed by a G-rich tail of 150-200 nucleotides [235]. Telomerase reverse transcriptase (TERT) is the enzymatic component of telomerase [236]. The *TERT* gene is made up of 15 introns, 16 exons, and a promoter core at chromosome 5p15.33 in humans [237]. This gene is 42kb long and can encode any of 22 mRNA isoforms [238]. The RNA component of telomerase is called Telomerase RNA Component (TERC; chromosome 3q26) and is essential for the production of these telomeric repeats [239]. TERC and TERT, as well as a variety of auxiliary proteins are required for proper formation and function of the telomerase complex [240]. These accessory proteins include dyskerin, NOP10, NHP2, GAR21, p23, and HSP90 [241]. Together, TERT and these proteins work together to bind TERT to TERC and to telomeres (Figure 1.5).

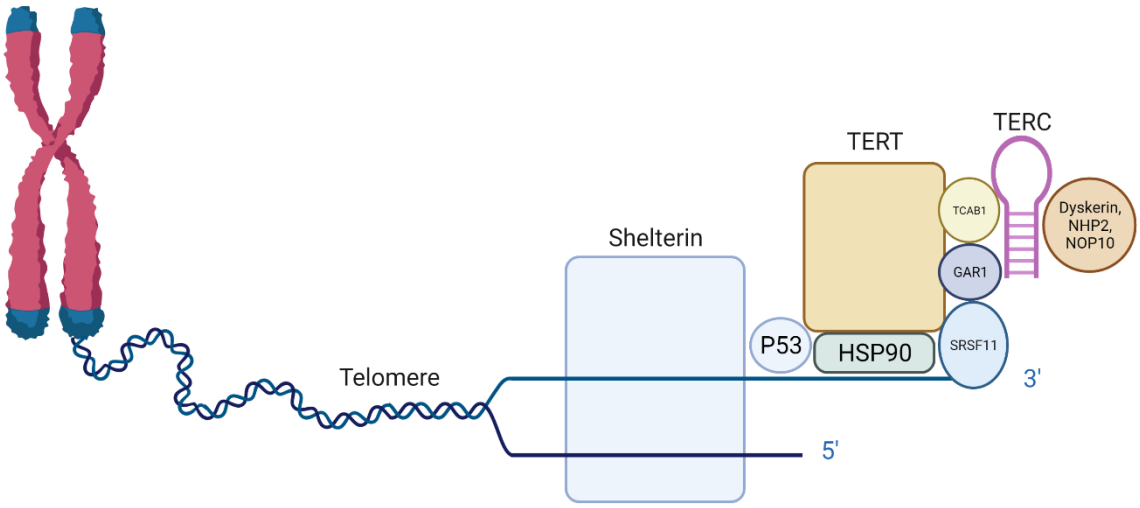

Figure 1.5. Organization of the telomerase complex and telomere associated proteins. TERT and TERC are bound through the actions of ATPases and during S phase of the cell cycle, this complex binds the shelterin protein complex on the telomere. The telomerase complex then acts to extend telomeres through the actions of TERT and TERC.

While TERT expression is undetectable in most somatic cells in postnatal stages, this protein has been identified in a subset of highly proliferative adult somatic cells in both mice and humans. TERT has further been identified as a marker of stem cells in a quiescent state across various adult mouse tissues. The reason that both highly proliferative cells and quiescent stem cells in the adult body express TERT is currently unknown. It is hypothesized that within highly proliferative cell types, such as cells within the epidermis of the skin, TERT is expressed at levels that will allow for repeated telomere extension and continued proliferation but at low enough levels to prevent cancer, and that in quiescent cell types such as qANSCs, TERT is expressed to fulfill another role. For that reason, it is important to understand both canonical and non-canonical roles of TERT. Overall, it is clear that understanding these cells would lend significant value to discovering the regeneration of adult tissues.

1.4.1. Canonical Roles of TERT

Telomerase functions to elongate telomeres after they are shortened following cell division [234, 242]. Most adult somatic cells do not express telomerase [243]. In most somatic cells, proliferation will cause shortening of telomeres, ultimately concluding with cellular senescence [244]. It is for this reason that shortened telomeres occur with aging [245, 246]. In addition to the "end-replication problem", telomeric DNA can be damaged and shortened by factors such as age, diet, stress, and more [247-249]. Upon senescence, the cell will utilize the checkpoint factors such as p16INK4a to prevent cell apoptosis or a cancerous phenotype [250, 251]. However, while the cell may avoid death or oncogenic activation, senescence will prevent the cell from proliferating again [252, 253]. In tissues where increased senescence occurs during aging, regeneration and repair are hindered and tissue function diminishes [254]. Therefore, the function of telomerase is vital for cells that require high levels of proliferation, as senescence or oncogenic phenotype can result when telomeres reach a dangerously short length [254].

High levels of telomerase activity and expression of both TERT and TERC are hallmarks of development. Here, telomerase functions to prevent senescence in ESCs [255]. While in cancerous cells telomerase functions to force immortality and unlimited proliferation, ESCs are able to proliferate and differentiate without becoming cancerous [256]. Importantly, TERT is expressed in around 90% of cancers, and is utilized for the unlimited proliferation of cancerous cells. The role of TERT in cancer has been covered in depth elsewhere but will not be a topic of interest here [257]. In humans, telomerase activity is reduced to undetectable levels from the neonatal period onward except for in certain cell types [255]. Section 1.5.2. will cover these tissues in more detail. As mammalian aging is directly correlated to telomere shortening, the loss of TERT and telomerase is of importance to our understanding of tissue regeneration and turnover.

Telomerase activity in humans is highly regulated by the expression of TERT, the rate-limiting subunit of telomerase, as TERC is expressed ubiquitously in all tissues [258, 259]. Regulation of the TERT gene at the transcriptional level as evidenced by multiple promoter

binding sites in the hTERT gene [260]. TERT mRNA is also regulated by pre-mRNA alternative splicing, which can affect telomerase activity [261]. Additionally, while TERC expression remains constant throughout differentiation of mouse erythroleukemia cells, mTERT expression undergoes changes throughout differentiation [259]. The discovery that telomerase activity was identified in immortalized cell lines where it prevented telomere shortening and chromosome instability [262] was integral to the development of TERT overexpressing immortalized cell lines [263]. TERT-immortalized cell lines include esophageal cells [264], fibroblasts [265], keratinocytes [266], and more. As TERC is expressed ubiquitously throughout the body, TERT overexpression is all that is required for immortalization. Importantly, TERT overexpression-based immortality does not cause major changes in cell physiology and cell cycle control. However, whether TERT overexpression affects non-canonical roles of TERT in these cell types is still not understood.

1.4.2. TERT Marks Adult Stem Cells in Human and Mouse Tissues

The role of TERT as a telomere-restoring protein supports the findings that tissues and organs where TERT is expressed often contain rapidly renewing cell types. This has been observed in both humans and mice [259, 267]. However, more murine tissues express TERT than in humans [259, 267]. In the adult mouse, mTERT mRNA expression has been identified in the brain, heart, lungs, liver, kidney, intestine, muscle, skin, testes, spleen, and thymus [259, 268]. Some adult tissues, such as the brain, exhibit TERT mRNA expression, but have low telomerase activity [268, 269]. Analysis of hTERT transcripts showed expression only in the spleen, testis, thymus, and bone marrow, with lower expression in the brain and uterus [267]. Support of hTERT expression in various human tissues can be found by analyzing Dyskeratosis congenita, a disease that results in the dysfunction of telomerase [270]. Patients exhibit issues with regeneration of the skin, gut, and bone marrow, and have reduced telomere length when compared with non-affected individuals [271]. Mouse TERT (mTERT) transcripts in the same

study were identified in more tissues than humans TERT (hTERT), including the mouse liver, spleen, testis, muscle, kidney, heart, thymus, lung, brain, bone marrow, and uterus [267]. It is important to note that lab mouse telomeres are significantly longer than human telomeres, which could be a confounding factor when interpreting TERT expression or telomerase activity between these organisms [272].

The skin is one such organ where the high turnover of epidermal cells requires proliferation to support the constant cell death. Here, human keratinocytes utilize telomerase activity to prevent senescence of the mitotic cells within this highly regenerative tissue [273]. While this discovery was made by analyzing telomerase activity, other studies have demonstrated the expression of hTERT in human skin samples from young, aged, and photo-aged skin [274]. Of note, hTERT levels are increased with photo-aging, indicating that the skin responds to sun damage by increasing TERT expression. Similarly, patients with psoriasis show increasing levels of TERT with psoriatic severity, indicating a role for TERT in injury response as well as basal turnover [275].

Immune cells are another cell type that exhibits TERT expression into adulthood in humans. B and T cells, also known as lymphocytes, migrate throughout the body through the bloodstream and perform immunological functions. Lymphocytes rely on proliferation to perform their immunological functions and are a highly proliferative cell population. For this reason, it is not surprising that these cells exhibit TERT expression and telomerase activity [276, 277]. While telomerase activity is increased transiently in T cell cultures, hTERT expression is decreased with differentiation of T cells [278]. This paired with the characteristic decrease of telomerase activity of T cells with aging, supports the function of telomerase to allow for proliferative ability of mitotic cell types with an age-associated decrease [279]. In fact, induction of TERT expression in T cells improves the proliferative potential of these cells [280].

Other adult somatic tissues where telomerase activity is present include the endometrial tissue and hair follicles, which rely on proliferation for basal upkeep [281, 282]. While telomerase

activity is an indicator of the presence of TERT, the identification of TERT+ cells was unknown until recently. TERT+ cells have now been identified within the endometrium [283] and intestinal crypts of adult mice utilizing mTert-GFP and mTert lineage tracing transgenic mice [284, 285]. However, unlike the skin or immune system where TERT was expressed by rapidly proliferating cell types, TERT+ cells in the endometrium and intestines were identified to be qASCs [284, 285]. These cells make up a small population of the proliferating cells within these regions and are often non-proliferating. TERT+ cells were identified in proximity to more differentiated intermediate progenitors but did not express markers for these cell types [284, 285]. In the intestine TERT+ cells give rise to various mature cell types after a lineage trace and respond to injury by proliferating [285]. Similarly, in the liver lineage traced TERT+ cells replenish the liver's hepatocyte population, are self-renewing, and respond to injury by regenerating the lost cell types [286]. More recently, TERT+ cells were identified as ASCs in adult mouse long bones [287] and adipose tissue [288]. Telomerase activity and TERT expression have also been identified in the adult brain, which will be covered in section 1.5.3.

It is important to note that while many TERT studies *in vivo* rely on transgenic mice, there are differences between mice and human telomerase activity, TERT expression, telomere length, and even transcriptional control that may result in imperfect translation of TERT research to humans. To start, murine telomerase activity is more widespread throughout tissues than in humans [267]. While hTERT mRNA expression is absent in the skeletal muscle, kidney, and lung, each of these tissues in the 8-week-old mouse exhibits mTERT expression [267]. This species difference is hypothesized to result from a nonconserved GC-box, which is present in mice but not humans [267]. Transcription factors that induce TERT expression include c-Myc [289], Sp1 [290], human papillomavirus 16 E6 [291], estrogen [290], and progesterone [292]. Negative regulators of TERT include Mad1 [293], p53 [294], and more (reviewed in [258]). TERT expression and activity are regulated not just at the transcriptional level, but also via mRNA splicing, post-translational modifications, subcellular localization, and assembly. In fact, phosphorylation of

TERT causes translocation of hTERT to the nucleus from the cytoplasm, which may control telomerase function [295]. Hypomethylation and hypermethylation of the hTERT promoter have been observed in cancer cells with varying effects on hTERT expression [296]. Indeed, hypermethylation upstream of the hTERT core promoter, which increases TERT expression, is often observed in various forms of cancer [297]. Due to the various regulatory processes of TERT expression, there may exist additional differences between humans and mice TERT expression that are currently unknown.

1.4.3. TERT and Telomerase in the Adult Mouse Brain

Telomerase activity has been mapped throughout the adult mouse brain to specific brain regions and cell types. These studies have determined that while most telomerase activity observed in development [298, 299] is lost after birth, some areas of the adult mouse brain retain activity into adulthood [269]. The brain regions where telomerase activity is retained include the V-SVZ and OB, two regions of the brain where adult neurogenesis is present [269]. Interestingly, telomerase activity in the V-SVZ is found within NSCs and intermediate progenitor cells, indicating that telomerase may be functioning to allow for repeated proliferation [269, 300]. Evidence for the role of TERT in ASCs is supported by the loss of this protein after differentiation. TERT expression is lost following differentiation of NSCs into astrocytes following TGF-B treatment [301] or NSCs into neurons following treatment with NGF [302, 303].

The role of TERT in the adult brain has not yet been well characterized, yet it is understood that TERT KO severely impacts basal brain processes. In the V-SVZ, KO of TERT decreases neurogenesis through a reduction in Sox2+ stem cells, DCX+ neuroblasts, and Ki67+ proliferative cells when compared to WT animals [304]. These effects were reversed following TERT re-expression in KO animals, utilizing a TERT-ER mouse line [304]. TERT-/- mice also exhibit inhibited spatial learning and memory formation, which is improved with lentiviral TERT overexpression in the hippocampus [305]. The learning and memory formation differences were

correlated with decreased branching point, dendrite length, and circuit incorporation of hippocampal neurons within the dentate gyrus of adult mice, implicating a role for this protein in adult neural plasticity [305]. Taken together, TERT clearly plays a role in adult brain plasticity, but the exact role of TERT in these regions remains unknown.

The differences observed between levels of TERT and telomerase activity provide evidence TERT does not function purely to extend telomeres. In the hippocampus, telomerase activity drops to nearly undetectable levels following P10 into adulthood, while mTERT mRNA remains at consistently low levels throughout adulthood [299, 306]. Many studies have also identified a role for TERT as a neuroprotective protein. Fu et al. demonstrate that TERT expression is required for embryonic neuron survival [307], and can protect neurons exposed to DNA damage [308]. This was also demonstrated in cerebellar Purkinje neurons, where X-ray radiation induced TERT expression in the nucleus, likely to repair damaged DNA, while glutamate exposure resulted in TERT expression in the mitochondria [309]. The role of TERT as a mitochondrial effector in the brain has been identified by a number of studies. One such study discovered that reducing TERT levels in neurons led to increased oxidative stress and mitochondrial dysfunction when responding to beta amyloid peptides [310]. Furthermore, an increase in TERT expression following dietary restriction or rapamycin treatment lowered radical oxygen species in the brains of aged mice [311]. In support of the role of TERT as a neuroprotective protein, ectopic expression of TERT prevented neuronal death following ischemia [312].

1.4.4. Non-Canonical Roles of TERT

Non-canonical roles of TERT reveal the ability of this protein to respond to damage or stressors [313]. When utilized for the purpose of telomere extension, TERT is localized to the nucleus and does not migrate throughout the cell during cell cycle progression [268]. While the canonical role of TERT is telomere extension, this protein also regulates non-telomeric DNA

damage, chromatin modulation, and transcription [313]. Although we are aware of various non-canonical roles of TERT both *in vitro* and *in vivo*, the reasons that certain cell types utilize TERT for these processes are poorly understood. For example, outside of the nucleus TERT plays a role in protecting mitochondrial DNA (mtDNA) following oxidative stress [313]. Why then, do embryonic neurons express TERT in the cytoplasm if their primary role is believed to be telomere extension for high levels of proliferation during development [307]? We must understand the canonical and non-canonical functions of TERT to fully glean the roles that TERT plays in adult stem cells throughout the body and the adult brain.

The hTERT gene has various transcripts that result from alternative splicing [314]. The full-length transcript is the only one associated with telomerase activity [314, 315]. The other known transcripts have been detected only in human fetal tissue [314]. Here, hTERT gene expression did not correlate with telomerase activity, and it was determined that the hTERT splice variants lacked critical enzymatic domains [314]. The function of these variants is currently unknown.

Non-canonical TERT functions can be measured through the inhibition of TERT compared to the inhibition of TERT to bind telomeres, wherein the non-canonical roles of TERT are still intact. When the binding of TERT to telomeres is inhibited in CD34+ hematopoietic precursors from bone marrow there is no change in differentiation capacity. However, when TERT is inhibited in totality, these cells showed decreased capacity to differentiate into myeloid and granulocyte lineages [316].

Cell survival and protection appear to be major non-canonical roles of the protein TERT. The apoptosis prevention factor protein nuclear factor kappa B (NF-KB) can induce TERT expression, potentially so that TERT can act to increase cell survival [317]. TERT expression can also be induced via the cell survival and immortalization factor c-Myc [318]. In fact, downregulation of TERT in embryonic neurons *in vitro* induces apoptosis [307, 310] whereas upregulation prevents cell death [307]. These results were replicated in human breast cancer cells [319].

However, rescue of TERT expression with a mutant hTERT that lacked the ability to extend telomeres was still able to prevent apoptosis [319]. Further evidence for the non-canonical role of TERT as an anti-apoptotic agent independent of its telomeric function has been accumulated in other cancerous cells *ex vivo* and *in vivo* [302, 320-323]. In many studies, the method of preventing apoptosis by TERT has been linked to improved mitochondrial function [311, 324, 325]. Indeed, TERT protects mtDNA [326, 327] and prevents mitochondrial dysfunction resulting from mtDNA damage (reviewed in [328]).

1.5. Adult Hypothalamic Neurogenesis in the Context of Metabolic Health

1.5.1 Interventions that Affect Hypothalamic Plasticity – Caloric Restriction and High Fat Diet

While the role of stem and progenitor cell in the hypothalamus remains unclear, hypothalamic plasticity in the form of gross proliferation and newborn neuron creation has been more comprehensively studied. Although these studies do not locate the stem cells that led to the production of newborn neurons and glia, they provide context to the role of various treatments and interventions that affect adult hypothalamic plasticity. In addition, these studies give insight into the role of hypothalamic neurogenesis and full body energy balance and metabolism. CNTF is a neurocytokine that causes leptin-independent weight loss through reduced food intake [329] for weeks or months after treatment has ended [330]. A landmark study on the effect of CNTF on hypothalamic neurogenesis revealed that a HFD followed by CNTF treatment increased BrdU+ cell numbers and revealed newborn neurons in the adult hypothalamus when compared to vehicle-treated animals [58]. Furthermore, the adult-born neurons expressed the orexigenic and anorexigenic markers NPY and POMC [58]. A subset of these neurons was responsive to leptin as well. Furthermore, the weight loss that accompanied proliferation in the hypothalamus was prevented with mitotic inhibition through the treatment with Ara-C [58].

Metabolic studies have also identified time-dependent, sex-dependent, and area-dependent neurogenic effects of high fat diet in the adult hypothalamus (Figure 1.6) [55, 133].

Lee et al., administered BrdU during the first 3 days of a 32-day HFD treatment and discovered decreased numbers of adult-born BrdU+ mature neurons in the ARC when compared to control diet animals [55]. A low protein diet had an even more intense effect [55]. The study of newborn neurons in the ME of female mice identified heightened proliferation with both HFD and low protein diet when compared to control diet, but no difference in male mice [55]. Additional studies on the role of caloric restriction (CR) during or following HFD revealed changes in proliferation of BrdU+ adult-born cells, wherein HFD followed by CR increased total proliferation in one study [133], but decreased ME proliferation in females (with no effect in males) in another [55]. However, the animals used in these studies as well as the length of the diet and CR were not identical, making it difficult if not impossible to draw direct comparisons. Finally, an analysis of gene expression following CR revealed Igf1r upregulation by 2-5-fold, which has previously been identified to induced tanycyte proliferation, indicating a possible role for tanycyte-driven CR-derived neurogenesis in the adult hypothalamus [331]. It is also important to note that HFD induces inflammatory responses [331], whereas CR reduces inflammation. The increased proliferation resulting from HFD treatment could be a combination of neurogenesis, gliogenesis, cell repair, or microglial activation and proliferation [331].

1.5.2 Role of the Immune System and Glial Cells in Adult Hypothalamic Plasticity

While neurons within the hypothalamus relay information across hypothalamic nuclei and throughout the body, the glial cell populations within the hypothalamus also retain important metabolic function yet are often overlooked. NG2+ GPCs in the mediobasal hypothalamus express the stem cell marker Sox2, proliferate, and give rise to oligodendrocytes [49]. Interestingly, lineage tracing studies also reveal newborn NeuN+ neurons in the adult mouse brain derived from NG2+ cells, implicating a neurogenic and gliogenic role for these cells [130]. NG2+ glia are also critical for the proper function of neurons within the ARC, with leptin responsive neurons relying on direct contact with NG2+ cells to respond to this circulating hormone [131].

Here, ablation of NG2+ glia in the ME via Ara-C treatment prevented neurons in the ARC from responding to leptin, resulting in significant body weight gain through increased food intake. Interestingly, this group had previously discovered that NG2 glia will regenerate completely following mitotic inhibition [130]. Indeed, the role of these glial cells appears to be critical for brain function in the context of leptin sensitivity.

Tanycytes, radial glial cells of the ventral third ventricle, are known to respond to dietary changes via the creation of newborn neurons within the hypothalamus [51, 52, 332]. After a high fat diet, young adult mice showed reductions in neurogenesis in the ARC, and female mice also had increased neurogenesis in the ME [55]. These newborn neurons within the ME were traced from Nestin+ cells and were determined to likely be progeny of tanycytes in proximity to the ME, as tanycytes are one of the few Nestin+ cell types in this niche. In addition, irradiation of the ME attenuated weight gain in female mice fed an HFD, resulting in significantly lower weight gain than their HFD-sham counterparts, providing evidence that adult-born neurons in the median eminence respond to HFD with increased body weight [55]. Interestingly, this effect was not seen in male mice, indicating that adult hypothalamic neurogenesis may be a sexually dimorphic method of body weight regulation and energy storage. See Appendix A for information on signaling pathways related to BMPs and their effects on adult plasticity and hypothalamic neurogenesis

Microglia are the resident immune cells of the brain and spinal cord (Section 1.1.3.3). These specialized cells can influence adult neurogenesis during both basal and HFD-induced inflammatory conditions wherein microglia are activated in the hypothalamus [333, 334]. Both food intake and energy expenditure are regulated at the axis of microglial activation and hypothalamic plasticity. As identified by Jin et al., microglial activation alters POMC neuron activity through changes to their inputs [335]. These changes to microglia had whole body effects including anorexia-derived weight loss [335]. In addition, hypothalamic inflammation if not reduced can eventually lead to neuronal apoptosis [336]. Interestingly, hypothalamic inflammation first occurs as a result of HFD in the mediobasal hypothalamus, which contains the ME, a key

proliferative niche of the hypothalamus [337]. In response, microglia will activate within the ARC and produce inflammatory cytokines [338]. To further support the importance of carefully comparing HFD-induced neurogenesis studies, it has been observed that 1wk HFD induces inflammation within the hypothalamus, which is then reduced after 2 weeks, and then again increased after 4 weeks [337]. Finally, although microglial activation in the adult brain is not specific to the hypothalamus, the hypothalamus exhibits microglial activation before other brain regions. For these reasons, it is crucial that future studies and the analysis of previous studies are sure to compare the hypothalamic microglial response and plastic effects of involved interventions only across similar treatments.

Microgliogenesis occurs throughout the adult brain. However, although hypothalamic inflammation is well studied, the role of microglial proliferation in this context has only just been realized. In addition to the regulatory roles played by microglia during HFD, these cells will also proliferate within the hypothalamus, specifically in the ARC after a 3-week HFD treatment [339]. Blocking mitosis of microglia (as well as other proliferative cells) via Ara-C resulted in reduced feeding, weight gain, and adiposity. The mitotic inhibition of microglia was paired with decreased proinflammatory cytokine expression indicating a reduction in inflammation [339]. These results must call into question previous hypothalamic neurogenic studies that utilize the number of BrdU+ or EdU+ cells to determine ‘neurogenesis’, as both NG2+ cells and microglia are a proliferative cell type within this niche.

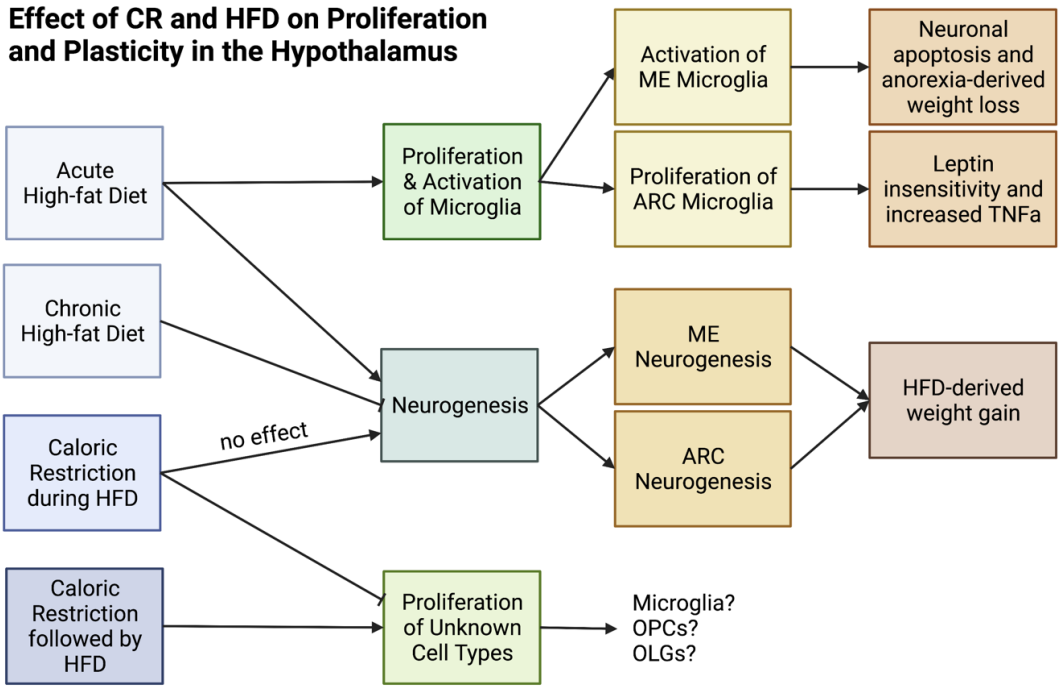

Figure 1.6. Effect of CR and HFD on Proliferation and Plasticity in the Hypothalamus.

Chapter 1 Acronym List

aANSCs – Activated adult neural stem cells

AgRP – Agouti-related peptide

AHN – Adult hippocampal neurogenesis

Ara-C – Cytosine arabinoside

ARC – Arcuate nucleus

ASC – Adult stem cell

ASCL1 – Achaete-scute homolog 1

aSVZ – anterior subventricular zone

BBB – Blood-brain barrier

BCSFB – Blood-CSF-barrier

BDNF – Brain-derived neurotrophic factor

BLBP – Brain lipid binding protein

BMP – Bone morphogenetic protein

BrdU – Bromodeoxyuridine

CNTF – Ciliary neurotrophic factor

CNS – Central nervous system

CP – Choroid plexus

CPEC – Choroid plexus epithelial cell

CSF – Cerebrospinal fluid

DCX – Doublecortin

DG – Dentate gyrus

EdU – 5-ethynyl-2'-deoxyuridine

EGFR – Epidermal growth factor receptor

ESC – Embryonic stem cell

GABA – Gamma aminobutyric acid

GBCs – Globose basal cells

GCL – Granule cell layer

GFAP – glial fibrillary acidic protein

GLAST – glutamate aspartate transporter

GPC – Glial precursor cell

HBCs – Horizontal basal cells

HFD – High fat diet

hTERT – human TERT

HSC – Hematopoietic stem cell

IGF-1 – Insulin-like growth factor 1

LVCPsec – Lateral ventricle choroid plexus secretome

MASH1 – Mammalian ASCL1 homolog

MBP – Myelin basic protein

ME – Median eminence

mtDNA – mitochondrial DNA

mTERT – mouse TERT

Myrf – Myelin regulatory factor

NeuN – Neuronal nuclear protein

NF-KB – nuclear factor kappa B

NG2 – Chondroitin sulfate proteoglycan NG2

NGF – Nerve growth factor

NMDA – N-methyl-D-aspartate

NPY – Neuropeptide Y

NVU – Neurovascular unit

OB – Olfactory bulb

OE – Olfactory epithelium

OPC – Oligodendrocyte progenitor cell

OSN – Olfactory sensory neuron

PDGFRa/B – Platelet-derived growth factor alpha/beta

POMC – Pro-opiomelanocortin

PSA-NCAM – polysialylated-neural cell adhesion molecule

pSTAT3 – phosphorylated signal transducer and activator of transcription 3

pSVZ – posterior subventricular zone

qASC – Quiescent adult stem cell

qANSC – Quiescent adult neural stem cell

Rax – Retina and anterior neural fold homeobox transcription factor

RMS – Rostral migratory stream

SGZ – Subgranular zone

Shh – Sonic hedgehog

TAC – Transit amplifying cell

TERC – Telomerase RNA component

TERT – Telomerase reverse transcriptase

Tfam – Mitochondrial transcription factor A

V-SVZ – Ventricular-subventricular zone

V3V – Ventral third ventricle

CHAPTER 2:

TELOMERASE REVERSE TRANSCRIPTASE (TERT)-EXPRESSING CELLS MARK A NOVEL STEM CELL POPULATION IN THE ADULT MOUSE BRAIN

Abstract

Telomerase reverse transcriptase (TERT) is expressed by quiescent adult stem cells (qASC) in numerous adult murine and human tissues but has never been explored in the adult brain. Here, we demonstrate that TERT+ cells in the adult mouse brain represent a novel population of multipotent qASCs. TERT+ cells were localized to numerous classical neuro/gliogenic niches including the ventricular-subventricular zone, hypothalamus and olfactory bulb, as well as newly discovered regions of adult tissue plasticity such as the meninges and choroid plexus (ChP). TERT+ cells expressed neural stem cell markers such as Nestin and Sox2, but not markers of activated stem/progenitor cells, nor markers of mature neuronal or glial cells. TERT+ qASCs also rarely expressed the proliferation marker Ki67, further confirming a quiescent phenotype. When cultured, TERT+ cells behaved like brain stem cells by forming neurospheres. Lineage tracing of TERT+ cells in adult transgenic mice revealed large-scale expansion of TERT+ progeny and differentiation in multiple brain regions to diverse cell types. Lineage-traced cells expressed markers of mature neurons, oligodendrocytes, astrocytes, ependymal cells, and choroid epithelial cells, thus demonstrating the striking multipotency of this stem cell population in basal tissue turnover. Together, these data demonstrate that TERT+ cells represent a new population of multipotent stem cells that contribute to basal brain plasticity and regeneration.

Introduction

The adult mammalian brain retains cellular plasticity and the ability to regenerate certain cell types, but adult neurogenesis is thought to occur only in restricted patterns and discrete niches of the adult brain [340]. Adult neurogenesis is well-studied in the ventricular-subventricular zone (V-SVZ) of the lateral ventricles and subgranular zone (SGZ) of the dentate gyrus (DG) in the hippocampus. However, numerous other adult brain niches have also demonstrated adult plasticity and capacity for neurogenesis. In the adult mammalian brain, the V-SVZ contains quiescent adult neural stem cells (qANSCs) known as Type B1 cells (reviewed in [134]). These cells can become activated and asymmetrically divide into self-renewing B1 cells and transit amplifying cells (TACS), also known as Type C cells. TACS then further divide to produce neuroblasts (Type A cells), which migrate rostrally within the rostral migratory stream (RMS) to the olfactory bulb (OB), where they differentiate into mature neurons that integrate into the neural circuitry [19]. In humans, V-SVZ-derived progenitors appear to migrate to the striatum instead of the OB [341]. Within the SGZ, quiescent radial glial-like stem cells (Type 1 cells) produce intermediate progenitor cells (Type 2 cells) via symmetric or asymmetric cell division. These cells produce adult-born neuronal cells that express doublecortin (DCX). DCX+ cells then migrate into the granule cell layer where they differentiate into mature DG neurons (reviewed in [342]). By contrast, in regions such as the hypothalamus and cortex, the cell types and mechanisms involved in adult neuro/gliogenesis are less well understood [343].

In the absence of a specific and unique marker for quiescent adult stem cells (qASCs) in the brain, explorations have relied on a combination of cellular markers. Sex determining region Y-box 2 (Sox2), glutamate aspartate transporter 1 (GLAST), and glial fibrillary acidic protein (GFAP) are often used to identify ANSCs in V-SVZ and SGZ. Further complicating these analyses, each of these markers is also expressed by other cell types throughout the brain, reducing their specificity. For example, GFAP and GLAST are expressed by mature glial cells in

addition to stem cells. Here, we propose that telomerase reverse transcriptase (TERT), the catalytic subunit of the enzyme telomerase, is a more specific and novel marker for a population of multipotent qASCs in numerous niches of the adult mouse brain.

TERT has previously been identified as a marker for slowly cycling or quiescent intestinal stem cells, as well as adult tissue stem/progenitor cells found in the testes, bone marrow, heart, thymus, spleen, liver, kidney, endometrium, heart, bone and adipose [268, 283-285, 287, 344-348]. However, until now TERT had never been investigated as a marker of ASCs in the brain. In both mice and humans, telomerase activity is high in the brain during development, but is dramatically reduced in the postnatal brain [255, 259]. In mice, telomerase activity declines in the brain before adulthood, except in specific neurogenic regions such as the V-SVZ and OB [268, 269, 349]. Numerous studies have pointed to TERT as a putative stem cell marker in the adult brain. For example, telomerase activity has been localized to cellular fractions containing Type A, B, and C neural progenitor cells (NPCs) from the adult mouse V-SVZ [269]. Differentiation of embryonic stem cells into astrocytes or neurons induces loss of telomerase activity [301, 303]. As mice age, they exhibit decreased TERT expression in the V-SVZ, which is accompanied by reduced proliferation and neurogenesis [350], consistent with a decline in the stem cell pool. Evidence for the importance of telomerase activity in neurogenic niches is supported by decreased levels of V-SVZ neurogenesis in mice with telomerase RNA component (TERC) deletion. In these mice, the stem cells in the V-SVZ are affected, while the proliferative ability of more committed/differentiated cells, such neuroblasts, remained unaffected [350]. Finally, tissue degeneration and decreased V-SVZ neurogenesis was reversed following TERT reactivation in TERT-ERT2 mice [304]. Together, these findings suggested that TERT plays an essential role in adult stem cell maintenance and in adult neurogenesis.

We now demonstrate for the first time that TERT+ cells in the adult mouse brain represent a rare, quiescent stem cell population, and that these cells possess the multipotent capability to

proliferate upon activation and to regenerate multiple brain regions by differentiating into numerous mature cell types

Materials and Methods

Mice

All procedures were approved by the University of Maine and Ohio State University IACUC. Mice were maintained on a 12 hr light/dark cycle, and food and water was provided *ad libitum*. Tg(Tert-GFP)22Brlt (*mTERT*-GFP) mice were described previously [284]. For lineage tracing studies, *mTert*-rtTA:: otet-Cre:: R26R$^{flox(mTmG)}$ mice were generated by crossing *mTERT*-rtTA mice [287] to otet-Cre:: R26R$^{flox(mTmG)}$ mice, which were generated by our lab by crossing B6.Cg-Tg(tet0-cre)1Jaw/J mice (The Jackson Lab) to B6.129(Cg)-Gt(ROSA)26Sor$^{tm4(ACTB-tdTomato,-EGFP)Luo}$ mice (The Jackson Lab). Recombination was induced via 2 mg/ml doxycycline (Sigma Aldrich) in 50 mg/ml sucrose water over the course of 2-21 days as indicated. To chase, doxycycline water was removed, and normal water was provided. Both male and female animals were utilized for most experiments (see Results section for specifics).

Immunostaining

Mice were anesthetized via intramuscular injection of 320 mg/kg body weight Ketamine and 24 mg/kg body weight Xylazine in 0.9% saline and then sacrificed via transcardial perfusion with 1X PBS followed by Histochoice Fixative, after loss of motor and ocular reflexes. Brains were post-fixed overnight at 4°C, then placed in 15% sucrose at 4°C for 2d, followed by 30% sucrose at 4°C for 2d. Brains were then divided into coronal or sagittal sections using adult mouse brain matrices and then frozen in optimal cutting temperature compound and stored at -20°C until slicing. Brains were sliced on a CM1950 or CM3050 S cryostat (Leica) at -20°C. Two slices of 7-10μm size were adhered to each slide. Slides were stored at -20°C until used for immunostaining, at which point

they were warmed up to room temperature and post-fixed with ice-cold acetone for 15min. Slides were washed for 5min in 1X IHC Select TBS Rinse Buffer shaking at 60rpm at room temperature (RT) between each step. Permeabilization for staining of nuclear antigens was performed with 0.3% Triton X-100 for 10min at RT. Permeabilization for staining of cytoplasmic antigens was performed with 0.3% Tween-20 for 10min at RT. Antigen retrieval was performed by microwaving slides in 1X DAKO Antigen Retrieval Solution on low for 10 minutes twice. Slides were then incubated in 0.3% Typogen Black in 70% EtOH for 20min at RT, blocked for 20 min at 37°C with Millipore Blocking Reagent, and incubated with primary antibody diluted in antibody diluent overnight at 4°C. Antibody concentrations are listed in the Key Resource Table. The next day, sections were incubated in Alexa Fluor secondary antibodies for 10m at RT, then counter-stained with 100ng/mL DAPI for 5min. Epifluorescence images were captures on Nikon E400 microscope with a Hamamatsu Flash 2.0. Confocal images were captures on either SP8 (Leica), Stellaris 5 (Leica), or LSM 900 (Zeiss) for co-expression analysis.

FACS

To obtain single cell suspensions of adult mouse brains, mice were sacrificed via CO_2 followed by cervical dislocation. Brains were isolated and washed with artificial cerebrospinal fluid (ACSF) (Ecocyte). Brains were then diced with a razor blade in a petri dish containing ice-cold ACSF with 1mg/mL pronase (Millipore-Sigma) until brain pieces were uniform sizes. Brains were then transferred to loosely capped 50mL falcon tubes placed in shaking water incubator (37°C and 90rpm) for 60-75min until cloudy. Every 5 minutes tubes were vortexed and then returned to shaking incubator. Samples were then centrifuged at 1600rpm for 4 minutes and supernatant decanted. Samples were then treated with ACSF with 5% fetal bovine serum (FBS) for 15 minutes while shaking at 90 rpm and 37°C. Trituration of each sample was performed with pasteur pipettes of 600µm, 300µm, and 150µm openings. Samples were centrifuged at 300 x g for 10min and

supernatant decanted. Debris removal solution (Miltenyi) was utilized to remove debris and myelin from the samples. In experiments where CD45 antibody was utilized for FACS, cells were then treated with 1X PBS with 0.5% BSA and 2% FBS for 20 min at 4°C, spun at 1800rpm for 5min, resuspended in 1X PBS with 5% FBS and 5mM EDTA with antibodies for 20min at 4°C, and then washed twice with 1X PBS with 0.5% BSA and 2% FBS. Cells were resuspended in ACSF with 10% FBS and stored on ice until sorting. Cells were sorted for endogenous membrane GFP fluorescent signal or Alexa Fluor 700 signal from CD45 antibody via BD FACSAria II (Jackson Laboratory, Bar Harbor, ME) or BD FACSAria III (OSUMC, Columbus, OH). Cells were sorted into Trizol (Ambion) and frozen at -80°C for qRT-PCR experiments or Neurosphere Basal Medium supplemented with Proliferation Supplement (STEMCELL Technologies), heparin, FGF2, and EGF (STEMCELL Technologies) for *in vitro* neurosphere culturing experiments according to methods from [351].

Neurosphere Formation Assay

Cells were sorted into 96-well low-attachment plates containing NeuroCult Basal Media (Mouse and Rat) (STEMCELL Technologies) with Proliferation Supplement (STEMCELL Technologies), 20ng/mL hrEGF (STEMCELL Technologies), 10ng/mL hrbFGF (STEMCELL Technologies), and 0.002% Heparin (w/v) (STEMCELL Technologies). Both GFP+ and GFP- cells were grown at 37°C with 5% CO_2 and 90% relative humidity for 14 days. Media was changed every 5-7 days. Cells were imaged every three days for a total of 22 days.

EdU Labeling

Neurospheres were removed from 96-well plates and pipetted into 8-well Seahorse XF HS miniplates (Agilent) coated with 15 µg/mL poly-L-ornithine and 10µg/mL laminin. Plates were spun

at 200 x g for 2 minutes until cells were adhered. Cells were incubated in 5μM EdU (ThermoFisher Scientific) in NeuroCult proliferation media with EGF and FGF for 24hr. Media was removed and cells were fixed with 4% PFA (pH 7.4) for 15min. Cells were washed twice with 3% BSA in PBS, then permeabilized with 0.5% Triton X-100 in PBS for 20min at RT. Cells were washed once with 3% BSA in PBS. Cells were incubated in Click-iT EdU reaction buffer for 30 minutes at RT (ThermoFisher Scientific). Cells were then washed once with 3% BSA in PBS followed by 1x PBS and incubated in 5μg Hoeschst 33342 for 30min at RT. Finally, cells were washed with 1X PBS, then imaged. After imaging, representative images were used for cell counting. Here, images from each of the 405, GFP, and 647 (EdU) channels were opened in FIJI (v1.543k). For each: images were converted to 8-bit, the threshold was adjusted, particles were analyzed with the parameters of size (inch^2): 0.001 – infinity, circularity 0.00-1.00, and the cell number was identified.

RNAscope

RNAscope was performed using the RNAscope Multiplex Fluorescent v2 Assay (ACD Bio). Slides with sagittal adult mouse brain sections from mice perfused with Amresco Histochoice Tissue Fixative and put through a sucrose gradient (15% to 30%) were frozen in OCT and sliced at 7um on a Leica Cryostat. Slides were washed in 1x PBS for 5min, then post-fixed in 4% PFA (pH 7.4) in 1X PBS at RT for 15min. Slides were washed in 1X PBS for 1min, and then dehydrates with 5min incubations of 50% EtOH, 70% EtOH, and 100% EtOH at RT. Tissues were dried on the benchtop for 5min. 5 drops of Hydrogen Peroxide (ACD Bio) was applied to each tissue and incubated for 10min at RT, then slides were washed with DI water for 5min, twice. Slides were boiled in antigen retrieval solution (ACD) at 100C for 15min, then rinsed with DI water for 5 minutes, twice. Slides were dehydrated in 100% EtOH for 5min at RT, then dried on the benchtop for 5min at RT. Pap-pen barriers were drawn around each tissue, and then slides were placed into a Hybridization Oven set at 40C with 5 drops of Protease III solution each, for 30min. Slides

were washed in DI water for 5min, twice. Probes were hybridized by adding 4 drops of the TERT probe, positive control probes, or negative control probes, and then incubating at 40C for 2hr. Slides were washed in 1X Wash Buffer for 2 min, then slides were washed in the same manner between each of the following steps. Tissues were incubated at 40C with each of FL v2 AMP1, AMP2, and AMP3 for 30min, 30 min, and 15min, respectively. For each channel, tissues were then incubated in FL v2 HRP (for that channel) for 15min at 40C, then FL v2 HRP blocker for 15min at 40C. Finally, slides were washed in 1x wash buffer, 4 drops of DAPI solution was added to each tissue for 30sec, and then cover slips with 1 drop of mounting medium were applied.

Intracerebroventricular administration of Ara-C

When mice reached 13 weeks of age, 2mg/ml doxycycline were administered in the drinking water for a 4-week pulse to mark mTERT expressing cells with GFP. 6 days prior to doxycycline removal, they received cytosine-β-D-arabinoside (2%; Ara-C) in 0.9% saline, or 0.9% saline alone into the right lateral ventricle via a mini-osmotic pump (ALZET) with cannulas implanted. Brain cannulation occurred at the following coordinates: anterior/posterior (A/P), -0.5mm; medial/lateral (M/L), -1.1mm; dorsal/ventral (D/V), -2.5mm (relative to Bregma and the surface of the brain; M/L coordinates are directed laterally to the right). After 6 days of Ara-C infusion, the mice were perfused and the brains were collected. **i.c.v. administration was performed by Jake Willows and Noelle Leon-Palmer.*

Statistical Analysis

All plots represent mean ± SEM. Statistical calculations were carried out in Excel or GraphPad Prism 9.0, utilizing the ANOVA or Student's T-test as indications of significance. For all figures, *$p<0.05$, **$p<0.01$.

Results

TERT+ cells in the brain of adult mTert-GFP direct reporter mice are localized to the V-SVZ and novel plastic regions

In the adult brain, prior work has demonstrated that adult stem/progenitor cells reside mainly within three anatomical regions: the V-SVZ, SGZ, and hypothalamus. To characterize the location and quantity of mTERT-GFP+ cells in the adult mouse brain, we examined a neurogenic-enriched area of the adult brain from *mTert*-GFP direct reporter mice [284]. This area contained the V-SVZ, SGZ, and hypothalamus (Figure 2.1A). Immunofluorescent analysis of all TERT-GFP+ cells revealed localization to some classical neurogenic niches as well as newly identified plastic niches (Figure 2.1B). TERT+ cells were detected at low numbers, as expected for qASCs. Most TERT+ cells were identified in the V-SVZ, LV ChP, D3V, D3V ChP, hypothalamus, and meninges, although other brain regions contained TERT+ cells as well (Figure 2.1B). No TERT+ cells were identified in the hippocampus (Figure 2.7). Interestingly, there were significantly more TERT+ cells per brain section, per mouse in the meninges when compared to the V-SVZ (Figure 2.1B, 2.2A). An analysis of TERT+ cells across 9 Bregma coordinates throughout the neurogenic enriched brain area (Figure 2.1A) identified that TERT+ cells were found at the same number throughout the neurogenic enriched brain area (Figure 2.1C). No difference was observed in the number of TERT+ cells per brain region across Bregma (Figure 2.1D). Fluorescence activated cell sorting (FACS) of TERT-GFP+ cells from full *mTert*-GFP brains revealed that only 0.1-0.3% of brain cells were TERT+ (Figure 2.2A). Taken together, TERT+ cells are found at low numbers throughout plastic niches of the adult mouse brain.

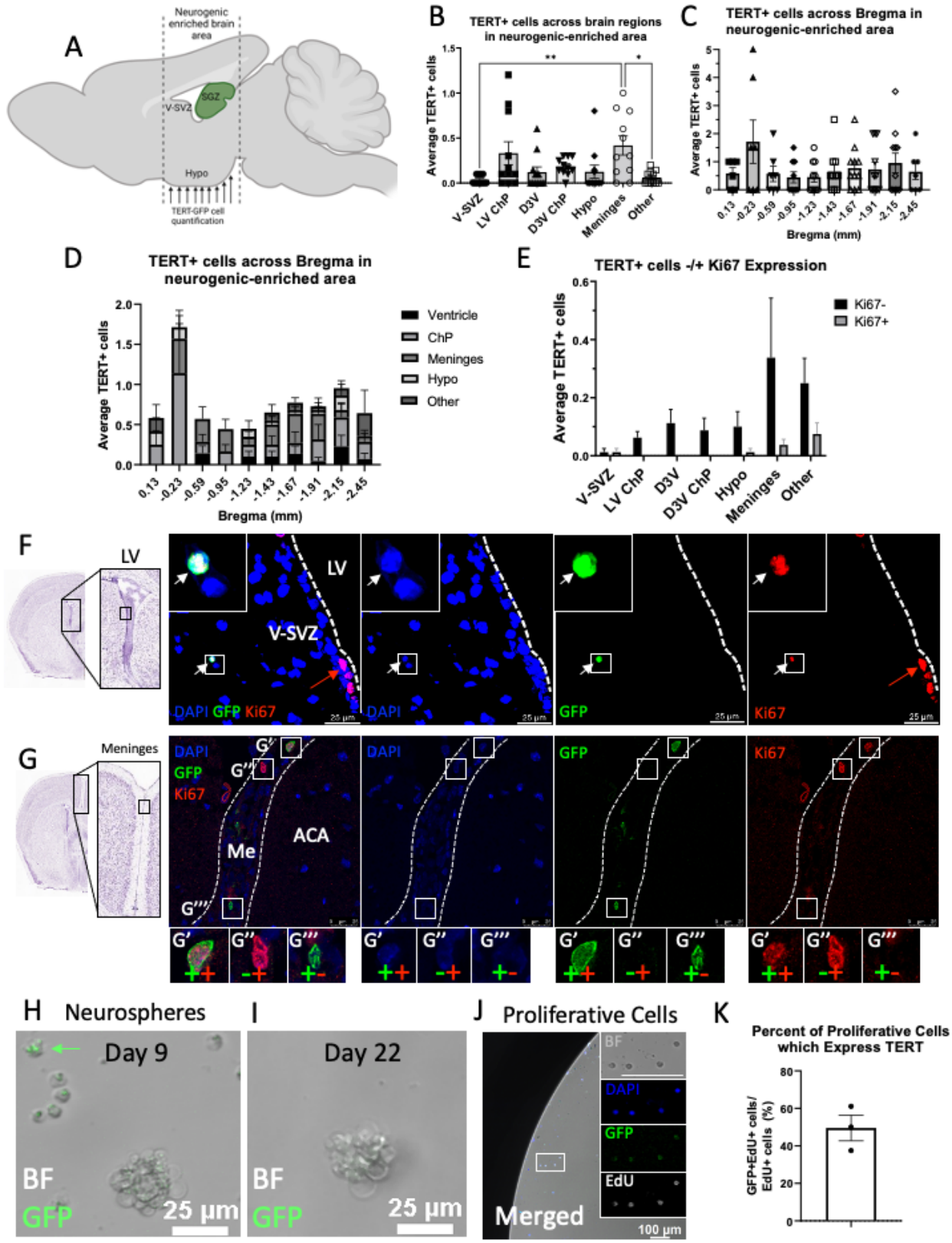
A
Neurogenic enriched brain area
SGZ
V-SVZ
Hypo
TERT-GFP cell quantification
B
TERT+ cells across brain regions in neurogenic-enriched area
Average TERT+ cells
V-SVZ
LV ChP
D3V
D3V ChP
Hypo
Meninges
Other
C
TERT+ cells across Bregma in neurogenic-enriched area
Average TERT+ cells
Bregma (mm)
D
TERT+ cells across Bregma in neurogenic-enriched area
Average TERT+ cells
Ventricle
ChP
Meninges
Hypo
Other
Bregma (mm)
E
TERT+ cells -/+ Ki67 Expression
Average TERT+ cells
Ki67-
Ki67+
F
LV
V-SVZ
DAPI GFP Ki67
DAPI
GFP
Ki67
G
Meninges
DAPI
GFP
Ki67
Me
ACA
H Neurospheres
Day 9
BF
GFP
25 µm
I
Day 22
BF
GFP
25 µm
J Proliferative Cells
BF
DAPI
GFP
EdU
Merged
100 µm
K
Percent of Proliferative Cells which Express TERT
GFP+EdU+ cells/ EdU+ cells (%)

Figure 2.1. TERT+ cells in the adult *mTert*-GFP mouse brain are quiescent stem cells localized to both well-studied and novel regions of adult brain plasticity.

(A) Mouse brain illustration of the neurogenic-enriched brain area used for immunostaining with arrows indicating coronal planes used for TERT-GFP+ cell analysis.

(B) Quantification of TERT + cells per region identified via immunostaining in adult *mTert*-GFP mouse brains. Cell quantification is graphed as the number of TERT+ cells per niche, per mouse. Dots represent individual animals. 8-20 coronal brain sections per mouse were analyzed from N=5 males and N=6 females at 12-weeks of age.

(C) Quantification of TERT+ cell numbers across Bregma coordinates through the neurogenic enriched brain area. Cell quantification is graphed as the sum of TERT+ cells across n=2 coronal brain sections per depth, per mouse. Dots represent individual animals. N=6-11 mice per depth.

(D) Quantification of TERT+ cells per region across Bregma coordinates through the neurogenic enriched brain area. Cell quantification is graphed as the sum of GFP+ cells per brain region across n=2 brain sections for each of N=6-11 mice.

(E) Quantification of co-staining for TERT-GFP and Ki67 in *mTert*-GFP mouse brains. Cell quantification is graphed as the average number of cells per brain region, per mouse, across n=16 brain sections for each of N=5 males and 5 females.

(F) Co-immunostaining of TERT+ cell in the V-SVZ with the proliferation marker Ki67. White arrow indicates TERT+Ki67+ cell. Red arrow indicates TERT-Ki67+ cells (N=5 males, 5 females, n=16 brain sections per animal).

(G) Representative image of co-immunostaining with Ki67 in the meninges of *mTert*-GFP mice. Green or red “+” or “-” indicates that the cells in indicated area were GFP+/GFP-, or Ki67+/Ki67-, respectively. Dots indicate individual animals. (N=4 males, 4 females, n=16 brain sections per animal).

(H-I) Representative neurosphere formation of FACS-sorted GFP+ cells grown with EGF and FGF with fluorescence analyzed on Day 9 (H) and Day 22 (I) (N=6).

J) EdU incorporation in TERT+ cells cultured with EdU for 24 hours at Day 9 (N=3 of 4 samples).

K) Quantification of GFP+EdU+ cells across the total number of EdU+ cells (N=3).

Scale bars are 25μm. Insets show 4x digital magnification of indicated area. Bar graphs show mean cells per brain section, per animals ± SEM with individual data points per animal. Grouped bar graphs show GFP+ cells per mouse, per brain section, at each depth ± SEM. Significance was determined via one-way ANOVA (*P < 0.05, **P < 0.01). V-SVZ: ventricular-subventricular zone, LV: lateral ventricle, ChP: choroid plexus, D3V: dorsal 3rd ventricle, Hypo: hypothalamus, Me: meninges, ACA: anterior cingulate area, BF: brightfield, EdU: 5-ethynyl-2´-deoxyuridine.

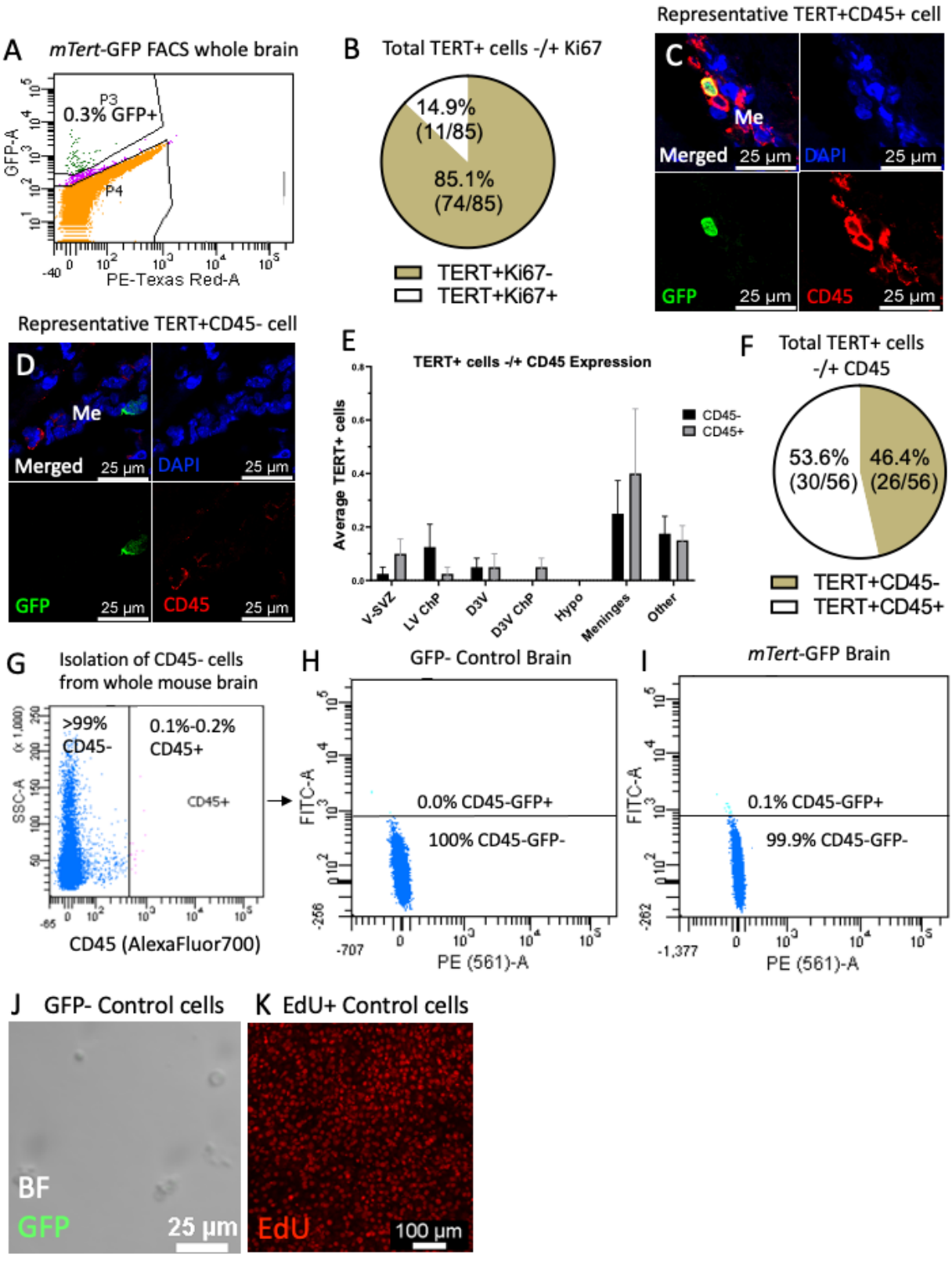
A
mTert-GFP FACS whole brain
P3
0.3% GFP+
P4
GFP-A
PE-Texas Red-A
B
Total TERT+ cells -/+ Ki67
14.9%
(11/85)
85.1%
(74/85)
TERT+Ki67-
TERT+Ki67+
Representative TERT+CD45+ cell
C
Me
Merged
25 µm
DAPI
25 µm
GFP
25 µm
CD45
25 µm
Representative TERT+CD45- cell
D
Me
Merged
25 µm
DAPI
25 µm
GFP
25 µm
CD45
25 µm
E
TERT+ cells -/+ CD45 Expression
Average TERT+ cells
CD45-
CD45+
V-SVZ
LV ChP
D3V
D3V ChP
Hypo
Meninges
Other
F
Total TERT+ cells
-/+ CD45
53.6%
(30/56)
46.4%
(26/56)
TERT+CD45-
TERT+CD45+
G
Isolation of CD45- cells
from whole mouse brain
>99%
CD45-
0.1%-0.2%
CD45+
CD45+
SSC-A
CD45 (AlexaFluor700)
H
GFP- Control Brain
0.0% CD45-GFP+
100% CD45-GFP-
FITC-A
PE (561)-A
I
mTert-GFP Brain
0.1% CD45-GFP+
99.9% CD45-GFP-
FITC-A
PE (561)-A
J
GFP- Control cells
BF
GFP
25 µm
K
EdU+ Control cells
EdU
100 µm

Figure 2.2: TERT+ cells in the adult mouse brain are rare, mostly quiescent, and include a subpopulation of CD45+ immune cells.

(A) Representative fluorescent activated cells sorting (FACS) plot of GFP+ cells from sorted adult *mTert*-GFP full mouse brains (N=16 males, 9 females). P3: GFP+, P4: GFP-. PE-Texas Red-A used to gate for autofluorescence.

(B) Quantification of total proliferative TERT+ cells across all tissues in the neurogenic enriched brain area stained for Ki67 from 10 *mTert-GFP* animals. (N=5 males, 5 females, n=8 sections per brain).

(C-D) Representative images of TERT+CD45+ (C) and TERT+CD45- (D) cells identified via immunofluorescence in the adult *mTert*-GFP mouse brain (identified in N=5 of 5 males, 5 of 5 females, n=8 brain sections per mouse).

(E) Quantification of co-staining for TERT-GFP and CD45 in *mTert*-GFP mouse brains. Cell quantification is graphed as the average number of cells per brain region across n=8 brain sections for each of N=5 males and 5 females.

(F) Quantification of total proliferative TERT+ cells across all tissues in the neurogenic enriched brain area stained for Ki67 from 10 *mTert-GFP* animals. (N=5 males, 5 females, n=8 sections per brain).

(G-I) Representative fluorescent activated cell sorting (FACS) plots showing identification of CD45- cells (G) followed by isolation of TERT-GFP+ cells from GFP- control brains (H) or full mTert-GFP full mouse brains (I) (N=6 males).

(J) FACS sorted GFP- cells from *mTert*-GFP animals do not express GFP (N=2 males).

(K) Proliferative 3T3-F4421A cells as a positive control for the EdU assay.

TERT+ cells in the adult mTert-GFP mouse brain are largely quiescent

Quiescent populations of stem cells are expected to slowly divide in order to prevent exhaustion of the stem cell pool. In adult murine brains where extended periods of stem cell proliferation have occurred, such as with aging, the stem cell pool becomes exhausted, resulting in reduced proliferation and neurogenesis [352]. Previously, it has been reported that TERT+ adult tissue stem cells in the intestines are slowly cycling and rarely express the proliferation marker Ki67 [284, 285]. Expression of TERT may act to restore telomere length after cell division and

prevent senescence into adulthood, which is a characteristic of stem cells. To assess the proliferative capacity of TERT+ cells in the adult mouse brain, we co-immunostained with the proliferation marker Ki67 in the neurogenic-enriched area of the adult brain in adult *mTert*-GFP mice [284]. TERT+Ki67- cells were identified in all brain regions of interest, while TERT+Ki67+ cells were found in the V-SVZ, hypothalamus, meninges, and other areas (Figure 2.1E). TERT+Ki67+ cells were not found in the LV ChP, D3V, or D3V ChP (Figure 2.1E). The majority of TERT+ cells analyzed across all brain sections were Ki67-negative, with only 14.9% of TERT+ cells expressing Ki67 (Figure 2.1E, 1.8B). We observed TERT+Ki67+ (Figures 2.1F, 2.1G'), TERT+Ki67- (Figure 2.1G''), and TERT-Ki67+ cells (Figure 2.1G'''), indicating that TERT expression is not cell-cycle specific, yet is rarely expressed by actively dividing cells. Taken together, TERT+ cells in the adult mouse brain are quiescent but have the ability to proliferate across various plastic niches.

TERT+ cells constitute immune and non-immune populations and form neurospheres in culture

Previous studies have identified subpopulations of TERT+ cells in various murine tissues as CD45+ immune cells originating from bone marrow [283, 285]. To determine whether TERT+ cells in the adult murine brain included a population of CD45+ immune cells, we performed immunostaining and identified both TERT+CD45+ and TERT+CD45- cells throughout the adult mouse brain (Figures 2.2C-F). Analysis of the total number of TERT+ cells across all brain sections examined revealed that 53.6% of TERT+ cells expressed CD45 (Figure 2.2F). Quantification of co-staining per region, per mouse, identified both CD45+ and CD45- TERT+ cells throughout most major TERT+ areas of the brain, although no TERT+CD45+ cells were identified in the hypothalamus (Figure 2.2E). FACS analysis of *mTert*-GFP brains where CD45+ cells were gated separately, revealed that 99% of brain cells were CD45- and that of these CD45- cells, only 0.1% were GFP+ (Figures 2.2G-I).

The ability of neural stem cells to form neurospheres in culture is a standard assay for characterizing their behavior [353]. To analyze the neurosphere-forming capabilities of a pure population of TERT+ stem cells from the brain, TERT+CD45- cells were sorted by FACS (to eliminate TERT+ immune cells) and plated into neurosphere growth media containing epidermal growth factor (EGF) and basic fibroblast growth factor (bFGF) (following the standard culture methods of [351]). The strategy for isolation of GFP+CD45- cells is outlined in Figures 2.2G-I. TERT+ cells did form classical neurospheres in culture (Figure 2.1H). GFP- cells sorted from *mTert*-GFP animals were used as controls (Figure 2.2J). Individual cells retained GFP expression in culture, while neurospheres exhibited a loss of GFP expression in culture over time (Figures 2.1H-I), likely due to the activation by the presence of growth factors in the culture media. Activation of TERT+ cells was further demonstrated through the incorporation of EdU over a 24-hour period (Figure 2.1J; N=3 of 4 animals, n=1 well per animal). 49.5% ± 5.6 of EdU+ cells were GFP+ (Figure 2.1K).

TERT+ cells express markers of quiescent stem cells but not of activated stem cells or intermediate neuronal progenitors.

There is currently no single, specific marker for qASCs in the adult brain. This is due to the fact that all previously identified stem cell markers are also expressed by various non-stem cell types [354]. For this reason, we investigated the expression profile of the stem cell markers Sox2, Nestin, and EGFR in TERT+ cells. Co-immunostaining was performed in adult *mTert*-GFP mouse brains. The neuronal lineage in both the V-SVZ and SGZ, consisting of qASCs which differentiate into neurons, is shown in Figure 2.3A with typical gene expression markers shown for reference (Figure 2.3A). Immunofluorescent staining for Sox2 co-expression in the neurogenic-enriched area of brains of adult *mTert*-GFP mice revealed populations of TERT+Sox2+ and TERT+Sox2- cells throughout all major TERT+ niches except for the V-SVZ

and D3V, which housed no TERT+Sox2+ cells (Figures 2.3B-D). Analysis of the total number of TERT+ cells across all brain sections examined revealed that 33.3% of TERT+ cells expressed Sox2 (Figure 2.4A). Immunostaining with Nestin uncovered 1 TERT+Nestin+ cell (Figure 2.3E) and 9 TERT+Nestin- cells (Figure 2.3F) showing 10% of TERT+ cells were Nestin+ (Figure 2.3E-F, 2.4B). These results indicate that a subset of TERT+ cells express various known stem cell markers, such as Sox2 and Nestin.

While subsets of TERT+ cells expressed Sox2 and Nestin, many TERT+ cells did not. To determine whether these were activated stem cells or differentiated cell types, we performed co-immunostaining with markers of activated stem cells as well as immature and mature neuronal cell types. The activated adult stem cell marker EGFR, which is also expressed by aASCs, TACS (V-SVZ), and Type II cells (DG), was never expressed by TERT+ cells in any brain region (Figures 2.3H-I, 2.4C). Additionally, TERT+ cells never expressed the more differentiated neuroblast marker DCX or the mature neuron marker neuronal nuclear protein (NeuN) (Figures 2.4D-G). Bone morphogenetic protein (BMP) receptor 1A (BMPR1A) is a protein that in the V-SVZ and SGZ allows for stem cells to respond to neuro/gliogenic BMP signals (reviewed in [355]). We did identify 1 TERT+ ASC with rare BMPR1A expression (Figure 2.4H). Taken together, these results show that TERT+ cells express quiescent and activated ASC markers, but are not activated intermediate neuronal progenitors or differentiated neuronal cell types.

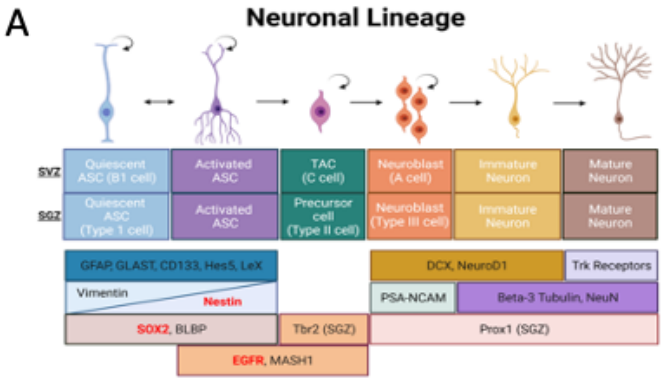
A
Neuronal Lineage
SVZ
SGZ
Quiescent ASC (B1 cell)
Activated ASC
TAC (C cell)
Neuroblast (A cell)
Immature Neuron
Mature Neuron
Quiescent ASC (Type 1 cell)
Activated ASC
Precursor cell (Type II cell)
Neuroblast (Type III cell)
Immature Neuron
Mature Neuron
GFAP, GLAST, CD133, Hes5, LeX
Vimentin
Nestin
SOX2, BLBP
Tbr2 (SGZ)
EGFR, MASH1
DCX, NeuroD1
Trk Receptors
PSA-NCAM
Beta-3 Tubulin, NeuN
Prox1 (SGZ)

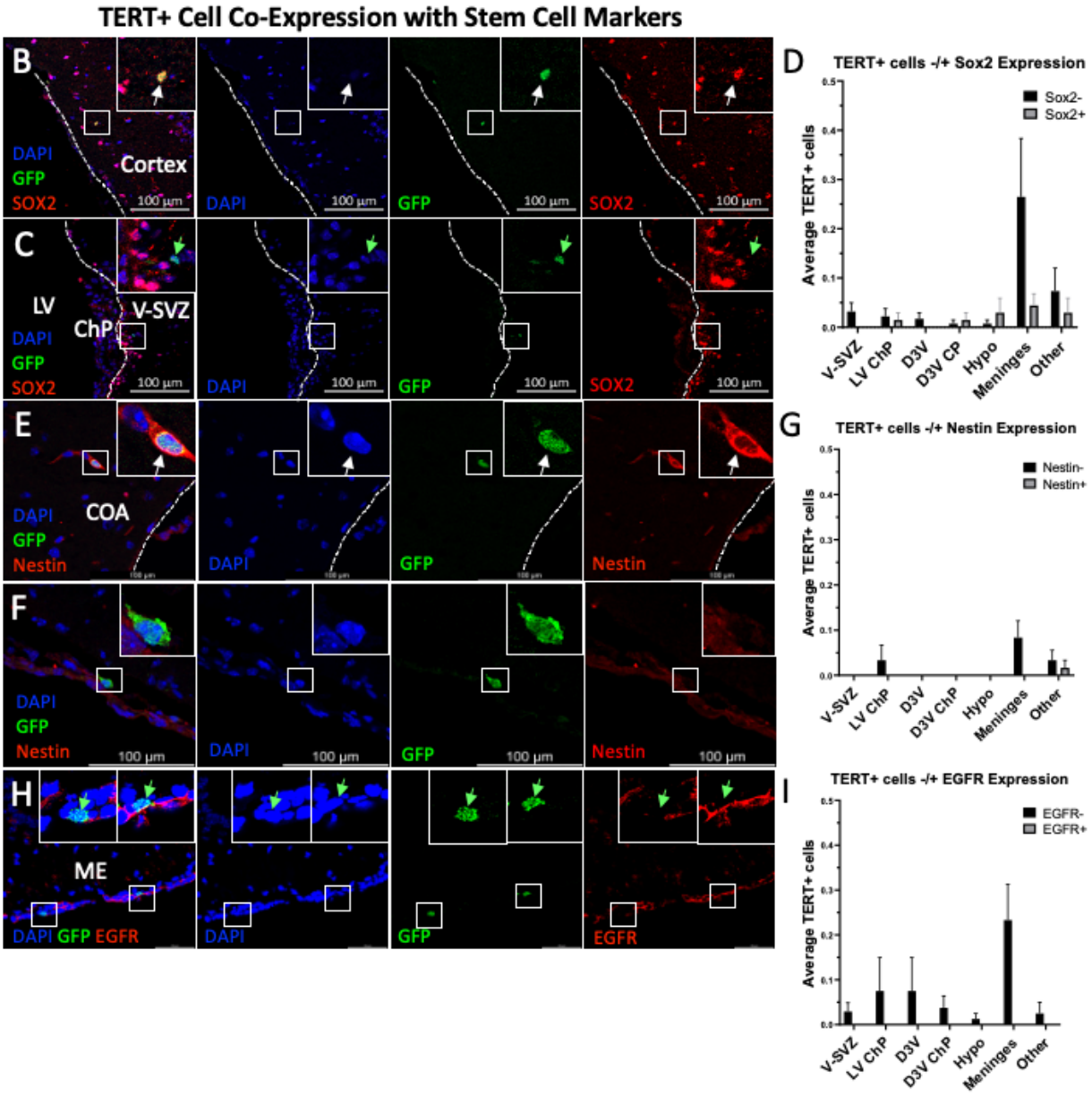
TERT+ Cell Co-Expression with Stem Cell Markers
B
DAPI
GFP
SOX2
Cortex
100 µm
C
LV
ChP
V-SVZ
E
COA
Nestin
F
H
ME
DAPI GFP EGFR
D
TERT+ cells -/+ Sox2 Expression
Sox2-
Sox2+
Average TERT+ cells
V-SVZ
LV ChP
D3V
D3V CP
Hypo
Meninges
Other
G
TERT+ cells -/+ Nestin Expression
Nestin-
Nestin+
I
TERT+ cells -/+ EGFR Expression
EGFR-
EGFR+

Figure 2.3. TERT+ cells express markers of quiescent stem cells, but not of activated stem cells, neuronal precursors, or mature neurons.

(A) Schematic depicting neuronal lineage markers from qASCs to mature neurons in the adult mouse brain. Markers with red text were stained for in this figure. SGZ-specific markers are denoted (SGZ). Curved arrows indicate the ability to proliferate, straight arrows indicate the ability to differentiate.

(B-C) Representative images of Sox2 staining in the adult *mTert*-GFP mouse brain. TERT+Sox2+ cells were identified in N=4 of 8 males and 3 of 9 females, n=4-8 brain sections (B). TERT+Sox2- cells were identified in N=4 of 8 males and 6 of 9 females, n=4-8 brain sections (C).

(D) Quantification of immunofluorescent co-staining analysis of the stem cell marker Sox2 in adult *mTert*-GFP mice. Cell quantification is graphed as the average number of cells per brain region across n=4-8 brain sections from N=8 males and N=9 females at 12 weeks of age.

(E-F) Representative images of Nestin staining in the adult *mTert*-GFP mouse brain. The rare TERT+Nestin+ cell was identified in N=1 of 10 mice (N=1 of 4 males and 0 of 6 females), n=4-6 brain sections (E). TERT+Nestin- cells were identified in N=5 of 10 mice (N=3 of 4 males and 2 of 6 females), n=4-8 brain sections (G).

(G) Quantification of immunofluorescent co-staining analysis of the stem cell marker Nestin in adult *mTert*-GFP mice. Cell quantification is graphed as the average number of cells per brain region across n=4-8 brain sections from N=4 males and N=6 females at 12 weeks of age.

(H) Representative image of EGFR staining in the adult *mTert*-GFP mouse brain. TERT+EGFR- cells were identified in N=8 of 10 mice (3 of 4 males, 5 of 6 females), n=4-6 brain sections.

(I) Quantification of immunofluorescent co-staining analysis of the stem cell marker Nestin in adult *mTert*-GFP mice. Cell quantification is graphed as the average number of cells per brain region across n=4-6 brain sections from N=4 males and N=6 females at 12 weeks of age.

Insets show indicated area at 3x digital zoom. White arrows indicate co-stained cells, green arrows indicate cells that express only TERT. Scale bars are 100μm except Figure H (50μm). Grouped bar graphs show mean cells per mouse, per brain section, at each brain region ± SEM. All images taken on SP8 or LSM 900 confocal microscopes. V-SVZ: ventricular-subventricular zone, LV: lateral ventricle, ChP: choroid plexus, COA: cortical amygdalar layer, ME: median eminence.

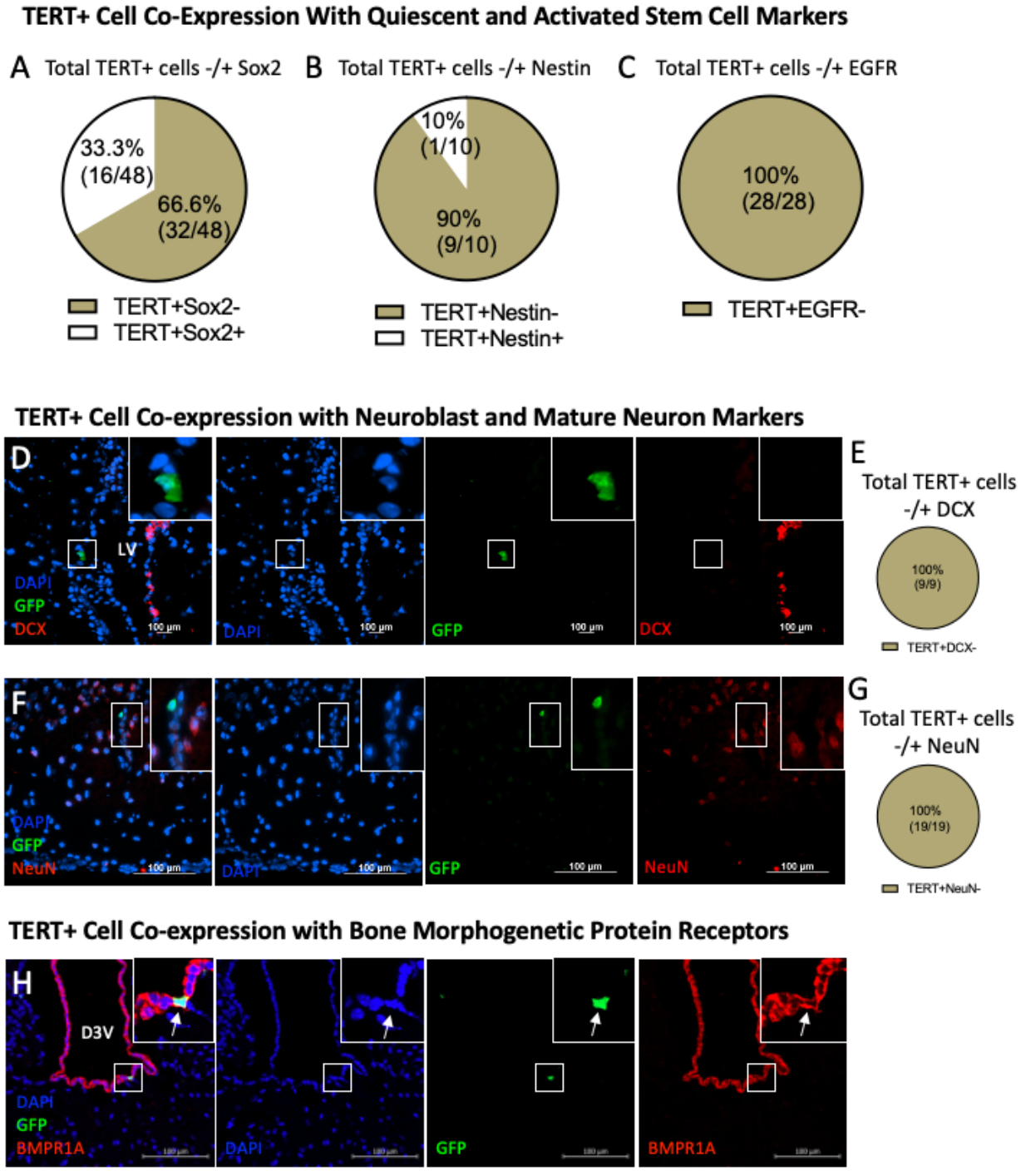
TERT+ Cell Co-Expression With Quiescent and Activated Stem Cell Markers
A Total TERT+ cells -/+ Sox2
33.3% (16/48)
66.6% (32/48)
TERT+Sox2-
TERT+Sox2+
B Total TERT+ cells -/+ Nestin
10% (1/10)
90% (9/10)
TERT+Nestin-
TERT+Nestin+
C Total TERT+ cells -/+ EGFR
100% (28/28)
TERT+EGFR-
TERT+ Cell Co-expression with Neuroblast and Mature Neuron Markers
D
LV
DAPI
GFP
DCX
100 µm
E
Total TERT+ cells -/+ DCX
100% (9/9)
TERT+DCX-
F
NeuN
G
Total TERT+ cells -/+ NeuN
100% (19/19)
TERT+NeuN-
TERT+ Cell Co-expression with Bone Morphogenetic Protein Receptors
H
D3V
BMPR1A

Figure 2.4: TERT+ cells express markers of quiescent stem cells, but not of activated stem cells, neuronal precursors, or mature neurons.

(A-C) Quantification of total TERT+ cells across all tissues in the neurogenic enriched brain area stained for Sox2 (A), Nestin (B), or EGFR (C) from 10 *mTert-GFP* animals. (N=4-8 males, 6-9 females, n=4-8 sections per brain).

(D-G) Representative images of TERT+ cells within the brain co-stained with DCX (D) with quantification across total TERT+ cells (E), or NeuN (F) with quantification across total TERT+ cells (G; for each marker, N=5 males, 5 females, n=4 sections per brain assessed).

(F) Brain section containing TERT+BMPR1A+ cell along D3V. 1 TERT+BMPR1A+ cell was identified across N=5 males, 5 females, n=8 sections per brain assessed.

Scale bars are all 100μm. Insets show indicated area at 2x digital zoom. LV: lateral ventricle, D3V: dorsal third ventricle

TERT+ cells do not express markers of glial progenitors or glia in the brains of TERT-GFP direct reporter mice

Adult gliogenesis, the generation of adult-born astrocytes and oligodendrocytes, occurs throughout the brain in a less restricted pattern than adult neurogenesis, due in part to the mitotic nature of mature astrocytes [356]. Since TERT+ cells were identified in neurogenic and non-neurogenic regions of the brain and expressed markers of adult stem cells but not differentiated neuronal cell types, we subsequently performed immunostaining for markers of glial precursor cells (GPCs) and mature glia. GPCs, which express neuron-glial antigen 2 (NG2), are found throughout the adult brain and have been described as arise from Sox2+ and Nestin+ stem cells [357]. Figure 2.5A depicts the changes gene expression across glial cell differentiation. Co-immunostaining revealed no co-expression of TERT with the GPC marker NG2, the oligodendrocyte-lineage marker oligodendrocyte transcription factor 2 (OLIG2), nor the astrocyte-lineage marker GFAP (Figures 2.5B-H). Images using the OLIG2 antibody in the V-SVZ confirmed labeling of mTERT-GFP with OLIG2+ cells (Figure 2.6A). These data indicated that TERT+ cells in the murine brain are not glial-committed precursors, mature astrocytes, or mature

oligodendrocytes. As GFAP is expressed by both astrocytes and ANSCs in the V-SVZ and SGZ [19], we had initially hypothesized that some TERT+ cells would be GFAP+. However, we saw no co-expression of TERT and GFAP in any brain region across numerous cohorts. Taken together, TERT+ cells in the adult mouse brain cannot be characterized as glial progenitors or mature glia.

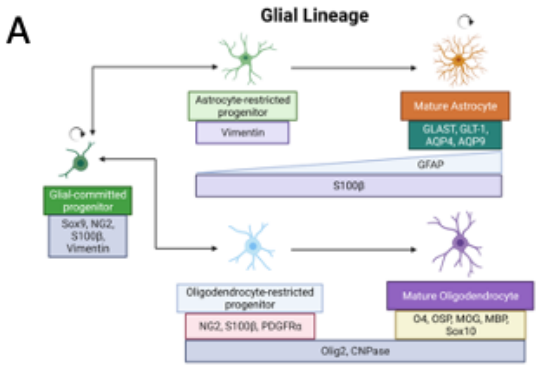
A
Glial Lineage
Astrocyte-restricted progenitor
Vimentin
Mature Astrocyte
GLAST, GLT-1, AQP4, AQP9
GFAP
S100β
Glial-committed progenitor
Sox9, NG2, S100β, Vimentin
Oligodendrocyte-restricted progenitor
NG2, S100β, PDGFRα
Mature Oligodendrocyte
O4, OSP, MOG, MBP, Sox10
Olig2, CNPase

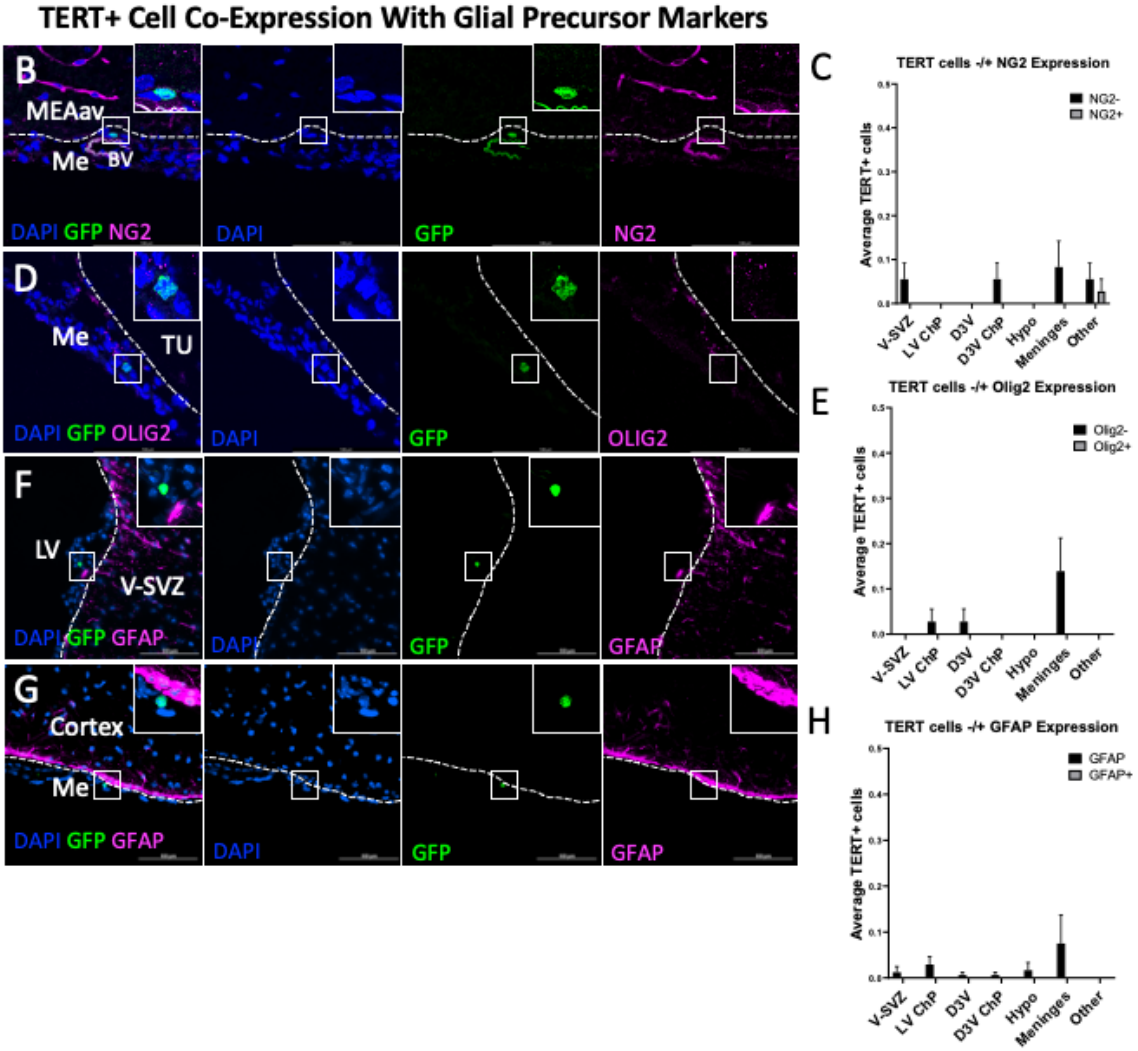
TERT+ Cell Co-Expression With Glial Precursor Markers
B
MEAav
Me
BV
DAPI GFP NG2
DAPI
GFP
NG2
C
TERT cells -/+ NG2 Expression
NG2-
NG2+
Average TERT+ cells
V-SVZ
LV ChP
D3V
D3V ChP
Hypo
Meninges
Other
D
Me
TU
DAPI GFP OLIG2
DAPI
GFP
OLIG2
E
TERT cells -/+ Olig2 Expression
Olig2-
Olig2+
Average TERT+ cells
V-SVZ
LV ChP
D3V
D3V ChP
Hypo
Meninges
Other
F
LV
V-SVZ
DAPI GFP GFAP
DAPI
GFP
GFAP
G
Cortex
Me
DAPI GFP GFAP
DAPI
GFP
GFAP
H
TERT cells -/+ GFAP Expression
GFAP
GFAP+
Average TERT+ cells
V-SVZ
LV ChP
D3V
D3V ChP
Hypo
Meninges
Other

Figure 2.5. TERT+ cells do not express markers of glial-committed progenitors or mature glia.

(A) Schematic depicting glial lineage markers from glial-committed progenitors to mature glial cell types in the adult mouse brain. Markers with red text were stained for in this figure.

(B-C) Immunostaining in the brains of adult *mTert*-GFP mice for the glial precursor cell marker NG2 identified no TERT+NG2+ cells (N=5 males, 5 females, n=4 sections per brain analyzed).

(D-E) Immunostaining in the brains of adult *mTert*-GFP mice for the progenitor/ mature oligodendrocyte marker OLIG2 identified no TERT+Olig2+ cells (N=5 males, 5 females, n=4 sections per brain analyzed).

(F-H) Immunostaining in the brains of adult *mTert*-GFP mice for the marker of immature/ mature astrocytes as well as qANSCs identified no TERT+GFAP+ cells (N=5 males, 5 females, n=4 sections per brain analyzed).

Insets show indicated area at 3x digital zoom. Scale bars are 100μm. MEAav: media amygdalar nucleus, anteroventral part, Me: meninges, TU: tuberal nucleus, LV: lateral ventricle, V-SVZ: ventricular-subventricular zone. Grouped bar graphs show mean cells per mouse, per section at each brain region ± SEM.

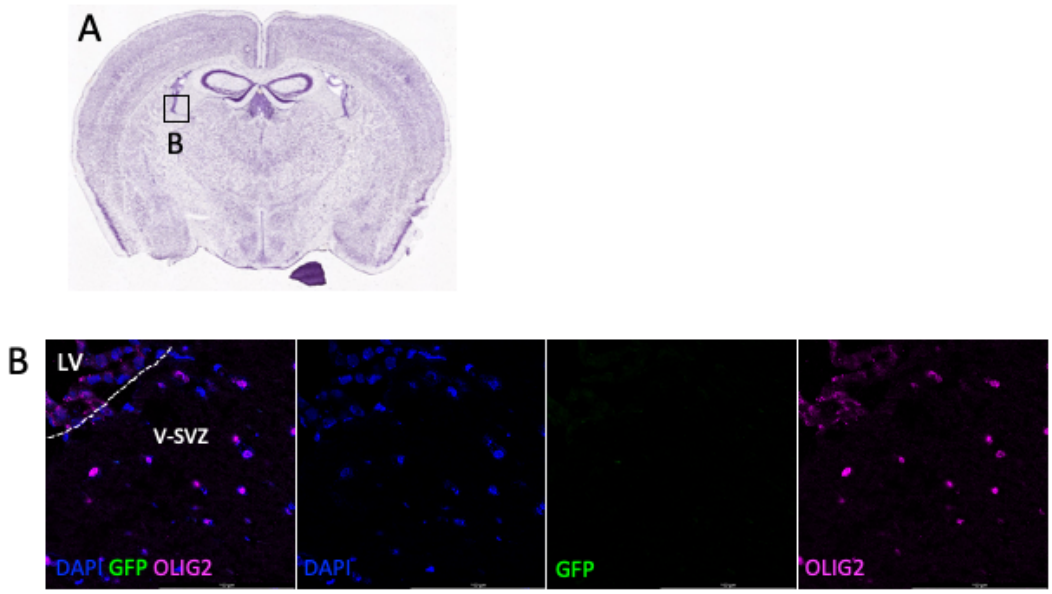

Figure 2.6: TERT+ cells do not express markers of glial-committed progenitors or mature glia.

(A) Schematic of a coronal mouse brain indicating area of Fig. 3B (Allen Brain Atlas).

(B) Positive control region for OLIG2 expression in the adult mouse brain. Scale bar is 100μm. LV: lateral ventricle, V-SVZ: ventricular-subventricular zone.

TERT+ stem cells trace to multiple areas of the adult mouse brain in a lineage-tracing mouse model

Based on the premise that TERT+ cells are qASCs, we tested the hypothesis that TERT+ cells would proliferate, differentiate, and migrate within the adult mouse brain using an inducible lineage tracing system [358]. Lineage tracing allows for an indelible tag such as the bioluminescent luciferase or the fluorescent protein GFP to be expressed by each TERT+ cell during a 'pulse' of the tetracycline derivative, doxycycline. If a cell population is labeled in this way, a 'chase' period after drug administration will allow for lineage tracing of these cells as they migrate, proliferate, or differentiate into mature cell types. Lineage tracing was performed with mTert-rtTA::oTet-Cre::R26R-mTmG (*mTert*-mTmG) animals [287]. In these animals, recombination after doxycycline administration resulted in loss of membrane tomato expression and activation of membrane (m)GFP expression through the doxycycline-inducible Tet-On system (Figure 2.7A). To better understand large-scale changes occurring throughout major TERT+ brain regions (i.e. proliferation and migration), various pulse-chase experiments were compared and three different pulse-chase durations were utilized in these studies: a 2-day pulse, 0-day chase, a 3-week pulse, 11-day chase, and a 3-week pulse, 14-week chase (Figure 2.7B). The 2-day pulse, 0-day chase was the shortest possible time required for mGFP induction and was used to compare to direct reporter mice [359]. The 3-week pulse, 11-day chase was chosen because adult-born neurons are created in approximately 2-4 weeks in the SGZ, V-SVZ, and hypothalamus [34, 58, 360-362] The 3-week pulse, 14-week chase was utilized to show long-term effects of TERT+ cell proliferation, migration, and differentiation in the adult brain similar to the IVIS-CT images.

Lineage tracing over the 3-week, 11-day pulse-chase period revealed expansion of *mTert*-driven mGFP signal throughout various brain regions when compared to *mTert*-GFP direct reporter mice (Figures 2.7C-R; see Figure Legend for N, n values). Immunostaining of *mTert*-

GFP brains revealed TERT+ cells in proximity to the walls of the lateral ventricles (Figure 2.7C). The expansion of this signal in the LV after a 3-week pulse, 11-day chase in *mTert*-mTmG animals appears to be minimal, as traced mGFP+ cells were also found at low numbers (Figure 2.7D). It is possible that TERT+ cells in the V-SVZ do not often give rise to V-SVZ or RMS cells under basal conditions, but instead respond to injury, metabolic, or other plasticity promoting cues.

In the OB of *mTert*-GFP mice, TERT+ cells were identified in the periglomerular layer (PGL; Figure 2.7E). Contrary to the low numbers of mGFP+ cells observed in the LV after lineage tracing, high mGFP+ cell numbers were observed in the PGL and the olfactory nerve layer (ONL) of the OB after a 3-week, 11-day pulse-chase, indicating proliferation and differentiation activity of the qASCs in this niche (Figure 2.7F). Traditional V-SVZ neurogenesis leads to the formation of adult-born neurons via migration of TACs and neuroblasts through the RMS into the GCL of the OB. In accordance with the low number of Tert-GFP+ and lineage traced mGFP+ cells in the V-SVZ (Fig. 4G-H), we also observed low numbers of mGFP+ cells within the GCL. These mGFP+ cells did not show a neuronal phenotype, indicating a possibly gliogenic pathway within or into the OB (Figure 2.8A). Progenitors and immature neurons that migrate to the OB via the RMS will integrate into the GCL more often than the PGL and ONL [24]. Although lineage tracing revealed mGFP+ cells within the RMS (Figure 2.8B), we never observed lineage traced cells with a neuronal morphology within the GCL that is typical of traditional V-SVZ-derived neurogenesis (Figure 2.8C). Instead, mGFP+ cells were found at low numbers in the mitral layer of the OB with similar morphology to the mGFP+ cells in the GCL (Figure 2.8E). It is therefore likely that adult neurogenesis from TERT+ stem cells in the olfactory epithelium (OE), as observed by luciferase signal after lineage tracing (Figures 2.7D and 2.7E) fueled the expansion of mGFP expression in the PGL and ONL [24].

In the hypothalamus, adult neurogenesis regulates energy balance and metabolism via the development of new adult-born proopiomelanocortin (POMC)+ and neuropeptide Y (NPY)+

neurons, as well as hypothalamic glial differentiation [58]. Metabolic interventions such as high fat diet increase neurogenesis in the median eminence (ME) of female mice while decreasing neurogenesis in the arcuate nucleus (ARC) of both male and female mice [55]. Additionally, treatment with the metabolic cytokine ciliary neurotrophic factor (CNTF), which causes weight loss in obese rodents and humans, increases cell proliferation in feeding centers of the murine hypothalamus, which is reversed with coadministration of the mitotic inhibitor cytosine-beta-d-arabinofuranoside (Ara-C), indicating that hypothalamic neurogenesis affects whole body energy balance [55, 58]. Immunofluorescent analysis revealed that the hypothalamus contained TERT+ cells in *mTert*-GFP direct reporter animals (Figure 2.7G). Interestingly, TERT+ cells were also identified nearby to the tanycyte region of the third ventricle (3V; Figure 2.8D). Tanycytes are radial glial-like cells that line the ventricles and are implicated in glucose-sensing and stem-like behavior [51]. Also, in the hypothalamus, we identified TERT+ cells in the ARC which contains POMC and NPY neurons (Figure 2.7G). Compared to direct reporter mice, a larger number of cells in the ARC and ME of the hypothalamus expressed mGFP after lineage-tracing, suggesting TERT+ cell contribution to tissue turnover in this niche (Figure 2.7H). This large-scale expression of mGFP when compared to the mTert-GFP hypothalamus (Figure 2.7G) may be attributed to the membrane expression of large cells such as traced neurons, astrocytes, and microglia, which all proliferate in the adult mouse hypothalamus, whereas the mTERT-GFP direct reporter animals express a fainter fluorophore that is not membrane-expressed.

Interestingly, in the hippocampal DG, no TERT+ cells were ever identified (Figure 2.7I). Lineage tracing also revealed no mGFP signal in any hippocampal region in mTert-mTmG animals after a 3-week pulse,11-day chase (Figure 2.7J).

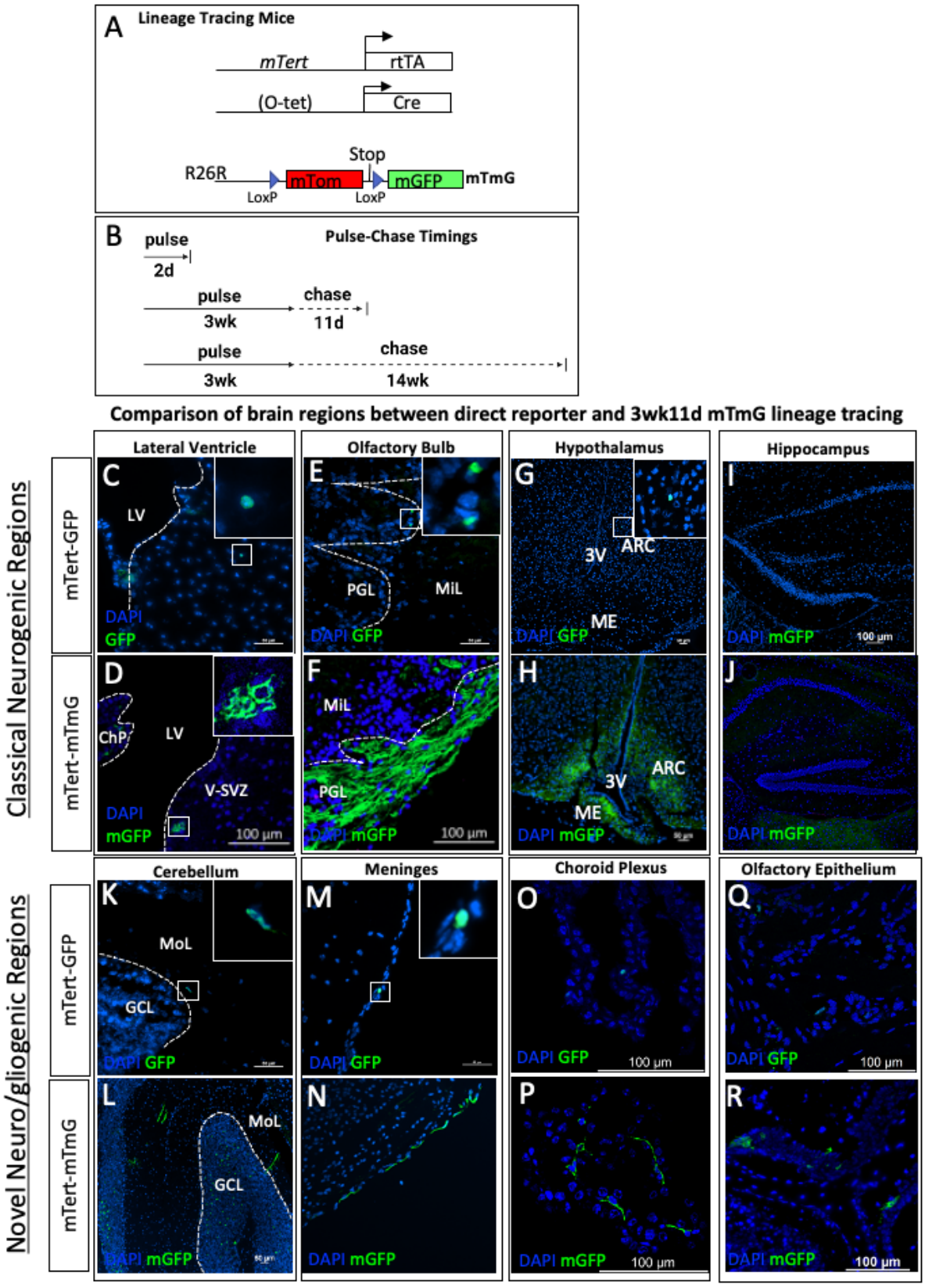
A
Lineage Tracing Mice
mTert
rtTA
(O-tet)
Cre
Stop
R26R
mTom
mGFP
mTmG
LoxP
LoxP
B
pulse
2d
Pulse-Chase Timings
pulse
3wk
chase
11d
pulse
3wk
chase
14wk
Comparison of brain regions between direct reporter and 3wk11d mTmG lineage tracing
Classical Neurogenic Regions
Novel Neuro/gliogenic Regions
mTert-GFP
mTert-mTmG
Lateral Ventricle
Olfactory Bulb
Hypothalamus
Hippocampus
Cerebellum
Meninges
Choroid Plexus
Olfactory Epithelium
LV
ChP
V-SVZ
PGL
MiL
3V
ARC
ME
MoL
GCL
DAPI
GFP
mGFP
100 μm

Figure 2.7: Lineage tracing reveals that mTert+ cells give rise to a heterogeneous population of cells in multiple plastic regions of the brain.

(A) Depiction of mTert-rtTA::oTet-Cre::R26R$^{(mTmG)}$ mouse model.

(B) Illustration of major pulse-chase timings utilized across both lineage-tracing mouse lines.

(C-J) Representative images of TERT+ cells from immunofluorescent analysis across classical neuro/gliogenic brain regions in direct reporter mice versus mTert-mTmG mice after a 3-week, 11-day pulse-chase. Images taken of *mTert*-GFP brains in the LV (C), OB (E), hypothalamus (G), and hippocampus (I) (N=2-11 of 11 mice showed this signal [N=2-5 of 5 males, 0-6 of 6 females], n=4-20 sections per brain analyzed). Representative images of adult mTmG lineage tracing mice after a 3-week, 11-day chase in the LV (D), OB (F), hypothalamus (H), and hippocampus (J); N=6-10 of 10 mice showed this signal; 3-4 of 4 males, 3-6 of 6 females, n=1-23 sections per brain analyzed).

(N-U) Immunofluorescent analysis across novel neuro/gliogenic regions in *mTert*-GFP (K,M,O,Q); N=2-6 of 6-10 mice showed this signal [N=1-3 of 3-5 males, 1-3 of 3-5 females], n=8-12 sections per brain analyzed) and mTmG mice after a 3-week pulse, 11-day chase (L,N,P,R; N=8-11 of 11 mice showed this signal [N=4 of 4 males, 4-7 of 7 females], n=1-19 sections per brain analyzed).

Scale bars are 100μm. Insets show indicated area at 3x digital zoom. LV: Lateral Ventricle, PGL: periglomerular layer, MiL: mitral layer, 3V: third ventricle.

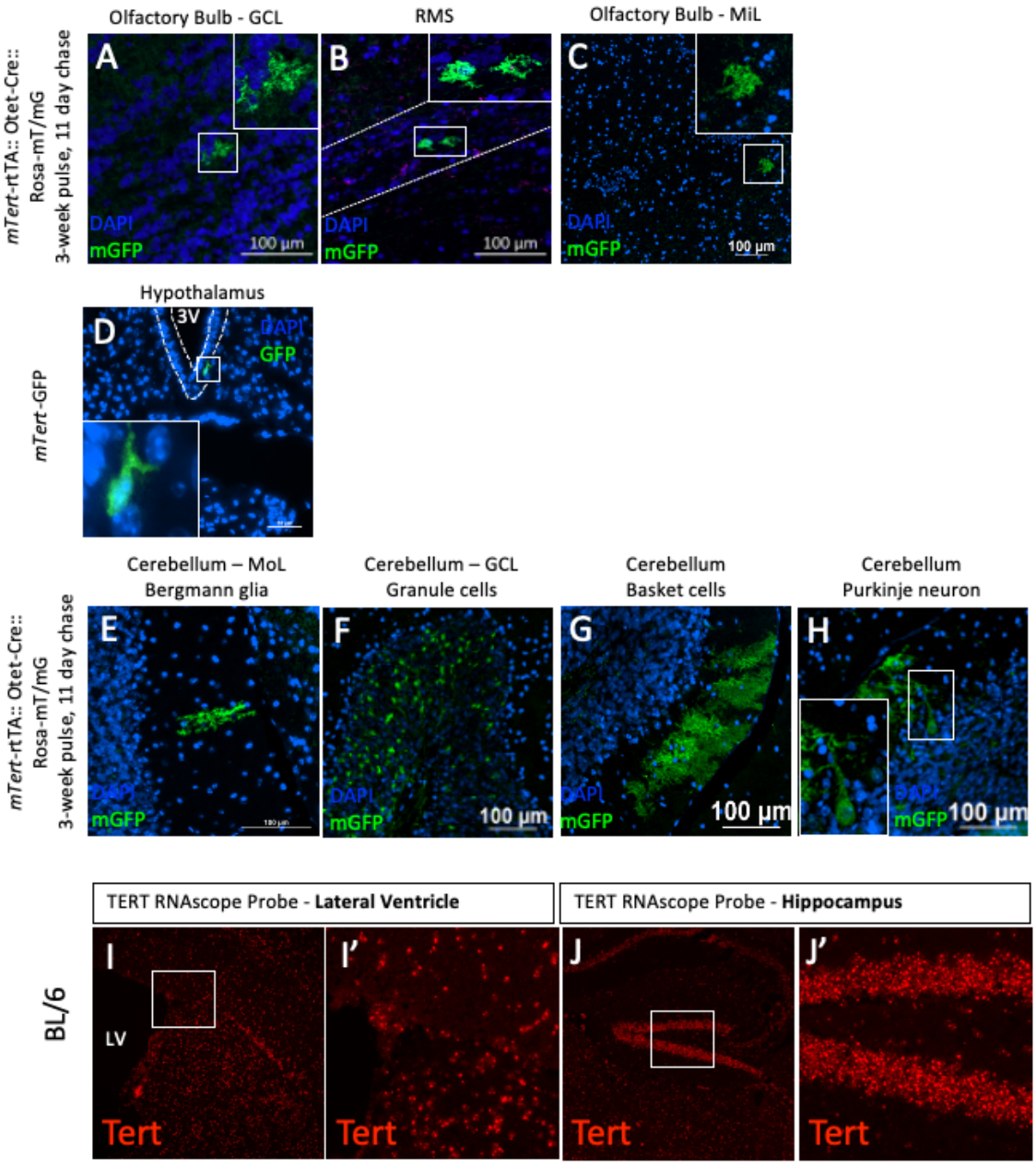
Olfactory Bulb - GCL
RMS
Olfactory Bulb - MiL
mTert-rtTA:: Otet-Cre:: Rosa-mT/mG 3-week pulse, 11 day chase
A
B
C
DAPI
mGFP
100 µm
Hypothalamus
mTert-GFP
D
3V
DAPI
GFP
Cerebellum – MoL Bergmann glia
Cerebellum – GCL Granule cells
Cerebellum Basket cells
Cerebellum Purkinje neuron
E
F
G
H
TERT RNAscope Probe - Lateral Ventricle
TERT RNAscope Probe - Hippocampus
BL/6
I
I'
J
J'
LV
Tert

Figure 2.8: Lineage tracing reveals that TERT+ cells give rise to a heterogeneous population of cells in multiple plastic regions of the brain.

(A) Representative image of TERT+ cells in the OB of *mTert*-GFP animals, specifically the GCL (A') and PGL (A'') of mTert-GFP brains (identified in N=2 of 5 mice [N=2 of 3 males, 0 of 3 females], n=8-14 sections per brain assessed).

(B) Representative image of mGFP+ cell within the GCL of *mTert*-mTmG mice after a 3-week, 11-day lineage tracing experiment (identified in N=8 of 10 mice [N=3 of 4 males, 5 of 6 females], n=13-23 sections per brain assessed).

(C) Representative image of mGFP+ cell within the RMS of *mTert*-mTmG mice after a 3-week, 11-day lineage tracing experiment (identified in N=3 of 10 mice [N=2 of 4 males, 1 of 6 females], n=1-5 sections per brain assessed).

(D) mGFP+ cells within the MiL after lineage trace (identified in N=2 of 10 mice [N=1 of 4 males, 1 of 6 females], n=13-22 sections per brain assessed.

(E) Hypothalamic TERT+ cell within the tanycytic layers of the third ventricle (3V) (identified in N=1 of 11 mice [N= 1of 5 males, 0 of 6 females], n=4-20 sections per brain assessed).

(F-I) Representative images of mGFP+ cells following a 3-week, 11-day pulse-chase in the cerebellum identifying Bergmann glia (F), granule cells G), basket cells (H), and Purkinje neurons (I) (seen in N=8-11 mice [N=4 of 4 males, 4-7 of 7 females], n=4-19 sections per brain assessed). Scale bars are 100μm.

J-K) TERT mRNA identified through RNAscope in the lateral ventricle and RMS (J) and hippocampus (K) of an adult WT BL/6 mouse (N=1).

TERT+ stem cells expand after lineage tracing in novel neuro/gliogenic niches of the adult mouse brain

TERT+ cells were also identified in brain regions where plastic potential has been observed but remains poorly understood. These regions, which included the cerebellum, meninges, and ChP, contain proliferative stem cells with the ability to differentiate [153, 363-365]. Within the cerebellum TERT+ cells were identified in direct reporter mice (Figure 2.7K). While TERT+ cells were sparse within the cerebellum, lineage tracing resulted in a large-scale expansion of mGFP signal throughout various cell types and regions of the cerebellum not seen

in *mTert*-GFP animals (Figures 2.7K and 2.7O). We confirmed traced cell types in the cerebellum that had the morphological identity of Bergmann glia (Figure 2.8E), granule cells (Figure 2.8F), basket cells (Figure 2.8G) and Purkinje neurons (Figure 2.8H). When compared to the rare TERT+ cells in *mTert*-GFP mice, the increased number of TERT-traced cells with the clear morphological identity of mature cell types within the cerebellum indicate TERT+ cells give rise to mature cell types.

The meninges also harbored TERT+ cells in *mTert*-GFP mice (Figure 2.7M). Lineage tracing revealed mGFP+ expression increased compared to direct reporter expression in the meninges (Figure 2.7N). These patterns were observed within the ChP as well (Figures 2.7O and 2.7P). These brain regions sit at the blood-brain barrier and blood-cerebrospinal fluid (CSF) barrier interface and play a major role in immune cell trafficking [366]. The ChP produces CSF, which in turn coordinates neurogenesis via the production of growth factors throughout the ventricular regions of the brain, including the lateral and third ventricles, and hypothalamus [135, 367]. Finally, In the OE, *mTert*-GFP animals showed low numbers of TERT+ cells (Figure 2.7Q). After a 3-week, 11-day lineage tracing experiment, mGFP+ cells were found at higher numbers throughout the OE compared to the direct reporter animals (Figure 2.7R), supporting the idea that newborn olfactory sensory neurons (OSNs) in this niche may be observed within the olfactory NL and PGL. Taken together, TERT+ cells give rise to adult-born cells in most, but not all classical and newly discovered neurogenic brain regions.

Lineage tracing of TERT+ cells increased mGFP expression with the pulse-chase duration

Expansion of the mGFP+ cell labeling over increasing pulse-chase times was observed in the OB, from the 2-day pulse, 0-day chase to the 3-week pulse, 14-week chase. It is important to note that these changes occur primarily in the ONL and PGL (Figures 2.9A-C). The fact that

TERT+ cells exist within the OB in direct reporter animals indicates the possibility of TERT+ cell proliferation within the OB instead of primarily via migration, however, the extent of GFP expression after a pulse-chase in the PGL and NL implies that this is in combination with neurogenesis in the OE so this may be an additional anatomical source of OB GFP signal. mGFP+ cell expansion was also identified in the cerebellum between the 2-day pulse, 0-day chase and 3-week pulse, 14-week chase (Figures 2.9D-E), but fluorescent intensity was reduced into the 3-week, 14-week pulse-chased cerebellum (Figure 2.9E). Within the hypothalamic ARC a trend was observed towards increased fluorescent intensity between 2-day pulse, 0-day chase and the other treatments (Figures 2.9G-H). The thalamus also showed a trend towards increased mGFP signal intensity between animals treated with a 2-day pulse, 0-day chase and 3-week pulse, 11-day chase (Figures 2.9H-I). Over all three pulse-chases, we rarely observed mGFP traced cells in the V-SVZ and RMS (Figures 2.10A-B).

Intracerebroventricular (*i.c.v.*) treatment with the mitotic inhibitor cytosine-beta-d-arabinofuranoside (Ara-C) resulted in a reduction of DCX+ cells along the lateral ventricle wall/V-SVZ (Figures 2.10C-E) but did not result in changes to the fluorescent intensity of lineage-traced mGFP expression in cells in the LV ChP (Figure 2.10F). Ara-C treatment did not significantly decrease mGFP expression in the OB, indicating that the mGFP signal within the OB likely does not originate from the V-SVZ (Figure 2.10G).

FACS analysis of a lineage-traced brains following a 3-week pulse, 11-day chase identified that mGFP cells accounted for 3.8% of the full adult mouse brain and formed neurospheres in culture, much higher numbers than what was observed in the *mTERT*-GFP direct reporter mice (Figure 2.10H), consistent with our immunostaining observations. These cells exhibited neurosphere formation as well (Figure 2.10H).

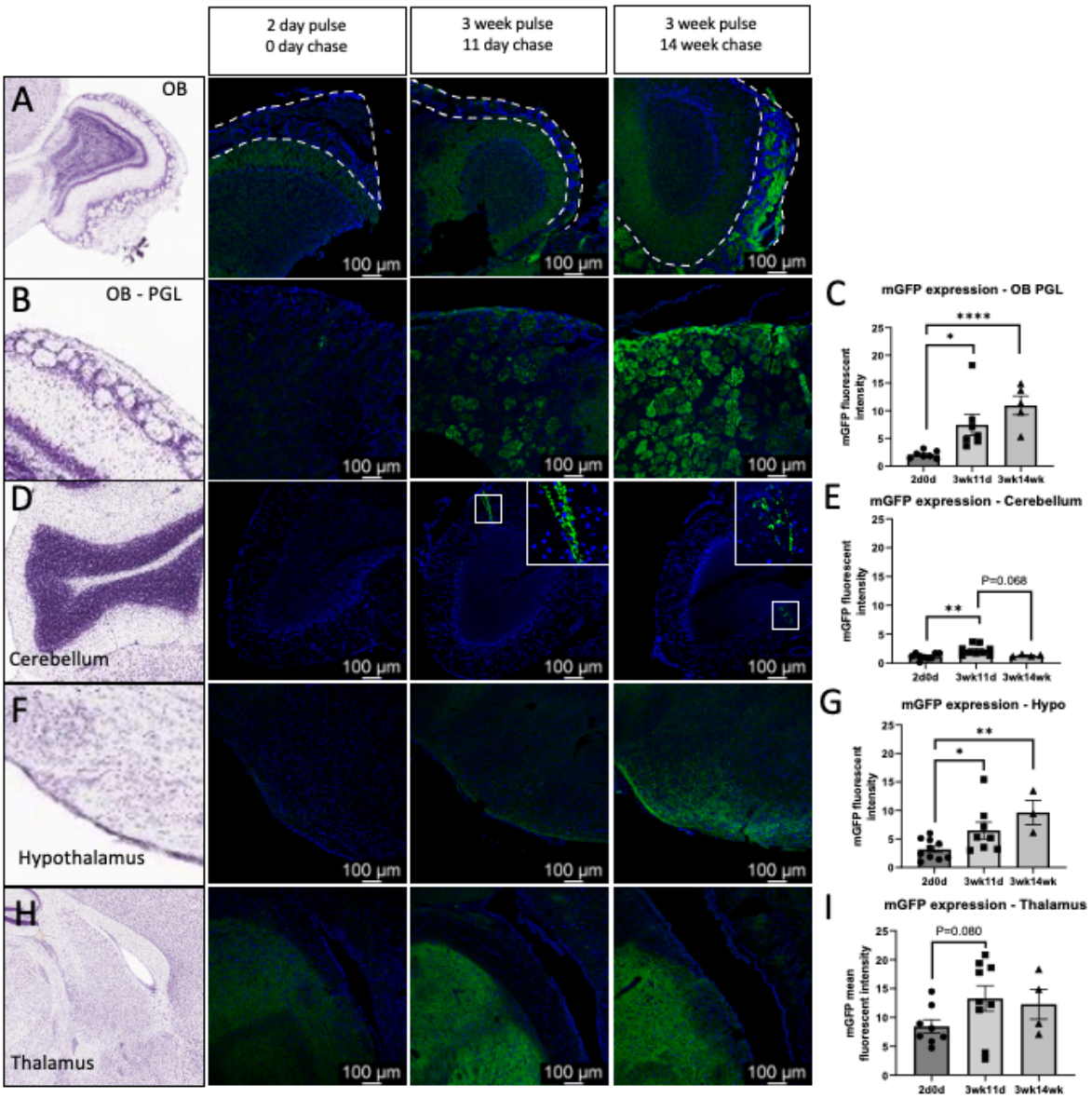
Comparison of brain regions after 3 lineage tracing durations
2 day pulse
0 day chase
3 week pulse
11 day chase
3 week pulse
14 week chase
A
OB
B
OB - PGL
D
Cerebellum
F
Hypothalamus
H
Thalamus
100 µm
C
mGFP expression - OB PGL
mGFP fluorescent intensity
2d0d
3wk11d
3wk14wk
E
mGFP expression - Cerebellum
P=0.068
G
mGFP expression - Hypo
I
mGFP expression - Thalamus
P=0.080
mGFP mean fluorescent intensity

Figure 2.9: Lineage tracing reveals numerous brain regions with high basal plasticity and differentiation of TERT+ precursors that increase with pulse-chase time. mTert-mTmG mouse brains were immunostained following a: 2-day pulse, 0-day chase (N=5 males, 5 females); 3-week pulse, 11-day chase (N=4 males, 8 females); or 3-week pulse, 14-week chase (N=6 females).

(A-N) Representative images of each of the OB (A), OB PGL (B), cerebellum (C), hypothalamus (D), and thalamus (E). Representative images of sagittal-view brain regions of interest were obtained from the Allen Brain Atlas. Quantification of mean fluorescent intensity of mGFP expression (± SEM) per mouse across lineage tracing in the OB PGL (C), cerebellum (E), hypothalamus (G), and thalamus (I). For each brain region imaged, N=4-10 mice, n=1 section per brain. Dots represent mean fluorescent intensity of individual animals (N=4-10; *P < 0.05, **P < 0.01, ****P < 0.001).

All scale bars are 100μm. All images taken at the same sagittal depth. Dotted lines indicate the PGL identified in the OB.

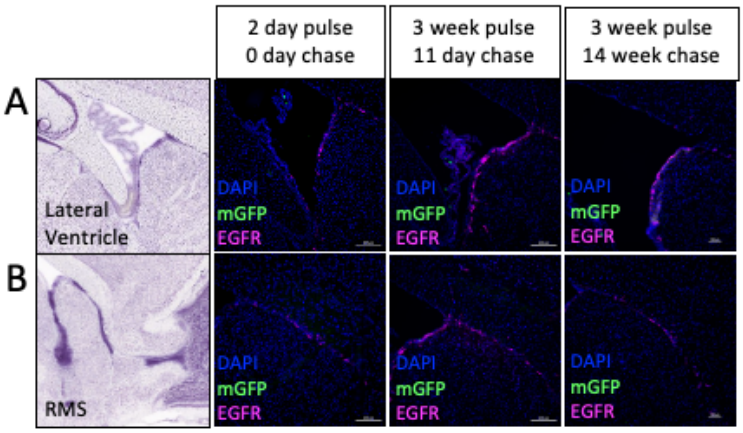
2 day pulse
0 day chase
3 week pulse
11 day chase
3 week pulse
14 week chase
A
B
Lateral
Ventricle
RMS
DAPI
mGFP
EGFR

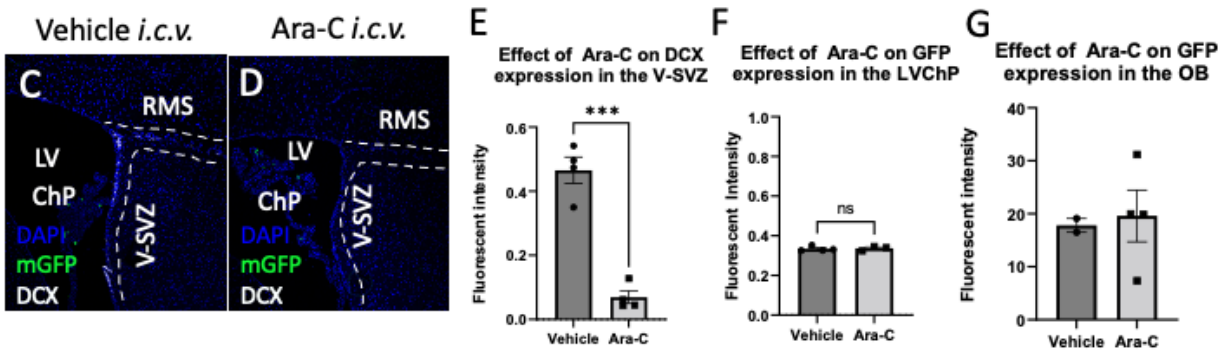
Vehicle *i.c.v.*
Ara-C *i.c.v.*
C
D
RMS
LV
ChP
V-SVZ
DAPI
mGFP
DCX
E
Effect of Ara-C on DCX expression in the V-SVZ
Fluorescent intensity
***
Vehicle
Ara-C
F
Effect of Ara-C on GFP expression in the LVChP
ns
G
Effect of Ara-C on GFP expression in the OB

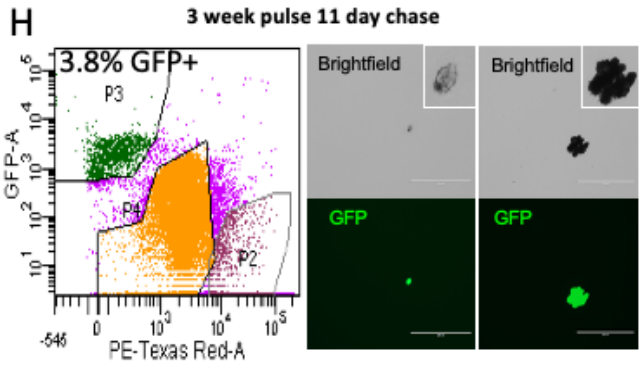
H
3 week pulse 11 day chase
3.8% GFP+
P3
P4
P2
GFP-A
PE-Texas Red-A
Brightfield
GFP

2.10: Lineage tracing of TERT+ cells revealed low numbers of traced cells in certain adult brain niches, which were unaffected by mitotic inhibition. Lineage traced cells were able to form neurospheres, and did not show increased expression of activation or differentiation markers.

(A-B) Representative images of each of the V-SVZ (A), and RMS (B). Representative images of sagittal-view brain regions of interest were obtained from the Allen Brain Atlas. mTert-mTmG mouse brains were immunostained following either a: 2-day pulse, 0-day chase (N=5 males, 5 females), 3-week pulse, 11-day chase (N=4 males, 8 females), or 3-week pulse, 14-week chase (N=6 females).

(C-D) Representative image of the LV of a vehicle treated mouse (C) and Ara-C treated mouse (D). For both, N=4 mice, n=1 section per brain assessed. Dotted lines indicate areas of the V-SVZ and RMS where DCX expression is observed under basal conditions.

(E) Fluorescent intensity of DCX signal in the V-SVZ of Ara-C or vehicle treated mice (N=4 mice, n=1 section per brain assessed).

(F-G) Fluorescent intensity of GFP signal in the LV ChP (G) or OB (H) of Ara-C or vehicle treated mice quantified by frame of vision (N=2-4 mice, n=1 section per brain assessed).

(H) FACS analysis of 3-week pulse, 11-day chase (J; N=4) lineage-traced mouse brains and the ability of GFP+ cells to form neurospheres in culture. P3: GFP+, P2, P4: GFP-. PE-Texas Red-A used to analyze membrane tomato signal.

Scale bars all 200μm except for D and E, which are 100μm. Bar graphs show mean +/- SEM. Dots indicate individual animals. ***P = 0.005.

TERT cells give rise to immature and mature neuronal cell types in lineage-tracing animals

In order to identify the cell types arising from lineage-traced TERT+ populations across the adult mouse brain, we co-stained mGFP+ cells from *mTert*-mTmG lineage traced mice with markers of activated ASCs, TACS, neuroblasts, and neurons. The brain regions where images were taken are represented in Figure 2.11A. The neuronal differentiation pathway is again shown in Figure 2.11B for reference. In the V-SVZ, the activation marker EGFR never co-localized to lineage traced mGFP+ cells after a 2-day, 0-day pulse-chase, nor the 3-week, 11-day pulse-chase, and only co-localized rarely with mGFP+ cells from 3-week, 14-week lineage-traced *mTert*-

mTmG animals (Figure 2.11C). While these data indicate that TERT+ cells often do not become activated, it does suggest that some animals may incur activation of TERT+ cells in the V-SVZ under certain situations and over longer time periods.

After a 3-week, 11-day lineage trace, mGFP+ cells in the ventricular lining and V-SVZ were negative for the stem cell marker Sox2 (Figure 2.12A). Interestingly, mGFP+Sox2+ cells were found in the midbrain (Figure 2.12B) and in the RMS after a 3-week, 11-day pulse-chase (Figures 2.11D and 2.8C). A subpopulation of mGFP+ cells in the RMS were DCX+ neuroblasts (Figure 2.11D). mGFP+ cells found in proximity to the RMS were DCX- and lacked the neuroblast phenotype (Figure 2.12C), indicating they may not be migrating neuronal precursors. The activation marker EGFR was co-expressed by lineage-traced mGFP+ cells in the brainstem after a 3-week, 11-day pulse-chase (Figure 2.12D). Finally, although no mGFP+ cells were found in the SGZ of the hippocampus after a 2-day, 0-day pulse-chase, nor following the 3-week, 11-day pulse-chase, we did observe 1 mGFP+ cell cluster in the DG of the hippocampus after the 3-week, 14-week pulse-chase (Figure 2.12E). This cluster of cells in the DG was EGFR+ (Figure 2.12E). Taken together, mGFP+ cells in the V-SVZ, RMS, and DG have the capacity to express markers of ASCs or progenitor cell types, indicating a cell type that has the potential to become activated in neurogenic brain regions, but TERT+ expression in these classical niches is far lower than in non-classical niches of the brain.

Lineage-traced cells co-expressed the mature neuron axonal marker NCAM in the olfactory bulb (Figure 2.11E). NCAM is expressed only in the ONL and PGL, and marks all PGL compartments due to expression of NCAM in olfactory sensory neurons [368]. mGFP signal was highly expressed in the ONL, but did not fill all PGL compartments after either a 3-week, 11-day nor after a 3-week, 14-week pulse-chase (Figure 2.11E). Unexpectedly, about half of female animals showed low or no mGFP signal in the ONL and PGL after a 3-week, 11-day pulse-chase, whereas all of the males had bright signal (Figure 2.12F). This was a rare display of sexual

dimorphism in these mouse models. The mature neuron marker TUJ1 was expressed by mGFP cells in the midbrain, identifying these cells as mature neurons (Figures 2.11F). Lineage-traced cells in the cerebellum also expressed TUJ1 and showed morphology indicative of mature neurons (Figure 2.11G). Taken together, it is clear that TERT+ cells give rise to a variety of neuronal cell types throughout the brain, which we confirmed by co-staining with mature cell markers, in both classic and non-classic neurogenic regions.

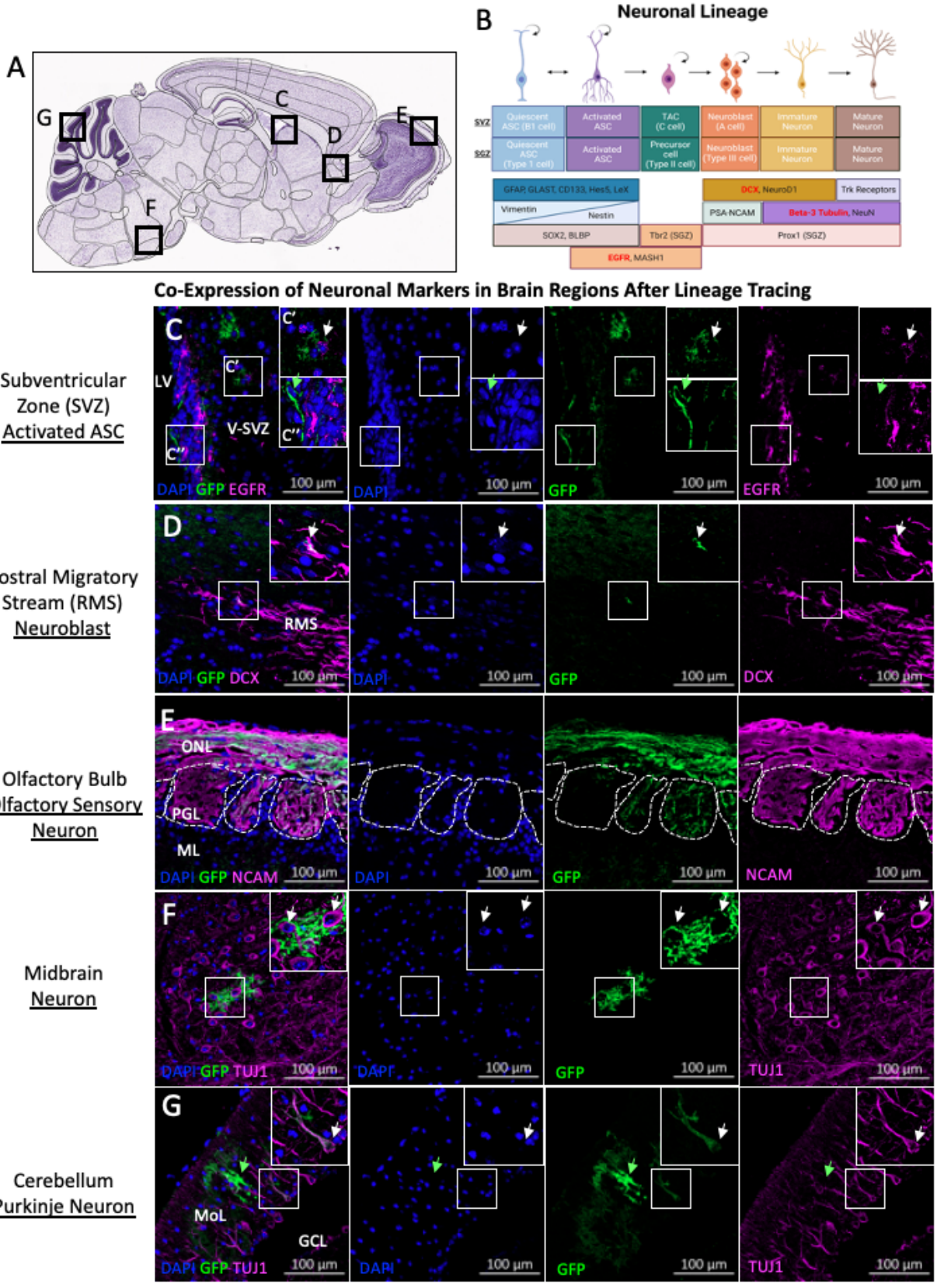
A
G
C
D
E
F
B
Neuronal Lineage
SVZ
SGZ
Quiescent ASC (B1 cell)
Activated ASC
TAC (C cell)
Neuroblast (A cell)
Immature Neuron
Mature Neuron
Quiescent ASC (Type 1 cell)
Activated ASC
Precursor cell (Type II cell)
Neuroblast (Type III cell)
Immature Neuron
Mature Neuron
GFAP, GLAST, CD133, Hes5, LeX
Vimentin
Nestin
SOX2, BLBP
Tbr2 (SGZ)
EGFR, MASH1
DCX, NeuroD1
Trk Receptors
PSA-NCAM
Beta-3 Tubulin, NeuN
Prox1 (SGZ)
Co-Expression of Neuronal Markers in Brain Regions After Lineage Tracing
Subventricular Zone (SVZ) Activated ASC
Rostral Migratory Stream (RMS) Neuroblast
Olfactory Bulb Olfactory Sensory Neuron
Midbrain Neuron
Cerebellum Purkinje Neuron
C
C'
C''
LV
V-SVZ
D
RMS
E
ONL
PGL
ML
F
G
MoL
GCL
DAPI GFP EGFR
DAPI
GFP
EGFR
DAPI GFP DCX
DCX
DAPI GFP NCAM
NCAM
DAPI GFP TUJ1
TUJ1
100 µm

Figure 2.11. Lineage tracing of TERT+ cells revealed immature and mature neuronal cell types throughout the adult mouse brain, confirming the multipotency of TERT+ ASCs.

(A) Sagittal mouse brain indicating the region each image was captured C-G (Allen Brain Atlas).

(B) Schematic depicting neuronal lineage markers; quiescent stem cell to mature neuron. Markers with red text were stained for in this image.

(C) Co-staining of lineage tracing mice after a 3-week, 14-week pulse-chase with the activated marker (EGFR). Both mGFP+EGFR+ (C', white arrow) and mGFP+EGFR- (C'', green arrow) cells were identified. No other mGFP+ cells expressed EGFR in the V-SVZ (N=5 males, 5 females with 2-day, 0-day pulse-chase, n=2 sections per brain; N=4 males, 4 females with 3-week, 11-day pulse-chase, n=2 sections per brain; N=6 females with 3-week, 14-week pulse-chase, n=2 sections per brain).

(D) Immunostaining of mTert-mTmG brains after a 3-week, 11-day pulse-chase stained with the neuroblast marker DCX in the RMS (seen in N=1 of 4 mice [N=1 of 2 males, 0 of 2 females], n=2 sections per brain analyzed)

(E) Representative image of co-immunostaining of OB stained with the olfactory sensory neuron marker NCAM after 3-week, 11-day pulse-chase (seen in N=4 of 5 mice [N=2 of 2 males, 2 of 3 females], n=2 sections per brain).

(F-G) Representative images of co-immunostaining with the mature neuron marker TUJ1 in the brainstem (F; N=2 of 4 mice [N=1 of 2 males, 1 of 2 females]) and cerebellum (G; N=3 of 4 mice [N=2 of 2 males, 1 of 2 females]) after a 3-week, 11-day pulse chase.

Scale bars are 100μm. Co-stained cells are indicated with white arrows. Cells that express mGFP only are indicated with green arrows. Insets show 4x digital magnification of indicated area. RMS: rostral migratory stream, MoL: molecular layer, GCL: granule cell layer, V-SVZ: ventricular-subventricular zone.

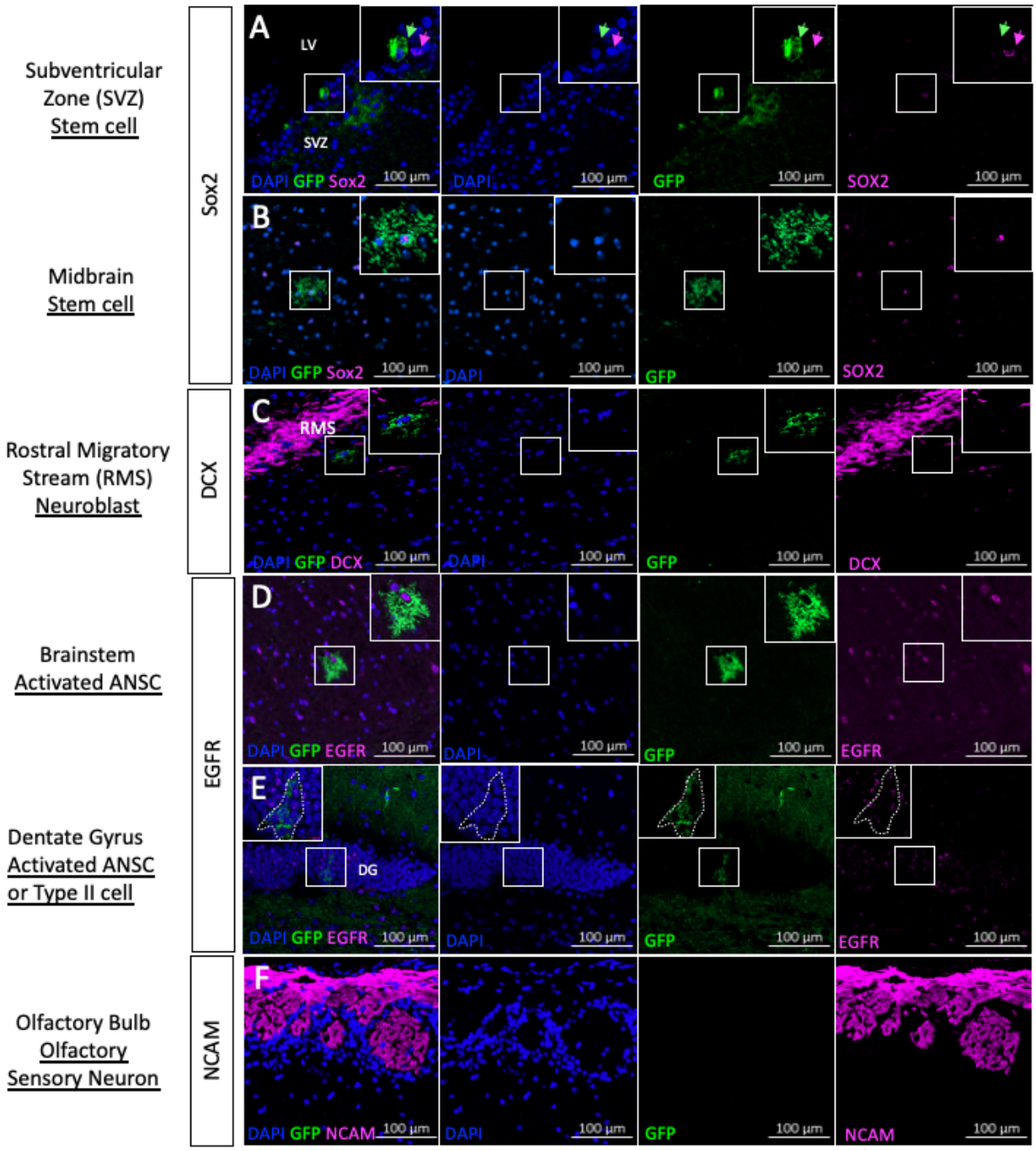
Subventricular Zone (SVZ) Stem cell
Midbrain Stem cell
Rostral Migratory Stream (RMS) Neuroblast
Brainstem Activated ANSC
Dentate Gyrus Activated ANSC or Type II cell
Olfactory Bulb Olfactory Sensory Neuron
Sox2
DCX
EGFR
NCAM
A
LV
SVZ
B
C
RMS
D
E
DG
F
DAPI GFP Sox2
DAPI
GFP
SOX2
DAPI GFP DCX
DCX
DAPI GFP EGFR
EGFR
DAPI GFP NCAM
NCAM
100 µm

Figure 2.12: Lineage trace of TERT cells leads to labeling of immature and mature neuronal cell types throughout the adult mouse brain.

(A-B) Representative images of 3-week, 11-day pulse-chased mTert-mTmG mouse brains stained for the stem cell marker Sox2 in the V-SVZ (A; N=2 of 2 females, n=2 sections per brain assessed) and midbrain (B; N=2 of 2 males, 2 of 2 females, n=2 sections per brain assessed).

(C) Representative image of mGFP+DCX- cell in proximity to RMS after 3-week, 11-day pulse-chase (cells identified in N=2 of 4 males, n=1-5 sections per brain assessed).

(D) Co-immunostaining with EGFR after 3-week, 11-day pulse-chase in the brainstem (N=1 of 2 males, n=2 sections per brain assessed).

(E) TERT+EGFR cell identified within the DG after a 3-week, 14-week pulse-chase. 1 mGFP+ cell was found within the DG across 78 brain sections in 3-week, 14-week pulse-chased animals (N=1 of 6 females, n=13 sections per brain analyzed). No mGFP+ cells were identified in the DG in 2-day, 0-day or 3-week, 11-day pulse-chased animals (N=4 males, 6-8 females, n=2 sections per brain analyzed).

(F) Representative image from a subset of female mice that showed little to no signal within the PGL or NL layers of the OB co-stained with the olfactory sensory neuron marker NCAM (N=3 of 10 mice [N=0 of 4 males, 3 of 6 females], n=2 sections per brain assessed).

(G) mGFP signal in the OB NL and PGL co-stained with Vimentin (N=7 of 10 mice [N=4 of 4 males, 3 of 6 females], n=2 sections per brain assessed). All images taken in sagittal plane. Scale bars are 100μm. Insets show 2x digital magnification. Arrows indicate expression of GFP (green), other indicated marker (magenta), or co-staining (white).

TERT cells give rise to various non-neuronal cell types including glia

After a 3-week, 11-day pulse-chase, mGFP+NG2+ cells were identified in the cerebellum (Figure 2.13C). These cells were therefore likely either GPCs or oligodendrocyte-restricted progenitors, whereas NG2+ cells in the meninges were not mGFP+ (Figure 2.14A). Lineage-tracing also revealed mGFP+OLIG2+ oligodendrocyte-lineage cells in a variety of brain regions, including the cerebellum, RMS, midbrain, and IoC (Figures 2.13D-2.13E and 2.14B-C). mGFP+GFAP+ cells in the astrocyte-lineage were observed in dense regions of the ventral hypothalamus (Figure 2.13F). Lineage-traced mGFP+ cells were identified lining all the ventricles

of the adult mouse brain and expressed ependymal markers Vimentin and GFAP (4^{th} ventricle shown in Figures 2.13G-2.14D). While rare, TERT-traced cells also expressed the microglial marker Iba1, indicating that TERT+ qASCs can differentiate into microglia in the adult mouse brain (Figure 2.14E). In addition to glial cell types, lineage tracing revealed mGFP+ mature ChP epithelial cells expressing AQP1 (Figure 2.14E). Taken together, TERT+ cells give rise to various glial cell types, in addition to neuronal cell types, throughout the adult mouse brain.

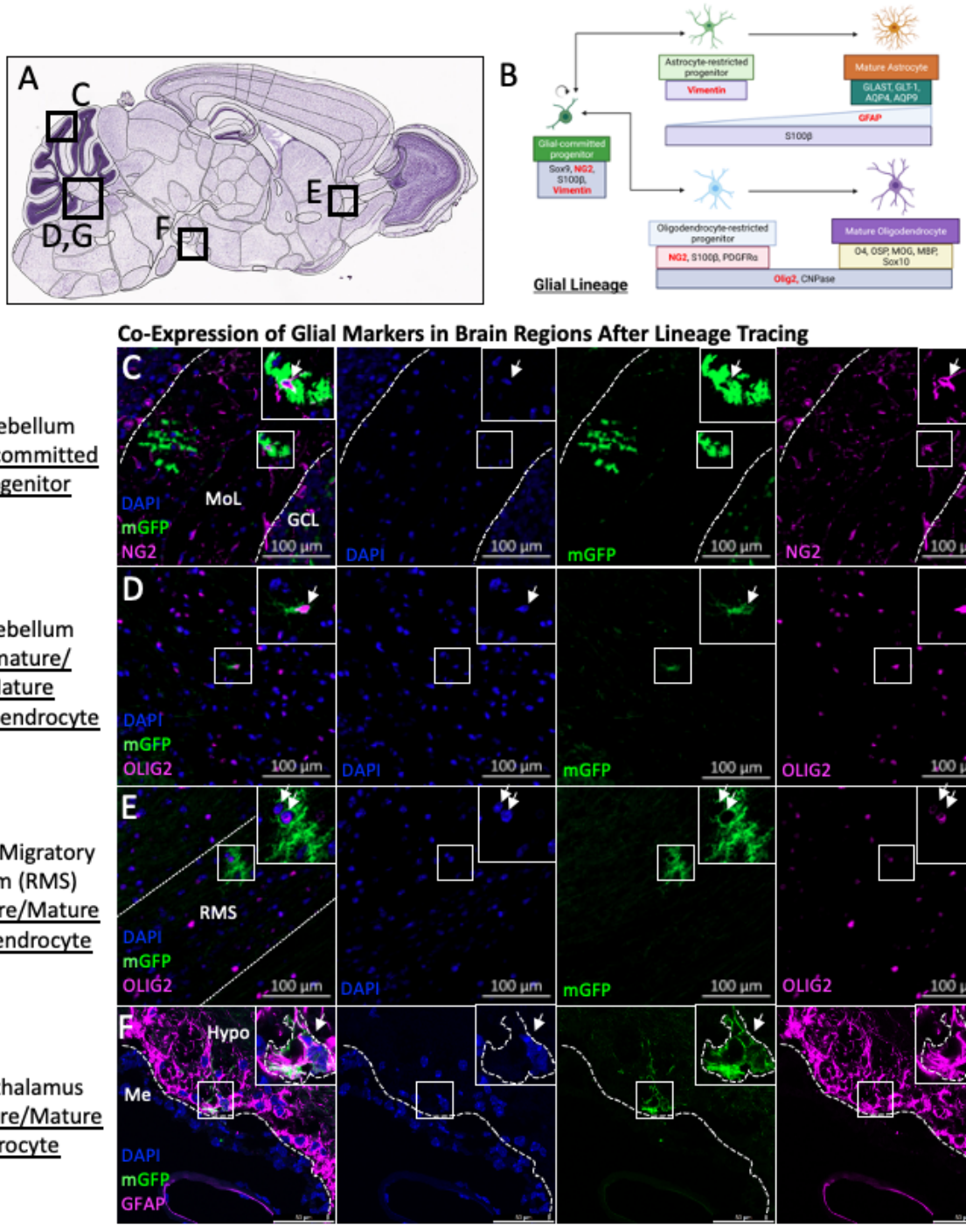
A
C
D,G
F
E
B
Astrocyte-restricted progenitor
Vimentin
Mature Astrocyte
GLAST, GLT-1, AQP4, AQP9
GFAP
S100β
Glial-committed progenitor
Sox9, NG2, S100β, Vimentin
Oligodendrocyte-restricted progenitor
NG2, S100β, PDGFRα
Mature Oligodendrocyte
O4, OSP, MOG, MBP, Sox10
Olig2, CNPase
Glial Lineage
Co-Expression of Glial Markers in Brain Regions After Lineage Tracing
Cerebellum
Glial-committed
Progenitor
Cerebellum
Immature/
Mature
Oligodendrocyte
Rostral Migratory
Stream (RMS)
Immature/Mature
Oligodendrocyte
Hypothalamus
Immature/Mature
Astrocyte
C
D
E
F
MoL
GCL
RMS
Hypo
Me
DAPI
mGFP
NG2
OLIG2
GFAP
100 µm

Figure 2.13. Lineage tracing of TERT+ cells revealed immature and mature glial cell types throughout the adult mouse brain, confirming the multipotency of TERT+ ASCs.

(A) Sagittal mouse brain indicating areas of images C-G (Allen Brain Atlas).

(B) Schematic depicting neuronal lineage markers of glial-committed progenitors through mature astrocytes and oligodendrocytes. Red text indicates markers stained in this figure.

(C-G) Co-staining of 3-week 11-day pulse-chased lineage tracing mice with the glial progenitor marker NG2 (C), the oligodendrocyte marker Olig2 (D-E), the hypothalamus (F), and the 4th ventricle (G) (N=4-5 of 5 males, 5-6 of 6 females showed this signal, n=2 sections per brain analyzed).

Scale bars are 100μm. White arrows indicate cells that co-express markers of interest. Insets show 2x digital zoom of indicated area. RMS: rostral migratory stream, MoL: molecular layer, GCL: granule cell layer, BV: blood vessel. 4V: 4th Ventricle

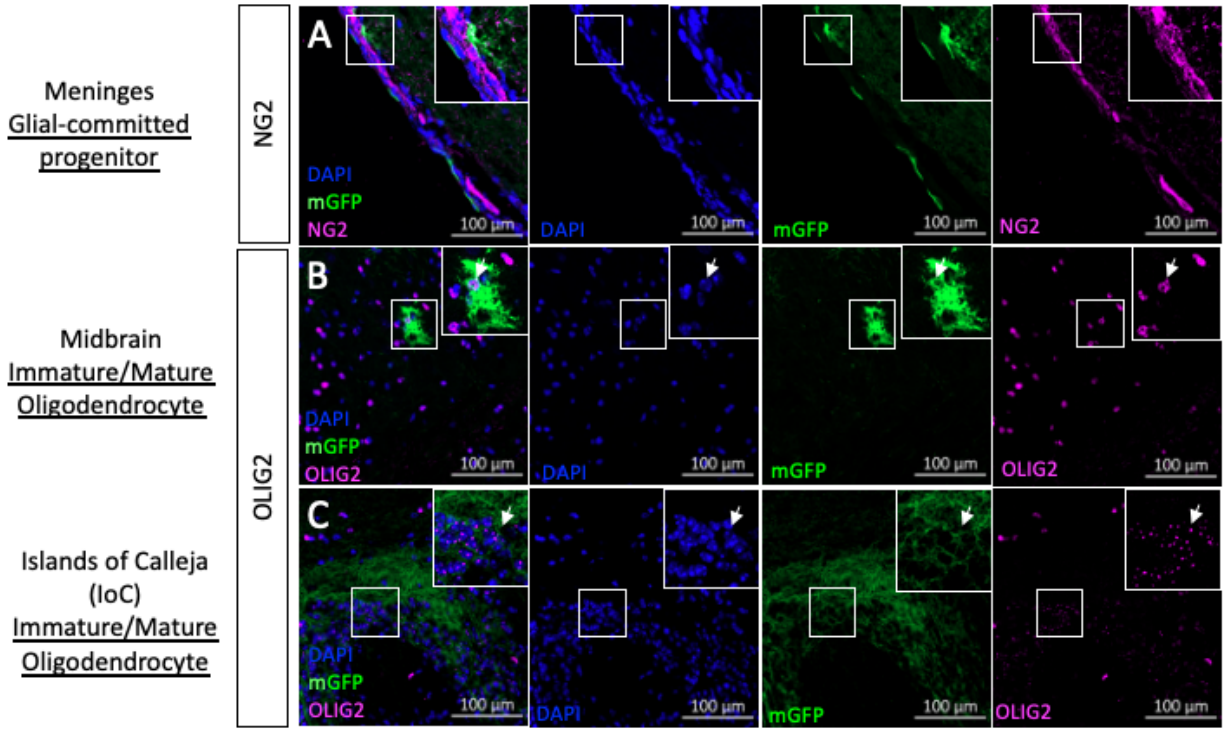

Figure 2.14: TERT+ cells give rise to numerous non-neuronal cell types, including glia, following lineage tracing

(A) Representative image of co-immunostaining with NG2 in 3-week, 11-day pulse-chased mTert-mTmG lineage tracing mice (N=5 of 5 mice [N=2 of 2 males, 3 of 3 females], n=2 sections per brain assessed).

(B-C) Representative OLIG2 co-staining with GFP in 3-week, 11-day pulse-chased mTert-mTmG mouse brains in the midbrain (B; N=3 of 4 mice [N=2 of 2 males, 1 of 2 females], n=2 sections per brain assessed) and IoC (C; N=4 of 4 mice [N=2 of 2 males, 2 of 2 females], n=2 sections per brain assessed).

(D) Representative co-staining of the astrocytic and ependymal marker GFAP in the 4V of 3-week, 11-day pulse-chased mTert-mTmG brains (identified in N=2 of 10 mice [N=2 of 4 males, 0 of 6 females], n=2 sections per brain assessed). Scale bars are 100μm. Insets show 2x digital zoom of indicated area. White arrows identify co-staining.

Discussion

Although adult neurogenesis was first discovered in avian brains in 1984 [369] and murine brains in 1992 [370, 371], the first evidence of human adult neurogenesis was as recent as 1998 [11]. The current understanding is that stem cells that can give rise to new mature neurons in the adult mammalian brain are restricted to certain neurogenic niches. Recently, these views have been challenged by the identification of stem cells that can give rise to neurons and glia in numerous other brain regions, such as the ChP [153], meninges [365], cerebellum [363], and more [343]. Here we report the identification of a rare, multipotent population of TERT+ qASCs in the adult murine brain. These TERT+ cells are distinct from GFAP+/Nestin+/Sox2+ cells, often termed quiescent adult neural stem cells (qANSCs) found within the SGZ or V-SVZ. While GFAP+/Sox2+/Nestin+ cells in the adult mouse brain are restricted to differentiation to neurons, astrocytes, and oligodendrocytes, TERT+ cells are truly multipotent and can differentiate into various subtypes of neurons, astrocytes, oligodendrocytes, ependymal cells, and choroid plexus epithelial cells. TERT+ qASCs are also less restricted anatomically than classical GFAP+

qANSCs, and we observe them in the basal state in numerous plastic brain regions. Due to the relative quiescence and multipotency of TERT+ cells, it is possible that previously described ANSCs in SVZ and SGZ may also be a mix of quiescent and activated stem cells and committed progenitors.

Despite the identification of molecular markers expressed by ANSCs in prior research, a specific and unique marker for qASCs in the adult mammalian brain had not yet been identified. Nestin, GFAP, GLAST, Sox2, and other markers have been proposed to mark slowly cycling multipotent stem cells, but each of these also marks multiple non-stem cell types throughout the brain. Nestin marks endothelial and meningeal cell types, GFAP and GLAST mark mature glia, and Sox2 is widely expressed throughout the brain. For these reasons, there is controversy in the field regarding the phenotype and localization of true qASCs in the brain [163]. TERT was an appealing candidate given the numerous prior studies investigating TERT+ qASCs in multiple tissues and organs. We now believe that TERT represents a more unique and specific marker of adult qASCs in the brain, as demonstrated by the low frequency of TERT+ cells in direct reporter mice and the ability of these cells to contribute to tissue turnover of mature numerous cell types as demonstrated in lineage tracing mice.

As discussed, a large percentage (53%) of TERT+ cells in the adult mouse brain express the immune cell marker CD45 (Figure 2.2). While TERT does mark a population of CD45+ immune cells in the brain these cells are likely circulating lymphocytes, as the majority of TERT+ CD45+ cells were identified in the ChP and meninges, brain regions with high immune infiltration. Human TERT (hTERT) is expressed by lymphocytes isolated from thymus, tonsil, and peripheral blood [372]. Therefore, TERT+CD45+ co-expressing cells may be infiltrating immune cells from the periphery via the bloodstream and glymphatic system. Previous studies have investigated the transdifferentiation of bone marrow derived TERT+CD45+ cells and concluded that TERT+CD45+ cells do not transdifferentiate into stroma, epithelium, and endothelium in the

endometrium [373]. Thus, TERT+CD45+ cells likely represent a committed or mature cell type that retains TERT expression, instead of a plastic cell type capable of renewing adult tissue like we describe here. Since CD45+ lymphocytes are post-mitotic, they are unlikely to contribute in any meaningful way to the lineage tracing observations in this study. It remains a possibility that a population of TERT+ cells are CD45-low microglia, which have mitotic properties. Further studies should investigate the role of TERT+ microglia in adult brain plasticity.

TERT+ cells represent a potentially heterogeneous population due to variable expression of CD45, Ki67, Nestin, and Sox2 observed in TERT-GFP+ cells. TERT was originally hypothesized to be expressed only by proliferative cells, since the telomerase enzyme, which is composed of TERT and a telomerase RNA component, prevents telomere shortening during chromosomal replication, thus allowing for continued cell division [374]. However, in other adult murine tissues such as the intestine, where TERT+ stem cells are low in number and rarely express Ki67, TERT clearly marks a population of adult tissue stem cells that are slowly cycling and quiescent. TERT may therefore carry out non-canonical functions in quiescent stem cells; indeed, tight mitochondrial control of the balance of glycolysis and oxidative phosphorylation is required in stem cells and TERT is understood to influence mitochondrial function distinct from its role in telomere extension [375]. The discovery of mostly non-proliferating, regenerative, multipotent TERT+ stem cells in the intestine, bone marrow, liver, adipose, long bone, kidney, heart, and now brain, is strong collective evidence for TERT as a marker of quiescent adult tissue stem cells [283-288, 344, 347, 348].

The ability of TERT+ cells to form neurospheres *in vitro* further supports these cells identity as neural stem cells, as the formation of neurospheres is a characteristic response, whereby proliferative stem cells can respond to cues such as the growth factors found in neurosphere culture media that activate the stem cells. As TERT+ cells appear to be quiescent *in vivo*, it is likely that the loss of GFP observed over time in neurospheres *in vitro* occurred due to activation

by EGF and bFGF in the culture media, leading to a proliferative and neurosphere-forming phenotype. Although TERT+ cells were activated in culture and could proliferate, as determined via EdU incorporation assays, TERT neurospheres were small, rarely reaching 50um. It is for this reason that no secondary sphere formation assays were assessed, although further experiments should be performed to determine whether TERT+ cells have the potential to grow enough for secondary sphere assays.

mTert-GFP direct reporter mice express GFP under the control of 4.4kb fragments of the mTert promoter region [284]. These cells express high levels of Tert mRNA transcripts as well as variable levels of GFP [284]. Analysis of this protein has been hindered by the lack of a specific TERT antibody. While the caveat remains that TERT-GFP+ cells could only be expressing the Tert mRNA and not translating to the TERT protein, prior studies have identified TERT-GFP+ cells exhibit telomerase activity, indicating the presence of functioning TERT protein within these cells [284]. mTert-rtTA::oTet-Cre::Rosa-mTmG mice have been validated previously as well in bone [287]. These TERT mouse models have also been utilized and validated in numerous prior tissue stem cell studies [283-285, 287, 288, 344, 347].

Although the V-SVZ and SGZ are classical neurogenic niches, there remains debate about how much the neurogenic capacity in these regions in rodent models translates to the adult human brain, as there are substantial discrepancies between human and mouse adult neurogenesis in both the V-SVZ and SGZ [376]. It is not yet fully understood where adult-born neurons from the human V-SVZ travel, as the human RMS remains elusive, however, some research indicates progeny of human V-SVZ ANSCs are destined for the striatum rather than the OB, which is much smaller in humans than mice [341]. In the human hippocampus, neurogenesis analysis relies heavily upon the presence of immature neurons, proliferative cells, and label retaining cells [11, 190, 194, 195, 197, 200]. Whether these immature neurons are derived from a population of stem cells within the niche, were created earlier in life as a pool of committed progenitors, or migrate

to the hippocampus from other brain regions, is currently unresolved. Additionally, depending on the analysis, adult human brains demonstrate rare or nonexistent hippocampal neurogenesis [196, 198, 199]. The underlying reason for the addition of these adult-born neurons in the striatum, and whether adult hippocampal neurogenesis in the DG persists past a few months into adult human life is still contested [190, 199, 201, 377-380]. Finally, it must be noted that while mTert mRNA expression and telomerase activity in the adult brain has been observed in mice [299]. In humans, while TERT expression has been observed [267, 298, 381], there is no evidence of human telomerase activity in the brain [298, 382]. In fact, human telomerase activity is decreased in the brain to undetectable levels after the 16th week of gestation [382].

It is possible that the most well-described adult neurogenic niches are mostly populated with committed neural progenitors and not multipotent qASCs, or they may represent a non-TERT separate pool of stem cells. This is supported by the rarity of TERT+ cells within the V-SVZ in both mTert-GFP and lineage tracing mice. Indeed, as we observed few TERT-traced cells within the RMS and GCL of the OB, it is likely that the V-SVZ/OB neurogenic axis does not populate the GCL with adult-born neurons as do GFAP+ cells within the V-SVZ. Previous studies have described the V-SVZ in TERT KO mice, wherein neurogenesis was significantly reduced [304]. TERT+ cells likely contribute to the neurogenesis in this region, although the process by which this occurs remains unknown. Our observations of TERT in the hippocampus in our two mouse models indicated that TERT+ cells may play a minimal role in adult neurogenesis in the SGZ. We only observed rare EGFR+ lineage-traced clusters of cells in the SGZ, even after a 3-week pulse, 14-week trace experiment in *mTert*-mTmG animals. The rarity of these events paired with the lack of TERT+ cells seen throughout the SGZ in mTert-GFP direct reporter mice, indicates that TERT-driven hippocampal neurogenesis may occur rarely, or at an extremely slow rate in the basal state. There is evidence that TERT overexpression in the hippocampus of Tert-/- mice improves the reduced dendrite outgrowth of DCX+ intermediate progenitors within the DG [305]. These

results indicate a role for TERT in the hippocampus. This paper utilizes TERT overexpression in a TERT KO mouse, which differs from our basal animals. The authors of this paper utilize TERT overexpression to reintroduce TERT expression in the brains of TERT KO mice, but by doing so may be introducing TERT expression to cells which may not express TERT under a basal state, which may explain the differences observed between the role of TERT expression and DCX+ intermediate progenitors and the lack of TERT in the DG observed by us. TERT+ cells and their progeny may be a rare quiescent stem cell population within these niches that do not proliferate or differentiate under basal conditions, in contrast to the intermediate progenitor cell types such as DCX+ neuroblasts. The lack of TERT+ cells in the DG and rarity of lineage tracing to hippocampal cell types do not support a role for TERT within the hippocampus during basal states. However, as both the V-SVZ and DG are areas of the brain that respond to various external stimuli, the potential for TERT effects in the hippocampus should be taken into consideration in further studies.

TERT+ cells and lineage-traced expansion of TERT+ cells and their progeny were identified through the adult mouse brain outside of the classical neuro/gliogenic niches, but within niches with prior evidence of adult neuro/gliogenesis. Lineage tracing revealed an increased number of GFP+ cells (meaning they derived from TERT+ precursors) compared to TERT direct reporter animals, across brain regions that included the meninges, ChP, cerebellum, brainstem, and thalamus. The presence of a rare population of TERT+ qASCs in these regions that gave rise to large numbers of multiple cell types clearly demonstrated that adult neuro/gliogenesis occurs in a far less restricted manner than previously believed. During development, neuroblasts migrate from the early postnatal V-SVZ to the medial prefrontal cortex, striatum, nucleus accumbens, and IoC. The cerebellum contained rare TERT+ cells in *mTERT*-GFP mice, but after lineage tracing, a large number of various mature cerebellar cell types were observed. While the cerebellum is known to harbor Sox2+ stem-like cells, the expansion of mature cell types from this stem cell

population is less than the V-SVZ or DG. Therefore, it was surprising to see such high levels of neuro/gliogenesis in the cerebellum after lineage tracing.

In the hypothalamus, a more recently identified neuro/gliogenic niche of the adult mouse brain, we identified expansion of mGFP+ cell signal within the ME and ARC. These cells did not co-express any glial cell markers. While these cells may have been neurons, which were created or expanded upon lineage tracing, these cells remain to be identified. In the hypothalamus, adult-born neurons and glia have been produced within the ARC and ME although the stem cell population that produces these cells is currently unknown. Additionally, this niche contains proliferative NG2+ glia and Olig2+ oligodendrocyte progenitor cells, which may contribute to the observed expansion of lineage traced mGFP+ signal.

Based on our data, we hypothesize that maintenance of a TERT+ population of ASCs in the brain is necessary to retain neurogenic and gliogenic potential throughout adulthood. Dysfunction in the maintenance of this population may play a role in the cognitive deficits seen in aging and neurodegenerative diseases. For example, TERT KO animals show decreased V-SVZ neurogenesis and stem cell numbers in adults, implicating TERT in stem cell renewal and niche function [304]. Consistent with this hypothesis, analysis of telomerase activity in the V-SVZ after injury shows that TERT+ cells may be injury-responsive [269]. In other adult tissues, TERT+ cells respond to injury by significantly increasing turnover and it is possible that these cells may not proliferate at high levels under homeostatic conditions, even in proliferative brain regions [285, 286]. The fact that telomerase activity in the V-SVZ is induced after injury may explain why low numbers of TERT+ cells and lineage-traced cells were observed in the V-SVZ during a basal state, as injury may be required for these cells to become activated.

In summary, we have identified a quiescent, multipotent stem cell population in the adult mouse brain which expresses TERT. These cells are located in various regions of the adult mouse brain and give rise to numerous adult-born mature cell types in the basal state of tissue turnover

and regeneration. Surprisingly, only a small population of TERT+ cells and their progeny were found in the traditional V-SVZ, RMS, and OB neurogenic niches, while no population of TERT+ cells existed in the SGZ. We hypothesize that the low number of GFP+ and mGFP+ cells identified in these classically neurogenic niches indicates that TERT+ cells may be a separate population of ASCs in the adult mammalian brain, or that they could have given rise to the stem/progenitor cells that have been previously studied in adult neurogenesis in these niches, earlier in development. It is also possible that these classical niches house activated stem cells or committed progenitors, but not qASCs, if TERT marks the sole qASC population in the brain. Intriguingly, TERT+ qASCs express only a subset of the markers previouly used for ANSCs, which could be because they are a true multipotent stem cell and not a purely neural/glial committed stem cell.

CHAPTER 3

SINGLE-CELL RNA SEQUENCING OF TERT LINEAGE-TRACED CELLS IN THE BRAIN REVEALS A ROLE OF TERT-DERIVED CELLS IN THE PROCESS OF NEUROPROTECTION AND NEURAL PLASTICITY IN RESPONSE TO CALORIC RESTRICTION

Abstract

Caloric Restriction (CR) as a dietary intervention extends lifespan and modulates adult neurogenesis throughout the adult brain, including the dentate gyrus (DG) of the hippocampus and the olfactory bulb (OB). However, the hypothalamus, which is another major neurogenic niche of the adult brain, and which coordinates energy balance throughout the body, has not been extensively studied in the context of CR. As neurogenesis within the hypothalamus is required for ciliary neurotrophic factor (CNTF)-induced weight loss and high-fat diet (HFD)-induced weight gain, it is understood that hypothalamic neurogenesis is vital for energy balance and metabolism. To understand the role of CR in adult hypothalamic neurogenesis, we performed single cell RNA sequencing (scRNAseq) using cells lineage traced from telomerase reverse transcriptase (TERT)-expressing cells in the adult mouse brain. TERT is expressed by a subset of adult stem cells (ASCs) that give rise to adult-born neurons and glia throughout the brain. CR treatment on adult mTert-rtTA::oTet-Cre::Rosa-mTmG lineage tracing animals revealed a decrease in TERT-traced cell signal within the median eminence (ME) of the hypothalamus, with no change in the arcuate nucleus (ARC), when compared to unrestricted diet (UR)-treated animals. CR treatment also revealed an increase in the neuroprotective gene brain lipid binding protein (BLBP) in TERT-traced cells after 1 month of CR. As neuroprotection is a classical response to inflammation, we then studied the role of TERT+ cells in the inflammatory process of aging. TERT+ cell numbers

varied with aging across neurogenic niches but remained a similar percentage of the full brain. However, TERT-traced cell signal increased significantly with aging, although label retention decreased. Aging was also required for the expression of BLBP in TERT-traced cells in the 4th ventricle. CR treatment in aged mice did not induce expression of neuroprotective or immune markers BLBP or Iba1 in TERT-traced cells within the hypothalamus. In all, lineage tracing of TERT+ ASCs in the adult mouse brain reveals hypothalamic changes in response to CR and full-brain changes in neuro/gliogenesis with aging.

Graphical Abstract

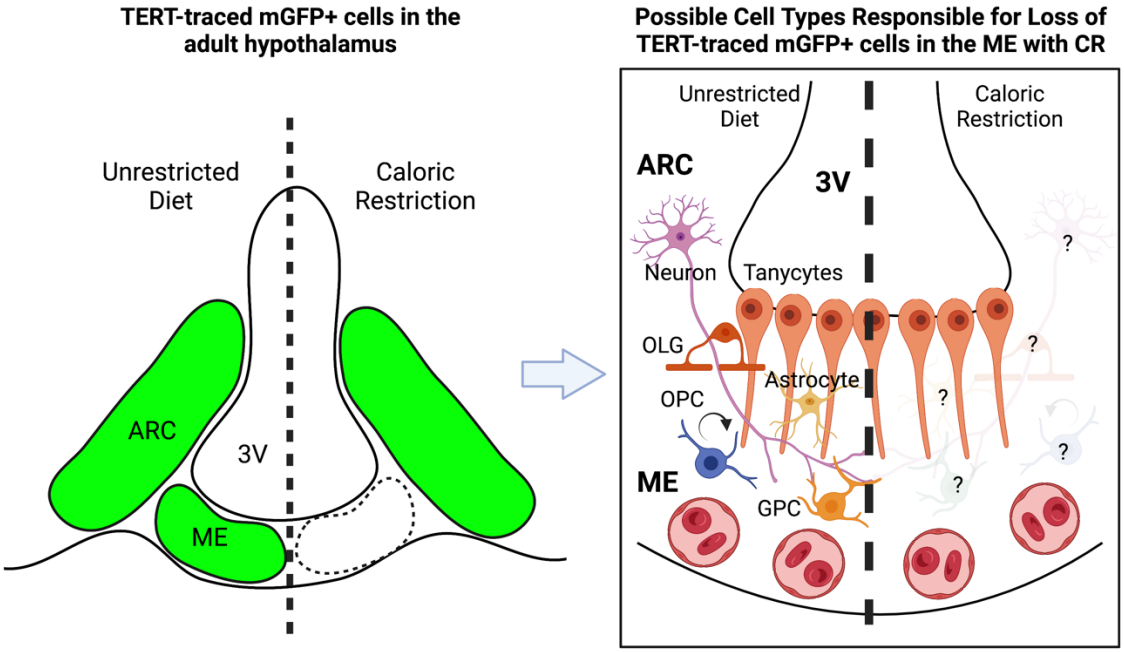

TERT-traced cell signal is reduced in the median eminence of the hypothalamus following caloric restriction, though the cell types responsible remain unknown. Green areas indicate the presence of membrane GFP (mGFP) after a pulse-chase in mTert-rtTA::oTet-Cre::Rosa-mTmG animals (left). Faded cell types identified via question marks identify populations of cells that may be TERT-traced and reduced with CR in the ME (right).
Abbreviations: TERT: telomerase reverse transcriptase, mGFP: membrane GFP, ARC: arcuate

nucleus, ME: median eminence, 3V: 3rd ventricle, CR: caloric restriction, OLG: oligodendrocyte, OPC: oligodendrocyte progenitor cell, GPC: glial precursor cell

Introduction

The mammalian hypothalamus produces adult-born neurons and glia through the processes of adult neuro/gliogenesis, as an adaptive response to respond to environmental stressors [59]. Under normal conditions, proliferation, and differentiation of quiescent adult stem cells (qASCs) and glial precursor cells (GPCs) in the hypothalamus produces adult-born neurons and glia [49, 58]. Both treatment with ciliary neurotrophic factor (CNTF), which reduces food intake and decreases body weight, or high-fat diet (HFD), increases hypothalamic neurogenesis and leads to adult-born orexigenic neuropeptide Y (NPY)-expressing and anorexigenic proopiomelanocortin (POMC)-positive neurons [383, 384]. Ablation of neurogenesis in the hypothalamus via mitotic inhibition prevents the weight loss associated with CNTF treatment [384]. Prevention of HFD-induced hypothalamic neurogenesis results in excessive obesity [55]. Taken together, hypothalamic neurogenesis is an important functional process in the adult brain, with full-body impacts.

HFD is a risk factor for diseases such as diabetes [385] and has multiple impacts on the mammalian brain, including in the neurogenic processes in the dentate gyrus (DG) of the hippocampus, where both acute and chronic HFD in the adult hippocampus reduce neurogenesis and ASC proliferation [386-388]. In the hypothalamus, HFD produces variable effects on adult neurogenesis depending on length of treatment, sex, and hypothalamic region [55]. In the median eminence (ME), neurogenesis increases with a 3-week HFD, while neurogenesis is decreased in the arcuate nucleus (ARC) [55]. Increased hypothalamic neurogenesis has been identified after as little as 3 days of HFD in adult mice [383]. Interestingly, these changes are associated with

hypothalamic reactive gliosis, which occurs prior to diet-induced obesity and results in neuronal apoptosis [337].

Caloric restriction (CR) is defined as a reduction in average daily caloric intake without malnutrition [389]. CR extends lifespan and appears to be a conserved metabolic response, as it has been identified to improve the lifespan of worms [390], mice [391], non-human primates [392-394], and humans [395, 396]. CR processes associated with aging include decreased metabolic rate and reduced oxidative damage [397]. In the adult brain, CR is correlated with increased neurogenesis and expression of brain-derived neurotrophic factor (BDNF) in the hippocampus [398-401]. The neurogenic effects of CR in the DG are observed between 2 weeks and 8 months and are therefore similar between acute and chronic treatment [398, 399]. In the V-SVZ and olfactory bulb (OB), CR increases neurogenesis in a time-dependent manner through the actions of acyl-ghrelin, indicating a connection between CR-induced plasticity and metabolic processes [402, 403]. In the adult mouse hypothalamus, CR in conjunction with HFD decreases adult hypothalamic proliferation specifically within the ME [55]. CR following HFD increases the number of label-retaining cells in adult mice, although these cells were not identified as neuronal [133] and may have resulted from the microglial proliferation in the hypothalamus that accompanies HFD [132, 404]. While further studies are required to understand the role of CR in the hypothalamus, gene expression analysis revealed decreased expression of insulin and ghrelin in an age-dependent manner, indicating that pathways which govern adult neurogenesis in response to CR in the V-SVZ and DG are also present in the hypothalamus [331].

Inflammation in the adult brain is characterized by activation of microglia, specialized macrophages seeded in the brain and spinal cord during development [405]. Microglia-driven inflammation decreases adult neurogenesis in the hippocampus [406-408]. In this niche, inflammation results in microglial phagocytosis of immature newborn neurons [409, 410] and neuroblasts [406, 411]. These effects are mirrored in the hypothalamus where the pro-

inflammatory HFD treatment is associated with microglial activation and neuronal death in adult mice [337, 404]. Acute HFD (3 days to 3 months) results in a period of proliferation in the hypothalamus [55, 133, 336, 337, 383], which is associated with increased microglial proliferation and activation [337, 404]. Chronic HFD (4 months to 8 months) leads to decreased neurogenesis in this niche paired with cell death [383, 412]. Indeed, a 4-month HFD induced IKKB/NF-KB-controlled apoptosis and impaired neuronal differentiation [412]. Interestingly, while both acute and chronic HFD are associated with hypothalamic inflammation, they exhibit opposite effects on neurogenesis. Unlike HFD, CR inhibits inflammation in humans [411, 413] and rodents [414], as both short-term and long-term CR decrease microglial activation [402]. While microglial activation is reduced with CR, glial activation appears to decrease in response to CR in some studies [415, 416] and decrease in others [417]. In the hypothalamus, CR reduces microglial activation after lipopolysaccharide (LPS) treatment [418]. These effects may be due to the decrease in expression of the inflammatory cytokines IFN-y, IL-6, and TNF-a [419-422] and the increase in BDNF and insulin growth factor 1 (IGF-1) expression [423-425].

Aging is associated with increased inflammation [426, 427] and decreased neurogenesis in the SGZ [428, 429], V-SVZ [430], and hypothalamus [431]. Age-related changes in neurogenesis can be attributed to inflammation [432], breakdown of the blood-brain barrier [433] and blood cerebrospinal fluid (CSF) barrier, and changes in the composition of the CSF [135]. Due to the anti-aging effects of CR in mice and humans, it is hypothesized that CR may reduce the effects of aging on neurogenesis. Indeed, CR attenuates the age-associated changes in mouse brains [434] including microglial activation [435]. CR may slow age-associated inflammation via the process of neuroprotection [436]. Neuroprotection is conferred in part by the expression of neurotrophins, which work to prevent neuronal apoptosis. Neurotrophins increased with CR include BDNF, neurotrophin-3 (NT-3), and glial cell line-derived neurotrophic factor

(GDNF) [400, 401, 423, 424, 437]. In fact, there is evidence that neurogenesis is enhanced in response to CR through the actions of BDNF [437].

The role of CR on adult hypothalamic neurogenesis remains less completely understood than the 'classic' neurogenic niches of the V-SVZ and DG. This is in part due to the lack of specific and unique markers of qASCs, and the questions that surround the process of neuronal differentiation in the hypothalamus [49]. Recent work has localized telomerase reverse transcriptase (TERT)-expressing qASCs to the adult mouse hypothalamus (Chapter 2). Lineage tracing of TERT+ cells in the adult mouse brain revealed the expansion of lineage-traced cells throughout the ARC and ME of the hypothalamus (Chapter 2). To understand the role of CR on hypothalamic neurogenesis we performed single cell RNA-sequencing (scRNAseq) on cells lineage traced from telomerase reverse transcriptase (TERT)-rtTA::oTet-Cre::Rosa-mTmG adult mice in the brain and further analyzed the relationship between TERT-traced cells and markers of neurogenesis and neuroprotection. TERT has been identified as a marker for qASCs in the adult mouse brain (Chapter 2).

Here, we describe the relationship between CR and neuroprotective gene expression by TERT-traced cells in the adult mouse brain, highlighting the importance of these adult-born cells in responding to metabolic intervention in the adult brain. Neuroprotective genes RBM3, CIRBP, and BLBP are upregulated in TERT-traced cells in response to CR in adult mTert-mTmG::oTet-Cre::Rosa-mTmG mice across various mature cell types. In addition, we identify the expansion of TERT-traced cells in the ME of the adult hypothalamus is reduced with CR. Overall, mature cell types traced from TERT+ stem cells in the brain clearly respond to metabolic cues and must be considered in future hypothalamic plasticity studies.

Materials and Methods

Mice

All procedures were approved by the Ohio State University IACUC. Mice were maintained on a 12 hr light/dark cycle, and food and water was provided ad libitum. mTert-rtTA:: otet-Cre:: $R26R^{flox(mTmG)}$ mice were generated by crossing mTERT-rtTA mice [2] to otet-Cre:: $R26R^{flox(mTmG)}$ mice, which were generated in our lab by crossing B6.Cg-Tg(tet0-cre)1Jaw/J mice (The Jackson Lab) to B6.129(Cg)-Gt(ROSA)26Sor$^{tm4(ACTB-tdTomato,-EGFP)Luo}$ mice (The Jackson Lab) (Jensen & Beaulieu). Recombination was induced via 2 mg/ml doxycycline (Sigma Aldrich) in 50 mg/ml sucrose water. To chase, doxycycline water was replaced with normal drinking water. Both male and female animals were utilized. For caloric restriction, animals were single caged and basal food intake was determined by weighing food daily over 7 days. For each of the calorie restricted animals, an amount of chow equal to 30% less than the average initial food intake was given per day. All unrestricted diet animals were given pair-fed chow. Ad libitum (ad lib) animals had unlimited access to food. Food intake was measured daily, and body weight was recorded twice per week throughout the study.

Body Composition Analysis

One day prior to perfusion animals underwent analysis of fat, lean, free water, and total water masses using the EchoMRI 3-in-1 body composition analyzer at the Ohio State University Small Animal Imaging Core. No anesthesia or special preparation was required.

Brain Dissociation, FACS, and Sample Collection

To obtain single cell suspensions of adult mouse brains, mice were sacrificed via CO_2 followed by cervical dislocation. Brains were isolated and washed with artificial cerebrospinal fluid (ACSF) (Ecocyte). Brains were then diced with a razor blade in a petri dish containing ice-cold ACSF with 1 mg/mL pronase (Millipore-Sigma) until brain pieces were uniform sizes. Brains were then transferred to loosely capped 50 mL falcon tubes placed in a shaking water incubator (37°C and 90 rpm) for 60-75 min until cloudy. Every 5 minutes the tubes were vortexed and then returned to the shaking incubator. Samples were then centrifuged at 1600 rpm for 4 min and supernatant decanted. Samples were then treated with ACSF with 5% fetal bovine serum (FBS) for 15 min while shaking at 90 rpm and 37°C. Trituration of each sample was performed with pasteur pipettes of 600 µm, 300 µm, and 150 µm openings. Samples were centrifuged at 300 x g for 10 min and supernatant decanted. Debris removal solution (Miltenyi) was utilized to remove debris and myelin from the samples. Cells were resuspended in ACSF with 10% FBS and stored on ice until sorting. Cells were sorted for endogenous membrane GFP fluorescent signal on a Kraken- BD Fortessa machine at the Nationwide Children's Hospital Flow Core. Cells were sorted into 1X PBS (Ca2+ and Mg2+ free) containing 0.04% w/v BSA. Cells were spun at 150 x g for 3 min and pellets were resuspended in 60 uL 1X PBS (Ca2+ and Mg2+ free) containing 0.04% w/v BSA. Samples were transferred to the Ohio State University Genomics Shared Resource, where cell number and viability were analyzed via hemocytometer.

Preparation of RNA-seq Libraries

For scRNAseq experiments, the following reagents were used: Chromium Next GEM Single Cell 3' Kit v3.1, 16 rxns (PN-1000268), Chromium Next GEM Chip G Single Cell Kit, 16 rxns (PN-1000127), Dual Index Kit TT Set A, 96 rxns (PN-1000215) were used according to the manufacturer's instructions for the GEM Single Cell 3' Kit v3.1, 16 rxns (PN-1000268).

EdU Administration

EdU in 0.9% NaCl was injected at 50mg/kg via intraperitoneal (i.p.) injections 18 days prior to perfusion using an EdU click reaction kit (Baseclick; BCK-EdU647).

Immunostaining

Mice were anesthetized via peritoneal injection of 320 mg/kg body weight Ketamine and 24 mg/kg body weight Xylazine in 0.9% saline and then sacrificed via transcardial perfusion with 1X PBS followed by Histochoice Fixative, after loss of motor and ocular reflexes. Brains were post-fixed overnight at 4°C, then placed in 15% sucrose at 4°C for 2 d, followed by 30% sucrose at 4°C for 2 d. Brains were then divided into coronal or sagittal sections using adult mouse brain matrices and then frozen in optimal cutting temperature compound (Sakura) and stored at -20°C until slicing. Brains were sliced on a CM1950 cryostat (Leica) at -20°C. Two slices of 7µm were adhered to each slide. Slides were stored at -20°C until used for immunostaining, at which point they were warmed up to room temperature and post-fixed with ice-cold acetone for 15 min. Slides were washed for 5 min in 1X IHC Select TBS Rinse Buffer shaking at 60 rpm at room temperature (RT) between each step. Permeabilization for staining of nuclear antigens was performed with 0.3% Triton X-100 for 10 min at RT. Permeabilization for staining of cytoplasmic antigens was performed with 0.3% Tween-20 for 10 min at RT. Antigen retrieval was performed by microwaving slides in 1X DAKO Antigen Retrieval Solution on low for 10 min twice. Slides were then incubated in 0.3% Typogen Black in 70% EtOH for 20 min at RT, blocked for 20 min at 37°C with Millipore Blocking Reagent, and incubated with primary antibody diluted in antibody diluent overnight at 4°C. Antibody concentrations are listed in the Key Resource Table. The next day, sections were incubated in Alexa Fluor secondary antibodies for 10 min at RT, then counter-stained with

100ng/mL DAPI for 5 min. Epifluorescence images were captured on Nikon E400 microscope with a Hamamatsu Flash 2.0. Confocal images were captured on a Stellaris 5 (Leica) for co-expression analysis.

Optical Clearing of Brain Sections

Adult male mTert-rtTA::oTet-Cre::Rosa-mTmG mice and Cre-, negative control mice were transcardially perfused with 1X PBS and 4% PFA after a 3-week, 11-day doxycycline pulse-chase. Brains were excised fully intact and post-fixed in 4% PFA overnight at 4°C and then again for 1hr at room temperature. Brains were washed in 1X PBS for an hour two times at room temperature and then cut into 1,000µm thick sagittal sections using a 500 µm brain block and placed back into 5 mL microcentrifuge tubes containing 1X PBS and proceeded to methanol pre-treatment as described by (Renier, N., 2014). Next, samples were incubated in 1X PBS/0.2% TritonX-100/20% DMSO/0.3M glycine at 37°C overnight on orbital shaker and then blocked in 1X PBS/0.2% TritonX-100/10% DMSO/6% donkey serum at 37°C for 3 days on an orbital shaker. Samples were then washed in 1X PBS/0.2% Tween-20 with 10µg/ml heparin for 1h twice at 37°C and then incubated in 1X PBS/0.2% Tween-20/10µg/ml heparin/5% DMSO/3% donkey serum containing a 1:500 concentration of rabbit anti-GFP Alexa Fluor 488 at 37°C on an orbital shaker for 2 days. Samples were then washed in 1X PBS/0.2% Tween-20 with 10µg/ml heparin for 1 hour at 37°C on orbital shaker, 3 times, and then once a day for 2 days. Tissues were then cleared with the iDISCO method detailed in Renier et al., 2014. Cleared brains were refractive index matched with, and imaged while submerged in, dibenzyl ether which is corrosive to most objective lenses and most plastics. To mitigate this, we took a glass bottom dish and coated any interior plastic with quick drying silicone elastomer (Kwik-Sil). Cleared brains were imaged on a Lecia Stellaris 5 confocal microscope with a white light laser (ex. 495, em. 505-600) intensity set to 20%. Images were captured with a 10X dry objective at 1024x1024 resolutions with pinhole set to 1 AU. Line scan speed was set to 600 Hz and lines were averaged 3 times per frame. Photons were captured

with Power HyD S detectors; gain set to 20%. Images were captured as Z-stacks; a total range of 500 µm with a 6 µm step-size (84 images per stack) Z-stacks were tiled together to form a complete image of each brain slice. These were then Z-maximum intensity projected into a comprehensive 2D image.

Fiji Analysis

Z-maximum intensity projections were opened in ImageJ (NIH, http://imagej.nih.gov/ij). For EdU+ cell counting, images were converted to 8-bit (Image -> Type -> 8-bit), thresholded (Image -> Adjust -> Threshold), and individual cells were quantified (Analyze -> Analyze Particles). For GFP fluorescence quantification, a region of interest (ROI) was identified (full brain was used for ROI), background subtraction was performed (Process -> Subtract Background), and images were measured (Analyze -> Measure) for fluorescent intensity.

Statistical analysis

All statistical analyses in this study were performed via student's t-test, as analyses were performed across two groups (aged vs. young or CR vs. UR). *P ≤ 0.05, **P ≤ 0.01, ***P ≤ 0.005, ****P ≤ 0.001.

Results

Caloric Restriction Induces Neuroprotective Changes in TERT-traced Cells

TERT+ qASCs in the adult mouse brain are multipotent and give rise to neurons, glia, ependyma, choroid plexus epithelial cells (CPECs) and other mature cell types. Due to the multi-faceted signaling changes affecting various cell types following CR, we hypothesized that single cell RNA sequencing (scRNAseq) of TERT-traced cells would reveal key signaling pathways by which these cells coordinated changes in neurogenesis and plasticity. Mice were administered CR or unrestricted (UR) diet for 33 days during a doxycycline pulse-chase (Figures 3.1A, B). CR resulted in a decreased change in percent body weight from initial after 15 days of caloric restriction (Figure 3.1C). Brains were then used for FACS isolation of GFP+ cells, followed by scRNAseq of samples from both CR and UR treated animals (Figure 3.1D, E). There were no significant differences in the cell number (Figure 3.1F), concentration of cDNA per sample (Figure 3.1G), or nucleotide concentration per library between CR and UR samples (Figure 3.1H). Cluster analysis and differential expression between CR and UR animals was performed by Kaitlyn Hajdarovic (Brown University) and are not shown in this dissertation. UMAP analysis of TERT-traced cells isolated from mTert-rtTA::oTet-Cre::Rosa-mTmG brains revealed TERT-traced arachnoid barrier cells, astrocytes, choroid plexus cells, dendritic cells, endothelial cells, microglia, macrophages, neurons, olfactory ensheathing glia, oligodendrocytes, and pericytes. Differential analysis of transcript expression across treatments identified both transcripts that were upregulated with CR and transcripts that were downregulated with CR (data analyzed by Kaitlyn Hajdarovic). The transcripts RBM3, CIRBP, and BLBP, which are all associated with neuroprotection, were all upregulated with CR. Cell-type specific differential expression analysis revealed CR-directed upregulation of BLBP in astrocytes, CIRBP in microglia, olfactory ensheathing glia, and oligodendrocytes, and RBM3 in choroid cells, microglia, olfactory

ensheathing glia, and oligodendrocytes (data analyzed by Kaitlyn Hajdarovic). Taken together, CR directs the expression of neuroprotective transcripts in TERT-traced cells across multiple cell types.

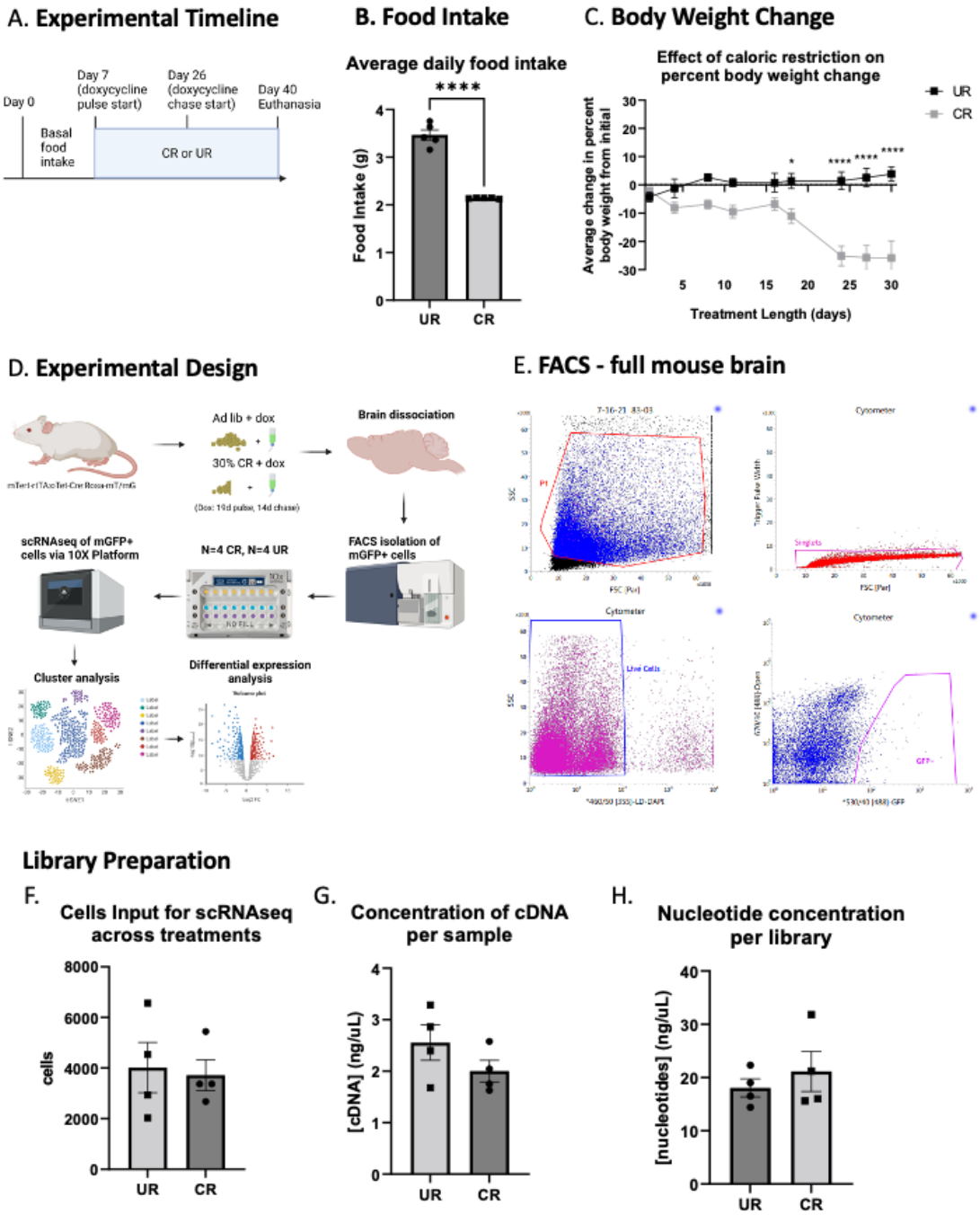

Figure 3.1 - Caloric Restriction Induced Neuroprotective Changes in TERT-traced Cells

A) Experimental timeline of caloric restriction concomitant with doxycycline pulse-chase in adult mTert-rtTA::oTet-Cre::Rosa-mTmG mice.

B) Daily food intake from D7-D40 of CR/UR-treated mice averaged per mouse (N=5 mice per group).

C) Average change in percent body weight from initial per group (N=5 mice per group).

D) Experimental design of scRNAseq of TERT-traced cells and downstream analysis (N=4 mice per group).

E) FACS plots detailing isolation of TERT-traced GFP-labeled cells from the adult mouse brain (N=5 mice per group).

F) Number of cells used for scRNASeq library preparation per sample (N=4 mice per group).

G) cDNA concentration per sample (N=4 mice per group).

H) Nucleotide concentration per library (N=4 mice per group).

Graphs show mean ± SEM. *P<0.05; **P<0.01, ***P<0.005, ****P<0.001.

Caloric Restriction-Induced Reduction in Adiposity and Increased Thermogenesis is Associated with Changes in TERT-traced Signal in the ME

CR-directed neurogenic modulation occurs throughout multiple plastic niches of the adult mouse brain, including the SGZ, V-SVZ, OB, and hypothalamus. In the hypothalamus, CR reduces proliferation in the ME, which has full-body implications as ME proliferation is required for weight gain on HFD. As scRNAseq did not elucidate the brain regions in which the identified TERT-traced cells were found, a replicate study was performed to identify changes in TERT-traced cells throughout the hypothalamus. Here, mice underwent a CR or UR intervention as discussed in Figure 3.1 (Figures 3.2A, B). CR once again resulted in a decreased change in percent body weight from initial (Figure 3.2C), in part due to a reduction in the weight of

perigonadal white adipose tissue (pgWAT; Figure 3.2D). Body composition analysis via Echo-MRI revealed decreased body weight with CR paired with decreased fat mass and adiposity (Figure 3.2E). These findings were paired with a trend towards increased lean mass in CR-treated mice and a significant increase in leanness (Figure 3.2E). There were no significant changes in free water or hydration ratio between groups (Figure 3.2E). Thermal imaging of interscapular brown adipose tissue (iBAT) revealed an increase in thermogenesis in CR-treated mice who lost at least 20% BW when compared to UR mice or CR-treated mice who did not lose 20% BW (Figure 3.2F). In the hypothalamus, TERT-traced GFP+ cells were localized to the arcuate nucleus (ARC) and median eminence (ME) (Figures 3.2G, H). There was no difference in GFP fluorescent intensity in the mGFP expression of the full hypothalamus with CR when compared to UR-treated mice (Figures 3.2G-I). Similarly, there was no difference in the GFP fluorescent intensity within the ARC of animals treated with CR or UR (Figures 3.2G'-H'; 3.2J). However, CR significantly reduced the expression of GFP fluorescent intensity in the ME (Figures 3.2G''-2H''; 3.2K). Taken together, CR improved the metabolic profile of adult mTert-rtTA::oTet-Cre::Rosa-mTmG, which was associated with reduced TERT-traced mGFP signal in the ME, but not ARC.

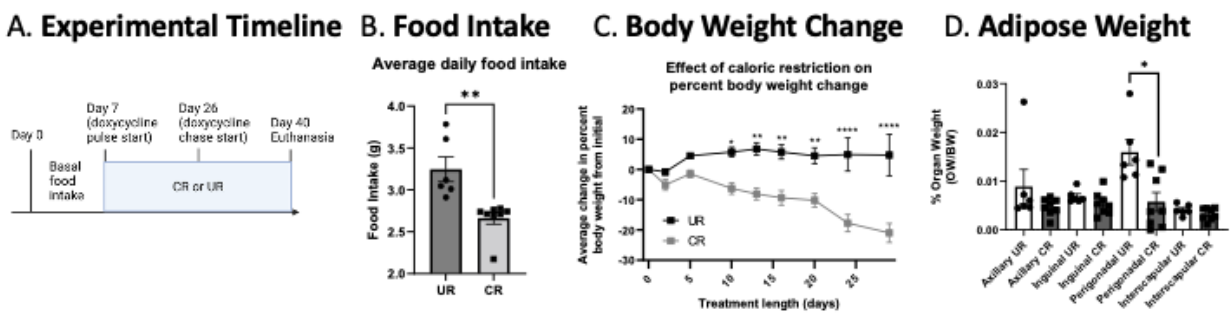
A. Experimental Timeline
B. Food Intake
C. Body Weight Change
D. Adipose Weight
Day 0
Day 7 (doxycycline pulse start)
Day 26 (doxycycline chase start)
Day 40 Euthanasia
Basal food intake
CR or UR
Average daily food intake
Food Intake (g)
UR
CR
Effect of caloric restriction on percent body weight change
Average change in percent body weight from initial
Treatment length (days)
% Organ Weight (OW/BW)
Axillary UR
Axillary CR
Inguinal UR
Inguinal CR
Perigonadal UR
Perigonadal CR
Interscapular UR
Interscapular CR

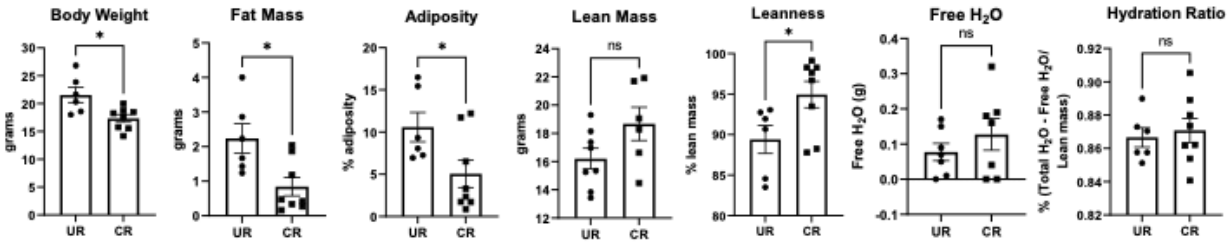
E. Body Composition of Caloric Restricted vs. Unrestricted Diet Groups (Echo-MRI)
Body Weight
Fat Mass
Adiposity
Lean Mass
Leanness
Free H2O
Hydration Ratio
grams
% adiposity
% lean mass
Free H2O (g)
% (Total H2O - Free H2O/ Lean mass)
UR
CR
ns

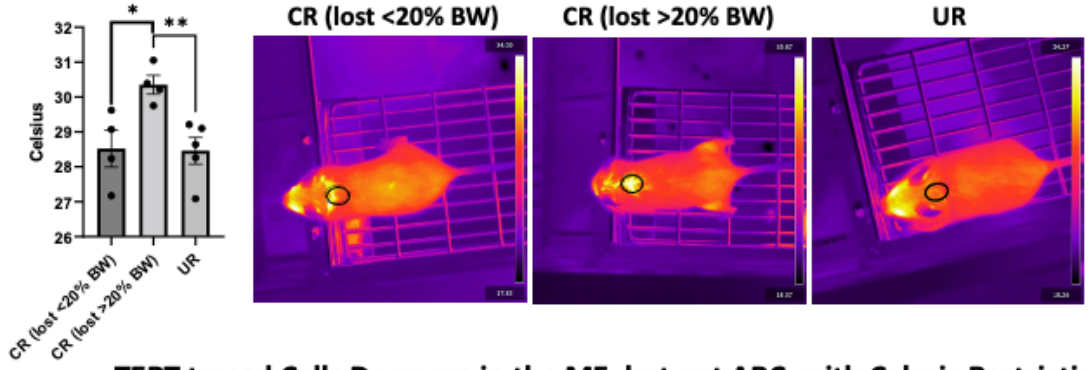
F. Thermal Imaging of BAT
Celsius
CR (lost <20% BW)
CR (lost >20% BW)
UR

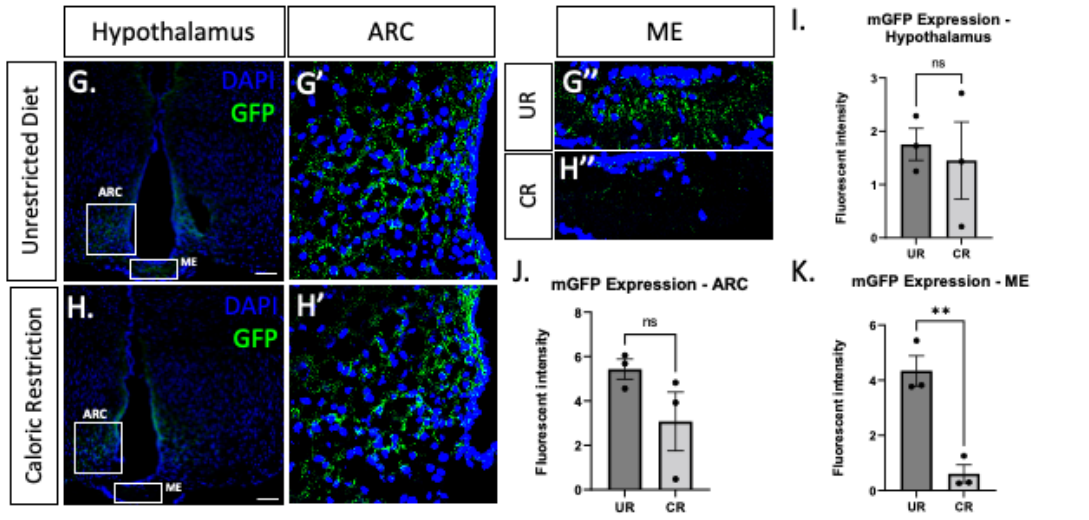
TERT-traced Cells Decrease in the ME, but not ARC, with Caloric Restriction
Hypothalamus
ARC
ME
Unrestricted Diet
Caloric Restriction
UR
CR
G.
G'
G''
H.
H'
H''
DAPI
GFP
I.
mGFP Expression - Hypothalamus
J.
mGFP Expression - ARC
K.
mGFP Expression - ME
Fluorescent intensity
ns

Figure 3.2 - Caloric Restriction-Induced Reduction in Adiposity and Increased Thermogenesis was Associated with Changes in TERT-traced Signal in the ME

A) Experimental timeline of caloric restriction concomitant with doxycycline pulse-chase in adult mTert-rtTA::oTet-Cre::Rosa-mTmG mice.

B) Daily food intake from D7-D40 of CR/UR-treated mice averaged per mouse (N=6-8 per group; N=2-3 female, N=4-5 male).

C) Average change in percent body weight from initial per group (N=6-8 per group).

D) Weight of adipose tissues per mouse at euthanasia (N=6-8 per group).

E) Body composition analysis via Echo-MRI of body weight, fat mass, adiposity (%fat), lean mass, leanness (%lean), Free H2O, and hydration ratio per mouse (N=6-8 per group).

F) Thermal imaging analysis of iBAT across CR mice with body weight loss <20%, CR mice with body weight loss >20%, and UR mice (N-6-8 per group).

G-H) Representative immunofluorescence of mGFP signal through the ARC and ME of the hypothalamus in coronal brain sections of UR (G) and CR mice (H). Insets are shown in G', G'' and H', H'' (N=3 mice per group).

I-K) Quantification of mGFP fluorescent intensity within the full hypothalamus (I), ARC (J), and ME (K; N=3 mice per group, n=2-4 brain sections per brain).

Insets show indicated area at 3x digital zoom. Scale bars are 100μm. Graphs show mean ± SEM. *P<0.05; **P<0.01, ***P<0.005, ****P<0.001.

<u>BLBP Expression is Unaffected by Caloric Restriction and is not Expressed by TERT-traced Cells in Ventricular Niches</u>

Increased BLBP expression in TERT-traced astrocytes after CR supports a neuroprotective phenotype, as BLBP expression is increased in astrocytes during reactive astrogliosis. In addition, the expression of BLBP in astrocyte-like cells has been associated with stemness of such BLBP+ cells, both in embryogenesis and adulthood. BLBP expression was examined through immunostaining of coronal brain sections to identify changes in BLBP

expression with caloric restriction in the neurogenic hypothalamus (Figures 3.3A-B) and V-SVZ (Figures 3.4A-B). Heightened fluorescent intensity of BLBP fluorescence may have resulted from CR when compared to UR in the hypothalamus and V-SVZ, but a low N-value prevented the analysis of this comparison (Figure 3.3C, 3.4C). However, there appeared to be no co-expression of BLBP in TERT-traced cells within the ME after either treatment (Figure 3.3D, E). In the ARC, where mGFP signal appears diffuse and often cannot be localized to specific cells, there was possible overlap of mGFP with BLBP, although the specific cells where co-localization may have occurred cannot be determined (Figure 3.3F, G). While co-expression of BLBP with mGFP has been identified in the lateral ventricle choroid plexus (Figure 3.4A), no co-expression of BLBP and mGFP occur within the neurogenic V-SVZ in either treatment (Figures 3.4A, B, D). In the 4th ventricle BLBP was expressed by ependymal cells (Figures 3.4E-G). However, BLBP was not expressed by TERT-traced cells in this niche (Figure 3.4G). Overall, while BLBP mRNA expression was increased in TERT-traced astrocytes with CR, no difference in BLBP expression was observed with CR in the V-SVZ or hypothalamus in adult animals, and co-expression with TERT-traced cells in neurogenic niches could not be identified.

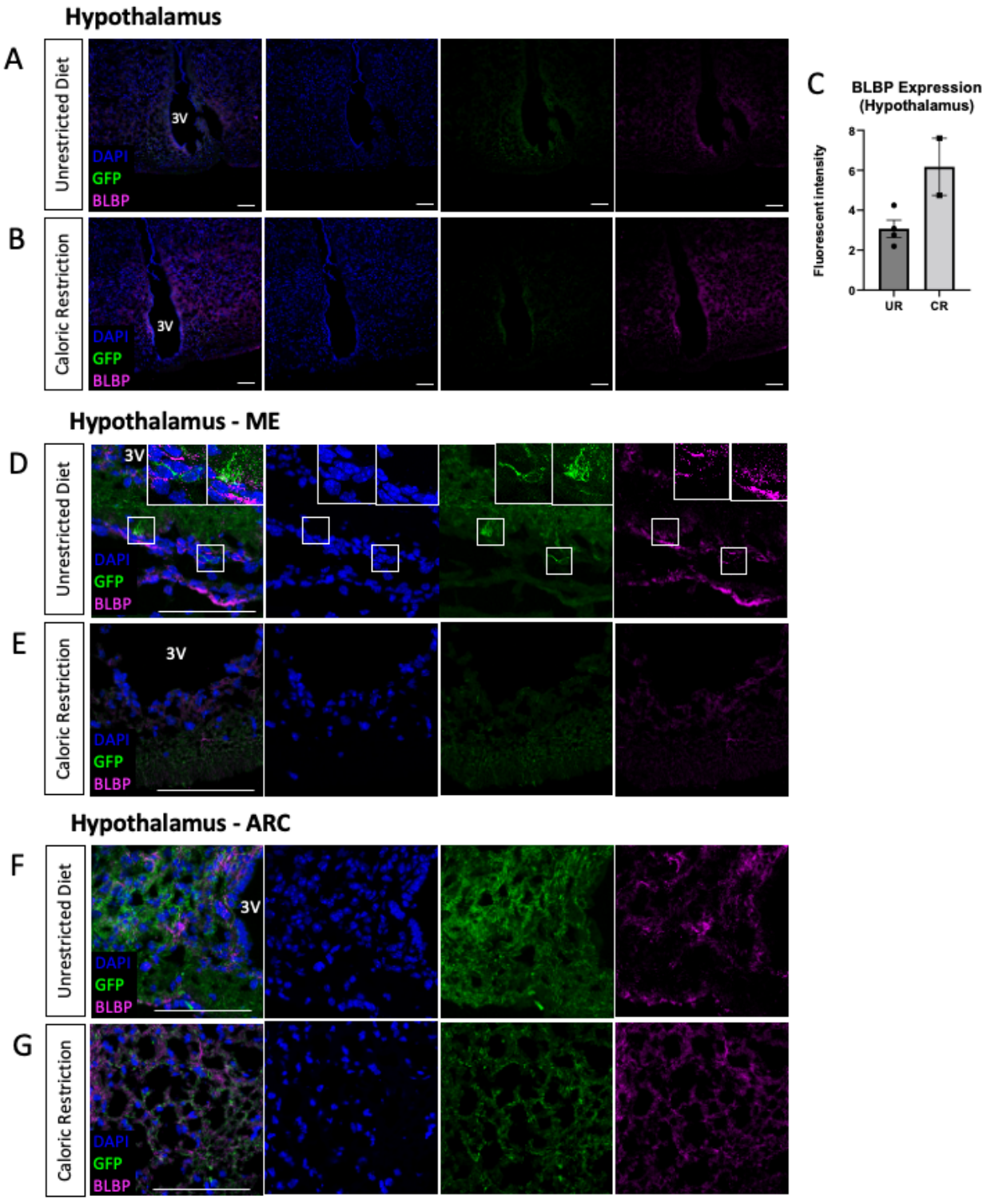
Hypothalamus
A
Unrestricted Diet
3V
DAPI
GFP
BLBP
B
Caloric Restriction
3V
DAPI
GFP
BLBP
C
BLBP Expression (Hypothalamus)
Fluorescent intensity
0
2
4
6
8
UR
CR
Hypothalamus - ME
D
Unrestricted Diet
3V
DAPI
GFP
BLBP
E
Caloric Restriction
3V
DAPI
GFP
BLBP
Hypothalamus - ARC
F
Unrestricted Diet
3V
DAPI
GFP
BLBP
G
Caloric Restriction
DAPI
GFP
BLBP

Figure 3.3 – BLBP Expression was Unaffected by Caloric Restriction and was not Expressed by TERT-traced Cells in Ventricular Niches

A-B) Representative immunofluorescence of mGFP and BLBP throughout the hypothalamus in coronal brain sections of UR (A) and CR mice (B; N=2-3 mice per group, n=1-2 sections per brain).

C) Quantification of the fluorescent intensity of BLBP in the hypothalamus (N=3 mice per group, n=1-2 sections per brain).

D-E) Representative immunofluorescence of mGFP and BLBP in the ME of UR (D) and CR mice (E; N=3 mice per group, n=1-2 sections per brain).

F-G) Representative immunofluorescence of mGFP and BLBP in the ME or UR (F) and CR mice (G; N=3 mice per group, n=1-2 sections per brain)

Insets show indicated area at 3x digital zoom. Scale bars are 100μm. Graphs show mean ± SEM. *P<0.05; **P<0.01, ***P<0.005, ****P<0.001.

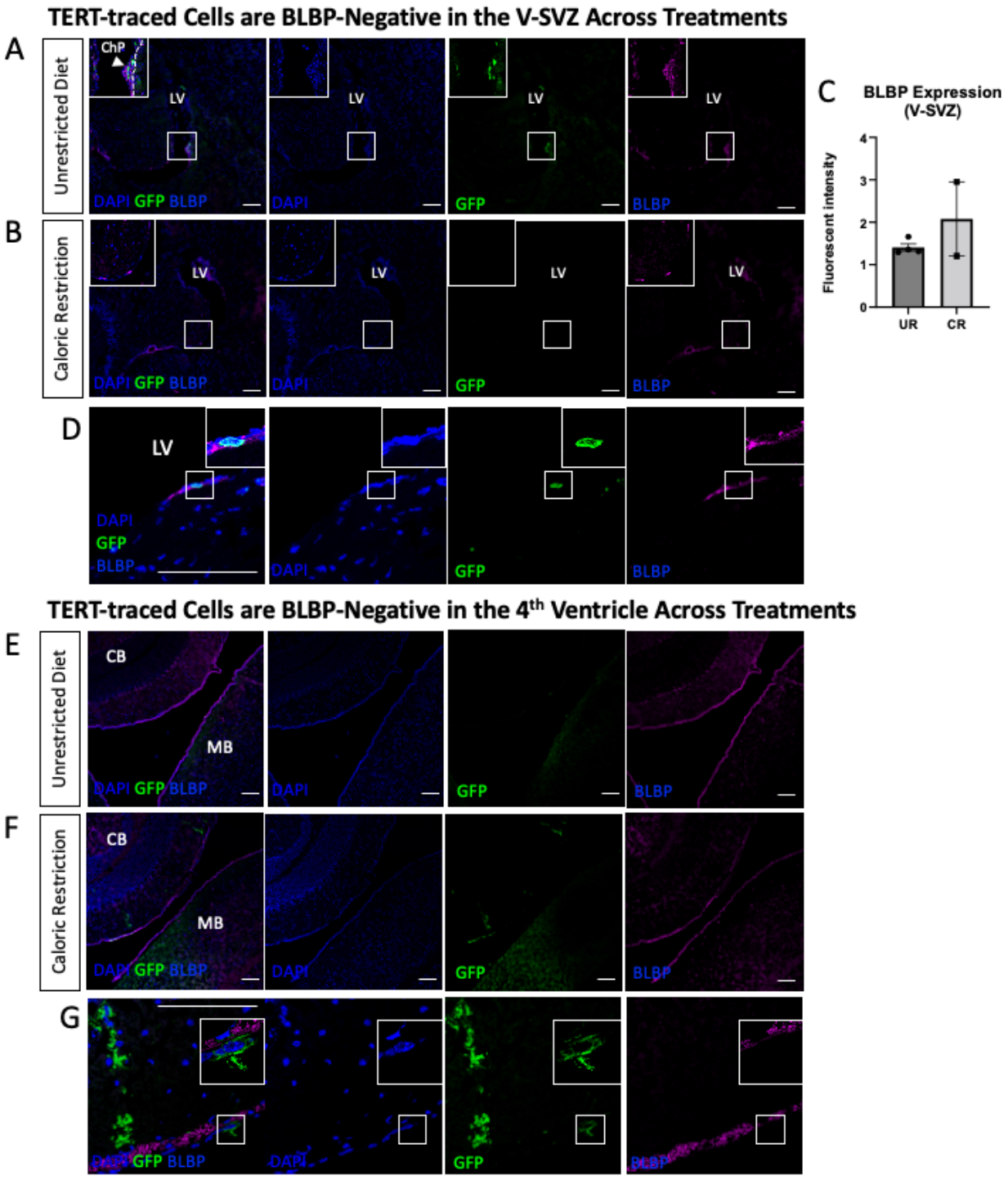
TERT-traced Cells are BLBP-Negative in the V-SVZ Across Treatments
A
Unrestricted Diet
ChP
LV
DAPI GFP BLBP
DAPI
GFP
BLBP
B
Caloric Restriction
C
BLBP Expression (V-SVZ)
Fluorescent intensity
UR
CR
D
TERT-traced Cells are BLBP-Negative in the 4th Ventricle Across Treatments
E
CB
MB
F
G

Figure 3.4 - TERT-traced cells in the V-SVZ and 4th Ventricle Rarely Expressed BLBP

A-B) Representative immunofluorescence of mGFP and BLBP in the V-SVZ and CP in UR (A) and CR animals (B; N=2-3 mice per group, n=1-2 slices per brain).

C) Quantification of BLBP fluorescent intensity within the V-SVZ and CP (N=2-4 mice per group, n=1-2 slices per brain).

D) Representative image of BLBP expression within the V-SVZ at 63x (N=2-4 mice per group, n=1-2 slices per brain)

E-G) Representative immunofluorescence of mGFP and BLBP in the 4th Ventricle of sagittal mouse brain sections of UR (E) and CR mice (F-G; N=3-6, n=1-2 sections per brain)

Insets show indicated area at 2x digital zoom. Scale bars are 100μm. Graphs show mean ± SEM. *P<0.05; **P<0.01, ***P<0.005, ****P<0.001.

No Effect was Observed on Proliferation within the V-SVZ or Hypothalamus in Response to CR

Proliferation of both stem and intermediate progenitor cells occurs throughout neurogenic regions of the mouse brain each day. While there have been many studies of cell survival and label retention with BrdU, few studies have examined basal proliferation at the time of perfusion. Additionally, no literature exists regarding the proliferative capacity of TERT-traced cells in the adult mouse hypothalamus. The number of proliferative cells in the V-SVZ was unchanged in CR mice when compared to UR (Figure 3.5A-C). Proliferation in the hypothalamus was rare, with most hypothalamic tissues containing no Ki67+ cells with either dietary treatment (Figure 3.5D-E). Additionally, while one set of proliferating cells were identified within the ME of one animal, the nature of the mGFP signal in the hypothalamus of mTert-rtTA::oTet-Cre::Rosa-mTmG animals prevented the clear identification of these cells as mGFP+ or mGFP- (Figure 3.5F). Within the V-SVZ and choroid plexus (ChP) of the lateral ventricles no TERT-traced cells were Ki67+ (Figure 3.5G), although Ki67+ cells were present in both areas. Taken together, this CR treatment did not

affect V-SVZ proliferation and TERT-traced cells are not proliferative after this pulse-chase period in the V-SVZ or hypothalamus.

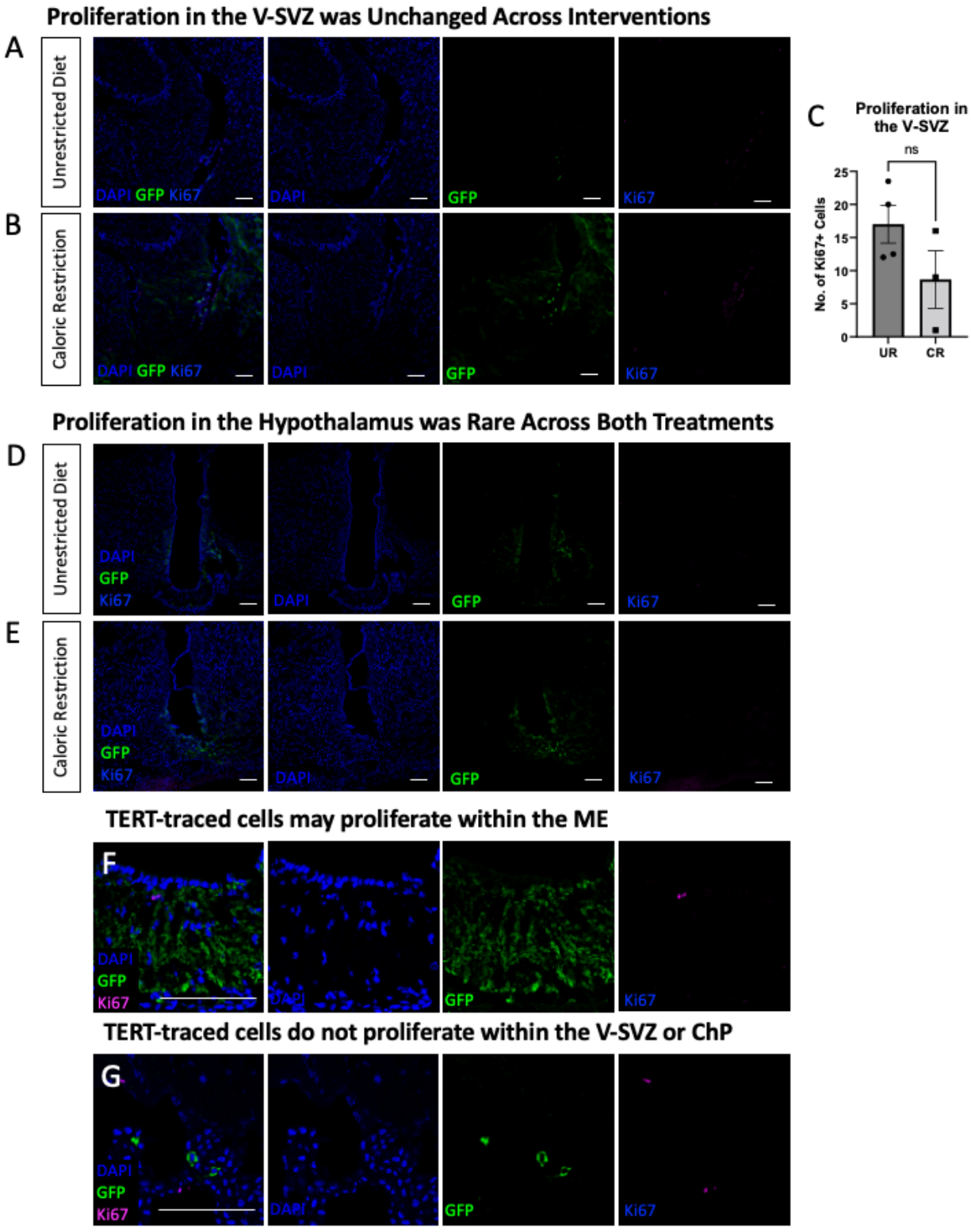
Proliferation in the V-SVZ was Unchanged Across Interventions
A
Unrestricted Diet
B
Caloric Restriction
DAPI GFP Ki67
DAPI
GFP
Ki67
C
Proliferation in the V-SVZ
ns
No. of Ki67+ Cells
25
20
15
10
5
0
UR
CR
Proliferation in the Hypothalamus was Rare Across Both Treatments
D
Unrestricted Diet
E
Caloric Restriction
TERT-traced cells may proliferate within the ME
F
TERT-traced cells do not proliferate within the V-SVZ or ChP
G

Figure 3.5 - Proliferation remained unchanged throughout the V-SVZ and Hypothalamus after CR

A-B) Representative immunofluorescence of mGFP and Ki67 in the V-SVZ

C) Quantification of Ki67 cell number in the V-SVZ (N=3 mice per group, n=1-2 sections per brain).

D-E) Representative immunofluorescence of mGFP and Ki67 in the hypothalamus in UR (D) and CR mice (E; N=3 mice per group, n=1-2 sections per brain).

F) Immunofluorescence of mGFP and Ki67+ cells in the ME (N=2 of 6 mice showed this signal, n=2 sections per brain).

G) Immunofluorescence of mGFP and Ki67+ cells in the V-SVZ and CP (N=6 of 6 mice; N=3 CR, N=3 UR showed this signal, n=2 sections per brain)

Scale bars are 100μm. Graphs show mean ± SEM. *P<0.05; **P<0.01, ***P<0.005, ****P<0.001.

Aging Increases TERT-traced Cell Signal in the Adult Mouse Brain

Aging reduces the number of proliferative stem and intermediate progenitor cells in the mouse and human brains. These changes are associated with cognitive decline and breakdown of critical regulatory barriers, such as the blood-brain barrier (BBB) and blood-cerebrospinal fluid barrier (BCSFB). The relationship between the BBB in the ME and the BCSFB in the hypothalamic third ventricle is therefore of critical importance regarding hypothalamic neurogenesis. To determine the effects of TERT lineage tracing and the relationship to proliferation and label retention in the adult mouse brain, young and aged mTert-rtTA::oTet-Cre::Rosa-mTmG mice were exposed to a 3-week doxycycline pulse, followed by an 11-day chase (Figure 3.6A). These mice were also injected with EdU on day 14 of the doxycycline pulse (Figure 3.6A). Animals were perfused following the doxycycline pulse-chase and a 1mm sagittal brain slice was cleared following the iDISCO protocol for each brain. Analysis of label retention through the quantification of EdU+ cells after the EdU ‘chase’ period revealed a decrease in the number of EdU+ cells with aging (Figure 3.6B). Interestingly, mGFP expression was significantly increased with aging

(Figure 3.6C). Representative images of the midsagittal slices used for these analyses reveal the expression of mGFP in the cerebellum, pontine reticular nucleus, median raphe nucleus, third ventricle, and olfactory bulb in aged brains, but only the third ventricle and olfactory bulb in young brains (Figures 3.6D, E).

Although TERT-traced mGFP expression increases with aging after a pulse-chase in mTert-rtTA::oTet-Cre::Rosa-mTmG animals, the number of TERT+ cells in the adult mouse brain remains unchanged (Figure 3.6A-B). Immunostaining of coronal brain slices from the neurogenic enriched brain area (Figure 3.6A) revealed that while TERT+ cell numbers increased in some regions, the number of TERT+ cells decreased in other regions (Figure 3.6A). Overall, TERT+ cells accounted for approximately 0.3% of the adult mouse brain, the same percentage as the aged mouse brain (Figure 3.6B). Immunostaining on thin sections of mTert-rtTA::oTet-Cre::Rosa-mTmG mice that underwent a 3-week doxycycline pulse, followed by an 11-day chase with EdU administration on day 14 (Figure 3.5A), revealing a high likelihood of increased expression of mGFP within the 4th ventricle and cerebellum with aging (Figures 3.5F-H). Here, only N=2 young animals could be assessed, preventing statistical analysis. To support these results, a replicate cohort of mTert-rtTA::oTet-Cre::Rosa-mTmG young and aged animals where animals did not receive EdU was assessed (Figure 3.6C). In these animals, decreased numbers of EGFR+ activated ANSCs (aANSCs) and TACS were observed with aging in the V-SVZ (Figure 3.6D), indicating a reduction in neurogenesis with aging in these mice similar to previously published results. mGFP expression in the cerebellum trended towards an increase with aging (Figure 3.6E) in support of our results in aged versus young mice from the previous experiment (Figure 3.5F-H). Interestingly, BLBP co-expression was observed in TERT-traced cells lining the 4th ventricle of aged brains (Figure 3.5I), identifying that TERT-traced ependymal cells of the 4th ventricle express BLBP with aging, but not in young brains exposed to CR or *ad lib* diet (Figure 3.6E-G).

A. **Experimental Outline**

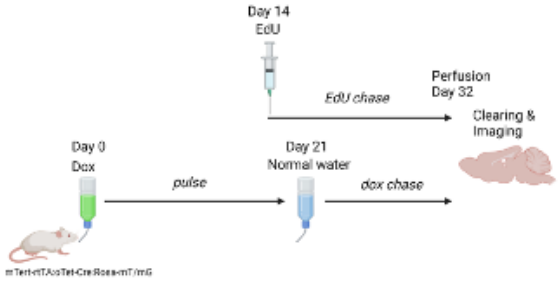

B. **Label Retention**

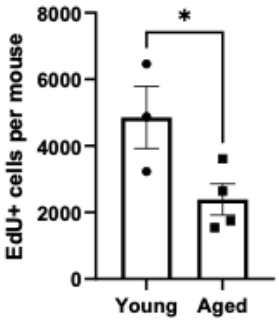

C. **mGFP Expression**

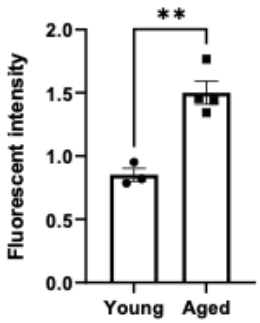

Brain Clearing

D. **Young (3wk/11d)**

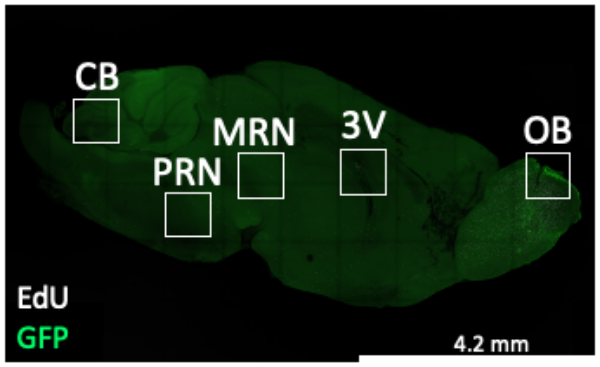

E. **Aged (3wk/11d)**

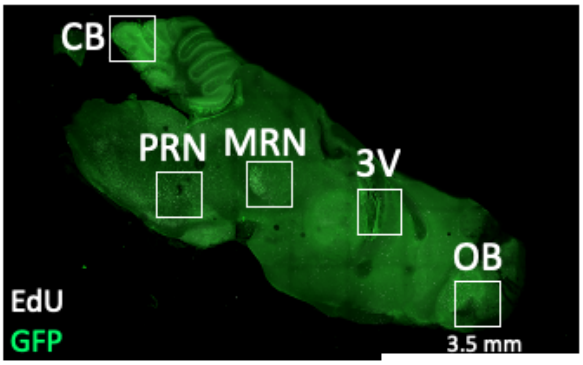

mGFP Expression Increases with Aging

G. **Young**

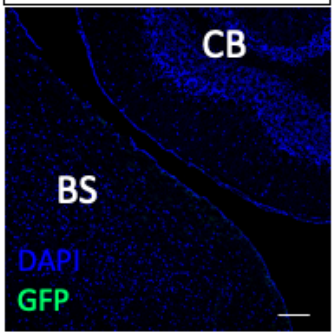

H. **Aged**

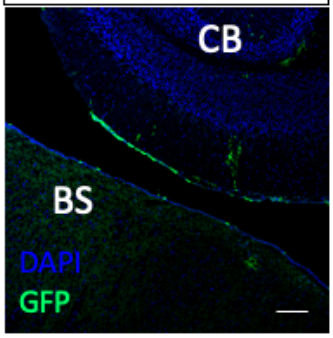

I. **GFP Expression 4th Ventricle**

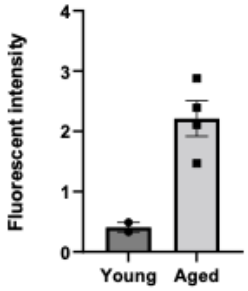

J. **BLBP Expression Occurs with Aging in TERT-traced cells**

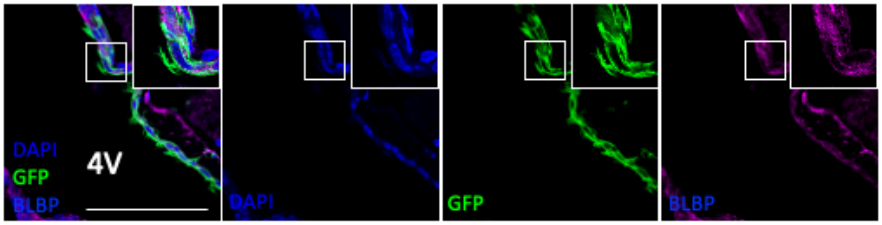

Figure 3.6 - Aging Increased TERT-traced Cell Signal in the Adult Mouse Brain

A) Experimental outline of EdU analysis of mTert-rtTA::oTet-Cre::Rosa-mTmG mice.

B) Quantification of the number of EdU+ cells throughout the adult and aged mouse brain (N=3-4 mice per group, n=1 cleared slice per brain).

C) Quantification of the fluorescent intensity of GFP throughout the adult and aged mouse brain (N=3-4 mice per group, n=1 cleared slice per brain).

D-E) Immunofluorescent analysis of mGFP and EdU in the young (D) and aged (E) mouse brain (N=3-4 mice per group, n=1 cleared slice per brain)

F-G) Representative immunofluorescence of mGFP in thin slices of the cerebellum (N=2-4 mice per group, n=1-2 slices per brain).

H) Quantification of mGFP fluorescent intensity in thin slices of the 4th ventricle (N=2-4 mice per group, n=1-2 slices per brain).

I) Co-expression of mGFP with BLBP in ependymal cells of the 4th ventricle (N=3-4 per group, n=2 slices per brain).

Insets show indicated area at 2x digital zoom. Scale bars are 100μm unless denoted otherwise. Graphs show mean ± SEM. *P<0.05; **P<0.01, ***P<0.005, ****P<0.001.

A. **TERT+ cells across brain regions in neurogenic-enriched area**

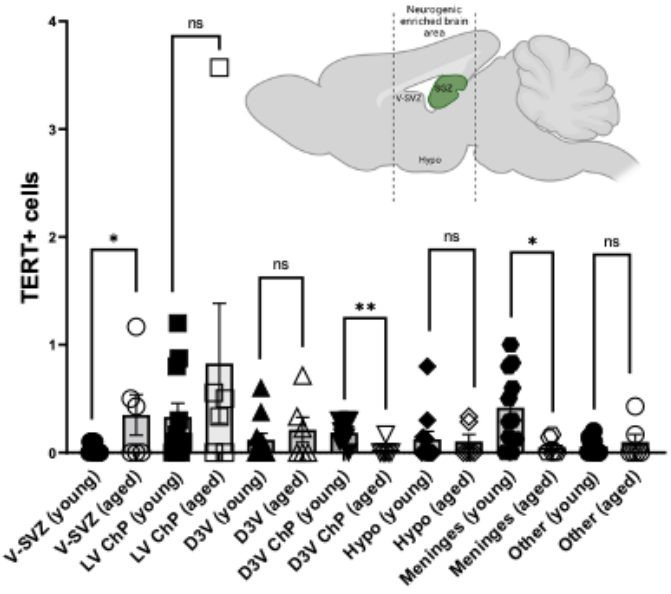

B. **FACS of TERT+ cells from full *mTert*-GFP mouse brains**

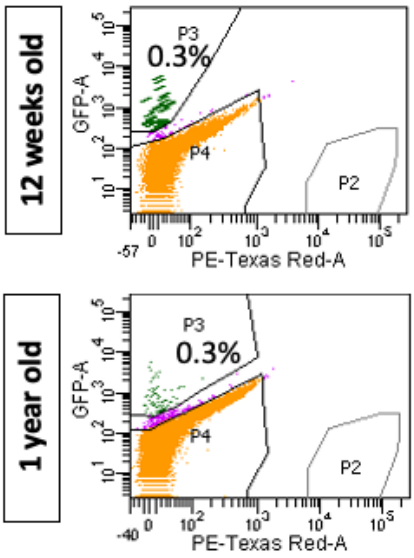

C. **Experimental Outline: Lineage Tracing**

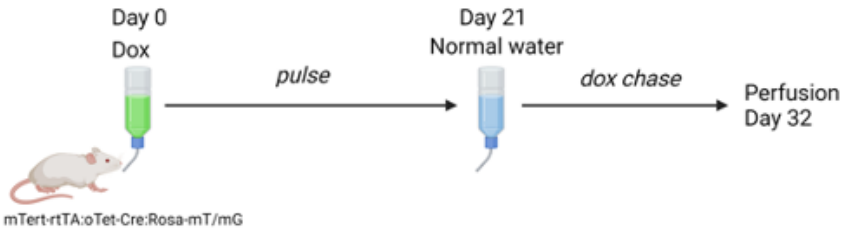

D. **Markers of Activation with Aging**

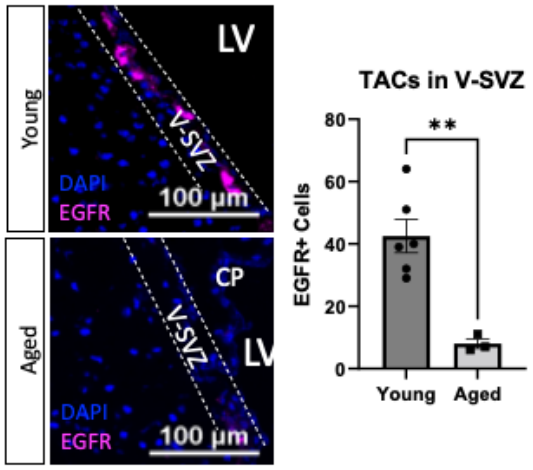

E. **mGFP Expression with Aging – Cereb.**

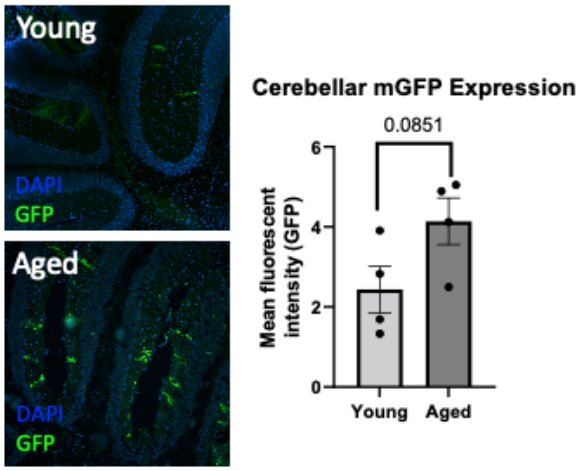

Figure 3.7 - Aging Modified TERT+ Cell Numbers and TERT-traced Cell Numbers Across Brain Regions

A) Quantification of TERT+ cells identified through immunofluorescence analysis of mTert-GFP mouse brain sections (N=6-10 mice per group, n=6-11 sections per brain).

B) FACS plots of full mTert-GFP mouse brains from adult and aged mice (N=7-25 mice per age)

C) Experimental outline of replicate lineage tracing experiment in aged and young mice.

D) Representative immunofluorescence of mGFP and EGFR in the V-SVZ of mTert-rtTA::oTet-Cre::Rosa-mTmG mice with a 3-week pulse, 11-day chase with quantification of the number of EGFR+ transit amplifying cells (TACs) per mouse (N=3-6 mice per group, n=1 section per brain).

E) Representative immunofluorescence of mGFP in the cerebellum of mTert-rtTA::oTet-Cre::Rosa-mTmG mice with a 3-week pulse, 11-day chase with quantification of the fluorescent intensity per mouse (N=4 mice per group, n=1-2 sections per brain).

Insets show indicated area at 2x digital zoom. Scale bars are 100μm. Graphs show mean ± SEM. *P<0.05; **P<0.01, ***P<0.005, ****P<0.001.

TERT-traced Microglia are Observed in the Aged Mouse Brain, but are Unaffected by CR

Aging is associated with changes in microglial shape and function, as well as full-brain inflammatory status. Behavioral changes also occur with aging, including cognitive decline. Caloric restriction in aged rodents has been identified as a treatment for the behavioral effects of aging through the reversal of age-associated expression of the inflammatory interleukin-6 (IL-6) [438]. To examine the relationship between aging and CR on TERT lineage tracing in the mouse brain, caloric restriction was performed on young and aged mTert-rtTA::oTet-Cre::Rosa-mTmG animals as per previous experimental plans (Figure 3.1A, 3.2A; Figure 3.8A). Body weight was significantly decreased in both young and aged mice when compared to UR controls (Figure 3.8B). Brain clearing of UR aged mice revealed similar TERT-traced mGFP+ signal in the cerebellum and 3rd ventricle when compared to CR aged mice (Figure 3.8C-D). However, CR-

treated animals showed reduced expression of mGFP in the olfactory glomerular and nerve layers (Figure 3.8C-D). Immunostaining was subsequently performed with sagittal sections of ad lib or CR-treated mice at each age group to identify the presence of TERT-traced microglia. In the hypothalamus, Iba1, a marker of microglial cells, was largely never co-expressed by TERT-traced cells with aging with ad lib or CR treatment (Figures 3.8E-F). However, 1 Iba1+mGFP+ cell was identified in the ME of *ad lib* aged mice (Figure 3.8G). Iba1+mGFP+ cells were also identified throughout the brain in the cortex (Figure 3.8H), meninges (Figure 3.9A), and thalamus (Figure 3.9B). While these cells were too rare for a quantitative comparison between ad lib and CR animals, the presence of mGFP+Iba1+ cells supported the results from the scRNAseq of separate microglial populations of TERT-traced cells (data analyzed by Kaitlyn Hajdarovic). Overall, CR with aging decreased TERT-traced signal in the OB but was not associated with changes in Iba1 in these cells. Taken together, the co-expression of Iba1 in TERT-traced cells throughout various brain regions points to a role of TERT+ cells and their progeny in the process of age-related inflammation.

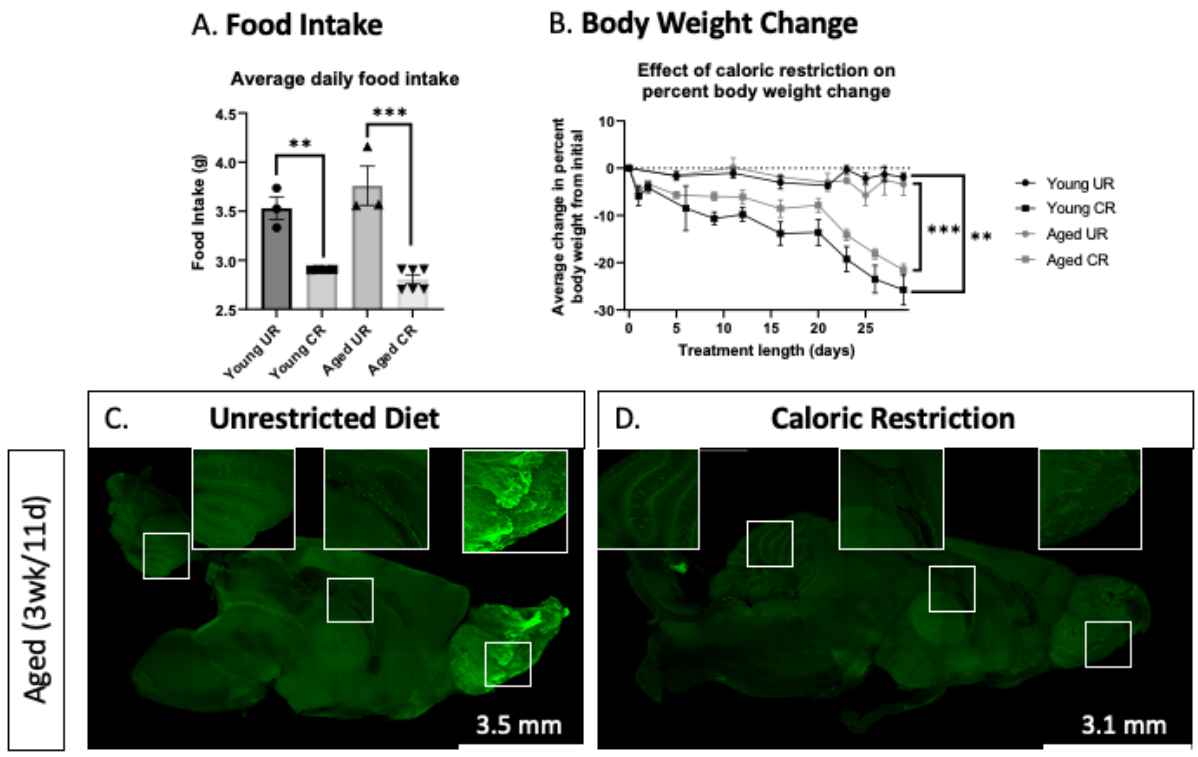

TERT-traced cells rarely express the microglial marker Iba1 in the aged mouse brain

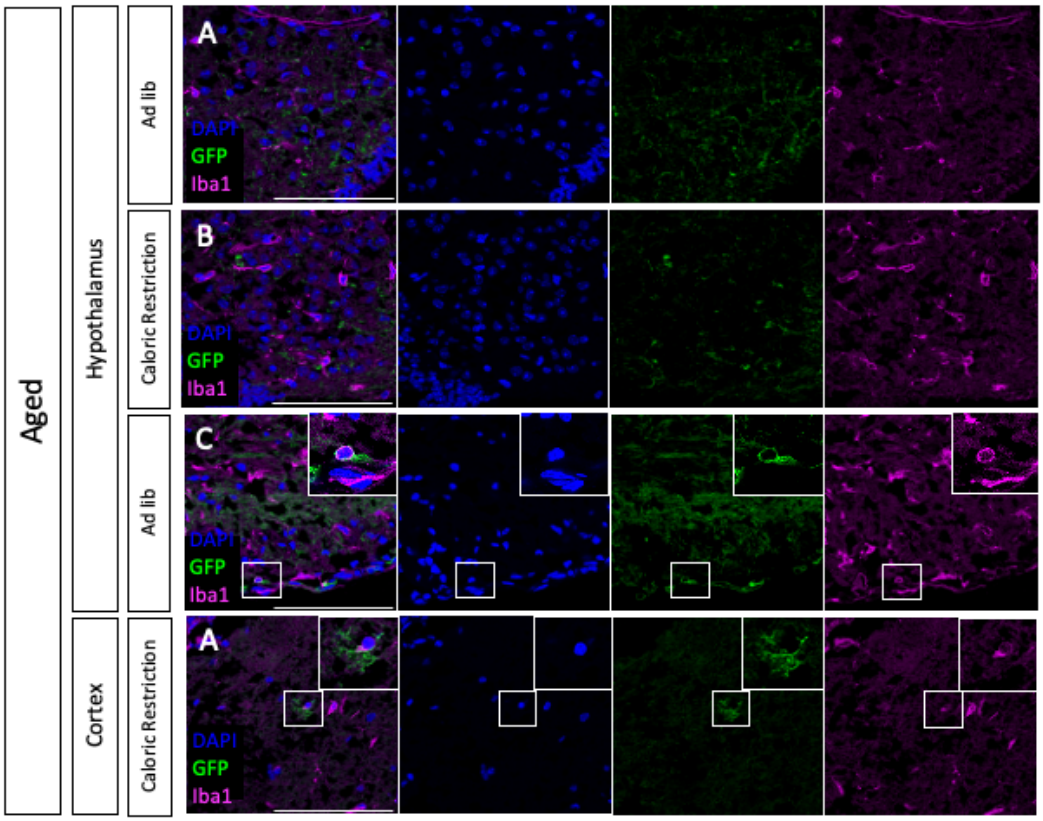

Figure 3.8 – TERT-traced Microglia were Observed in the Aged Mouse Brain, but were Unaffected by CR

A) Daily food intake from D7-D40 of CR/UR-treated mice averaged per mouse (N=3-6 mice per group).

B) Average change in percent body weight from initial per group (N=3-6 mice per group).

C-D) Immunofluorescent analysis of mGFP and EdU in aged UR (C) and aged CR mice (D; N=2-6 mice per group, n=1 section per brain).

E-F) Representative immunofluorescent image of BLBP expression in sagittal slices of the aged mouse brain with ad lib diet (E) or CR (F; N=3-6, n=1-2 sections per brain)

G-H) Iba1 expression in sagittal slices of the aged mouse brain with UR (E) or CR (F; N=3-6, n=1-2 sections per brain)

Insets show indicated area at 2x digital zoom. Scale bars are 100μm unless denoted otherwise. Graphs show mean ± SEM. *P<0.05; **P<0.01, ***P<0.005, ****P<0.001.

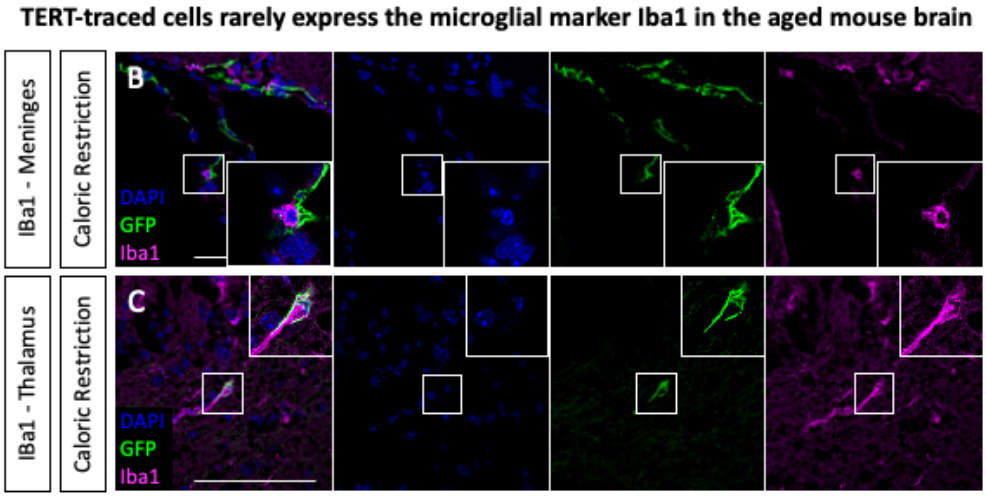

Figure 3.9 - TERT-traced Cells Expressed the Microglial Marker Iba1 in the Meninges and Thalamus

A-B) mGFP+ cells co-express Iba1 in the ME (C; N=1), cerebral cortex (D; N=1), meninges (E; N=1), and thalamus (F; N=1).

Insets show indicated area at 2x digital zoom. Scale bars are 100μm.

Discussion

Adult neurogenesis throughout the mouse and human brains remains incompletely understood, in part due to the lack of specific and unique markers for adult stem cells in the brain [163]. In the mouse brain, the V-SVZ and SGZ are highly proliferative niches that are home to ANSCs, which produce adult-born neurons and glia throughout adulthood [340]. While a population of stem cells has been identified in these niches in mice, the study of neurogenesis in the adult human brain has been hindered by debate regarding the potential of the human brain to

produce adult-born neurons and glia beyond childhood [190, 196, 198, 199]. It remains a possibility that a population of quiescent and multipotent stem cells exist within these niches within the mouse and human but have not yet been identified. The identification of these qASCs will also answer questions regarding plasticity in additional neuro/gliogenic niches of the adult brain, including the hypothalamus. Currently the hypothalamus is known to house various stem-like cell types, including alpha and beta tanycytes, and Olig2+Sox2+ OPCs, although the cell types that differentiate into newborn neurons and glia during basal conditions *in vivo* remain unknown [49]. In addition, the production of adult-born neurons and glia in the niche hint towards a qASC population, although definitive evidence remains to be collected towards this cell type. We have previously shown the potential for TERT+ cells in the mouse brain to be this cell type.

A lineage-tracing study of mTert-rtTA::oTet-Cre::Rosa-mTmG mice followed by scRNAseq of TERT-traced cells labeled with mGFP reveals the differentiation of TERT+ cells to neurons, microglia, astrocytes, oligodendrocytes, choroid plexus epithelial cells (CPECs), endothelial cells, and more. There was no difference in the number of cell types identified with CR compared to animals with UR. However, differential analysis of bulk and cell-specific gene expression between CR and UR animals revealed an increase in neuroprotective genes with CR. This matches with previous studies that correlate CR with increased neuroprotection and neurogenesis in the adult mouse brain [401, 402, 418]. This study identifies Rbm3 and Cirbp as significantly upregulated with CR in TERT-traced microglia, OEGs, and oligodendrocytes. In the adult mouse brain, Rbm3 promotes neuronal differentiation and neural progenitor proliferation, while decreasing neuronal apoptosis, following hypoxic ischemia [439]. Primary neural progenitor cells isolated from the SGZ of adult mice support the role of RBM3 as neuroprotective, as RBM3 KO animals showed significantly fewer proliferation events when compared to WT animals [440]. CIRBP prevents apoptosis in neural stem cells and prevents differentiation *in vitro* [441]. In the mouse hippocampus, CIRBP increases in response to both cold exposure and brain ischemia

[442]. CIRBP has also been shown to attenuate apoptosis through the ERK and MAPK pathways [443, 444].

Cold exposure reduces inflammation and induces anti-apoptotic effects by inhibiting caspase-depenent and caspase-independent pathways [445]. This treatment is also largely anti-inflammatory, as it also reduces neutrophils and activated microglia, ROS [446], and pro-inflammatory cytokines [447] in the adult mouse brain. Interestingly, both RBM3 and CIRBP are expressed during cold exposure, indicating a role for these genes in this anti-inflammatory and pro-neuroprotective intervention [448-450]. In the central nervous system (CNS), cold exposure reduces the severity of EAE by reducing neuroinflammation through large-scale changes in macrophages and dendritic cells [451]. Taken together, the increased expression of both RBM3 and CIRBP in multiple cell types with caloric restriction are likely performing anti-inflammatory and neuroprotective effects in the adult mouse brain, although further studies are required to determine the pathways utilized.

BLBP is expressed by radial glial cells in the embryonic ventricular zone and postnatal brain [452]. In the V-SVZ, BLBP is expressed by GFAP+ B cells as well as Hes5+ proliferative progenitors [453], although whereas GFAP and Hes5 are expressed by more quiescent B cells (Type 1 and Type 2), BLBP is expressed by Type 2 and Type 3 B-cells [453]. Similar to the qANSC markers GFAP and GLAST, BLBP is also expressed by cells within the astrocyte lineage of adult animals [454]. In the present study we analyzed TERT-traced cells with common markers of both qASNCs and astrocytes to confirm that there were no qANSC cells within our astrocyte cluster. This provided evidence for the increased expression of BLBP with CR to be specific to astrocytes. BLBP expression in astrocytes in the adult CNS is often concurrent with reactive astroglia [454-456]. The process of reactive gliosis includes upregulation of GFAP, vimentin, and nestin, morphological changes including cytoskeletal hypertrophy, and can result in glial scars forming from proliferating scar astrocytes in proximity to tissue lesions [454, 457]. Indeed, BLBP

expression is identified in proliferative astrocytes resulting from demyelination and cortical stab injuries [458]. In addition, BLBP expression in astrocytes is correlated with remyelination through activation of oligodendrocyte progenitor cells in multiple sclerosis (MS), and expression of BLBP in astrocytes decreases with disease progression [454]. In rat glioma cells as well as cultured astrocytes, proliferation is induced with BLBP [458, 459]. Taken together, BLBP upregulation in astrocytes within TERT-traced cells likely indicates a reactive phenotype for these cells in response to this treatment.

CR decreased the mGFP signal intensity from TERT-traced cells in the ME of the hypothalamus, but not the ARC. This pattern reflects the findings of Lee et al., [55], where CR during HFD reduced label retention in the ME, but not the ARC of adult mice. Interestingly, neurogenesis (Hu+BrdU+/Hu+ cells) was not identified to be significantly affected by HFD in the ME in that study. Instead, label retention was significantly altered, as the ratio of BrdU+ nuclei over total nuclei decreased with CR [55]. This group was unable to identify the cell types responsible for the changes occurring with CR, although there are several possibilities. Other cell types found in the ME include tanycytes, glial precursor cells (GPCs), astrocytes, oligodendrocytes, OPCs, and microglia [50, 53]. Gliogenesis encompasses the processes of astrogliogenesis, oligodendrogenesis, and microgliognesis, and likely accounts for the observed increase in proliferation after CR during HFD [55]. In the current study, co-staining experiments have not identified the TERT-traced cell population within the ME, as these cells were largely negative for markers of microglia (Iba1), tanycytes (Vimentin), neurons (NeuN), and astrocytes (GFAP). What then are TERT-traced cells in the ME and why do they decrease with CR? Furthermore, is the decrease in mGFP signal in the ME indicative of cell death of TERT-traced cells, reduced proliferation or differentiation of TERT-traced cells, or changes in the morphology of these TERT-traced cells?

In the ARC and ME the mGFP signal from TERT-traced cells appears to spread out across the entirety of these regions. For this reason, it is unlikely that only one cell type would lead to the mGFP expression observed, as cells such as microglia, astrocytes, or OPCs are spread nearly uniformly throughout the hypothalamus. For this reason, it remains a possibility that the mGFP signal observed originates from neurons within the ARC. This would explain the high density of mGFP signal within this brain region after a lineage trace. However, NPY/AgRP and POMC neurons within the ARC reach into the paraventricular nucleus (PVN) and lateral hypothalamus (LH), and there is no evidence for mGFP signal within this brain region in CR or UR treated animals. As the mGFP expression occurs throughout the full cell membrane, we would expect mGFP to be identified within the cell body, as well as axons and dendrites, and as none are observed within the PVN, we cannot conclude that the mGFP+ cells in the ARC and ME are NPY/AgRP and POMC neurons.

However, there are other neuronal subtypes in the ARC which extend axons into the ME, including dopamine/tyrosine hydroxylase neurons, gonadotropin-releasing hormone (GnRH) neurons, and growth hormone-releasing hormone (GHRH) neurons [460-462]. Of great importance to the analysis of the results in this study is the identification of axonal degeneration in the ME in response to aging [463]. Perhaps axons reaching into the ME from ARC neurons are degenerating in response to CR in the adult mouse brain, resulting in decreased mGFP signal in the ME. Future studies should identify whether ARC-ME neuron subtypes in these animals express mGFP after a lineage tracing experiment (Figure 3.7). While it is possible that the mGFP+ signal observed in these regions originates from neurons whose axons and dendrites reside within the ARC and ME, future studies could be clouded by the fact that the cell bodies of these neurons may be found outside of these regions or even the hypothalamus. The hypothalamus is connected through long-range neuronal pathways to the hippocampus and amygdala, receives input through various bodily systems, and through the periventricular axon system and neuropeptidergic

hypothalamic network (Figure 3.10). Therefore, there is a distinct possibility that the mGFP observed in the hypothalamus in mTert-rtTA::oTet-Cre::Rosa-mTmG animals after a pulse-chase experiment is expressed by neuronal cell types with cell bodies outside of the hypothalamus (see Conclusions and Future Directions for more on the possible axonal connections between the olfactory epithelium and hypothalamus).

Initially, the qASC population in the adult hypothalamus was hypothesized to be tanycytes, radial glial cells that line the hypothalamic third ventricle [95]. Support of this hypothesis was identified in the *in vitro* formation and multipotent differentiation of neurospheres derived from these cells [96]. Lineage tracing studies of tanycytes further supported the formation of adult-born neurons and glia from these cells [3, 6, 96]. The newborn cells were identified within the ARC and ME, several cell layers away from the tanycytes. The growing consensus hinted at a cell type that could produce adult-born cells that would migrate down the tanycyte process into the hypothalamic parenchyma [97]. However, due to the promiscuity of the promoters utilized for lineage tracing studies and the differences between *in vitro* and *in vivo* tanycyte function, these studies have not conclusively identified tanycytes as adult stem cells in this niche. In fact, Rax+ tanycytes were recently identified as non-proliferative in a basal state [3].

Instead, both Olig2+Sox2+ OPCs and NG2+ GPCs have been identified in the hypothalamic parenchyma as a population of progenitor cells. NG2+ GPCs in the ME are proliferative in adult mice under basal conditions and indicate an active progenitor cell population within this niche [94]. While Zilka-Falb et al. and others describe NG2+ cells as oligodendrocyte progenitors due to the ability of NG2+ cells to differentiate into mature oligodendrocytes *in vitro* and after transplantation, NG2+ cells throughout the mammalian brain are largely GPCs which can produce adult-born astrocytes or oligodendrocytes [98]. Therefore, it cannot be ruled out that the NG2+ cell population in the ME produces both astrocytes and oligodendrocytes in this niche. Furthermore, OPCs in the ME have recently been found to undergo variable proliferation and

differentiation depending on nutritional state [464]. NG2+ cells in the ME have also been identified to maintain dendritic processes of ARC neurons in the ME, indicating other roles of these GPCs outside of proliferation and differentiation [99]. It is important to note that tanycytes can contribute to injury-induced tissue repair, however, it is likely that under basal conditions hypothalamic plasticity is regulated by other cell types in this niche.

Basal proliferation in the hypothalamus occurs at lower levels than the classical neurogenic niches of the V-SVZ and DG. The high proliferative capacity of the intermediate progenitor cells in these niches allows for thousands of newborn neurons to be produced daily. Proliferation occurs more rarely in the hypothalamus, with a recent study identifying approximately 1.5 Ki67+ cells/ mm^2 in 40um-thick sections of 8-week-old C57BL/6J mice [465]. In contrast, Ki67+ cells in the SGZ of 50um-thick sections from 8-week-old mice were found at approximately 500 Ki67+ cells/ mm^2 [466]. This matches with our results which showed minimal numbers of Ki67+ cells in any hypothalamic region, and points to the importance of other methods of studying adult neurogenesis in the hypothalamus.

Aging reduces adult neurogenesis in all brain regions. Interestingly, aged mTert-rtTA::oTet-Cre::Rosa-mTmG animals that underwent a 3-week pulse of doxycycline followed by an 11-day chase showed increased fluorescent intensity of GFP across cleared sagittal brain slices when compared to young adult mice (Figure 3.5C-E). A study of EdU+ label-retaining cells that had incorporated EdU on day 14 of the doxycycline pulse revealed a decrease in EdU+ cells by the end of the study in aged animals (Figure 3.5B), modeling previous research on adult neurogenesis in aging. Further evidence for the decrease in neurogenesis with aging in lineage-tracing mice was illustrated through the decrease in EGFR+ aANSCs and TACs in the V-SVZ (Figure 3.6D). It can therefore be concluded that these animals respond to aging with a decrease in proliferation.

It is curious that we would see an increase in the mGFP signal of TERT-traced cells across the mouse brain through clearing of sagittal brain sections (Figures 3.5C-E). Importantly, the increase in mGFP expression across the mouse brain was not fully due to increased mGFP expression in the regions of low mGFP expression in young mice, such as the olfactory bulb or LVCP. Instead, large numbers of mGFP+ cells were identified in brain regions such as the PVN, MRN, and other regions within the midbrain and brainstem (Figures 3.5D-E). It therefore remains possible that TERT-traced cells within these regions become more proliferative with aging, or that TERT expression is induced by more cells within these brain regions with aging. Further studies are required to determine the number and proliferative capacity of TERT+ cells in these brain regions, although we have shown that TERT+ cell numbers can vary significantly between young and aged mTert-GFP mice (Figure 3.6A).

The timing of EdU administration in this study must also be taken into consideration. Doxycycline was administered to adult or aged animals for 3 weeks, followed by an 11-day chase, with a single injection of EdU at day 14 of the doxycycline. 14 days into the doxycycline pulse, TERT+ cells will have already been marked and begun activating, proliferating, migrating, and differentiating. For this reason, the EdU administration may label proliferative cells that are no longer TERT+ but are lineage-traced from TERT+ cells which would include intermediate progenitor cell types such as neuroblasts, which have been observed in TERT-tracing experiments previously (Chapter 2). In addition, the administration of EdU only once during this experiment likely prevented the labeling of most TERT+ cells, as only approximately 15% of TERT+ cells express Ki67 in the adult mouse brain (Chapter 2). The results of EdU+mGFP+ co-expression, while currently undiscovered, must be considered in this light.

To study the role of TERT+ cells in the adult and aged mouse brain to produce adult-born microglia, as identified through scRNAseq, sagittal brain sections were stained with the microglial marker Iba1. While Iba1 expression was identified throughout all brain regions in both adult and

aged mice, TERT-traced Iba1+ microglia were rare in all brain regions. These cells were identified once per every few brain sections and did not compose any significant population of microglia (Figure 3.9). Due to the increase in Rbm3 and Cirbp in TERT-traced microglia in the adult mouse brain with CR (data analyzed by Kaitlyn Hajdarovic), we hypothesized that TERT-traced microglia would have a neuroprotective function in the aged mouse brain with CR treatment. While TERT-traced microglia were identified in both treatments in aged animals, including within the hypothalamus, the low number of microglia observed prevented quantification of TERT-traced microglia. Further studies should be done to identify the levels of Rbm3 and Cirbp in TERT-traced Iba1+ microglia, but current analysis is hindered by low cell counts.

Overall, this study highlights the role of TERT+ qASCs in the adult mouse brain to respond to the neurogenic and anti-inflammatory process of CR, including within the hypothalamus. scRNAseq uncovered a role of TERT-traced cell types throughout the brain to respond to CR by inducing a neuroprotective phenotype through the expression of Blbp, Rbm3, and Cirbp. We have also identified a loss of mGFP signal in the ME with CR, indicating a loss of TERT-traced cells in this niche. Currently, the TERT-traced cells within the ME remain unclear, as the ME contains various proliferative and stem-like cell types, including Olig2+Sox2+ OPCs and NG2+ GPCs, as well as tanycytes, as well as mature cell types including oligodendrocytes, astrocytes, and axons from neurons in the ARC. Furthermore, an interesting dichotomy was discovered between the decrease in proliferative potential and increase in mGFP signal from TERT-traced cells within the aging brain. Further studies are required to understand the role of TERT-traced microglia in the adult brain. While there have been some studies pointing towards the expression of TERT by microglial cell types, it remains possible that TERT+ cells can produce CR-responsive microglia. The implications of these cells in the adult and aged mouse brain to respond to inflammatory signals by producing neuroprotective transcripts may unveil a valuable role of TERT+ cells and their progeny in the mouse brain.

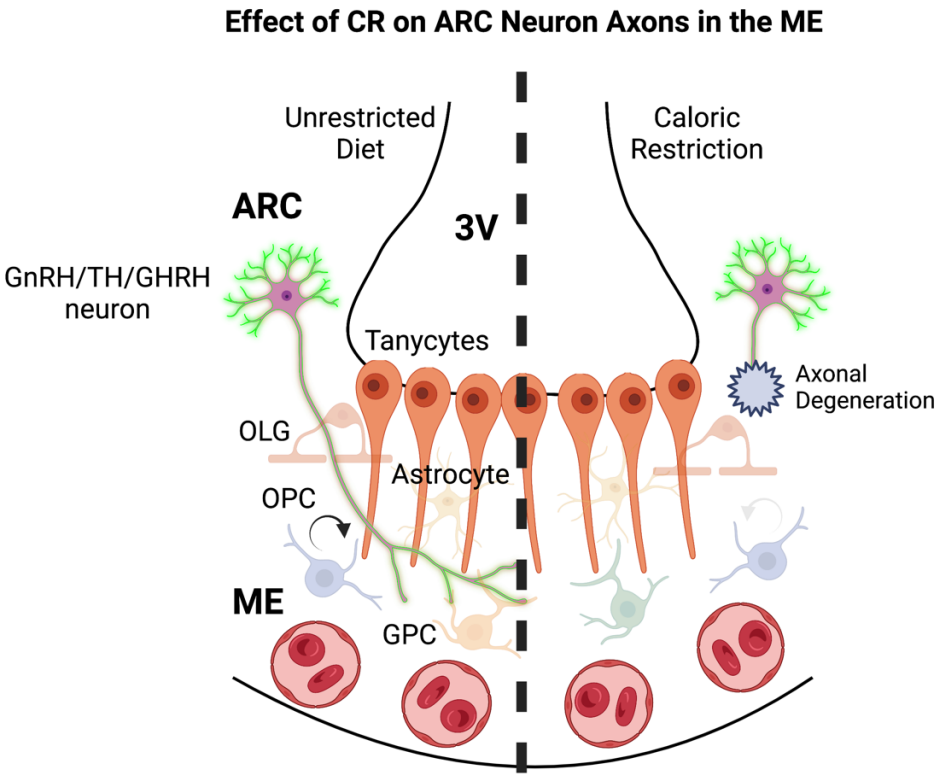

Figure 3.10 – Axonal degeneration may result in TERT-traced mGFP+ GnRH, TH, and/or GHRH neurons in response to CR. Abbreviations: ARC: arcuate nucleus, ME: median eminence, 3V: 3rd ventricle, CR: caloric restriction, OLG: oligodendrocyte, OPC: oligodendrocyte progenitor cell, GPC: glial precursor cell. Green, fluorescent outline indicates expression of mGFP in neurons.

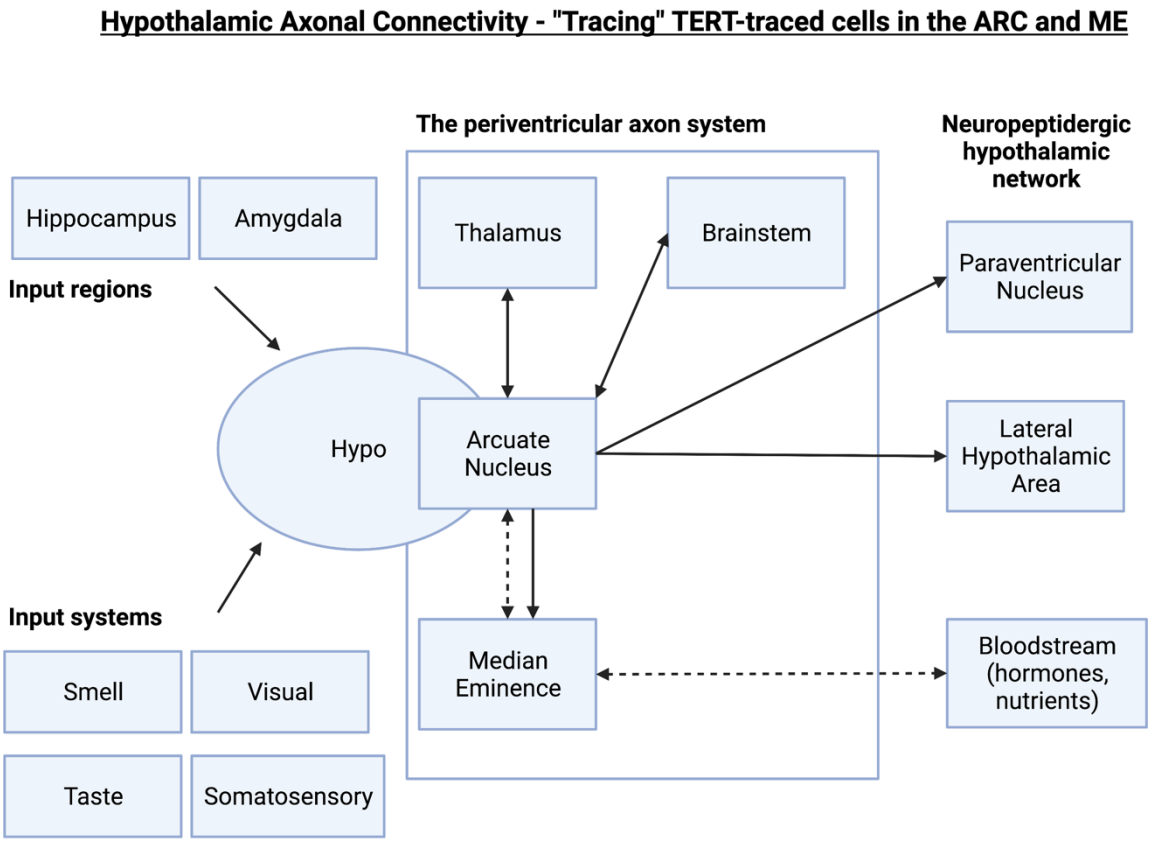

Figure 3.11 – Hypothalamic-centric axonal connectivity in the adult mouse brain. Dotted arrows indicate movement of hormones and nutrients. Solid arrows indicate neuronal connection of brain regions.

Chapter 4

OVERALL CONCLUSION AND FUTURE DIRECTIONS

Overall Conclusions

These studies have identified TERT+ cells in the adult mouse brain as qASCs which form neurospheres and proliferate *in vitro* and which express stem cell markers, but not markers of activated or mature cell types *in vivo.* TERT+ cells in adult mouse brains differentiate into mature cell types in both classical and novel neuro/gliogenic niches. Furthermore, we have identified TERT+ as well as TERT-traced intermediate progenitor cells and mature cell types labeled with mGFP throughout various brain regions (Figure 4.1) in mTert-rtTA::oTet-Cre::Rosa-mTmG mice. Multiple populations of TERT-traced cells adopt a neuroprotective transcriptional profile following CR treatment implicating these cells in functional roles in response to changes in energy balance. CR results in a significant reduction in mGFP signal in the ME, a brain region known to undergo changes in proliferation and neurogenesis with dietary intervention. Finally, a higher amount of mGFP signal is identified through the brains of aged lineage-traced mice when compared to adults, pointing to the possibility of differences in proliferation and/or TERT expression with aging.

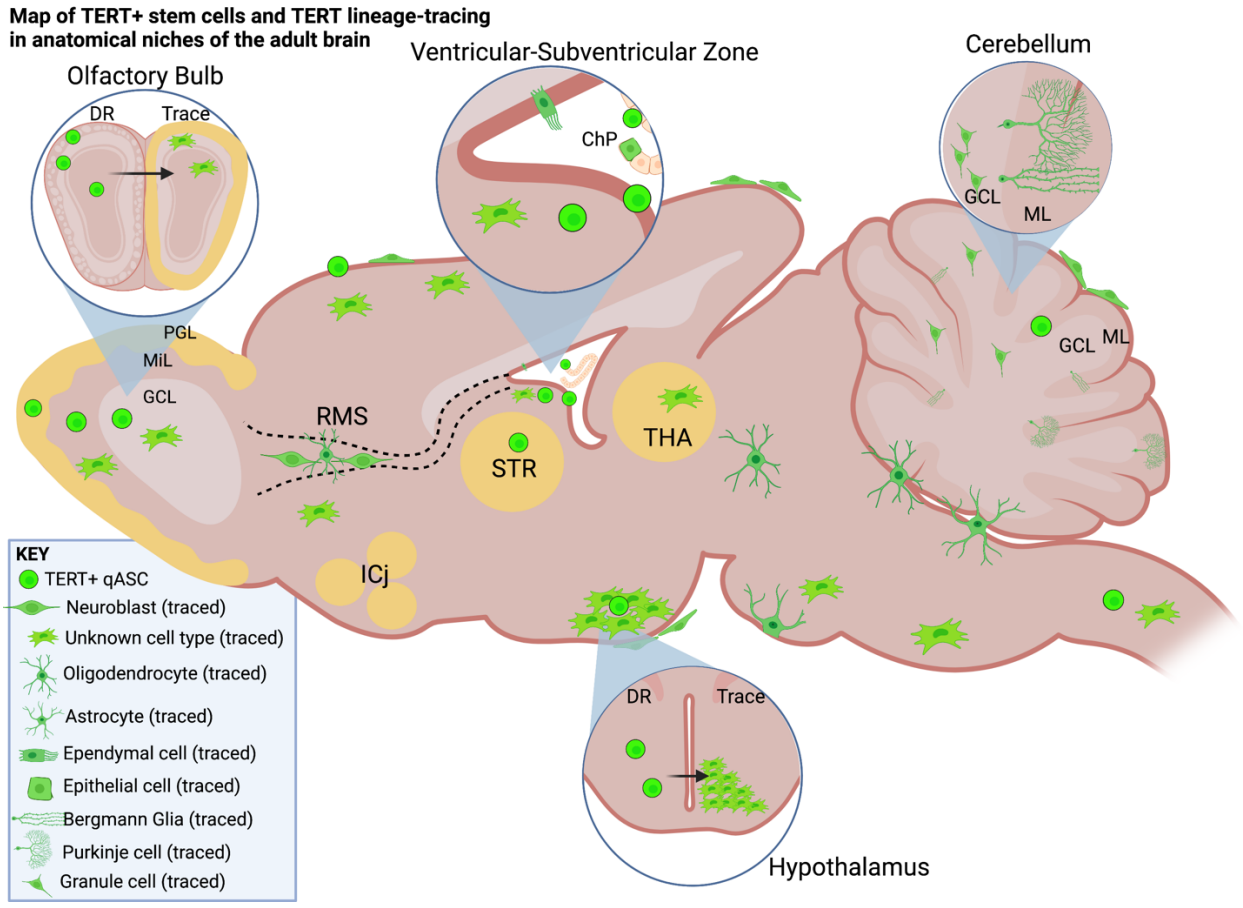

Figure 4.1 - Map of TERT+ stem cells and TERT lineage-tracing in anatomical niches of the adult brain. DR: direct reporter, Trace: lineage tracing mouse line after a lineage-trace with doxycycline, PGL: periglomerular layer, MiL: mitral layer, GCL: granule cell layer, RMS: rostral migratory stream, ICj: Islands of Calleja, STR: Striatum, THA: thalamus, ML: molecular layer.

Future Directions

The role of TERT-directed neurogenesis in the olfactory epithelium in hypothalamic neurogenesis and energy balance

The current lack of a specific and unique marker for qANSCs in the adult brain has hindered our understanding of adult neural plasticity. The reliance on markers that overlap with other cell types and tools which mark proliferating cell types has yielded information on the

process of neurogenesis but has left out critical information on the first steps of the process regarding the stem cells that produce these adult-born intermediate and mature cell types.

One such brain region where adult neurogenesis is well understood from a 'classical' angle is the OB, where V-SVZ-derived neuroblasts differentiate into adult-born olfactory granule neurons. Due to the lack of evidence of adult-born neurons or an RMS in the human brain, other options should be explored. We identified TERT+ cells in the olfactory bulb throughout the PGL, MiL, and GCL, while lineage tracing resulted in a vast majority of the resulting TERT-traced cells in the PGL layer. The phenotype and expression of NCAM in these cells is evidence that these are axons from OSNs in the OE. Further analysis of the OE revealed TERT+ and TERT-traced cells within this niche (Chapter 2, Figure 4). Much is known regarding the role of stem cells in the OE and the production of OSNs that interact with the OB in both mice and humans. However, as is the case in the brain, the specific qASC population in the OE is unidentified. There are significant similarities in the stem cell populations in the OE and the brain including the expression of stem cell markers Nestin and Sox2 and therefore, much can be learned from the neural tissue of the OE. For this reason, a more complete understanding of the role of adult neurogenesis in the OE should be investigated.

The following experiments can be performed to better understand the role of TERT+ cells in neurogenesis within the OE.

Discover the cell types and molecular mechanisms involved in TERT+ cell activation and neurogenesis in the olfactory epithelium

- Experiment 1 (mechanisms of TERT cell action with and without stimulation): scRNAseq & IF analysis of pathway transcripts of interest
    - *Questions:* What are TERT+ ASCs? What markers do they express? What cells do TERT+ cells create? How are these cells different after neurogenic stimuli (CR)? How is TERT-mediated adult neuro/gliogenesis affected by neurogenic CR?

Which pathways can we validate from scRNAseq via IF? What are the cellular processes utilized by various mGFP cells?

  - *Hypothesis:* TERT+ cells will express various SC markers and produce multi-lineage progeny and CR will induce increased neurogenesis in the hypothalamus and areas of proliferation/ differentiation and will also express high levels of growth factors of interest (Noggin, EGF, FGF, etc.)

- Experiment 2 (*in vitro* mechanisms of TERT cell action): Seahorse/ cell culture with TERT+ cells and administration of various compounds (BMP4, EGF, FGF)
  - *Questions:* Do TERT+ cells have metabolic characteristics of qASCs? How do TERT+ cells respond to various neuro/gliogenic stimuli? Which pathways can we validate from scRNAseq via Seahorse?
  - *Hypothesis:* TERT+ cells will have robust mitochondrial profiles with great capacity for survival under ischemic conditions; additionally, they will show decreased glycolysis after treatment with noggin, EGF, FGF2, and other activating factors.
- Experiment 3 (*in vivo* mechanisms of TERT cell action): *in vivo* administration followed by IF/ WB/ qRT-PCR
  - *Questions:* What are the effects of *in vivo* administration of growth factors/ signaling molecules/ other on TERT cell activation, quiescence, proliferation, differentiation, and more in different brain regions?
  - *Hypothesis:* Compounds that led to changes in TERT proliferation and differentiation from scRNAseq, Seahorse, or cell culture, will cause changes in TERT+ cell and TERT+ cell progeny in the adult mouse brain
- Experiment 4 (TERT+ cell types and effects after regeneration): IF of mTert-GFP and mTert-rtTA (pulse-chased) brains and OE (with and without intranasal treatment with ZnSO4, which destroys OSNs)

- *Questions:* How does OE/OB cell ablation affect mGFP TERT progeny? What cell types are TERT+ cells in the OE? What are the effects of OE/OB cell ablation on mGFP signal in other brain regions?
- *Hypothesis:* TERT+ cells in the OE will show markers of HBCs and GBC_{stem} cells and will regenerate the OE after injury (as well as in basal conditions at different levels). TERT+ cells in the OE will express proteins expected in the BMP pathway/ other pathways discovered via scRNAseq/ Seahorse.

Determine whether OSNs from TERT+ cells in the OE communicate with the hypothalamus to control energy balance and metabolism

In addition to better understanding TERT+ cells, we can utilize TERT+ cells in the OE to better understand the relationship between olfaction, the hypothalamus, and metabolic status. Nearly half of Americans are obese, increasing our population's chances of heart disease, stroke, type 2 diabetes, and metabolic syndrome [1]. Obesity results from various environmental, physical, and neurological variables. The hypothalamus of the brain regulates signaling to and from the liver, adipose, and stomach to regulate both food intake as well as energy expenditure. Plasticity within this brain region has been identified in the form of neurogenesis, gliogenesis, and synaptic plasticity and can modulate energy input as well as energy output. However, because hypothalamic neurogenesis has only recently been discovered, our understanding of the dynamic processes within the adult hypothalamus are incomplete [2].

Creation or destruction of of adult-born of olfactory sensory neurons (ONSs) within the olfactory epithelia (OE) and subsequent olfactory changes can modify food intake, adipose thermogenesis and browning, and full body glucose homeostasis [3]. It is understood that neurons within the olfactory bulb communicate with the hypothalamus, but their effect on hypothalamic plasticity remains unknown [4]. We have recently discovered telomerase reverse transcriptase

(TERT) expressing cells in the adult mouse brain give rise to newborn ONSs in the OE as well as unknown cell types in the hypothalamus. Importantly, destruction of OSNs in the OE via zinc sulfate leads to loss of TERT+ progenitors in the hypothalamus after a lineage-trace (Figure 4.2)

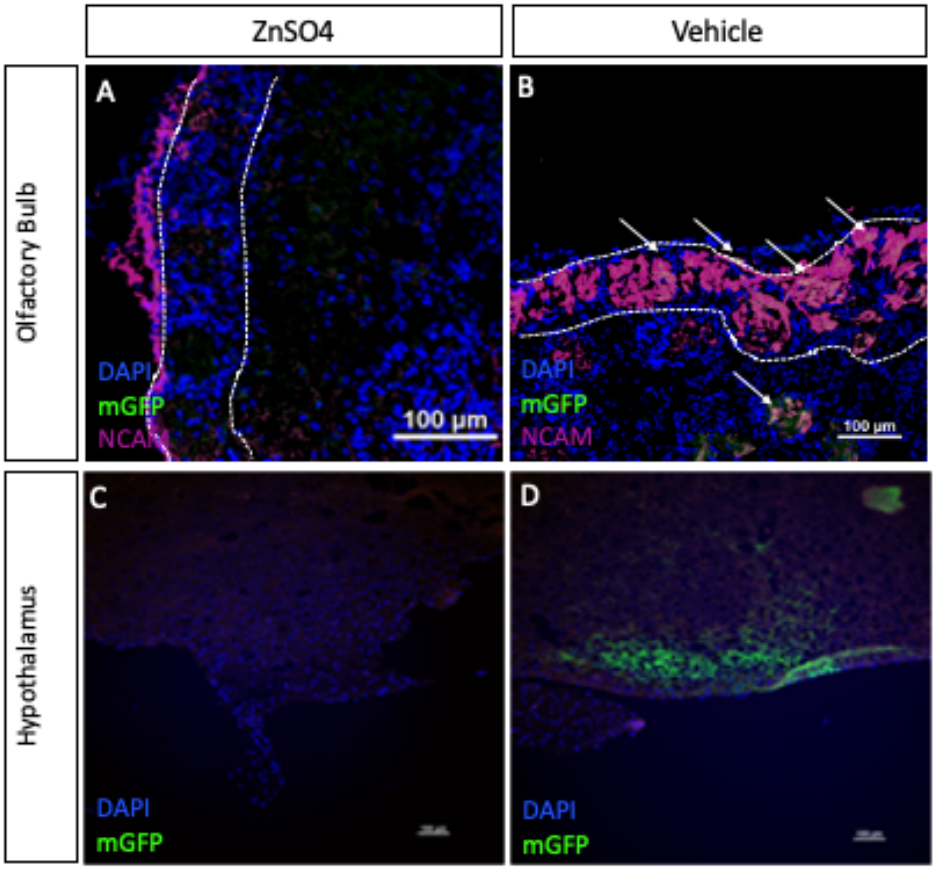

Figure 4.2 - Lineage tracing followed by ZnSO4 OSN ablation revealed loss of hypothalamic mGFP signal in adult mTert-rtTA::oTet-Cre::Rosa-mTmG mice.

A-B) Representative image of immunostaining of OB mGFP signal after ZnSO4 intranasal treatment (A) or vehicle (B; N=1-3 mice per treatment, n=1-2 tissues per brain)

C-D) Hypothalamic mGFP signal after ZnSO4 intranasal treatment (C) or vehicle (D; N=1-3 mice per treatment, n=1-2 tissues per brain).

Scale bars are 100um.

We hypothesize that adult born OSNs that arise from TERT+ cells in the OE communicate with the hypothalamus to induce energy balance changes in the adult body (Figure 4.3). This research will uncover previously unknown hypothalamic energy pathways from the OE and olfactory bulb that have been shown to influence metabolic changes. Unlike other approaches that do not investigate the interconnected olfactory and hypothalamic pathways, our approach will allow us to identify how these olfactory signals induce plastic changes within the hypothalamus and study the newborn cells. The proposed work addresses a current obesity epidemic, and specific experiments are detailed below.

- Experiment 5 (Hypothalamic & full-body effects of $ZnSO_4$ in OE): Analysis will be performed on hypothalamus; IF for mGFP signal to determine if loss of signal is changes in proliferation vs. changes in axonal outgrowth from OE/OB/olfactory cortex
    - *Questions:* What are the effects of OE/OB cell death OR regeneration on mGFP signal in the hypothalamus? What are the effects of OE/OB cell death OR regeneration on energy balance and metabolism (BAT, WAT, Liver, glucose/ insulin, etc.)
    - *Hypothesis:* OE cell death will lead to decreased olfaction and improved metabolic state through decreased hypothalamic TERT related signaling/ neurogenesis and metabolic tissue changes, while allowing for OE regeneration will show opposite effects.
- Experiment 6 (OE/OB-Hypo retrograde tracing): *in vivo* administration of cholera toxin from hypothalamic nuclei, staining for neurons in OE/OB that also express cholera toxin after trace period
    - *Questions:* Are mGFP cells in the hypothalamus in direct communication with mGFP+ cells in the OE/OB?

- *Hypothesis:* OE/OB cells that express mGFP or OE/OB cells that are in proximity to mGFP cells will express cholera toxin fluorophores after retrograde trace from the ARC or ME of the hypothalamus.

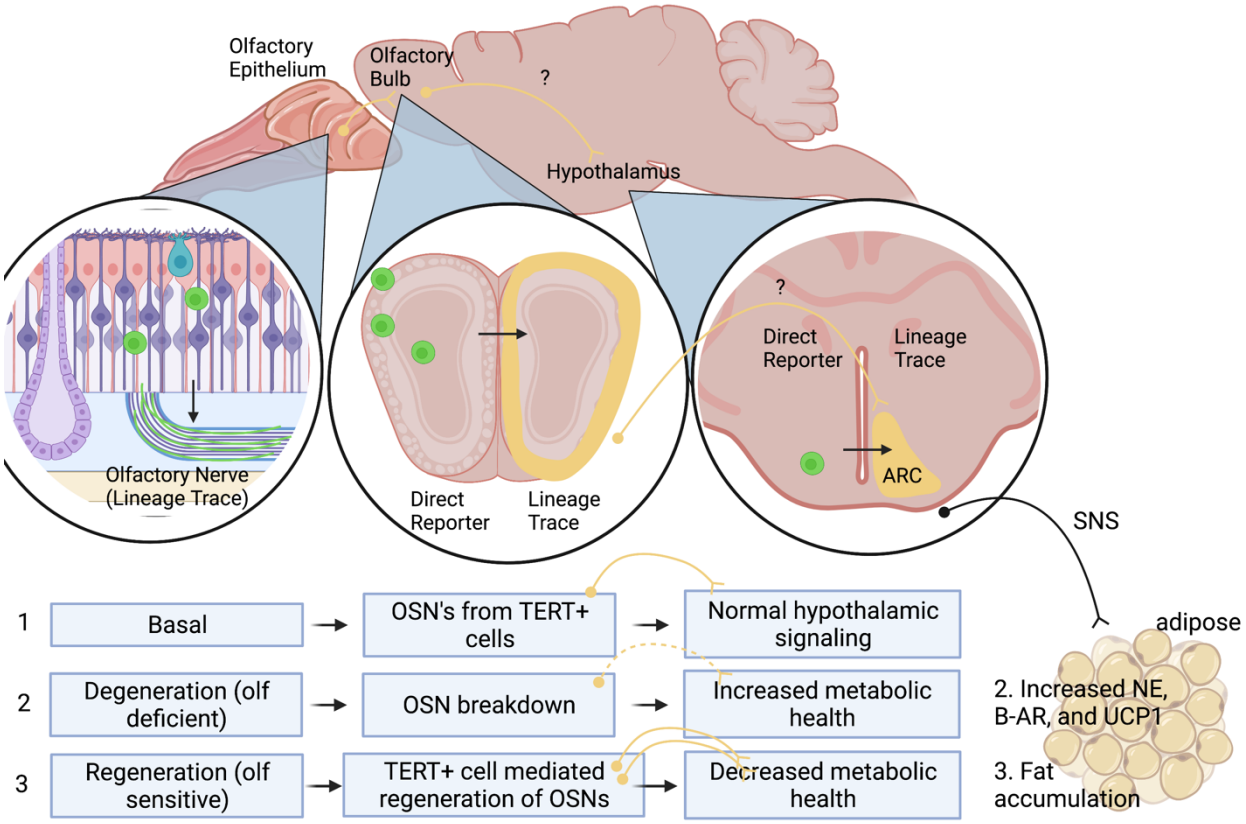

Figure 4.3 - Working Model: TERT ASCs in the OE coordinate hypothalamus-adipose SNS.

REFERENCES

1. Colodner, K.J., et al., *Proliferative potential of human astrocytes.* J Neuropathol Exp Neurol, 2005. **64**(2): p. 163-9.

2. Yamaguchi, M., et al., *Neural stem cells and neuro/gliogenesis in the central nervous system: understanding the structural and functional plasticity of the developing, mature, and diseased brain.* The Journal of Physiological Sciences, 2016. **66**(3): p. 197-206.

3. Chang, A., et al., *NG2-positive oligodendrocyte progenitor cells in adult human brain and multiple sclerosis lesions.* J Neurosci, 2000. **20**(17): p. 6404-12.

4. Altman, J. and G.D. Das, *Autoradiographic and histological evidence of postnatal hippocampal neurogenesis in rats.* J Comp Neurol, 1965. **124**(3): p. 319-35.

5. Kaplan, M.S. and J.W. Hinds, *Neurogenesis in the adult rat: electron microscopic analysis of light radioautographs.* Science, 1977. **197**(4308): p. 1092-4.

6. Rakic, P., *Limits of neurogenesis in primates.* Science, 1985. **227**(4690): p. 1054-6.

7. Goldman, S.A. and F. Nottebohm, *Neuronal production, migration, and differentiation in a vocal control nucleus of the adult female canary brain.* Proc Natl Acad Sci U S A, 1983. **80**(8): p. 2390-4.

8. Stanfield, B.B. and J.E. Trice, *Evidence that granule cells generated in the dentate gyrus of adult rats extend axonal projections.* Exp Brain Res, 1988. **72**(2): p. 399-406.

9. Cameron, H.A., P. Tanapat, and E. Gould, *Adrenal steroids and N-methyl-D-aspartate receptor activation regulate neurogenesis in the dentate gyrus of adult rats through a common pathway.* Neuroscience, 1998. **82**(2): p. 349-54.

10. Gould, E., et al., *Neurogenesis in the dentate gyrus of the adult tree shrew is regulated by psychosocial stress and NMDA receptor activation.* J Neurosci, 1997. **17**(7): p. 2492-8.

11. Eriksson, P.S., et al., *Neurogenesis in the adult human hippocampus.* Nat Med, 1998. **4**(11): p. 1313-7.

12. Hu, V.W., et al., *3H-thymidine is a defective tool with which to measure rates of DNA synthesis.* FASEB J, 2002. **16**(11): p. 1456-7.

13. Cifuentes, M., et al., *A comparative analysis of intraperitoneal versus intracerebroventricular administration of bromodeoxyuridine for the study of cell proliferation in the adult rat brain.* J Neurosci Methods, 2011. **201**(2): p. 307-14.

14. Taupin, P., *BrdU immunohistochemistry for studying adult neurogenesis: paradigms, pitfalls, limitations, and validation.* Brain Res Rev, 2007. **53**(1): p. 198-214.

15. Zeng, C., et al., *Evaluation of 5-ethynyl-2'-deoxyuridine staining as a sensitive and reliable method for studying cell proliferation in the adult nervous system.* Brain Res, 2010. **1319**: p. 21-32.

16. Lois, C., J.M. Garcia-Verdugo, and A. Alvarez-Buylla, *Chain migration of neuronal precursors.* Science, 1996. **271**(5251): p. 978-81.

17. Levy, F., et al., *Adult Neurogenesis in Sheep: Characterization and Contribution to Reproduction and Behavior.* Front Neurosci, 2017. **11**: p. 570.

18. Seri, B., et al., *Astrocytes give rise to new neurons in the adult mammalian hippocampus.* J Neurosci, 2001. **21**(18): p. 7153-60.

19. Doetsch, F., et al., *Subventricular zone astrocytes are neural stem cells in the adult mammalian brain.* Cell, 1999. **97**(6): p. 703-16.

20. Gomez-Lopez, S., R.G. Lerner, and C. Petritsch, *Asymmetric cell division of stem and progenitor cells during homeostasis and cancer.* Cell Mol Life Sci, 2014. **71**(4): p. 575-97.

21. Kam, M., et al., *The cellular composition and morphological organization of the rostral migratory stream in the adult human brain.* J Chem Neuroanat, 2009. **37**(3): p. 196-205.

22. Whitman, M.C. and C.A. Greer, *Adult neurogenesis and the olfactory system.* Prog Neurobiol, 2009. **89**(2): p. 162-75.

23. Belluzzi, O., et al., *Electrophysiological differentiation of new neurons in the olfactory bulb.* J Neurosci, 2003. **23**(32): p. 10411-8.

24. Lledo, P.M. and M. Valley, *Adult Olfactory Bulb Neurogenesis.* Cold Spring Harb Perspect Biol, 2016. **8**(8).

25. Carlen, M., et al., *Functional integration of adult-born neurons.* Curr Biol, 2002. **12**(7): p. 606-8.

26. Carleton, A., et al., *Becoming a new neuron in the adult olfactory bulb.* Nat Neurosci, 2003. **6**(5): p. 507-18.

27. Saghatelyan, A., et al., *Activity-dependent adjustments of the inhibitory network in the olfactory bulb following early postnatal deprivation.* Neuron, 2005. **46**(1): p. 103-16.

28. Rochefort, C., et al., *Enriched odor exposure increases the number of newborn neurons in the adult olfactory bulb and improves odor memory.* J Neurosci, 2002. **22**(7): p. 2679-89.

29. Brown, J., et al., *Enriched environment and physical activity stimulate hippocampal but not olfactory bulb neurogenesis.* Eur J Neurosci, 2003. **17**(10): p. 2042-6.

30. Liu, Y., et al., *Glial fibrillary acidic protein-expressing neural progenitors give rise to immature neurons via early intermediate progenitors expressing both glial fibrillary acidic protein and neuronal markers in the adult hippocampus.* Neuroscience, 2010. **166**(1): p. 241-51.

31. Garcia, A.D., et al., *GFAP-expressing progenitors are the principal source of constitutive neurogenesis in adult mouse forebrain.* Nat Neurosci, 2004. **7**(11): p. 1233-41.

32. Fortin, N.J., K.L. Agster, and H.B. Eichenbaum, *Critical role of the hippocampus in memory for sequences of events.* Nat Neurosci, 2002. **5**(5): p. 458-62.

33. Kee, N., et al., *Preferential incorporation of adult-generated granule cells into spatial memory networks in the dentate gyrus.* Nat Neurosci, 2007. **10**(3): p. 355-62.

34. Kempermann, G., *Why new neurons? Possible functions for adult hippocampal neurogenesis.* J Neurosci, 2002. **22**(3): p. 635-8.

35. Kempermann, G., H.G. Kuhn, and F.H. Gage, *More hippocampal neurons in adult mice living in an enriched environment.* Nature, 1997. **386**(6624): p. 493-5.

36. Rhodes, J.S., et al., *Exercise increases hippocampal neurogenesis to high levels but does not improve spatial learning in mice bred for increased voluntary wheel running.* Behav Neurosci, 2003. **117**(5): p. 1006-16.

37. Tashiro, A., H. Makino, and F.H. Gage, *Experience-specific functional modification of the dentate gyrus through adult neurogenesis: a critical period during an immature stage.* J Neurosci, 2007. **27**(12): p. 3252-9.

38. van Praag, H., et al., *Running enhances neurogenesis, learning, and long-term potentiation in mice.* Proc Natl Acad Sci U S A, 1999. **96**(23): p. 13427-31.

39. van Praag, H., et al., *Exercise enhances learning and hippocampal neurogenesis in aged mice.* J Neurosci, 2005. **25**(38): p. 8680-5.

40. Hastings, N.B. and E. Gould, *Rapid extension of axons into the CA3 region by adult-generated granule cells.* J Comp Neurol, 1999. **413**(1): p. 146-54.

41. Laplagne, D.A., et al., *Functional convergence of neurons generated in the developing and adult hippocampus.* PLoS Biol, 2006. **4**(12): p. e409.

42. Laplagne, D.A., et al., *Similar GABAergic inputs in dentate granule cells born during embryonic and adult neurogenesis.* Eur J Neurosci, 2007. **25**(10): p. 2973-81.

43. Kempermann, G., et al., *Milestones of neuronal development in the adult hippocampus.* Trends Neurosci, 2004. **27**(8): p. 447-52.

44. van Praag, H., et al., *Functional neurogenesis in the adult hippocampus.* Nature, 2002. **415**(6875): p. 1030-4.

45. Jessberger, S. and G. Kempermann, *Adult-born hippocampal neurons mature into activity-dependent responsiveness.* Eur J Neurosci, 2003. **18**(10): p. 2707-12.

46. Shors, T.J., *Acute stress rapidly and persistently enhances memory formation in the male rat.* Neurobiol Learn Mem, 2001. **75**(1): p. 10-29.

47. Shors, T.J., *Opposite effects of stressful experience on memory formation in males versus females.* Dialogues Clin Neurosci, 2002. **4**(2): p. 139-47.

48. Drapeau, E., et al., *Spatial memory performances of aged rats in the water maze predict levels of hippocampal neurogenesis.* Proc Natl Acad Sci U S A, 2003. **100**(24): p. 14385-90.

49. Mu, W., et al., *Hypothalamic Rax(+) tanycytes contribute to tissue repair and tumorigenesis upon oncogene activation in mice.* Nat Commun, 2021. **12**(1): p. 2288.

50. Zilkha-Falb, R., N. Kaushansky, and A. Ben-Nun, *The Median Eminence, A New Oligodendrogenic Niche in the Adult Mouse Brain.* Stem cell reports, 2020. **14**(6): p. 1076-1092.

51. Goodman, T. and M.K. Hajihosseini, *Hypothalamic tanycytes-masters and servants of metabolic, neuroendocrine, and neurogenic functions.* Front Neurosci, 2015. **9**: p. 387.

52. Rodriguez, E.M., et al., *Hypothalamic tanycytes: a key component of brain-endocrine interaction.* Int Rev Cytol, 2005. **247**: p. 89-164.

53. Yin, W. and A.C. Gore, *The hypothalamic median eminence and its role in reproductive aging.* Ann N Y Acad Sci, 2010. **1204**: p. 113-22.

54. Markakis, E.A., et al., *Novel neuronal phenotypes from neural progenitor cells.* J Neurosci, 2004. **24**(12): p. 2886-97.

55. Lee, D.A., et al., *Dietary and sex-specific factors regulate hypothalamic neurogenesis in young adult mice.* Front Neurosci, 2014. **8**: p. 157.

56. Xu, Y., et al., *Neurogenesis in the ependymal layer of the adult rat 3rd ventricle.* Exp Neurol, 2005. **192**(2): p. 251-64.

57. Chaker, Z., et al., *Hypothalamic neurogenesis persists in the aging brain and is controlled by energy-sensing IGF-I pathway.* Neurobiol Aging, 2016. **41**: p. 64-72.

58. Kokoeva, M.V., H. Yin, and J.S. Flier, *Neurogenesis in the hypothalamus of adult mice: potential role in energy balance.* Science, 2005. **310**(5748): p. 679-83.

59. Pierce, A.A. and A.W. Xu, *De novo neurogenesis in adult hypothalamus as a compensatory mechanism to regulate energy balance.* J Neurosci, 2010. **30**(2): p. 723-30.

60. Miranda, M., et al., *Brain-Derived Neurotrophic Factor: A Key Molecule for Memory in the Healthy and the Pathological Brain.* Front Cell Neurosci, 2019. **13**: p. 363.

61. Rasika, S., A. Alvarez-Buylla, and F. Nottebohm, *BDNF mediates the effects of testosterone on the survival of new neurons in an adult brain.* Neuron, 1999. **22**(1): p. 53-62.

62. Zhou, J., et al., *The BDNF content of postnatal and adult rat brain: the effects of 6-hydroxydopamine lesions in adult brain.* Brain Res Dev Brain Res, 1996. **97**(2): p. 297-303.

63. Nagahara, A.H. and M.H. Tuszynski, *Potential therapeutic uses of BDNF in neurological and psychiatric disorders.* Nat Rev Drug Discov, 2011. **10**(3): p. 209-19.

64. Pencea, V., et al., *Infusion of brain-derived neurotrophic factor into the lateral ventricle of the adult rat leads to new neurons in the parenchyma of the striatum, septum, thalamus, and hypothalamus.* J Neurosci, 2001. **21**(17): p. 6706-17.

65. Rios, M., *BDNF and the central control of feeding: accidental bystander or essential player?* Trends Neurosci, 2013. **36**(2): p. 83-90.

66. Tsuchida, A., et al., *Acute effects of brain-derived neurotrophic factor on energy expenditure in obese diabetic mice.* Int J Obes Relat Metab Disord, 2001. **25**(9): p. 1286-93.

67. !!! INVALID CITATION !!! [58].

68. Luzzati, F., et al., *Quiescent neuronal progenitors are activated in the juvenile guinea pig lateral striatum and give rise to transient neurons.* Development, 2014. **141**(21): p. 4065-75.

69. Bordiuk, O.L., et al., *Cell proliferation and neurogenesis in adult mouse brain.* PLoS One, 2014. **9**(11): p. e111453.

70. Shipp, S., *Structure and function of the cerebral cortex.* Curr Biol, 2007. **17**(12): p. R443-9.

71. Scharff, C., *Chasing fate and function of new neurons in adult brains.* Curr Opin Neurobiol, 2000. **10**(6): p. 774-83.

72. Snyder, L.H., A.P. Batista, and R.A. Andersen, *Coding of intention in the posterior parietal cortex.* Nature, 1997. **386**(6621): p. 167-70.

73. Magavi, S.S., B.R. Leavitt, and J.D. Macklis, *Induction of neurogenesis in the neocortex of adult mice.* Nature, 2000. **405**(6789): p. 951-5.

74. Mombaerts, P., et al., *Visualizing an olfactory sensory map.* Cell, 1996. **87**(4): p. 675-86.

75. Schwob, J.E., et al., *Stem and progenitor cells of the mammalian olfactory epithelium: Taking poietic license.* J Comp Neurol, 2017. **525**(4): p. 1034-1054.

76. Schwob, J.E., S.L. Youngentob, and R.C. Mezza, *Reconstitution of the rat olfactory epithelium after methyl bromide-induced lesion.* J Comp Neurol, 1995. **359**(1): p. 15-37.

77. Caggiano, M., J.S. Kauer, and D.D. Hunter, *Globose basal cells are neuronal progenitors in the olfactory epithelium: a lineage analysis using a replication-incompetent retrovirus.* Neuron, 1994. **13**(2): p. 339-52.

78. Graziadei, P.P. and G.A. Graziadei, *Neurogenesis and neuron regeneration in the olfactory system of mammals. I. Morphological aspects of differentiation and structural organization of the olfactory sensory neurons.* J Neurocytol, 1979. **8**(1): p. 1-18.

79. Huard, J.M., et al., *Adult olfactory epithelium contains multipotent progenitors that give rise to neurons and non-neural cells.* J Comp Neurol, 1998. **400**(4): p. 469-86.

80. Leung, C.T., P.A. Coulombe, and R.R. Reed, *Contribution of olfactory neural stem cells to tissue maintenance and regeneration.* Nat Neurosci, 2007. **10**(6): p. 720-6.

81. Schwob, J.E., *Neural regeneration and the peripheral olfactory system.* Anat Rec, 2002. **269**(1): p. 33-49.

82. Chen, X., H. Fang, and J.E. Schwob, *Multipotency of purified, transplanted globose basal cells in olfactory epithelium.* J Comp Neurol, 2004. **469**(4): p. 457-74.

83. Riera, C.E., et al., *The Sense of Smell Impacts Metabolic Health and Obesity.* Cell Metab, 2017. **26**(1): p. 198-211 e5.

84. Ge, W.P., et al., *Local generation of glia is a major astrocyte source in postnatal cortex.* Nature, 2012. **484**(7394): p. 376-80.

85. Sohn, J., et al., *The subventricular zone continues to generate corpus callosum and rostral migratory stream astroglia in normal adult mice.* J Neurosci, 2015. **35**(9): p. 3756-63.

86. Zimmermann, T., et al., *Neural stem cell lineage-specific cannabinoid type-1 receptor regulates neurogenesis and plasticity in the adult mouse hippocampus.* Cereb Cortex, 2018. **28**(12): p. 4454-4471.

87. Horner, P.J., M. Thallmair, and F.H. Gage, *Defining the NG2-expressing cell of the adult CNS.* J Neurocytol, 2002. **31**(6-7): p. 469-80.

88. Peters, A., K. Josephson, and S.L. Vincent, *Effects of aging on the neuroglial cells and pericytes within area 17 of the rhesus monkey cerebral cortex.* Anat Rec, 1991. **229**(3): p. 384-98.

89. Sofroniew, M.V. and H.V. Vinters, *Astrocytes: biology and pathology.* Acta Neuropathol, 2010. **119**(1): p. 7-35.

90. Genc, S., I.A. Kurnaz, and M. Ozilgen, *Astrocyte-neuron lactate shuttle may boost more ATP supply to the neuron under hypoxic conditions--in silico study supported by in vitro expression data.* BMC Syst Biol, 2011. **5**: p. 162.

91. Bezzi, P., et al., *Neuron-astrocyte cross-talk during synaptic transmission: physiological and neuropathological implications.* Prog Brain Res, 2001. **132**: p. 255-65.

92. Khan, Z.U., et al., *An astroglia-linked dopamine D2-receptor action in prefrontal cortex.* Proc Natl Acad Sci U S A, 2001. **98**(4): p. 1964-9.

93. Delgado, A.C., et al., *Release of stem cells from quiescence reveals gliogenic domains in the adult mouse brain.* Science, 2021. **372**(6547): p. 1205-1209.

94. Mohn, T.C. and A.O. Koob, *Adult Astrogenesis and the Etiology of Cortical Neurodegeneration.* J Exp Neurosci, 2015. **9**(Suppl 2): p. 25-34.

95. Buffo, A., et al., *Origin and progeny of reactive gliosis: A source of multipotent cells in the injured brain.* Proc Natl Acad Sci U S A, 2008. **105**(9): p. 3581-6.

96. Buffo, A., et al., *Expression pattern of the transcription factor Olig2 in response to brain injuries: implications for neuronal repair.* Proc Natl Acad Sci U S A, 2005. **102**(50): p. 18183-8.

97. Nave, K.A. and H.B. Werner, *Myelination of the nervous system: mechanisms and functions.* Annu Rev Cell Dev Biol, 2014. **30**: p. 503-33.

98. Perez-Cerda, F., M.V. Sanchez-Gomez, and C. Matute, *Pio del Rio Hortega and the discovery of the oligodendrocytes.* Front Neuroanat, 2015. **9**: p. 92.

99. Franklin, R.J. and S.A. Goldman, *Glia Disease and Repair-Remyelination.* Cold Spring Harb Perspect Biol, 2015. **7**(7): p. a020594.

100. Shi, J., A. Marinovich, and B.A. Barres, *Purification and characterization of adult oligodendrocyte precursor cells from the rat optic nerve.* J Neurosci, 1998. **18**(12): p. 4627-36.

101. Clarke, L.E., et al., *Properties and fate of oligodendrocyte progenitor cells in the corpus callosum, motor cortex, and piriform cortex of the mouse.* J Neurosci, 2012. **32**(24): p. 8173-85.

102. Levine, J.M., F. Stincone, and Y.S. Lee, *Development and differentiation of glial precursor cells in the rat cerebellum.* Glia, 1993. **7**(4): p. 307-21.

103. Rivers, L.E., et al., *PDGFRA/NG2 glia generate myelinating oligodendrocytes and piriform projection neurons in adult mice.* Nat Neurosci, 2008. **11**(12): p. 1392-401.

104. Menn, B., et al., *Origin of oligodendrocytes in the subventricular zone of the adult brain.* J Neurosci, 2006. **26**(30): p. 7907-18.

105. McKenzie, I.A., et al., *Motor skill learning requires active central myelination.* Science, 2014. **346**(6207): p. 318-22.

106. Birey, F., et al., *Genetic and Stress-Induced Loss of NG2 Glia Triggers Emergence of Depressive-like Behaviors through Reduced Secretion of FGF2.* Neuron, 2015. **88**(5): p. 941-956.

107. Diers-Fenger, M., et al., *AN2/NG2 protein-expressing glial progenitor cells in the murine CNS: isolation, differentiation, and association with radial glia.* Glia, 2001. **34**(3): p. 213-28.

108. Yeung, M.S., et al., *Dynamics of oligodendrocyte generation and myelination in the human brain.* Cell, 2014. **159**(4): p. 766-74.

109. Ginhoux, F., et al., *Fate mapping analysis reveals that adult microglia derive from primitive macrophages.* Science, 2010. **330**(6005): p. 841-5.

110. Alliot, F., I. Godin, and B. Pessac, *Microglia derive from progenitors, originating from the yolk sac, and which proliferate in the brain.* Brain Res Dev Brain Res, 1999. **117**(2): p. 145-52.

111. Tremblay, M.E., *The role of microglia at synapses in the healthy CNS: novel insights from recent imaging studies.* Neuron Glia Biol, 2011. **7**(1): p. 67-76.

112. Korin, B., et al., *High-dimensional, single-cell characterization of the brain's immune compartment.* Nat Neurosci, 2017. **20**(9): p. 1300-1309.

113. Soulet, D. and S. Rivest, *Microglia.* Curr Biol, 2008. **18**(12): p. R506-8.

114. Benarroch, E.E., *Microglia: Multiple roles in surveillance, circuit shaping, and response to injury.* Neurology, 2013. **81**(12): p. 1079-88.

115. Torres, L., et al., *Dynamic microglial modulation of spatial learning and social behavior.* Brain Behav Immun, 2016. **55**: p. 6-16.

116. Lopez-Redondo, F., et al., *Glutamate transporter GLT-1 is highly expressed in activated microglia following facial nerve axotomy.* Brain Res Mol Brain Res, 2000. **76**(2): p. 429-35.

117. Akiyoshi, R., et al., *Microglia Enhance Synapse Activity to Promote Local Network Synchronization.* eNeuro, 2018. **5**(5).

118. Costello, D.A., et al., *Interleukin-1alpha and HMGB1 mediate hippocampal dysfunction in SIGIRR-deficient mice.* J Neurosci, 2011. **31**(10): p. 3871-9.

119. Huang, Y., et al., *Repopulated microglia are solely derived from the proliferation of residual microglia after acute depletion.* Nat Neurosci, 2018. **21**(4): p. 530-540.

120. Lawson, L.J., V.H. Perry, and S. Gordon, *Turnover of resident microglia in the normal adult mouse brain.* Neuroscience, 1992. **48**(2): p. 405-15.

121. Tonchev, A.B., et al., *Differential proliferative response in the postischemic hippocampus, temporal cortex, and olfactory bulb of young adult macaque monkeys.* Glia, 2003. **42**(3): p. 209-24.

122. Reu, P., et al., *The Lifespan and Turnover of Microglia in the Human Brain.* Cell Rep, 2017. **20**(4): p. 779-784.

123. Zhan, L., et al., *Proximal recolonization by self-renewing microglia re-establishes microglial homeostasis in the adult mouse brain.* PLoS Biol, 2019. **17**(2): p. e3000134.

124. Levison, S.W. and J.E. Goldman, *Both oligodendrocytes and astrocytes develop from progenitors in the subventricular zone of postnatal rat forebrain.* Neuron, 1993. **10**(2): p. 201-12.

125. Levison, S.W. and J.E. Goldman, *Multipotential and lineage restricted precursors coexist in the mammalian perinatal subventricular zone.* J Neurosci Res, 1997. **48**(2): p. 83-94.

126. Steiner, B., et al., *Differential regulation of gliogenesis in the context of adult hippocampal neurogenesis in mice.* Glia, 2004. **46**(1): p. 41-52.

127. Bonaguidi, M.A., et al., *In vivo clonal analysis reveals self-renewing and multipotent adult neural stem cell characteristics.* Cell, 2011. **145**(7): p. 1142-55.

128. Eckenhoff, M.F. and P. Rakic, *Nature and fate of proliferative cells in the hippocampal dentate gyrus during the life span of the rhesus monkey.* J Neurosci, 1988. **8**(8): p. 2729-47.

129. Robins, S.C., et al., *alpha-Tanycytes of the adult hypothalamic third ventricle include distinct populations of FGF-responsive neural progenitors.* Nat Commun, 2013. **4**: p. 2049.

130. Robins, S.C., et al., *Evidence for NG2-glia derived, adult-born functional neurons in the hypothalamus.* PLoS One, 2013. **8**(10): p. e78236.

131. Djogo, T., et al., *Adult NG2-Glia Are Required for Median Eminence-Mediated Leptin Sensing and Body Weight Control.* Cell Metab, 2016. **23**(5): p. 797-810.

132. Andre, C., et al., *Inhibiting Microglia Expansion Prevents Diet-Induced Hypothalamic and Peripheral Inflammation.* Diabetes, 2017. **66**(4): p. 908-919.

133. McNay, D.E., et al., *Remodeling of the arcuate nucleus energy-balance circuit is inhibited in obese mice.* J Clin Invest, 2012. **122**(1): p. 142-52.

134. Lim, D.A. and A. Alvarez-Buylla, *The Adult Ventricular-Subventricular Zone (V-SVZ) and Olfactory Bulb (OB) Neurogenesis.* Cold Spring Harb Perspect Biol, 2016. **8**(5).

135. Silva-Vargas, V., et al., *Age-Dependent Niche Signals from the Choroid Plexus Regulate Adult Neural Stem Cells.* Cell Stem Cell, 2016. **19**(5): p. 643-652.

136. Ganat, Y.M., et al., *Early postnatal astroglial cells produce multilineage precursors and neural stem cells in vivo.* J Neurosci, 2006. **26**(33): p. 8609-21.

137. Doetsch, F., et al., *EGF converts transit-amplifying neurogenic precursors in the adult brain into multipotent stem cells.* Neuron, 2002. **36**(6): p. 1021-34.

138. Gil-Perotin, S., et al., *Adult neural stem cells from the subventricular zone: a review of the neurosphere assay.* Anat Rec (Hoboken), 2013. **296**(9): p. 1435-52.

139. Jensen, J.B. and M. Parmar, *Strengths and limitations of the neurosphere culture system.* Mol Neurobiol, 2006. **34**(3): p. 153-61.

140. Campos, L.S., *Neurospheres: insights into neural stem cell biology.* J Neurosci Res, 2004. **78**(6): p. 761-9.

141. Engstrom, C.M., et al., *A method for clonal analysis of epidermal growth factor-responsive neural progenitors.* J Neurosci Methods, 2002. **117**(2): p. 111-21.

142. Gritti, A., et al., *Epidermal and fibroblast growth factors behave as mitogenic regulators for a single multipotent stem cell-like population from the subventricular region of the adult mouse forebrain.* J Neurosci, 1999. **19**(9): p. 3287-97.

143. Morshead, C.M. and D. van der Kooy, *Disguising adult neural stem cells.* Curr Opin Neurobiol, 2004. **14**(1): p. 125-31.

144. Tropepe, V., et al., *Distinct neural stem cells proliferate in response to EGF and FGF in the developing mouse telencephalon.* Dev Biol, 1999. **208**(1): p. 166-88.

145. Bez, A., et al., *Neurosphere and neurosphere-forming cells: morphological and ultrastructural characterization.* Brain Res, 2003. **993**(1-2): p. 18-29.

146. Lobo, M.V., et al., *Cellular characterization of epidermal growth factor-expanded free-floating neurospheres.* J Histochem Cytochem, 2003. **51**(1): p. 89-103.

147. Suslov, O.N., et al., *Neural stem cell heterogeneity demonstrated by molecular phenotyping of clonal neurospheres.* Proc Natl Acad Sci U S A, 2002. **99**(22): p. 14506-11.

148. Imura, T., H.I. Kornblum, and M.V. Sofroniew, *The predominant neural stem cell isolated from postnatal and adult forebrain but not early embryonic forebrain expresses GFAP.* J Neurosci, 2003. **23**(7): p. 2824-32.

149. Laywell, E.D., et al., *Identification of a multipotent astrocytic stem cell in the immature and adult mouse brain.* Proc Natl Acad Sci U S A, 2000. **97**(25): p. 13883-8.

150. Ramalho-Santos, M., et al., *"Stemness": transcriptional profiling of embryonic and adult stem cells.* Science, 2002. **298**(5593): p. 597-600.

151. Rodriguez-Jimenez, F.J., et al., *Organized Neurogenic-Niche-Like Pinwheel Structures Discovered in Spinal Cord Tissue-Derived Neurospheres.* Front Cell Dev Biol, 2019. **7**: p. 334.

152. Bolos, M., et al., *Neurogenic effects of beta-amyloid in the choroid plexus epithelial cells in Alzheimer's disease.* Cell Mol Life Sci, 2013. **70**(15): p. 2787-97.

153. Itokazu, Y., et al., *Choroid plexus ependymal cells host neural progenitor cells in the rat.* Glia, 2006. **53**(1): p. 32-42.

154. Bifari, F., et al., *Meninges harbor cells expressing neural precursor markers during development and adulthood.* Front Cell Neurosci, 2015. **9**: p. 383.

155. Decimo, I., et al., *Meninges: from protective membrane to stem cell niche.* Am J Stem Cells, 2012. **1**(2): p. 92-105.

156. Kierdorf, K., et al., *Macrophages at CNS interfaces: ontogeny and function in health and disease.* Nat Rev Neurosci, 2019. **20**(9): p. 547-562.

157. Lee, J.Y. and S.H. Hong, *Hematopoietic Stem Cells and Their Roles in Tissue Regeneration.* Int J Stem Cells, 2020. **13**(1): p. 1-12.

158. Mezey, E., et al., *Turning blood into brain: cells bearing neuronal antigens generated in vivo from bone marrow.* Science, 2000. **290**(5497): p. 1779-82.

159. Krause, D.S., et al., *Multi-organ, multi-lineage engraftment by a single bone marrow-derived stem cell.* Cell, 2001. **105**(3): p. 369-77.

160. Rodriguez-Perez, L.M., et al., *Immunocytochemical characterisation of the wall of the bovine lateral ventricle.* Cell Tissue Res, 2003. **314**(3): p. 325-35.

161. De Nevi, E., et al., *Immunohistochemical study of doublecortin and nucleostemin in canine brain.* Eur J Histochem, 2013. **57**(1): p. e9.

162. Fasemore, T.M., et al., *The Distribution of Ki-67 and Doublecortin-Immunopositive Cells in the Brains of Three Strepsirrhine Primates: Galago demidoff, Perodicticus potto, and Lemur catta.* Neuroscience, 2018. **372**: p. 46-57.

163. Petrik, D. and J.M. Encinas, *Perspective: Of Mice and Men - How Widespread Is Adult Neurogenesis?* Front Neurosci, 2019. **13**: p. 923.

164. Bergmann, O., K.L. Spalding, and J. Frisen, *Adult Neurogenesis in Humans.* Cold Spring Harb Perspect Biol, 2015. **7**(7): p. a018994.

165. DeSesso, J.M., A.R. Scialli, and J.F. Holson, *Apparent lability of neural tube closure in laboratory animals and humans.* Am J Med Genet, 1999. **87**(2): p. 143-62.

166. Rice, D. and S. Barone, Jr., *Critical periods of vulnerability for the developing nervous system: evidence from humans and animal models.* Environ Health Perspect, 2000. **108 Suppl 3**: p. 511-33.

167. Clancy, B., et al., *Extrapolating brain development from experimental species to humans.* Neurotoxicology, 2007. **28**(5): p. 931-7.

168. Finlay, B.L. and R.B. Darlington, *Linked regularities in the development and evolution of mammalian brains.* Science, 1995. **268**(5217): p. 1578-84.

169. Kriegstein, A. and A. Alvarez-Buylla, *The glial nature of embryonic and adult neural stem cells.* Annu Rev Neurosci, 2009. **32**: p. 149-84.

170. Apfelbach, R., et al., *The effects of predator odors in mammalian prey species: a review of field and laboratory studies.* Neurosci Biobehav Rev, 2005. **29**(8): p. 1123-44.

171. Lois, C. and A. Alvarez-Buylla, *Long-distance neuronal migration in the adult mammalian brain.* Science, 1994. **264**(5162): p. 1145-8.

172. Rokni, D., et al., *An olfactory cocktail party: figure-ground segregation of odorants in rodents.* Nat Neurosci, 2014. **17**(9): p. 1225-32.

173. Kirschenbaum, B., et al., *In vitro neuronal production and differentiation by precursor cells derived from the adult human forebrain.* Cereb Cortex, 1994. **4**(6): p. 576-89.

174. Kukekov, V.G., et al., *Multipotent stem/progenitor cells with similar properties arise from two neurogenic regions of adult human brain.* Exp Neurol, 1999. **156**(2): p. 333-44.

175. Quinones-Hinojosa, A. and K. Chaichana, *The human subventricular zone: a source of new cells and a potential source of brain tumors.* Exp Neurol, 2007. **205**(2): p. 313-24.

176. Curtis, M.A., et al., *Human neuroblasts migrate to the olfactory bulb via a lateral ventricular extension.* Science, 2007. **315**(5816): p. 1243-9.

177. Sanai, N., et al., *Corridors of migrating neurons in the human brain and their decline during infancy.* Nature, 2011. **478**(7369): p. 382-6.

178. Bergmann, O., et al., *The age of olfactory bulb neurons in humans.* Neuron, 2012. **74**(4): p. 634-9.

179. Spalding, K.L., et al., *Dynamics of hippocampal neurogenesis in adult humans.* Cell, 2013. **153**(6): p. 1219-1227.

180. Sahay, A., et al., *Increasing adult hippocampal neurogenesis is sufficient to improve pattern separation.* Nature, 2011. **472**(7344): p. 466-70.

181. Blumcke, I., et al., *Increase of nestin-immunoreactive neural precursor cells in the dentate gyrus of pediatric patients with early-onset temporal lobe epilepsy.* Hippocampus, 2001. **11**(3): p. 311-21.

182. Boldrini, M., et al., *Antidepressants increase neural progenitor cells in the human hippocampus.* Neuropsychopharmacology, 2009. **34**(11): p. 2376-89.

183. Boekhoorn, K., M. Joels, and P.J. Lucassen, *Increased proliferation reflects glial and vascular-associated changes, but not neurogenesis in the presenile Alzheimer hippocampus.* Neurobiol Dis, 2006. **24**(1): p. 1-14.

184. Jin, K., et al., *Increased hippocampal neurogenesis in Alzheimer's disease.* Proc Natl Acad Sci U S A, 2004. **101**(1): p. 343-7.

185. Monje, M.L., et al., *Impaired human hippocampal neurogenesis after treatment for central nervous system malignancies.* Ann Neurol, 2007. **62**(5): p. 515-20.

186. Allen, K.M., S.J. Fung, and C.S. Weickert, *Cell proliferation is reduced in the hippocampus in schizophrenia.* Aust N Z J Psychiatry, 2016. **50**(5): p. 473-80.

187. Le Maitre, T.W., et al., *Effects of Alcohol Abuse on Proliferating Cells, Stem/Progenitor Cells, and Immature Neurons in the Adult Human Hippocampus.* Neuropsychopharmacology, 2018. **43**(4): p. 690-699.

188. Lucassen, P.J., et al., *Regulation of adult neurogenesis by stress, sleep disruption, exercise and inflammation: Implications for depression and antidepressant action.* Eur Neuropsychopharmacol, 2010. **20**(1): p. 1-17.

189. Crews, L., et al., *Increased BMP6 levels in the brains of Alzheimer's disease patients and APP transgenic mice are accompanied by impaired neurogenesis.* J Neurosci, 2010. **30**(37): p. 12252-62.

190. Moreno-Jimenez, E.P., et al., *Evidences for Adult Hippocampal Neurogenesis in Humans.* J Neurosci, 2021. **41**(12): p. 2541-2553.

191. D'Alessio, L., et al., *Dentate gyrus expression of nestin-immunoreactivity in patients with drug-resistant temporal lobe epilepsy and hippocampal sclerosis.* Seizure, 2015. **27**: p. 75-9.

192. D'Alessio, L., et al., *Doublecortin (DCX) immunoreactivity in hippocampus of chronic refractory temporal lobe epilepsy patients with hippocampal sclerosis.* Seizure, 2010. **19**(9): p. 567-72.

193. Epp, J.R., C.L. Beasley, and L.A. Galea, *Increased hippocampal neurogenesis and p21 expression in depression: dependent on antidepressants, sex, age, and antipsychotic exposure.* Neuropsychopharmacology, 2013. **38**(11): p. 2297-306.

194. Cipriani, S., et al., *Hippocampal Radial Glial Subtypes and Their Neurogenic Potential in Human Fetuses and Healthy and Alzheimer's Disease Adults.* Cereb Cortex, 2018. **28**(7): p. 2458-2478.

195. Dennis, C.V., et al., *Human adult neurogenesis across the ages: An immunohistochemical study.* Neuropathol Appl Neurobiol, 2016. **42**(7): p. 621-638.

196. Paredes, M.F., et al., *Does Adult Neurogenesis Persist in the Human Hippocampus?* Cell Stem Cell, 2018. **23**(6): p. 780-781.

197. Knoth, R., et al., *Murine features of neurogenesis in the human hippocampus across the lifespan from 0 to 100 years.* PLoS One, 2010. **5**(1): p. e8809.

198. Sorrells, S.F., et al., *Human hippocampal neurogenesis drops sharply in children to undetectable levels in adults.* Nature, 2018. **555**(7696): p. 377-381.

199. Sorrells, S.F., et al., *Positive Controls in Adults and Children Support That Very Few, If Any, New Neurons Are Born in the Adult Human Hippocampus.* J Neurosci, 2021. **41**(12): p. 2554-2565.

200. Boldrini, M., et al., *Human Hippocampal Neurogenesis Persists throughout Aging.* Cell Stem Cell, 2018. **22**(4): p. 589-599 e5.

201. Flor-Garcia, M., et al., *Unraveling human adult hippocampal neurogenesis.* Nat Protoc, 2020. **15**(2): p. 668-693.

202. Franjic, D., et al., *Transcriptomic taxonomy and neurogenic trajectories of adult human, macaque, and pig hippocampal and entorhinal cells.* Neuron, 2022. **110**(3): p. 452-469 e14.

203. Palmer, T.D., et al., *Fibroblast growth factor-2 activates a latent neurogenic program in neural stem cells from diverse regions of the adult CNS.* J Neurosci, 1999. **19**(19): p. 8487-97.

204. Urban, N. and F. Guillemot, *Neurogenesis in the embryonic and adult brain: same regulators, different roles.* Front Cell Neurosci, 2014. **8**: p. 396.

205. Wardle, R.A. and M.M. Poo, *Brain-derived neurotrophic factor modulation of GABAergic synapses by postsynaptic regulation of chloride transport.* J Neurosci, 2003. **23**(25): p. 8722-32.

206. Liddelow, S.A., *Development of the choroid plexus and blood-CSF barrier.* Front Neurosci, 2015. **9**: p. 32.

207. Bowyer, J.F., et al., *A visual description of the dissection of the cerebral surface vasculature and associated meninges and the choroid plexus from rat brain.* J Vis Exp, 2012(69): p. e4285.

208. Daneman, R. and A. Prat, *The blood-brain barrier.* Cold Spring Harb Perspect Biol, 2015. **7**(1): p. a020412.

209. Brightman, M.W., et al., *Osmotic opening of tight junctions in cerebral endothelium.* J Comp Neurol, 1973. **152**(4): p. 317-25.

210. Brightman, M.W. and T.S. Reese, *Junctions between intimately apposed cell membranes in the vertebrate brain.* J Cell Biol, 1969. **40**(3): p. 648-77.

211. Coomber, B.L. and P.A. Stewart, *Morphometric analysis of CNS microvascular endothelium.* Microvasc Res, 1985. **30**(1): p. 99-115.

212. Reese, T.S. and M.J. Karnovsky, *Fine structural localization of a blood-brain barrier to exogenous peroxidase.* J Cell Biol, 1967. **34**(1): p. 207-17.

213. Ottone, C. and S. Parrinello, *Multifaceted control of adult SVZ neurogenesis by the vascular niche.* Cell Cycle, 2015. **14**(14): p. 2222-5.

214. Andreu-Agullo, C., et al., *Vascular niche factor PEDF modulates Notch-dependent stemness in the adult subependymal zone.* Nat Neurosci, 2009. **12**(12): p. 1514-23.

215. Montagne, A., et al., *Blood-brain barrier breakdown in the aging human hippocampus.* Neuron, 2015. **85**(2): p. 296-302.

216. Tavazoie, M., et al., *A specialized vascular niche for adult neural stem cells.* Cell Stem Cell, 2008. **3**(3): p. 279-88.

217. Kuhn, H.G., H. Dickinson-Anson, and F.H. Gage, *Neurogenesis in the dentate gyrus of the adult rat: age-related decrease of neuronal progenitor proliferation.* J Neurosci, 1996. **16**(6): p. 2027-33.

218. Watters, A.K., et al., *Identification and dynamic regulation of tight junction protein expression in human neural stem cells.* Stem Cells Dev, 2015. **24**(12): p. 1377-89.

219. Urban, N., et al., *Return to quiescence of mouse neural stem cells by degradation of a proactivation protein.* Science, 2016. **353**(6296): p. 292-5.

220. Hall, C.N., et al., *Oxidative phosphorylation, not glycolysis, powers presynaptic and postsynaptic mechanisms underlying brain information processing.* J Neurosci, 2012. **32**(26): p. 8940-51.

221. Mukherjee, S., et al., *REST regulation of gene networks in adult neural stem cells.* Nat Commun, 2016. **7**: p. 13360.

222. Baser, A., et al., *Onset of differentiation is post-transcriptionally controlled in adult neural stem cells.* Nature, 2019. **566**(7742): p. 100-104.

223. Webb, A.E., et al., *FOXO3 shares common targets with ASCL1 genome-wide and inhibits ASCL1-dependent neurogenesis.* Cell Rep, 2013. **4**(3): p. 477-91.

224. Scharfman, H., et al., *Increased neurogenesis and the ectopic granule cells after intrahippocampal BDNF infusion in adult rats.* Exp Neurol, 2005. **192**(2): p. 348-56.

225. Zigova, T., et al., *Intraventricular administration of BDNF increases the number of newly generated neurons in the adult olfactory bulb.* Mol Cell Neurosci, 1998. **11**(4): p. 234-45.

226. Ahn, S. and A.L. Joyner, *In vivo analysis of quiescent adult neural stem cells responding to Sonic hedgehog.* Nature, 2005. **437**(7060): p. 894-7.

227. Angot, E., et al., *Chemoattractive activity of sonic hedgehog in the adult subventricular zone modulates the number of neural precursors reaching the olfactory bulb.* Stem Cells, 2008. **26**(9): p. 2311-20.

228. Balordi, F. and G. Fishell, *Hedgehog signaling in the subventricular zone is required for both the maintenance of stem cells and the migration of newborn neurons.* J Neurosci, 2007. **27**(22): p. 5936-47.

229. Ables, J.L., et al., *Notch1 is required for maintenance of the reservoir of adult hippocampal stem cells.* J Neurosci, 2010. **30**(31): p. 10484-92.

230. Nomura, T., et al., *EphB signaling controls lineage plasticity of adult neural stem cell niche cells.* Cell Stem Cell, 2010. **7**(6): p. 730-43.

231. Lie, D.C., et al., *Wnt signalling regulates adult hippocampal neurogenesis.* Nature, 2005. **437**(7063): p. 1370-5.

232. Yu, J.M., et al., *Increase in proliferation and differentiation of neural progenitor cells isolated from postnatal and adult mice brain by Wnt-3a and Wnt-5a.* Mol Cell Biochem, 2006. **288**(1-2): p. 17-28.

233. Greider, C.W. and E.H. Blackburn, *A telomeric sequence in the RNA of Tetrahymena telomerase required for telomere repeat synthesis.* Nature, 1989. **337**(6205): p. 331-7.

234. Blasco, M.A., *Telomeres and human disease: ageing, cancer and beyond.* Nat Rev Genet, 2005. **6**(8): p. 611-22.

235. Xu, L., S. Li, and B.A. Stohr, *The role of telomere biology in cancer.* Annu Rev Pathol, 2013. **8**: p. 49-78.

236. Harrington, L., et al., *A mammalian telomerase-associated protein.* Science, 1997. **275**(5302): p. 973-7.

237. Akincilar, S.C., et al., *Long-Range Chromatin Interactions Drive Mutant TERT Promoter Activation.* Cancer Discov, 2016. **6**(11): p. 1276-1291.

238. Hrdlickova, R., J. Nehyba, and H.R. Bose, Jr., *Alternatively spliced telomerase reverse transcriptase variants lacking telomerase activity stimulate cell proliferation.* Mol Cell Biol, 2012. **32**(21): p. 4283-96.

239. Feng, J., et al., *The RNA component of human telomerase.* Science, 1995. **269**(5228): p. 1236-41.

240. Trybek, T., et al., *Telomeres and telomerase in oncogenesis.* Oncol Lett, 2020. **20**(2): p. 1015-1027.

241. Jafri, M.A., et al., *Roles of telomeres and telomerase in cancer, and advances in telomerase-targeted therapies.* Genome Med, 2016. **8**(1): p. 69.

242. Bourgeron, T., et al., *The asymmetry of telomere replication contributes to replicative senescence heterogeneity.* Sci Rep, 2015. **5**: p. 15326.

243. Collins, K. and J.R. Mitchell, *Telomerase in the human organism.* Oncogene, 2002. **21**(4): p. 564-79.

244. Newbold, R.F., *Genetic control of telomerase and replicative senescence in human and rodent cells.* Ciba Found Symp, 1997. **211**: p. 177-89; discussion 189-97.

245. Hastie, N.D., et al., *Telomere reduction in human colorectal carcinoma and with ageing.* Nature, 1990. **346**(6287): p. 866-8.

246. Lindsey, J., et al., *In vivo loss of telomeric repeats with age in humans.* Mutat Res, 1991. **256**(1): p. 45-8.

247. Harley, C.B., *Telomere loss: mitotic clock or genetic time bomb?* Mutat Res, 1991. **256**(2-6): p. 271-82.

248. Shammas, M.A., *Telomeres, lifestyle, cancer, and aging.* Curr Opin Clin Nutr Metab Care, 2011. **14**(1): p. 28-34.

249. Wright, W.E. and J.W. Shay, *The two-stage mechanism controlling cellular senescence and immortalization.* Exp Gerontol, 1992. **27**(4): p. 383-9.

250. Shay, J.W., *Telomerase therapeutics: telomeres recognized as a DNA damage signal: commentary re: K. Kraemer et al., antisense-mediated hTERT inhibition specifically reduces the growth of human bladder cancer cells. Clin. Cancer Res., 9: 3794-3800, 2003.* Clin Cancer Res, 2003. **9**(10 Pt 1): p. 3521-5.

251. Wright, W.E., O.M. Pereira-Smith, and J.W. Shay, *Reversible cellular senescence: implications for immortalization of normal human diploid fibroblasts.* Mol Cell Biol, 1989. **9**(7): p. 3088-92.

252. Shawi, M. and C. Autexier, *Telomerase, senescence and ageing.* Mech Ageing Dev, 2008. **129**(1-2): p. 3-10.

253. Shay, J.W. and W.E. Wright, *Senescence and immortalization: role of telomeres and telomerase.* Carcinogenesis, 2005. **26**(5): p. 867-74.

254. Pan, C., et al., *Changes in telomerase activity and telomere length during human T lymphocyte senescence.* Exp Cell Res, 1997. **231**(2): p. 346-53.

255. Wright, W.E., et al., *Telomerase activity in human germline and embryonic tissues and cells.* Dev Genet, 1996. **18**(2): p. 173-9.

256. Podlevsky, J.D. and J.J. Chen, *It all comes together at the ends: telomerase structure, function, and biogenesis.* Mutat Res, 2012. **730**(1-2): p. 3-11.

257. Pestana, A., et al., *TERT biology and function in cancer: beyond immortalisation.* J Mol Endocrinol, 2017. **58**(2): p. R129-R146.

258. Cong, Y.S., W.E. Wright, and J.W. Shay, *Human telomerase and its regulation.* Microbiol Mol Biol Rev, 2002. **66**(3): p. 407-25, table of contents.

259. Greenberg, R.A., et al., *Expression of mouse telomerase reverse transcriptase during development, differentiation and proliferation.* Oncogene, 1998. **16**(13): p. 1723-30.

260. Kyo, S., et al., *Understanding and exploiting hTERT promoter regulation for diagnosis and treatment of human cancers.* Cancer Sci, 2008. **99**(8): p. 1528-38.

261. Kilian, A., et al., *Isolation of a candidate human telomerase catalytic subunit gene, which reveals complex splicing patterns in different cell types.* Hum Mol Genet, 1997. **6**(12): p. 2011-9.

262. Counter, C.M., et al., *Telomere shortening associated with chromosome instability is arrested in immortal cells which express telomerase activity.* EMBO J, 1992. **11**(5): p. 1921-9.

263. Nugent, C.I. and V. Lundblad, *The telomerase reverse transcriptase: components and regulation.* Genes Dev, 1998. **12**(8): p. 1073-85.

264. Palanca-Wessels, M.C., et al., *Genetic analysis of long-term Barrett's esophagus epithelial cultures exhibiting cytogenetic and ploidy abnormalities.* Gastroenterology, 1998. **114**(2): p. 295-304.

265. Venetsanakos, E., et al., *Induction of tubulogenesis in telomerase-immortalized human microvascular endothelial cells by glioblastoma cells.* Exp Cell Res, 2002. **273**(1): p. 21-33.

266. Thi, M.M., et al., *Characterization of hTERT-immortalized osteoblast cell lines generated from wild-type and connexin43-null mouse calvaria.* Am J Physiol Cell Physiol, 2010. **299**(5): p. C994-C1006.

267. Horikawa, I., et al., *Differential cis-regulation of human versus mouse TERT gene expression in vivo: identification of a human-specific repressive element.* Proc Natl Acad Sci U S A, 2005. **102**(51): p. 18437-42.

268. Martin-Rivera, L., et al., *Expression of mouse telomerase catalytic subunit in embryos and adult tissues.* Proc Natl Acad Sci U S A, 1998. **95**(18): p. 10471-6.

269. Caporaso, G.L., et al., *Telomerase activity in the subventricular zone of adult mice.* Mol Cell Neurosci, 2003. **23**(4): p. 693-702.

270. Mitchell, J.R., E. Wood, and K. Collins, *A telomerase component is defective in the human disease dyskeratosis congenita.* Nature, 1999. **402**(6761): p. 551-5.

271. Vulliamy, T.J., et al., *Very short telomeres in the peripheral blood of patients with X-linked and autosomal dyskeratosis congenita.* Blood Cells Mol Dis, 2001. **27**(2): p. 353-7.

272. Wright, W.E. and J.W. Shay, *Telomere dynamics in cancer progression and prevention: fundamental differences in human and mouse telomere biology.* Nat Med, 2000. **6**(8): p. 849-51.

273. Harle-Bachor, C. and P. Boukamp, *Telomerase activity in the regenerative basal layer of the epidermis inhuman skin and in immortal and carcinoma-derived skin keratinocytes.* Proc Natl Acad Sci U S A, 1996. **93**(13): p. 6476-81.

274. Attia, E.A., et al., *Study of telomerase reverse transcriptase (hTERT) expression in normal, aged, and photo-aged skin.* Int J Dermatol, 2010. **49**(8): p. 886-93.

275. Mahmoud, M.A., et al., *Expression of telomerase reverse transcriptase in psoriatic lesional skin.* Dis Markers, 2006. **22**(4): p. 265-9.

276. Broccoli, D., J.W. Young, and T. de Lange, *Telomerase activity in normal and malignant hematopoietic cells.* Proc Natl Acad Sci U S A, 1995. **92**(20): p. 9082-6.

277. Liu, K., et al., *Constitutive and regulated expression of telomerase reverse transcriptase (hTERT) in human lymphocytes.* Proc Natl Acad Sci U S A, 1999. **96**(9): p. 5147-52.

278. Chiu, C.P., et al., *Differential expression of telomerase activity in hematopoietic progenitors from adult human bone marrow.* Stem Cells, 1996. **14**(2): p. 239-48.

279. Patrick, M. and N.P. Weng, *Expression and regulation of telomerase in human T cell differentiation, activation, aging and diseases.* Cell Immunol, 2019. **345**: p. 103989.

280. Rufer, N., et al., *Transfer of the human telomerase reverse transcriptase (TERT) gene into T lymphocytes results in extension of replicative potential.* Blood, 2001. **98**(3): p. 597-603.

281. Brien, T.P., et al., *Telomerase activity in benign endometrium and endometrial carcinoma.* Cancer Res, 1997. **57**(13): p. 2760-4.

282. Hiyama, E., et al., *Telomerase activity in human intestine.* Int J Oncol, 1996. **9**(3): p. 453-8.

283. Cousins, F.L., et al., *Telomerase Reverse Transcriptase Expression in Mouse Endometrium During Reepithelialization and Regeneration in a Menses-Like Model.* Stem Cells Dev, 2019. **28**(1): p. 1-12.

284. Breault, D.T., et al., *Generation of mTert-GFP mice as a model to identify and study tissue progenitor cells.* Proc Natl Acad Sci U S A, 2008. **105**(30): p. 10420-5.

285. Montgomery, R.K., et al., *Mouse telomerase reverse transcriptase (mTert) expression marks slowly cycling intestinal stem cells.* Proc Natl Acad Sci U S A, 2011. **108**(1): p. 179-84.

286. Lin, S., et al., *Distributed hepatocytes expressing telomerase repopulate the liver in homeostasis and injury.* Nature, 2018. **556**(7700): p. 244-248.

287. Carlone, D.L., et al., *Telomerase expression marks transitional growth-associated skeletal progenitor/stem cells.* Stem Cells, 2021. **39**(3): p. 296-305.

288. Lynes, M.D., et al., *Telomerase reverse transcriptase expression marks a population of rare adipose tissue stem cells.* Stem Cells, 2021 (accepted manuscript).

289. Wang, J., et al., *Myc activates telomerase.* Genes Dev, 1998. **12**(12): p. 1769-74.

290. Kyo, S., et al., *Estrogen activates telomerase.* Cancer Res, 1999. **59**(23): p. 5917-21.

291. Oh, S.T., S. Kyo, and L.A. Laimins, *Telomerase activation by human papillomavirus type 16 E6 protein: induction of human telomerase reverse transcriptase expression through Myc and GC-rich Sp1 binding sites.* J Virol, 2001. **75**(12): p. 5559-66.

292. Wang, Z., et al., *Progesterone regulates human telomerase reverse transcriptase gene expression via activation of mitogen-activated protein kinase signaling pathway.* Cancer Res, 2000. **60**(19): p. 5376-81.

293. Xu, D., et al., *Switch from Myc/Max to Mad1/Max binding and decrease in histone acetylation at the telomerase reverse transcriptase promoter during differentiation of HL60 cells.* Proc Natl Acad Sci U S A, 2001. **98**(7): p. 3826-31.

294. Kanaya, T., et al., *Adenoviral expression of p53 represses telomerase activity through down-regulation of human telomerase reverse transcriptase transcription.* Clin Cancer Res, 2000. **6**(4): p. 1239-47.

295. Liu, K., R.J. Hodes, and N. Weng, *Cutting edge: telomerase activation in human T lymphocytes does not require increase in telomerase reverse transcriptase (hTERT) protein but is associated with hTERT phosphorylation and nuclear translocation.* J Immunol, 2001. **166**(8): p. 4826-30.

296. Castelo-Branco, P., et al., *Methylation of the TERT promoter and risk stratification of childhood brain tumours: an integrative genomic and molecular study.* Lancet Oncol, 2013. **14**(6): p. 534-42.

297. Seynnaeve, B., et al., *Genetic and Epigenetic Alterations of TERT Are Associated with Inferior Outcome in Adolescent and Young Adult Patients with Melanoma.* Sci Rep, 2017. **7**: p. 45704.

298. Ishaq, A., et al., *Telomerase Activity is Downregulated Early During Human Brain Development.* Genes (Basel), 2016. **7**(6).

299. Klapper, W., T. Shin, and M.P. Mattson, *Differential regulation of telomerase activity and TERT expression during brain development in mice.* J Neurosci Res, 2001. **64**(3): p. 252-60.

300. Ostenfeld, T., et al., *Human neural precursor cells express low levels of telomerase in vitro and show diminishing cell proliferation with extensive axonal outgrowth following transplantation.* Exp Neurol, 2000. **164**(1): p. 215-26.

301. Miura, T., et al., *Neural stem cells lose telomerase activity upon differentiating into astrocytes.* Cytotechnology, 2001. **36**(1-3): p. 137-44.

302. Kondo, S., et al., *Antisense telomerase treatment: induction of two distinct pathways, apoptosis and differentiation.* FASEB J, 1998. **12**(10): p. 801-11.

303. Kruk, P.A., et al., *Telomere reduction and telomerase inactivation during neuronal cell differentiation.* Biochem Biophys Res Commun, 1996. **224**(2): p. 487-92.

304. Jaskelioff, M., et al., *Telomerase reactivation reverses tissue degeneration in aged telomerase-deficient mice.* Nature, 2011. **469**(7328): p. 102-6.

305. Zhou, Q.G., et al., *Hippocampal TERT Regulates Spatial Memory Formation through Modulation of Neural Development.* Stem Cell Reports, 2017. **9**(2): p. 543-556.

306. Mattson, M.P. and W. Klapper, *Emerging roles for telomerase in neuronal development and apoptosis.* J Neurosci Res, 2001. **63**(1): p. 1-9.

307. Fu, W., et al., *The catalytic subunit of telomerase is expressed in developing brain neurons and serves a cell survival-promoting function.* J Mol Neurosci, 2000. **14**(1-2): p. 3-15.

308. Lu, C., W. Fu, and M.P. Mattson, *Telomerase protects developing neurons against DNA damage-induced cell death.* Brain Res Dev Brain Res, 2001. **131**(1-2): p. 167-71.

309. Eitan, E., et al., *Excitotoxic and Radiation Stress Increase TERT Levels in the Mitochondria and Cytosol of Cerebellar Purkinje Neurons.* Cerebellum, 2016. **15**(4): p. 509-17.

310. Zhu, H., W. Fu, and M.P. Mattson, *The catalytic subunit of telomerase protects neurons against amyloid beta-peptide-induced apoptosis.* J Neurochem, 2000. **75**(1): p. 117-24.

311. Miwa, S., et al., *Decreased mTOR signalling reduces mitochondrial ROS in brain via accumulation of the telomerase protein TERT within mitochondria.* Aging (Albany NY), 2016. **8**(10): p. 2551-2567.

312. Kang, H.J., et al., *Ectopic expression of the catalytic subunit of telomerase protects against brain injury resulting from ischemia and NMDA-induced neurotoxicity.* J Neurosci, 2004. **24**(6): p. 1280-7.

313. Thompson, C.A.H. and J.M.Y. Wong, *Non-canonical Functions of Telomerase Reverse Transcriptase: Emerging Roles and Biological Relevance.* Curr Top Med Chem, 2020. **20**(6): p. 498-507.

314. Ulaner, G.A., et al., *Telomerase activity in human development is regulated by human telomerase reverse transcriptase (hTERT) transcription and by alternate splicing of hTERT transcripts.* Cancer Res, 1998. **58**(18): p. 4168-72.

315. Ulaner, G.A., et al., *Regulation of telomerase by alternate splicing of human telomerase reverse transcriptase (hTERT) in normal and neoplastic ovary, endometrium and myometrium.* Int J Cancer, 2000. **85**(3): p. 330-5.

316. Jose, S.S., et al., *The Telomerase Complex Directly Controls Hematopoietic Stem Cell Differentiation and Senescence in an Induced Pluripotent Stem Cell Model of Telomeropathy.* Frontiers in Genetics, 2018. **9**.

317. Yin, L., A.K. Hubbard, and C. Giardina, *NF-kappa B regulates transcription of the mouse telomerase catalytic subunit.* J Biol Chem, 2000. **275**(47): p. 36671-5.

318. Fuhrmann, G., et al., *The MYC dualism in growth and death.* Mutat Res, 1999. **437**(3): p. 205-17.

319. Cao, Y., et al., *TERT regulates cell survival independent of telomerase enzymatic activity.* Oncogene, 2002. **21**(20): p. 3130-8.

320. Del Bufalo, D., et al., *Involvement of hTERT in apoptosis induced by interference with Bcl-2 expression and function.* Cell Death Differ, 2005. **12**(11): p. 1429-38.

321. Folini, M., et al., *Antisense oligonucleotide-mediated inhibition of hTERT, but not hTERC, induces rapid cell growth decline and apoptosis in the absence of telomere shortening in human prostate cancer cells.* Eur J Cancer, 2005. **41**(4): p. 624-34.

322. Massard, C., et al., *hTERT: a novel endogenous inhibitor of the mitochondrial cell death pathway.* Oncogene, 2006. **25**(33): p. 4505-14.

323. Yatabe, N., et al., *2-5A antisense therapy directed against human telomerase RNA inhibits telomerase activity and induces apoptosis without telomere impairment in cervical cancer cells.* Cancer Gene Ther, 2002. **9**(7): p. 624-30.

324. Indran, I.R., M.P. Hande, and S. Pervaiz, *hTERT overexpression alleviates intracellular ROS production, improves mitochondrial function, and inhibits ROS-mediated apoptosis in cancer cells.* Cancer Res, 2011. **71**(1): p. 266-76.

325. Moon, D.O., et al., *Sulforaphane decreases viability and telomerase activity in hepatocellular carcinoma Hep3B cells through the reactive oxygen species-dependent pathway.* Cancer Lett, 2010. **295**(2): p. 260-6.

326. Ahmed, S., et al., *Telomerase does not counteract telomere shortening but protects mitochondrial function under oxidative stress.* J Cell Sci, 2008. **121**(Pt 7): p. 1046-53.

327. Martens, A., et al., *Telomerase Does Not Improve DNA Repair in Mitochondria upon Stress but Increases MnSOD Protein under Serum-Free Conditions.* Int J Mol Sci, 2019. **21**(1).

328. Rosen, J., et al., *Non-canonical functions of Telomerase Reverse Transcriptase - Impact on redox homeostasis.* Redox Biol, 2020. **34**: p. 101543.

329. Gloaguen, I., et al., *Ciliary neurotrophic factor corrects obesity and diabetes associated with leptin deficiency and resistance.* Proc Natl Acad Sci U S A, 1997. **94**(12): p. 6456-61.

330. Ettinger, M.P., et al., *Recombinant variant of ciliary neurotrophic factor for weight loss in obese adults: a randomized, dose-ranging study.* JAMA, 2003. **289**(14): p. 1826-32.

331. Wu, P., et al., *Systematic gene expression profile of hypothalamus in calorie-restricted mice implicates the involvement of mTOR signaling in neuroprotective activity.* Mech Ageing Dev, 2009. **130**(9): p. 602-10.

332. Bolborea, M. and N. Dale, *Hypothalamic tanycytes: potential roles in the control of feeding and energy balance.* Trends Neurosci, 2013. **36**(2): p. 91-100.

333. Gao, Y., et al., *Hormones and diet, but not body weight, control hypothalamic microglial activity.* Glia, 2014. **62**(1): p. 17-25.

334. Wang, X.L. and L. Li, *Microglia Regulate Neuronal Circuits in Homeostatic and High-Fat Diet-Induced Inflammatory Conditions.* Front Cell Neurosci, 2021. **15**: p. 722028.

335. Jin, S., et al., *Hypothalamic TLR2 triggers sickness behavior via a microglia-neuronal axis.* Sci Rep, 2016. **6**: p. 29424.

336. Moraes, J.C., et al., *High-fat diet induces apoptosis of hypothalamic neurons.* PLoS One, 2009. **4**(4): p. e5045.

337. Thaler, J.P., et al., *Obesity is associated with hypothalamic injury in rodents and humans.* J Clin Invest, 2012. **122**(1): p. 153-62.

338. Morari, J., et al., *Fractalkine (CX3CL1) is involved in the early activation of hypothalamic inflammation in experimental obesity.* Diabetes, 2014. **63**(11): p. 3770-84.

339. Andre, D.M., et al., *High-fat diet-induced obesity impairs insulin signaling in lungs of allergen-challenged mice: Improvement by resveratrol.* Sci Rep, 2017. **7**(1): p. 17296.

340. Ming, G.L. and H. Song, *Adult neurogenesis in the mammalian brain: significant answers and significant questions.* Neuron, 2011. **70**(4): p. 687-702.

341. Ernst, A., et al., *Neurogenesis in the striatum of the adult human brain.* Cell, 2014. **156**(5): p. 1072-83.

342. Abbott, L.C. and F. Nigussie, *Adult neurogenesis in the mammalian dentate gyrus.* Anat Histol Embryol, 2020. **49**(1): p. 3-16.

343. Jurkowski, M.P., et al., *Beyond the Hippocampus and the SVZ: Adult Neurogenesis Throughout the Brain.* Front Cell Neurosci, 2020. **14**: p. 576444.

344. Deane, J.A., et al., *The mouse endometrium contains epithelial, endothelial and leucocyte populations expressing the stem cell marker telomerase reverse transcriptase.* Mol Hum Reprod, 2016. **22**(4): p. 272-84.

345. Lin, S., et al., *Distributed hepatocytes expressing telomerase repopulate the liver in homeostasis and injury.* Nature, 2018. **556**(7700): p. 244-248.

346. Lynes MD, D.C., KL Townsend, DT Braeault, Y-H Tseng, *Telomerase reverse transcriptase expression marks a population of rare adipose tissue stem cells.* 2021 (accepted manuscript).

347. Richardson, G.D., et al., *Telomerase expression in the mammalian heart.* Faseb j, 2012. **26**(12): p. 4832-40.

348. Song, J., et al., *Characterization and fate of telomerase-expressing epithelia during kidney repair.* J Am Soc Nephrol, 2011. **22**(12): p. 2256-65.

349. Zhou, Q.G., et al., *Hippocampal telomerase is involved in the modulation of depressive behaviors.* J Neurosci, 2011. **31**(34): p. 12258-69.

350. Ferron, S.R., et al., *Telomere shortening in neural stem cells disrupts neuronal differentiation and neuritogenesis.* J Neurosci, 2009. **29**(46): p. 14394-407.

351. Usta, S.N., et al., *Chemically defined serum-free and xeno-free media for multiple cell lineages.* Ann Transl Med, 2014. **2**(10): p. 97.

352. Mira, H., et al., *Signaling through BMPR-IA regulates quiescence and long-term activity of neural stem cells in the adult hippocampus.* Cell Stem Cell, 2010. **7**(1): p. 78-89.

353. Reynolds, B.A. and R.L. Rietze, *Neural stem cells and neurospheres--re-evaluating the relationship.* Nat Methods, 2005. **2**(5): p. 333-6.

354. Zhang, J. and J. Jiao, *Molecular Biomarkers for Embryonic and Adult Neural Stem Cell and Neurogenesis.* Biomed Res Int, 2015. **2015**: p. 727542.

355. Jensen, G.S., N.E. Leon-Palmer, and K.L. Townsend, *Bone morphogenetic proteins (BMPs) in the central regulation of energy balance and adult neural plasticity.* Metabolism, 2021. **123**: p. 154837.

356. Rusznak, Z., et al., *Adult Neurogenesis and Gliogenesis: Possible Mechanisms for Neurorestoration.* Exp Neurobiol, 2016. **25**(3): p. 103-12.

357. Nishiyama, A., et al., *Identity, distribution, and development of polydendrocytes: NG2-expressing glial cells.* J Neurocytol, 2002. **31**(6-7): p. 437-55.

358. Carlone, D.L., *Identifying Adult Stem Cells Using Cre-Mediated Lineage Tracing.* Curr Protoc Stem Cell Biol, 2016. **36**: p. 5a.2.1-5a.2.18.

359. Muzumdar, M.D., et al., *A global double-fluorescent Cre reporter mouse.* Genesis, 2007. **45**(9): p. 593-605.

360. Lugert, S., et al., *Quiescent and active hippocampal neural stem cells with distinct morphologies respond selectively to physiological and pathological stimuli and aging.* Cell Stem Cell, 2010. **6**(5): p. 445-56.

361. Ortega-Perez, I., K. Murray, and P.M. Lledo, *The how and why of adult neurogenesis.* J Mol Histol, 2007. **38**(6): p. 555-62.

362. Petreanu, L. and A. Alvarez-Buylla, *Maturation and death of adult-born olfactory bulb granule neurons: role of olfaction.* J Neurosci, 2002. **22**(14): p. 6106-13.

363. Ahlfeld, J., et al., *Neurogenesis from Sox2 expressing cells in the adult cerebellar cortex.* Sci Rep, 2017. **7**(1): p. 6137.

364. Nakagomi, T., et al., *Ischemia-induced neural stem/progenitor cells in the pia mater following cortical infarction.* Stem Cells Dev, 2011. **20**(12): p. 2037-51.

365. Decimo, I., et al., *Meninges: A Widespread Niche of Neural Progenitors for the Brain.* Neuroscientist, 2020: p. 1073858420954826.

366. Tumani, H., A. Huss, and F. Bachhuber, *The cerebrospinal fluid and barriers - anatomic and physiologic considerations.* Handb Clin Neurol, 2017. **146**: p. 21-32.

367. Lun, M.P., E.S. Monuki, and M.K. Lehtinen, *Development and functions of the choroid plexus-cerebrospinal fluid system.* Nat Rev Neurosci, 2015. **16**(8): p. 445-57.

368. Feinstein, P., et al., *Axon guidance of mouse olfactory sensory neurons by odorant receptors and the beta2 adrenergic receptor.* Cell, 2004. **117**(6): p. 833-46.

369. Paton, J.A. and F.N. Nottebohm, *Neurons generated in the adult brain are recruited into functional circuits.* Science, 1984. **225**(4666): p. 1046-8.

370. Richards, L.J., T.J. Kilpatrick, and P.F. Bartlett, *De novo generation of neuronal cells from the adult mouse brain.* Proc Natl Acad Sci U S A, 1992. **89**(18): p. 8591-5.

371. Reynolds, B.A. and S. Weiss, *Generation of neurons and astrocytes from isolated cells of the adult mammalian central nervous system.* Science, 1992. **255**(5052): p. 1707-10.

372. Liu, J.P., *Studies of the molecular mechanisms in the regulation of telomerase activity.* FASEB J, 1999. **13**(15): p. 2091-104.

373. Ong, Y.R., et al., *Bone Marrow Stem Cells Do Not Contribute to Endometrial Cell Lineages in Chimeric Mouse Models.* Stem Cells, 2018. **36**(1): p. 91-102.

374. Zvereva, M.I., D.M. Shcherbakova, and O.A. Dontsova, *Telomerase: structure, functions, and activity regulation.* Biochemistry (Mosc), 2010. **75**(13): p. 1563-83.

375. Zheng, Q., J. Huang, and G. Wang, *Mitochondria, Telomeres and Telomerase Subunits.* Front Cell Dev Biol, 2019. **7**: p. 274.

376. Charvet, C.J. and B.L. Finlay, *Comparing Adult Hippocampal Neurogenesis Across Species: Translating Time to Predict the Tempo in Humans.* Front Neurosci, 2018. **12**: p. 706.

377. Gandhi, S., J. Gupta, and P.P. Tripathi, *The Curious Case of Human Hippocampal Neurogenesis.* ACS Chem Neurosci, 2019. **10**(3): p. 1131-1132.

378. Lucassen, P.J., et al., *Adult neurogenesis, human after all (again): Classic, optimized, and future approaches.* Behav Brain Res, 2020. **381**: p. 112458.

379. Seki, T., *Understanding the Real State of Human Adult Hippocampal Neurogenesis From Studies of Rodents and Non-human Primates.* Front Neurosci, 2020. **14**: p. 839.

380. Kempermann, G., et al., *Human Adult Neurogenesis: Evidence and Remaining Questions.* Cell Stem Cell, 2018. **23**(1): p. 25-30.

381. Spilsbury, A., et al., *The role of telomerase protein TERT in Alzheimer's disease and in tau-related pathology in vitro.* J Neurosci, 2015. **35**(4): p. 1659-74.

382. Ulaner, G.A. and L.C. Giudice, *Developmental regulation of telomerase activity in human fetal tissues during gestation.* Mol Hum Reprod, 1997. **3**(9): p. 769-73.

383. Gouaze, A., et al., *Cerebral cell renewal in adult mice controls the onset of obesity.* PLoS One, 2013. **8**(8): p. e72029.

384. Kokoeva, M.V., H. Yin, and J.S. Flier, *Evidence for constitutive neural cell proliferation in the adult murine hypothalamus.* J Comp Neurol, 2007. **505**(2): p. 209-20.

385. Duan, Y., et al., *Inflammatory Links Between High Fat Diets and Diseases.* Frontiers in Immunology, 2018. **9**.

386. Chiazza, F., et al., *Short high fat diet triggers reversible and region specific effects in DCX(+) hippocampal immature neurons of adolescent male mice.* Sci Rep, 2021. **11**(1): p. 21499.

387. Lindqvist, A., et al., *High-fat diet impairs hippocampal neurogenesis in male rats.* Eur J Neurol, 2006. **13**(12): p. 1385-8.

388. Park, H.R., et al., *A high-fat diet impairs neurogenesis: involvement of lipid peroxidation and brain-derived neurotrophic factor.* Neurosci Lett, 2010. **482**(3): p. 235-9.

389. Speakman, J.R. and S.E. Mitchell, *Caloric restriction.* Mol Aspects Med, 2011. **32**(3): p. 159-221.

390. Braeckman, B.P., L. Demetrius, and J.R. Vanfleteren, *The dietary restriction effect in C. elegans and humans: is the worm a one-millimeter human?* Biogerontology, 2006. **7**(3): p. 127-33.

391. Weindruch, R., *Effect of caloric restriction on age-associated cancers.* Exp Gerontol, 1992. **27**(5-6): p. 575-81.

392. Ingram, D.K., et al., *Dietary restriction and aging: the initiation of a primate study.* J Gerontol, 1990. **45**(5): p. B148-63.

393. Kemnitz, J.W., *Calorie restriction and aging in nonhuman primates.* ILAR J, 2011. **52**(1): p. 66-77.

394. Lane, M.A., et al., *Dietary restriction in nonhuman primates: progress report on the NIA study.* Ann N Y Acad Sci, 1992. **673**: p. 36-45.

395. Fontana, L., et al., *Long-term calorie restriction is highly effective in reducing the risk for atherosclerosis in humans.* Proc Natl Acad Sci U S A, 2004. **101**(17): p. 6659-63.

396. Meyer, T.E., et al., *Long-term caloric restriction ameliorates the decline in diastolic function in humans.* J Am Coll Cardiol, 2006. **47**(2): p. 398-402.

397. Nisoli, E., et al., *Calorie restriction promotes mitochondrial biogenesis by inducing the expression of eNOS.* Science, 2005. **310**(5746): p. 314-7.

398. Bondolfi, L., et al., *Impact of age and caloric restriction on neurogenesis in the dentate gyrus of C57BL/6 mice.* Neurobiol Aging, 2004. **25**(3): p. 333-40.

399. Hornsby, A.K., et al., *Short-term calorie restriction enhances adult hippocampal neurogenesis and remote fear memory in a Ghsr-dependent manner.* Psychoneuroendocrinology, 2016. **63**: p. 198-207.

400. Lee, J., et al., *Dietary restriction increases the number of newly generated neural cells, and induces BDNF expression, in the dentate gyrus of rats.* J Mol Neurosci, 2000. **15**(2): p. 99-108.

401. Lee, J., K.B. Seroogy, and M.P. Mattson, *Dietary restriction enhances neurotrophin expression and neurogenesis in the hippocampus of adult mice.* J Neurochem, 2002. **80**(3): p. 539-47.

402. Apple, D.M., et al., *Calorie restriction protects neural stem cells from age-related deficits in the subventricular zone.* Aging (Albany NY), 2019. **11**(1): p. 115-126.

403. Ratcliff, M., et al., *Calorie restriction activates new adult born olfactory-bulb neurones in a ghrelin-dependent manner but acyl-ghrelin does not enhance subventricular zone neurogenesis.* J Neuroendocrinol, 2019. **31**(7): p. e12755.

404. Klein, C., et al., *High-fat Diet and Physical Exercise Differentially Modulate Adult Neurogenesis in the Mouse Hypothalamus.* Neuroscience, 2019. **400**: p. 146-156.

405. Li, Q. and B.A. Barres, *Microglia and macrophages in brain homeostasis and disease.* Nat Rev Immunol, 2018. **18**(4): p. 225-242.

406. Ekdahl, C.T., et al., *Inflammation is detrimental for neurogenesis in adult brain.* Proc Natl Acad Sci U S A, 2003. **100**(23): p. 13632-7.

407. Green, H.F. and Y.M. Nolan, *GSK-3 mediates the release of IL-1beta, TNF-alpha and IL-10 from cortical glia.* Neurochem Int, 2012. **61**(5): p. 666-71.

408. Johansson, A., et al., *The relative impact of chronic food restriction and acute food deprivation on plasma hormone levels and hypothalamic neuropeptide expression.* Peptides, 2008. **29**(9): p. 1588-95.

409. Sierra, A., et al., *Surveillance, phagocytosis, and inflammation: how never-resting microglia influence adult hippocampal neurogenesis.* Neural Plast, 2014. **2014**: p. 610343.

410. Sierra, A., et al., *Microglia shape adult hippocampal neurogenesis through apoptosis-coupled phagocytosis.* Cell Stem Cell, 2010. **7**(4): p. 483-95.

411. Monje, M.L., H. Toda, and T.D. Palmer, *Inflammatory blockade restores adult hippocampal neurogenesis.* Science, 2003. **302**(5651): p. 1760-5.

412. Li, J., Y. Tang, and D. Cai, *IKKbeta/NF-kappaB disrupts adult hypothalamic neural stem cells to mediate a neurodegenerative mechanism of dietary obesity and pre-diabetes.* Nat Cell Biol, 2012. **14**(10): p. 999-1012.

413. Colman, R.J., et al., *Caloric restriction delays disease onset and mortality in rhesus monkeys.* Science, 2009. **325**(5937): p. 201-4.

414. Spaulding, C.C., R.L. Walford, and R.B. Effros, *Calorie restriction inhibits the age-related dysregulation of the cytokines TNF-alpha and IL-6 in C3B10RF1 mice.* Mech Ageing Dev, 1997. **93**(1-3): p. 87-94.

415. Kaur, M., S. Sharma, and G. Kaur, *Age-related impairments in neuronal plasticity markers and astrocytic GFAP and their reversal by late-onset short term dietary restriction.* Biogerontology, 2008. **9**(6): p. 441-54.

416. Sharma, S. and G. Kaur, *Dietary restriction enhances kainate-induced increase in NCAM while blocking the glial activation in adult rat brain.* Neurochem Res, 2008. **33**(7): p. 1178-88.

417. Harrison, L., et al., *Profound weight loss induces reactive astrogliosis in the arcuate nucleus of obese mice.* Mol Metab, 2019. **24**: p. 149-155.

418. Radler, M.E., M.W. Hale, and S. Kent, *Calorie restriction attenuates lipopolysaccharide (LPS)-induced microglial activation in discrete regions of the hypothalamus and the subfornical organ.* Brain Behav Immun, 2014. **38**: p. 13-24.

419. Fontana, L., et al., *Effects of 2-year calorie restriction on circulating levels of IGF-1, IGF-binding proteins and cortisol in nonobese men and women: a randomized clinical trial.* Aging Cell, 2016. **15**(1): p. 22-7.

420. Mulrooney, T.J., et al., *Influence of caloric restriction on constitutive expression of NF-kappaB in an experimental mouse astrocytoma.* PLoS One, 2011. **6**(3): p. e18085.

421. Piccio, L., J.L. Stark, and A.H. Cross, *Chronic calorie restriction attenuates experimental autoimmune encephalomyelitis.* J Leukoc Biol, 2008. **84**(4): p. 940-8.

422. Ugochukwu, N.H., J.D. Mukes, and C.L. Figgers, *Ameliorative effects of dietary caloric restriction on oxidative stress and inflammation in the brain of streptozotocin-induced diabetic rats.* Clin Chim Acta, 2006. **370**(1-2): p. 165-73.

423. Duan, W., Z. Guo, and M.P. Mattson, *Brain-derived neurotrophic factor mediates an excitoprotective effect of dietary restriction in mice.* J Neurochem, 2001. **76**(2): p. 619-26.

424. Maswood, N., et al., *Caloric restriction increases neurotrophic factor levels and attenuates neurochemical and behavioral deficits in a primate model of Parkinson's disease.* Proc Natl Acad Sci U S A, 2004. **101**(52): p. 18171-6.

425. Mattson, M.P. and R. Wan, *Beneficial effects of intermittent fasting and caloric restriction on the cardiovascular and cerebrovascular systems.* J Nutr Biochem, 2005. **16**(3): p. 129-37.

426. Chung, H.Y., et al., *Redefining Chronic Inflammation in Aging and Age-Related Diseases: Proposal of the Senoinflammation Concept.* Aging Dis, 2019. **10**(2): p. 367-382.

427. Ferrucci, L. and E. Fabbri, *Inflammageing: chronic inflammation in ageing, cardiovascular disease, and frailty.* Nat Rev Cardiol, 2018. **15**(9): p. 505-522.

428. Bernal, G.M. and D.A. Peterson, *Neural stem cells as therapeutic agents for age-related brain repair.* Aging Cell, 2004. **3**(6): p. 345-51.

429. Rao, M.S., et al., *Newly born cells in the ageing dentate gyrus display normal migration, survival and neuronal fate choice but endure retarded early maturation.* Eur J Neurosci, 2005. **21**(2): p. 464-76.

430. Daynac, M., et al., *Age-related neurogenesis decline in the subventricular zone is associated with specific cell cycle regulation changes in activated neural stem cells.* Sci Rep, 2016. **6**: p. 21505.

431. Matsuzaki, K., et al., *Aging attenuates acquired heat tolerance and hypothalamic neurogenesis in rats.* J Comp Neurol, 2015. **523**(8): p. 1190-201.

432. Valero, J., et al., *Impact of Neuroinflammation on Hippocampal Neurogenesis: Relevance to Aging and Alzheimer's Disease.* J Alzheimers Dis, 2017. **60**(s1): p. S161-S168.

433. Knox, E.G., et al., *The blood-brain barrier in aging and neurodegeneration.* Mol Psychiatry, 2022.

434. Wong, A.M., et al., *Macrosialin increases during normal brain aging are attenuated by caloric restriction.* Neurosci Lett, 2005. **390**(2): p. 76-80.

435. Olmedillas Del Moral, M., et al., *Effect of Caloric Restriction on the in vivo Functional Properties of Aging Microglia.* Front Immunol, 2020. **11**: p. 750.

436. Koubova, J. and L. Guarente, *How does calorie restriction work?* Genes Dev, 2003. **17**(3): p. 313-21.

437. Lee, J., W. Duan, and M.P. Mattson, *Evidence that brain-derived neurotrophic factor is required for basal neurogenesis and mediates, in part, the enhancement of neurogenesis by dietary restriction in the hippocampus of adult mice.* J Neurochem, 2002. **82**(6): p. 1367-75.

438. Niraula, A., J.F. Sheridan, and J.P. Godbout, *Microglia Priming with Aging and Stress.* Neuropsychopharmacology, 2017. **42**(1): p. 318-333.

439. Zhu, X., et al., *RBM3 promotes neurogenesis in a niche-dependent manner via IMP2-IGF2 signaling pathway after hypoxic-ischemic brain injury.* Nat Commun, 2019. **10**(1): p. 3983.

440. Yan, J., et al., *The RNA-Binding Protein RBM3 Promotes Neural Stem Cell (NSC) Proliferation Under Hypoxia.* Front Cell Dev Biol, 2019. **7**: p. 288.

441. Saito, K., N. Fukuda, and N. Hayashi, *Moderate Low Temperature Preserves the Stemness of Neural Stem Cells (Methods)*, in *Stem Cells and Cancer Stem Cells, Volume 10: Therapeutic Applications in Disease and Injury*, M.A. Hayat, Editor. 2013, Springer Netherlands: Dordrecht. p. 137-145.

442. Liu, A., et al., *Effects of hypothermia and cerebral ischemia on cold-inducible RNA-binding protein mRNA expression in rat brain.* Brain Res, 2010. **1347**: p. 104-10.

443. Artero-Castro, A., et al., *Cold-inducible RNA-binding protein bypasses replicative senescence in primary cells through extracellular signal-regulated kinase 1 and 2 activation.* Mol Cell Biol, 2009. **29**(7): p. 1855-68.

444. Sakurai, T., et al., *Cirp protects against tumor necrosis factor-alpha-induced apoptosis via activation of extracellular signal-regulated kinase.* Biochim Biophys Acta, 2006. **1763**(3): p. 290-5.

445. Yenari, M.A. and H.S. Han, *Neuroprotective mechanisms of hypothermia in brain ischaemia.* Nat Rev Neurosci, 2012. **13**(4): p. 267-78.

446. Perrone, S., et al., *Whole body hypothermia and oxidative stress in babies with hypoxic-ischemic brain injury.* Pediatr Neurol, 2010. **43**(4): p. 236-40.

447. Zhao, H., et al., *Akt contributes to neuroprotection by hypothermia against cerebral ischemia in rats.* J Neurosci, 2005. **25**(42): p. 9794-806.

448. Chip, S., et al., *The RNA-binding protein RBM3 is involved in hypothermia induced neuroprotection.* Neurobiol Dis, 2011. **43**(2): p. 388-96.

449. Han, H.S. and M.A. Yenari, *Effect on gene expression of therapeutic hypothermia in cerebral ischemia.* Future Neurology, 2007. **2**(4): p. 435-440.

450. Saito, K., et al., *Moderate low temperature preserves the stemness of neural stem cells and suppresses apoptosis of the cells via activation of the cold-inducible RNA binding protein.* Brain Res, 2010. **1358**: p. 20-9.

451. Spiljar, M., et al., *Cold exposure protects from neuroinflammation through immunologic reprogramming.* Cell Metab, 2021. **33**(11): p. 2231-2246 e8.

452. Feng, L., M.E. Hatten, and N. Heintz, *Brain lipid-binding protein (BLBP): a novel signaling system in the developing mammalian CNS.* Neuron, 1994. **12**(4): p. 895-908.

453. Giachino, C., et al., *Molecular diversity subdivides the adult forebrain neural stem cell population.* Stem Cells, 2014. **32**(1): p. 70-84.

454. Kipp, M., et al., *BLBP-expression in astrocytes during experimental demyelination and in human multiple sclerosis lesions.* Brain Behav Immun, 2011. **25**(8): p. 1554-68.

455. Sirko, S., et al., *Reactive glia in the injured brain acquire stem cell properties in response to sonic hedgehog. [corrected].* Cell Stem Cell, 2013. **12**(4): p. 426-39.

456. Sirko, S., et al., *Astrocyte reactivity after brain injury-: The role of galectins 1 and 3.* Glia, 2015. **63**(12): p. 2340-61.

457. Sofroniew, M.V., *Astrogliosis.* Cold Spring Harb Perspect Biol, 2014. **7**(2): p. a020420.

458. Li, H., et al., *Low-dose DHA-induced astrocyte proliferation can be attenuated by insufficient expression of BLBP in vitro.* Prostaglandins Other Lipid Mediat, 2018. **134**: p. 114-122.

459. Han, X., et al., *Brain lipid-binding protein promotes proliferation and modulates cell cycle in C6 rat glioma cells.* Int J Oncol, 2017. **51**(5): p. 1439-1448.

460. Yin, W. and A.C. Gore, *The hypothalamic median eminence and its role in reproductive aging.* Annals of the New York Academy of Sciences, 2010. **1204**: p. 113-122.

461. Zhang, X. and A.N. van den Pol, *Dopamine/Tyrosine Hydroxylase Neurons of the Hypothalamic Arcuate Nucleus Release GABA, Communicate with Dopaminergic and Other Arcuate Neurons, and Respond to Dynorphin, Met-Enkephalin, and Oxytocin.* J Neurosci, 2015. **35**(45): p. 14966-82.

462. Mano-Otagiri, A., et al., *Growth Hormone-Releasing Hormone (GHRH) Neurons in the Arcuate Nucleus (Arc) of the Hypothalamus Are Decreased in Transgenic Rats Whose Expression of Ghrelin Receptor Is Attenuated: Evidence that Ghrelin Receptor Is Involved in the Up-Regulation of GHRH Expression in the Arc.* Endocrinology, 2006. **147**(9): p. 4093-4103.

463. Brawer, J.R. and R.J. Walsh, *Response of tanycytes to aging in the median eminence of the rat.* Am J Anat, 1982. **163**(3): p. 247-56.

464. Kohnke, S., et al., *Nutritional regulation of oligodendrocyte differentiation regulates perineuronal net remodeling in the median eminence.* Cell Reports, 2021. **36**(2): p. 109362.

465. Ohira, K., *Change of hypothalamic adult neurogenesis in mice by chronic treatment of fluoxetine.* BMC Research Notes, 2022. **15**(1).

466. Chen, G.-Y., et al., *Mediator Med23 Regulates Adult Hippocampal Neurogenesis.* Frontiers in Cell and Developmental Biology, 2020. **8**.

467. Urist, M.R., *Bone: formation by autoinduction.* Science, 1965. **150**(3698): p. 893-9.

468. Bakrania, P., et al., *Mutations in BMP4 cause eye, brain, and digit developmental anomalies: overlap between the BMP4 and hedgehog signaling pathways.* Am J Hum Genet, 2008. **82**(2): p. 304-19.

469. Massague, J., *TGF-beta signal transduction.* Annu Rev Biochem, 1998. **67**: p. 753-91.

470. Nickel, J., et al., *Intricacies of BMP receptor assembly.* Cytokine Growth Factor Rev, 2009. **20**(5-6): p. 367-77.

471. Wang, R.N., et al., *Bone Morphogenetic Protein (BMP) signaling in development and human diseases.* Genes Dis, 2014. **1**(1): p. 87-105.

472. Whittle, A.J., et al., *BMP8B increases brown adipose tissue thermogenesis through both central and peripheral actions.* Cell, 2012. **149**(4): p. 871-85.

473. Zhao, G.Q., *Consequences of knocking out BMP signaling in the mouse.* Genesis, 2003. **35**(1): p. 43-56.

474. Fukuda, S. and T. Taga, *[Roles of BMP in the development of the central nervous system].* Clin Calcium, 2006. **16**(5): p. 781-85.

475. Townsend, K.L., et al., *Reestablishment of Energy Balance in a Male Mouse Model With POMC Neuron Deletion of BMPR1A.* Endocrinology, 2017. **158**(12): p. 4233-4245.

476. Townsend, K.L., et al., *Bone morphogenetic protein 7 (BMP7) reverses obesity and regulates appetite through a central mTOR pathway.* FASEB J, 2012. **26**(5): p. 2187-96.

477. Wrana, J.L., et al., *TGF beta signals through a heteromeric protein kinase receptor complex.* Cell, 1992. **71**(6): p. 1003-14.

478. de Caestecker, M., *The transforming growth factor-beta superfamily of receptors.* Cytokine Growth Factor Rev, 2004. **15**(1): p. 1-11.

479. Gilboa, L., et al., *Bone morphogenetic protein receptor complexes on the surface of live cells: a new oligomerization mode for serine/threonine kinase receptors.* Mol Biol Cell, 2000. **11**(3): p. 1023-35.

480. Liu, F., et al., *Human type II receptor for bone morphogenic proteins (BMPs): extension of the two-kinase receptor model to the BMPs.* Mol Cell Biol, 1995. **15**(7): p. 3479-86.

481. Nohe, A., et al., *The mode of bone morphogenetic protein (BMP) receptor oligomerization determines different BMP-2 signaling pathways.* J Biol Chem, 2002. **277**(7): p. 5330-8.

482. Kawabata, M., T. Imamura, and K. Miyazono, *Signal transduction by bone morphogenetic proteins.* Cytokine Growth Factor Rev, 1998. **9**(1): p. 49-61.

483. Rosenzweig, B.L., et al., *Cloning and characterization of a human type II receptor for bone morphogenetic proteins.* Proc Natl Acad Sci U S A, 1995. **92**(17): p. 7632-6.

484. Nohno, T., et al., *Identification of a human type II receptor for bone morphogenetic protein-4 that forms differential heteromeric complexes with bone morphogenetic protein type I receptors.* J Biol Chem, 1995. **270**(38): p. 22522-6.

485. Yamashita, H., et al., *Osteogenic protein-1 binds to activin type II receptors and induces certain activin-like effects.* J Cell Biol, 1995. **130**(1): p. 217-26.

486. Macias-Silva, M., et al., *Specific activation of Smad1 signaling pathways by the BMP7 type I receptor, ALK2.* J Biol Chem, 1998. **273**(40): p. 25628-36.

487. ten Dijke, P., et al., *Identification of type I receptors for osteogenic protein-1 and bone morphogenetic protein-4.* J Biol Chem, 1994. **269**(25): p. 16985-8.

488. Katagiri, T. and T. Watabe, *Bone Morphogenetic Proteins.* Cold Spring Harb Perspect Biol, 2016. **8**(6).

489. Nishitoh, H., et al., *Identification of type I and type II serine/threonine kinase receptors for growth/differentiation factor-5.* J Biol Chem, 1996. **271**(35): p. 21345-52.

490. Bragdon, B., et al., *Bone morphogenetic proteins: a critical review.* Cell Signal, 2011. **23**(4): p. 609-20.

491. Savage, C., et al., *Caenorhabditis elegans genes sma-2, sma-3, and sma-4 define a conserved family of transforming growth factor beta pathway components.* Proc Natl Acad Sci U S A, 1996. **93**(2): p. 790-4.

492. Sekelsky, J.J., et al., *Genetic characterization and cloning of mothers against dpp, a gene required for decapentaplegic function in Drosophila melanogaster.* Genetics, 1995. **139**(3): p. 1347-58.

493. Heldin, C.H., K. Miyazono, and P. ten Dijke, *TGF-beta signalling from cell membrane to nucleus through SMAD proteins.* Nature, 1997. **390**(6659): p. 465-71.

494. Hart, C.G. and S. Karimi-Abdolrezaee, *Bone morphogenetic proteins: New insights into their roles and mechanisms in CNS development, pathology and repair.* Exp Neurol, 2020. **334**: p. 113455.

495. Hegarty, S.V., G.W. O'Keeffe, and A.M. Sullivan, *BMP-Smad 1/5/8 signalling in the development of the nervous system.* Prog Neurobiol, 2013. **109**: p. 28-41.

496. Colak, D., et al., *Adult neurogenesis requires Smad4-mediated bone morphogenic protein signaling in stem cells.* J Neurosci, 2008. **28**(2): p. 434-46.

497. Lim, D.A., et al., *Noggin antagonizes BMP signaling to create a niche for adult neurogenesis.* Neuron, 2000. **28**(3): p. 713-26.

498. Yousef, H., et al., *Age-Associated Increase in BMP Signaling Inhibits Hippocampal Neurogenesis.* Stem Cells, 2015. **33**(5): p. 1577-88.

499. Holley, S.A., et al., *The Xenopus dorsalizing factor noggin ventralizes Drosophila embryos by preventing DPP from activating its receptor.* Cell, 1996. **86**(4): p. 607-17.

500. Zimmerman, L.B., J.M. De Jesus-Escobar, and R.M. Harland, *The Spemann organizer signal noggin binds and inactivates bone morphogenetic protein 4.* Cell, 1996. **86**(4): p. 599-606.

501. Mikawa, S. and K. Sato, *Noggin expression in the adult rat brain.* Neuroscience, 2011. **184**: p. 38-53.

502. Charytoniuk, D.A., et al., *Distribution of bone morphogenetic protein and bone morphogenetic protein receptor transcripts in the rodent nervous system and up-regulation of bone morphogenetic protein receptor type II in hippocampal dentate gyrus in a rat model of global cerebral ischemia.* Neuroscience, 2000. **100**(1): p. 33-43.

503. Chen, H.L., et al., *Expression of bone morphogenetic proteins in the brain during normal aging and in 6-hydroxydopamine-lesioned animals.* Brain Res, 2003. **994**(1): p. 81-90.

504. Gross, R.E., et al., *Bone morphogenetic proteins promote astroglial lineage commitment by mammalian subventricular zone progenitor cells.* Neuron, 1996. **17**(4): p. 595-606.

505. Peretto, P., et al., *BMP mRNA and protein expression in the developing mouse olfactory system.* J Comp Neurol, 2002. **451**(3): p. 267-78.

506. Fan, X.T., et al., *Effect of antisense oligonucleotide of noggin on spatial learning and memory of rats.* Acta Pharmacol Sin, 2003. **24**(5): p. 394-7.

507. Hayashi, Y., et al., *BMP6 expression in the adult rat central nervous system.* J Chem Neuroanat, 2019. **98**: p. 41-54.

508. Kusakawa, Y., S. Mikawa, and K. Sato, *BMP5 expression in the adult rat brain.* Neuroscience, 2015. **284**: p. 972-987.

509. Mikawa, S., C. Wang, and K. Sato, *Bone morphogenetic protein-4 expression in the adult rat brain.* J Comp Neurol, 2006. **499**(4): p. 613-25.

510. Sato, T., S. Mikawa, and K. Sato, *BMP2 expression in the adult rat brain.* J Comp Neurol, 2010. **518**(22): p. 4513-30.

511. Yamashita, K., S. Mikawa, and K. Sato, *BMP3 expression in the adult rat CNS.* Brain Res, 2016. **1643**: p. 35-50.

512. Takahara, K., G.E. Lyons, and D.S. Greenspan, *Bone morphogenetic protein-1 and a mammalian tolloid homologue (mTld) are encoded by alternatively spliced transcripts which are differentially expressed in some tissues.* J Biol Chem, 1994. **269**(51): p. 32572-8.

513. Yan, Y., et al., *The cell-specific upregulation of bone morphogenetic protein-10 (BMP-10) in a model of rat cortical brain injury.* J Mol Histol, 2012. **43**(5): p. 543-52.

514. Enzmann, G.U., et al., *Consequences of noggin expression by neural stem, glial, and neuronal precursor cells engrafted into the injured spinal cord.* Exp Neurol, 2005. **195**(2): p. 293-304.

515. Miyagi, M., et al., *Bone morphogenetic protein receptor expressions in the adult rat brain.* Neuroscience, 2011. **176**: p. 93-109.

516. Zhang, D., et al., *Development of bone morphogenetic protein receptors in the nervous system and possible roles in regulating trkC expression.* J Neurosci, 1998. **18**(9): p. 3314-26.

517. Kusakawa, Y., S. Mikawa, and K. Sato, *BMP7 expression in the adult rat brain.* IBRO Rep, 2017. **3**: p. 72-86.

518. Ogawa, C., et al., *BMP9 expression in the adult rat brain.* J Chem Neuroanat, 2021. **113**: p. 101933.

519. Dattatreyamurty, B., et al., *Cerebrospinal fluid contains biologically active bone morphogenetic protein-7.* Exp Neurol, 2001. **172**(2): p. 273-81.

520. Frayling, C., R. Britton, and N. Dale, *ATP-mediated glucosensing by hypothalamic tanycytes.* J Physiol, 2011. **589**(Pt 9): p. 2275-86.

521. Elizondo-Vega, R.J., A. Recabal, and K. Oyarce, *Nutrient Sensing by Hypothalamic Tanycytes.* Front Endocrinol (Lausanne), 2019. **10**: p. 244.

522. Joppe, S.E., et al., *Bone morphogenetic protein dominantly suppresses epidermal growth factor-induced proliferative expansion of adult forebrain neural precursors.* Front Neurosci, 2015. **9**: p. 407.

523. Samanta, J., et al., *BMPR1a signaling determines numbers of oligodendrocytes and calbindin-expressing interneurons in the cortex.* J Neurosci, 2007. **27**(28): p. 7397-407.

524. Gomes, W.A., M.F. Mehler, and J.A. Kessler, *Transgenic overexpression of BMP4 increases astroglial and decreases oligodendroglial lineage commitment.* Dev Biol, 2003. **255**(1): p. 164-77.

525. Chmielnicki, E., et al., *Adenovirally expressed noggin and brain-derived neurotrophic factor cooperate to induce new medium spiny neurons from resident progenitor cells in the adult striatal ventricular zone.* J Neurosci, 2004. **24**(9): p. 2133-42.

526. Pous, L., et al., *Fibrinogen induces neural stem cell differentiation into astrocytes in the subventricular zone via BMP signaling.* Nat Commun, 2020. **11**(1): p. 630.

527. Brederlau, A., et al., *The bone morphogenetic protein type Ib receptor is a major mediator of glial differentiation and cell survival in adult hippocampal progenitor cell culture.* Mol Biol Cell, 2004. **15**(8): p. 3863-75.

528. Scholze, A.R., et al., *BMP signaling in astrocytes downregulates EGFR to modulate survival and maturation.* PLoS One, 2014. **9**(10): p. e110668.

529. Kempermann, G. and F.H. Gage, *New nerve cells for the adult brain.* Sci Am, 1999. **280**(5): p. 48-53.

530. Seki, T. and Y. Arai, *Age-related production of new granule cells in the adult dentate gyrus.* Neuroreport, 1995. **6**(18): p. 2479-82.

531. Bond, A.M., G.L. Ming, and H. Song, *Adult Mammalian Neural Stem Cells and Neurogenesis: Five Decades Later.* Cell Stem Cell, 2015. **17**(4): p. 385-95.

532. Gould, E., et al., *Learning enhances adult neurogenesis in the hippocampal formation.* Nat Neurosci, 1999. **2**(3): p. 260-5.

533. Bonaguidi, M.A., et al., *Noggin expands neural stem cells in the adult hippocampus.* J Neurosci, 2008. **28**(37): p. 9194-204.

534. Bond, A.M., et al., *BMP signaling regulates the tempo of adult hippocampal progenitor maturation at multiple stages of the lineage.* Stem Cells, 2014. **32**(8): p. 2201-14.

535. Coskun, V., et al., *Retroviral manipulation of the expression of bone morphogenetic protein receptor Ia by SVZa progenitor cells leads to changes in their p19(INK4d) expression but not in their neuronal commitment.* Int J Dev Neurosci, 2001. **19**(2): p. 219-27.

536. Gajera, C.R., et al., *LRP2 in ependymal cells regulates BMP signaling in the adult neurogenic niche.* J Cell Sci, 2010. **123**(Pt 11): p. 1922-30.

537. Morell, M., Y.C. Tsan, and K.S. O'Shea, *Inducible expression of noggin selectively expands neural progenitors in the adult SVZ.* Stem Cell Res, 2015. **14**(1): p. 79-94.

538. Gobeske, K.T., et al., *BMP signaling mediates effects of exercise on hippocampal neurogenesis and cognition in mice.* PLoS One, 2009. **4**(10): p. e7506.

539. Armenteros, T., et al., *BMP and WNT signalling cooperate through LEF1 in the neuronal specification of adult hippocampal neural stem and progenitor cells.* Sci Rep, 2018. **8**(1): p. 9241.

540. Shou, J., P.C. Rim, and A.L. Calof, *BMPs inhibit neurogenesis by a mechanism involving degradation of a transcription factor.* Nat Neurosci, 1999. **2**(4): p. 339-45.

541. Valenzuela, D.M., et al., *Identification of mammalian noggin and its expression in the adult nervous system.* J Neurosci, 1995. **15**(9): p. 6077-84.

542. Soderstrom, S., H. Bengtsson, and T. Ebendal, *Expression of serine/threonine kinase receptors including the bone morphogenetic factor type II receptor in the developing and adult rat brain.* Cell Tissue Res, 1996. **286**(2): p. 269-79.

543. Cameron, H.A. and E. Gould, *Adult neurogenesis is regulated by adrenal steroids in the dentate gyrus.* Neuroscience, 1994. **61**(2): p. 203-9.

544. Gould, E., et al., *Neurogenesis in adulthood: a possible role in learning.* Trends Cogn Sci, 1999. **3**(5): p. 186-192.

545. Guizzetti, M., T.J. Kavanagh, and L.G. Costa, *Measurements of astrocyte proliferation.* Methods Mol Biol, 2011. **758**: p. 349-59.

546. Gomez-Nicola, D., et al., *Regulation of microglial proliferation during chronic neurodegeneration.* J Neurosci, 2013. **33**(6): p. 2481-93.

547. Bradl, M. and H. Lassmann, *Oligodendrocytes: biology and pathology.* Acta Neuropathol, 2010. **119**(1): p. 37-53.

548. Das, A.T., L. Tenenbaum, and B. Berkhout, *Tet-On Systems For Doxycycline-inducible Gene Expression.* Curr Gene Ther, 2016. **16**(3): p. 156-67.

549. Lee, C.M., et al., *Single-cell RNA-seq analysis revealed long-lasting adverse effects of tamoxifen on neurogenesis in prenatal and adult brains.* Proc Natl Acad Sci U S A, 2020. **117**(32): p. 19578-19589.

550. Smith, B.M., et al., *Oral and injected tamoxifen alter adult hippocampal neurogenesis in female and male mice.* eNeuro, 2022.

551. Lynes, M.D., et al., *Telomerase Reverse Transcriptase Expression Marks a Population of Rare Adipose Tissue Stem Cells.* Stem Cells, 2022. **40**(1): p. 102-111.

552. Redelsperger, I.M., et al., *Stability of Doxycycline in Feed and Water and Minimal Effective Doses in Tetracycline-Inducible Systems.* J Am Assoc Lab Anim Sci, 2016. **55**(4): p. 467-74.

553. Jensen, G.J., et al., *Telomerase reverse transcriptase (TERT)-expressing cells mark a novel stem cell population in the adult mouse brain.* In Peer Review.

554. Bocker, R., et al., *Comparison of distribution of doxycycline in mice after oral and intravenous application measured by a high-performance liquid chromatographic method.* Arzneimittelforschung, 1981. **31**(12): p. 2116-7.

555. Lucchetti, J., et al., *Plasma and Brain Concentrations of Doxycycline after Single and Repeated Doses in Wild-Type and APP23 Mice.* J Pharmacol Exp Ther, 2019. **368**(1): p. 32-40.

556. Sun, Y., X. Chen, and D. Xiao, *Tetracycline-inducible expression systems: new strategies and practices in the transgenic mouse modeling.* Acta Biochim Biophys Sin (Shanghai), 2007. **39**(4): p. 235-46.

557. Lee, P., et al., *Conditional lineage ablation to model human diseases.* Proc Natl Acad Sci U S A, 1998. **95**(19): p. 11371-6.

558. Shi, S.R., et al., *Evaluation of the value of frozen tissue section used as "gold standard" for immunohistochemistry.* Am J Clin Pathol, 2008. **129**(3): p. 358-66.

559. Bratthauer, G.L., *Preparation of Frozen Sections for Analysis*, in *Immunocytochemical Methods and Protocols*, C. Oliver and M.C. Jamur, Editors. 2010, Humana Press: Totowa, NJ. p. 67-73.

560. Cawthorne, C., et al., *Comparison of doxycycline delivery methods for Tet-inducible gene expression in a subcutaneous xenograft model.* J Biomol Tech, 2007. **18**(2): p. 120-3.

561. Hristovska, I., et al., *Ketamine/xylazine and barbiturates modulate microglial morphology and motility differently in a mouse model.* PLoS One, 2020. **15**(8): p. e0236594.

562. Pereira, G.C., et al., *Anesthesia can alter the levels of corticosterone and the phosphorylation of signaling molecules.* BMC Res Notes, 2021. **14**(1): p. 363.

563. Renier, N., et al., *iDISCO: a simple, rapid method to immunolabel large tissue samples for volume imaging.* Cell, 2014. **159**(4): p. 896-910.

564. Markakis, E.A. and F.H. Gage, *Adult-generated neurons in the dentate gyrus send axonal projections to field CA3 and are surrounded by synaptic vesicles.* J Comp Neurol, 1999. **406**(4): p. 449-60.

565. Evans, J., et al., *Characterization of mitotic neurons derived from adult rat hypothalamus and brain stem.* J Neurophysiol, 2002. **87**(2): p. 1076-85.

566. Parent, A., F. Cicchetti, and T.G. Beach, *Calretinin-immunoreactive neurons in the human striatum.* Brain Res, 1995. **674**(2): p. 347-51.

567. Rich, E.L. and M. Shapiro, *Rat prefrontal cortical neurons selectively code strategy switches.* J Neurosci, 2009. **29**(22): p. 7208-19.

568. Suzuki, S.O. and J.E. Goldman, *Multiple cell populations in the early postnatal subventricular zone take distinct migratory pathways: a dynamic study of glial and neuronal progenitor migration.* J Neurosci, 2003. **23**(10): p. 4240-50.

569. Figueres-Onate, M., R. Sanchez-Gonzalez, and L. Lopez-Mascaraque, *Deciphering neural heterogeneity through cell lineage tracing.* Cell Mol Life Sci, 2021. **78**(5): p. 1971-1982.

570. Hammelrath, L., et al., *Morphological maturation of the mouse brain: An in vivo MRI and histology investigation.* Neuroimage, 2016. **125**: p. 144-152.

571. Sanchez-Gonzalez, R., A. Bribian, and L. Lopez-Mascaraque, *Cell Fate Potential of NG2 Progenitors.* Sci Rep, 2020. **10**(1): p. 9876.

572. Suzuki, T., et al., *Cells of NG2 lineage increase in glomeruli of mice following podocyte depletion.* Am J Physiol Renal Physiol, 2018. **315**(5): p. F1449-F1464.

573. Chou, Y.H., et al., *Nestin promotes the phosphorylation-dependent disassembly of vimentin intermediate filaments during mitosis.* Mol Biol Cell, 2003. **14**(4): p. 1468-78.

574. Hendrickson, M.L., et al., *Expression of nestin by neural cells in the adult rat and human brain.* PLoS One, 2011. **6**(4): p. e18535.

575. DeCarolis, N.A., et al., *In vivo contribution of nestin- and GLAST-lineage cells to adult hippocampal neurogenesis.* Hippocampus, 2013. **23**(8): p. 708-19.

576. Ihrie, R.A. and A. Alvarez-Buylla, *Cells in the astroglial lineage are neural stem cells.* Cell and Tissue Research, 2008. **331**(1): p. 179-191.

APPENDICES

Appendix A

BONE MORPHOGENETIC PROTEINS (BMPS) IN THE CENTRAL REGULATION OF ENERGY BALANCE AND ADULT NEURAL PLASTICITY

Published in Metabolism: Clinical and Experimental 123(3698):154837

DOI: 10.1016/j.metabol.2021.154837

Authors: Gabriel S. Jensen, Noelle E. Leon-Palmer, and Kristy L. Townsend

Sections, figures, and tables in this dissertation are GJ contributions

1. Introduction

Bone morphogenetic proteins (BMPs) are multi-functional growth factors belonging to the Transforming Growth Factor-β (TGF-β) superfamily [467]. BMPs were first discovered in the 1960's, and while initially believed to only be involved in bone formation, BMPs are now understood to be involved in numerous cell regulatory processes. These include cell growth, proliferation, differentiation, migration, and apoptosis, as well as the development and life-long function of various tissues and organs such as the brain [468-471]. Knockouts of many BMPs are lethal during embryogenesis and often result in marked defects or pathologies, which can include decreased metabolic health and obesity [472, 473]. BMP signaling is critically important for the development and maintenance of the central nervous system (CNS) and peripheral nervous system (PNS) [474]. In adulthood, previous studies by us and others have highlighted the roles of BMP7 and BMP8b, as well as BMP receptor 1A (BMPR1A), in reducing body weight by modulating signaling, appetite, and sympathetic outflow to adipose depots [472, 475, 476].

2. The Basics of BMP Signaling

BMP signaling is initiated at the cell surface by the binding of a BMP ligand to type I or type II transmembrane serine/ threonine kinase receptors forming a tetrameric receptor complex [469, 477]. After ligand binding, the type II receptor dimer phosphorylates the type I receptor dimer, activating the downstream signaling cascades [478]. The mode of ligand binding and tetrameric receptor formation differs between BMPs. BMP2 and BMP4 have a higher affinity for type I receptors, leading to the recruitment of type II receptors, while BMP6 and BMP7 bind type II receptors and recruit type I receptors [478-480]. BMP type II receptors can also form tetrameric complexes prior to ligand binding to affect downstream signaling [479]. In fibroblasts where BMP type II receptors were mutated to prevent preassembled receptor complexes, BMP2 treatment preferentially activated SMAD1 signaling, at the expense of the p38 Mitogen-Activated Protein Kinase (MAPK) pathway *in vitro* [481].

BMP ligands each bind preferentially to certain type I and type II receptors, with higher affinities for three type I BMP receptors: BMPR1A (ALK3), BMPR1B (ALK6) and ActR1A (ALK2), and three type II receptors: BMPRII, and the activin receptors ActRIIA, and ActRIIB [482-487]. BMPR1A, BMPR1B, and BMPRII are specific to BMP2, BMP4, BMP5, BMP6, BMP7, BMP8, and BMP8b ligands, but activin receptors have the ability to bind activin ligands and to a lesser degree BMP3, BMP9, BMP10, BMP12, BMP13, BMP14, and BMP15 [488]. BMP binding affinity may play a role in regulating signaling. BMP7 binds BMPR1B with higher affinity than BMPR1A, while BMP4 binds both type I receptors with the same affinity [487, 489]. Other receptors in the TGF-β superfamily, including ALK1, ALK4, and ALK5 have the ability to bind BMPs, but the binding occurs less frequently [470, 490].

The SMAD pathway is the canonical signaling pathway downstream of BMP receptor phosphorylation. The SMAD nomenclature is derived from the homologues for SMAD, SMA (small worm phenotype) in *Caenorhabditis elegans (C. elegans)* and MAD (Mothers Against Decapentaplegic) in *Drosophila melanogaster (D. melanogaster)* [491, 492]. Activation of the

SMAD pathway begins with phosphorylation of a receptor activated SMAD (R-SMAD) by a type I BMP receptor. R-SMADs include SMAD1, SMAD5, and SMAD8/9. Phosphorylated R-SMADs will then bind to SMAD4, a co-mediator SMAD (co-SMAD) and translocate to the nucleus where the complex can act as a transcription factor [493]. This process can be modulated by inhibitory SMADs (I-SMADs), including SMAD6 and SMAD7, which bind to co-SMAD to prevent nuclear binding and downstream processing [493]. SMAD4 has been used to explore the role of BMPs, including in the CNS, as SMAD4 knockout models halt downstream BMP-SMAD signaling [493].

BMP signaling pathways in the CNS have been well studied during development [494, 495]. Much remains to be studied regarding BMP signaling pathways in the adult brain, including specific cell types and discrete brain regions where BMP signaling occurs. In the subventricular zone (SVZ) of the lateral ventricles, a region with well-described adult neurogenesis, the presence of p-SMAD1/5/8 signaling is correlated to the presence of BMP2, BMP4, BMP6, and BMP7, as well as Noggin, BMPRII and SMAD4. Additionally, SMAD4 KO from stem cells and glia in the SVZ, as well as infusion of the inhibitor Noggin, led to major changes in proliferation and neurogenesis, indicating the utilization of the SMAD signaling pathway in the regulation of adult brain plasticity [496, 497]. BMP-related downstream SMAD signaling is also observed in the hippocampus of the adult murine brain, another region with high adult neural plasticity, where differences in pSMAD1/5/8-positive progenitor cells are linked to age-associated changes in BMP ligand expression [498]. Non-canonical BMP signaling occurs in the brain as well, as intracerebroventricular (*i.c.v.*) administration of BMP7 to adult mice induced a central rapamycin-sensitive mTOR-p70S6 kinase pathway in the hypothalamus [476]. In this study, BMP7 treatment of hypothalamic neuronal cells resulted in increased pSMAD1/5/8 and phosphorylated Ribosomal Protein S6 Kinase (p-p70S6K) protein levels *in vitro* (Fig. A2A) [476]. While the role of these signaling pathways in various processes are incompletely understood, it is clear that BMP signaling induces both canonical and non-canonical signaling in the adult brain.

The effects of BMPs are also regulated across different tissues through the inherent diversity of the many BMP ligands (BMP1-15) [490], the regulation of the extracellular matrix (ECM) environment, the specificity of the downstream signaling pathways activated, and the action of endogenous antagonists. BMP antagonists include Noggin [497, 499, 500]. It is important to note that Noggin is endogenously expressed throughout the mouse [497] and rat [501] adult CNS, including the neuro/gliogenic SVZ of the lateral ventricles, ependymal lining of the lateral ventricles, hippocampus, hypothalamus, cortex, striatum, and the olfactory bulbs (OBs) [497, 501]. These areas also express BMPs and/or BMP receptors (Fig A1A, B, E) [502] and are niches of adult neural plasticity, highlighting the importance of BMP regulation within the stem cell niches of the adult mammalian brain.

3. Localization and Expression of BMPs in the Adult Brain

Temporal and spatial changes in expression of BMP ligands and receptors occur throughout development as well as adulthood [503-505]. In the hippocampus and substantia nigra, expression of BMP4, BMP6, and noggin increases into adulthood, then decreases as the animal reaches old age [503, 506]. In neurogenic niches of the adult brain, changes in Noggin expression, BMP ligand levels, and downstream signaling pathways have been shown to regulate adult neurogenesis and gliogenesis [496]. Dynamic expression patterns of BMP ligands and receptors may therefore work to balance BMP signaling in the brain from development through adulthood in response to changing needs.

There is widespread transcript and protein expression of BMP ligands and receptors throughout the adult brain (Table A1). BMP2, BMP3, BMP4, BMP5, BMP6, BMP7, and BMP9 are broadly distributed across the brain, as are the receptors BMPR1A, BMPRII, and to a lesser extent BMPR1B. In each of these brain areas, regional and cell type specific differences were observed. Most cell types in the brain, including neurons, astrocytes, oligodendrocytes, and ependymal cells express BMP2, BMP3, BMP4, BMP5, and BMP6 [507-511]. However, these BMPs are not

expressed by immune cells such as microglia or macrophages. BMP6 is the only BMP ligand studied that has been found to be expressed by oligodendrocytes [507]. Currently, comparative expression levels have not been performed across BMP ligands, but expression across brain regions has been performed for many individual BMPs. BMP1 is not expressed in the adult brain [512]. BMP8b has been located to the cortex, striatum, hippocampus, hypothalamus, and medulla [472]. BMP10 has only been observed in the cortex, although this study did not search elsewhere in the brain [513]. BMP12, and BMP13 have been identified in the adult spinal cord, but not the brain [514]. BMP8, BMP14, and BMP15 have not been characterized within the adult brain [494, 502]. The BMP inhibitor Noggin has been identified in many overlapping brain regions and appears to follow similar spatial and temporal patterns of expression [496, 497, 506]. As BMPs require proteolytic processing to yield mature proteins from their initial pro-proteins, additional complexity can be attributed to the diverse BMP processing across tissue regions and cell types (Reviewed in [494]).

BMPRII and BMPR1A expression is diverse in the adult mouse and rat brain [502, 515, 516]. *In situ* hybridization studies in the adult mouse show that the highest expression of BMPRII is within the OB, hippocampus, and cerebellum [502]. BMPR1A and BMPRII regional expression differences have been observed as BMPRII is expressed in the granule cell layer of the cerebellum or the glomerular layer of the OB, while BMPR1A is not [502, 515]. BMPR1A, BMPR1B, and BMPII receptors are co-localized with a variety of cell types in the adult CNS, including neurons, astrocytes, oligodendrocytes, ependyma, and microglia indicating the importance of BMP signaling throughout the entire adult brain [515].

Appendix Table A1 – BMP Ligand and Receptor Localization in the Adult Brain

Ligand/ Receptor	Location	Function Studied?	Model	Method	RNA or Protein	Citation
BMP1	None	No	Mouse, Human	NB	RNA	Takahara, 1994 [512]
BMP2	SEZ, CC	Not directly	Mouse	ISH	RNA	Colak, 2008 [496]
	SVZ	Not directly	Mouse	RT-PCR	RNA	Lim, 2000 [497]
	CTX, HIP, STR, SN	Not directly	Rat	RT-PCR	RNA	Chen, 2003 [503]
	OB, CTX, CC, HIP, THA, HYP, MB, CB, BS, SVZ, ChP	No	Rat	IHC	Protein	Sato, 2010 [510]
BMP3	OB, CTX, CC, NA, HIP, THA, HYP, MB, BS, CB, SVZ, ChP	No	Rat	IHC	Protein	Yamashita, 2016 [511]
BMP4	Fiber tracts, CB, CC, CTX	No	Rat	ISH	RNA	Charytoniuk, 2000 [502]
	OB	No	Mouse	WB, IHC	Protein	Peretto, 2002 [505]
	SEZ, CC	Not directly	Mouse	ISH	RNA	Colak, 2008 [496]
	SVZ	Not directly	Mouse	RT-PCR, IHC	RNA & Protein	Lim, 2000 [497]
	CTX, HIP, STR, SN	Not directly	Rat	RT-PCR	RNA	Chen, 2003 [503]
	OB, CTX, HIP, THA, HYP, MB, CB, BS, SVZ, ChP	No	Rat	IHC	Protein	Mikawa, 2006 [509]
	HIP	No	Rat	RT-PCR, ISH	RNA	Fan, 2003 [506]
BMP5	CTX, HIP, STR, SN	Not directly	Rat	RT-PCR	RNA	Chen, 2003 [503]
	OB, CTX, HIP, THA, HYP, MB, CB, BS, CC, SVZ, ChP	No	Rat	IHC, WB	Protein	Kusakawa, 2015 [508]

Table A1 continued

BMP6	Meninges	No	Rat	ISH	RNA	Charytoniuk, 2000 [502]
	OB	No	Mouse	WB, IHC	Protein	Peretto, 2002 [505]
	SEZ, CC	Not directly	Mouse	ISH	RNA	Colak, 2008 [496]
	CTX, HIP, STR, SN	Not directly	Rat	RT-PCR	RNA	Chen, 2003 [503]
	OB, CTX, HIP, THA, HYP, MB, CB, BS, CC, SVZ, ChP	No	Rat	IHC	Protein	Hayashi, 2019 [507]
BMP7	Meninges, Septal regions	No	Rat	ISH, IHC	RNA & Protein	Charytoniuk, 2000 [502]
	ChP, HYP, HIP	Yes	Mouse	ISH	RNA	Townsend, 2012 [476]
	OB	No	Mouse	WB	Protein	Peretto, 2002 [505]
	SEZ, CC	Not directly	Mouse	ISH	RNA	Colak, 2008 [496]
	CTX, HIP, STR, SN	No	Rat	RT-PCR	RNA	Chen, 2003 [503]
	OB, CTX, HIP, THA, HYP, MB, CB, BS, SVZ, ChP	No	Rat	IHC	Protein	Kusakawa, 2017 [517]
	SVZ	Yes	Mouse	IHC	Protein	Lim, 2000 [497]
BMP8a	None		Rat	RT-PCR	RNA	Charytoniuk, 2000 [502]
BMP8b	CTX, STR, HIP, HYP, MED	Yes	Mouse	ISH, RT-PCR	RNA	Whittle, 2012 [472]
BMP9	OB, CTX, HIP, THA, HYP, MB, CB, BS, SVZ	No	Rat	IHC	Protein	Ogawa, 2021 [518]
BMP10	CTX	No		IHC, WB, RT-PCR	RNA & Protein	Yan, 2012 [513]
BMP11	Not studied	-	-	-	-	-
BMP12	Not studied	-	-	-	-	-
BMP13	Not studied	-	-	-	-	-
BMP14	Not studied	-	-	-	-	-
BMP15	Not studied	-	-	-	-	-
Noggin	SEZ, Septum	Yes	Mouse	ISH	RNA	Colak, 2008 [496]
	HIP	Yes	Mouse	ISH	RNA	Fan, 2003 [506]
	CTX, HIP, STR, SN	Yes	Rat	RT-PCR	RNA	Chen, 2003 [503]

Table A1 continued

	Ependyma of LV	Yes	Mouse	RT-PCR, IHC	RNA, Protein	Lim, 2000 [497]
	OB, CTX, HIP, THA, HYP, MB, HB, CB	No	Rat	NB, ISH	RNA	Valenzuela, 1995 [541]
	OB, CTX, HIP, CB, THA, HYP, MB, SN, SVZ, ChP	No	Rat	IHC	Protein	Mikawa, 2011 [501]
BMPRII	SEZ	No	Mouse	ISH	RNA	Colak, 2008 [496]
	SVZ	No	Mouse	RT-PCR	RNA	Lim, 2000 [497]
	OB, CTX, STR, HIP, THA, AMG, SN, CB	No	Rat	ISH	RNA	Söderström, 1996 [542]
	OB, THA, BS, CB, HYP, HIP, CTX, STR	No	Rat	NB	RNA	Charytoniuk, 2000 [502]
	CTX, OB, HIP, CB, HYP, SN	No	Rat	ISH	RNA	Charytoniuk, 2000 [502]
	HYP	No	Mouse	ISH	RNA	Townsend, 2012 [476]
	OB, HIP, AMG, THA, HYP, MB, BS, CTX	No	Rat	IHC	Protein	Miyagi, 2011 [515]
BMPR1A	SVZ	Yes	Mouse	RT-PCR	RNA	Lim, 2000 [497]
	CTX, HIP, THA, OB, CB, BS, ChP	No	Mouse	ISH	RNA	Zhang, 1998 [516]
	HYP	Yes	Mouse	IHC	Protein	Townsend, 2017 [475]
	OB, HIP, AMG, THA, HYP, MB, BS, CTX	No	Rat	IHC	Protein	Miyagi, 2011 [515]
BMPR1B	SVZ	No	Mouse	RT-PCR	RNA	Lim, 2000 [497]
	Anterior olfactory nuclei	No	Mouse	ISH	RNA	Zhang, 1998 [516]
	OB, HIP, AMG, THA, HYP, MB, BS, CTX	No	Rat	IHC	Protein	Miyagi, 2011 [515]

Table A1. Expression of BMP ligands and receptors in the adult brain. Acronyms – SEZ: sub-ependymal zone, CC: corpus callosum, SVZ: subventricular zone, CTX: Cortex, OB: Olfactory bulb, STR: striatum, HIP: hippocampus, THA: thalamus, AMG: amygdala, SN: substantia nigra, HYP: hypothalamus, MB: midbrain, BS: brainstem, ChP: choroid plexus, CB: cerebellum, MED: Medulla, ISH: *in situ* hybridization, IHC: immunohistochemistry, RT-PCR: real-time polymerase chain reaction, WB: Western Blot, NB: Northern Blot

3.1 – BMP Expression within Neurogenic Niches

Within the adult hippocampus, radial glial-like stem cells within the subgranular zone (SGZ) of the dentate gyrus (DG) proliferate and differentiate to produce transit amplifying cells (TACs), which then differentiate into neuroblasts. These cells migrate into the granule cell layer of the hippocampus and mature into adult-born neurons. BMP ligands, receptors, and inhibitors are expressed here, and actively play a role in modulating adult plasticity (Fig A1D) [502, 506]. BMP2, BMP3, BMP4, BMP5, BMP6, BMP7, BMP9, Noggin, BMPR1A, BMPR1B, and BMPRII are all expressed in various areas of the hippocampus including the DG [501, 507-511, 517, 518]. BMP2, BMP3, BMP4, BMP5, BMP6, and BMP9 expression was localized to pyramidal cells and granule neurons, but BMP7 was not expressed in either cell type. In contrast BMP7 was expressed in astrocyte-like cells throughout the hippocampus [517]. BMP2 expression was found in astrocyte-like cells as well [510]. BMP receptor expression also showed notable differences in this region, as BMPR1A and BMPRII showed weak expression compared to BMPRIB. BMPR1A was expressed by astrocyte-like cells and some pyramidal neurons. BMPR1B and BMPRII were expressed by pyramidal cells [515].

The SVZ, located adjacent to the ependymal cells of the lateral ventricles, contains slowly cycling radial glial like neural stem cells (NSCs). These cells give rise to TACs, which in turn proliferate and differentiate into neuroblasts (Fig A1B). Neuroblasts migrate through the rostral migratory stream to the olfactory bulb where they differentiate into interneurons that integrate into

existing neural circuitry [19]. BMP ligands, receptors, inhibitors, and downstream gene expression targets can be found in all SVZ cell types (Fig A1B). BMP2, BMP4, BMPR1A, and BMPRII are all expressed by NSCs, TACs, and neuroblasts [497] (Fig A1B). However, only neuroblasts, the most differentiated and committed of these progenitors, express BMPR1B [497] (Fig A1B), which may provide specificity for BMP signals impacting neuroblast differentiation. BMP2 and BMP4 expression are 20 to 25-fold higher in ANSCs and TACs compared to neuroblasts [497] and may be maintaining an undifferentiated state. BMP2, BMP3, BMP4, BMP5, BMP6, BMP7, BMP9, Noggin, BMPR1A, BMPR1B, and BMPRII as well as downstream signaling molecules p-SMAD1/5/8, SMAD4, and SMAD transcriptional targets Id1and Id3 are all expressed by cells within the SVZ and ependymal niche of adult mice and rats, although many have not been localized to specific cell types (Fig A1B) [496, 497]. This full spectrum of BMP signaling molecules in this neurogenic niche provides insight into the importance and complexity of BMP signaling in adult neural plasticity.

BMPs also have the potential to influence brain regions far from where they are expressed, due to the brain's ventricular transport system. Our previous work in Lac-Z-BMP7 reporter mice, as well as the work of others, has demonstrated that the metabolically relevant ligand BMP7 is expressed in the choroid plexus of the lateral ventricles of the mouse brain [476, 502] (Fig A1B). As BMP7 has been found to circulate within the cerebrospinal fluid (CSF) [519], BMP7 could be produced in the choroid plexus, secreted into the CSF, and bind BMP receptors on cells that lie at the CSF-brain interface [519] (Fig A1B). BMP2, BMP3, BMP4, BMP5, and BMP6 are also expressed in the choroid plexus and may be circulating within the CSF, but that is currently unknown [507-511].

To respond to BMPs moving throughout the CSF, ependymal cells and other cells lining the ventricular system of the adult mouse brain express BMP receptors. We have found that BMPR1A is highly expressed on hypothalamic tanycytes, which line the walls of the ventral third

ventricle (V3V) (unpublished observations) (Fig A1E). Tanycytes are ependymal, radial glial-like cells whose cell bodies are positioned along the wall of the V3V with long apical processes extending out into the parenchyma of the hypothalamus [52]. The positioning of these cells between the CSF and the hypothalamic parenchyma allows these cells to respond to cues in the CSF, including glucose, histamine, and acetylcholine, and to communicate bidirectionally with the hypothalamus and the CSF [520]. Their processes also project to the median eminence (ME) at the ventral portion of the hypothalamic third ventricle, where fenestrated capillaries result in a lack of blood-brain barrier, thus allowing these tanycytes to sense factors within the blood and respond accordingly [521]. The high expression of BMPR1A receptors on tanycytes puts them in an opportune position to respond to BMPs circulating in the CSF.

In addition to the CSF and vasculature, expression of BMP2, BMP3, BMP4, BMP5, BMP6, BMP7, BMP8b, and BMP9 have been identified along the ependyma of the ventricles and throughout most hypothalamic regions (Fig A1E). Here, BMP2, BMP4, BMP6, and BMP9 are expressed within the arcuate nucleus (ARC) [507, 509, 510, 518]. BMP3, BMP5, BMP6, BMP7, and Noggin are expressed within the paraventricular nucleus (PVH), with BMP7 being expressed by oxytocin-positive neurons in this region [507, 508, 511, 517]. BMP3, BMP4, BMP5, BMP6, and BMP9 are expressed in the supraoptic nucleus (SON) [507-509, 511, 518]. BMP3, BMP5, BMP6, and BMP9 are expressed in the ventromedial hypothalamic nucleus (VMH) [507, 508, 511, 518]. BMP3, BMP4, BMP5, BMP6, BMP7, and BMP9 are expressed along the ependyma of the V3V, which may include tanycytes, although the specific cell types have not been studied [507-509, 511, 517, 518]. Interestingly, tanycytes are also proliferative, stem-like cells, which play a role in adult hypothalamic plasticity [332]. Therefore, it is possible that tanycytes utilize BMP signaling to regulate hypothalamic neuro/gliogenesis and energy balance.

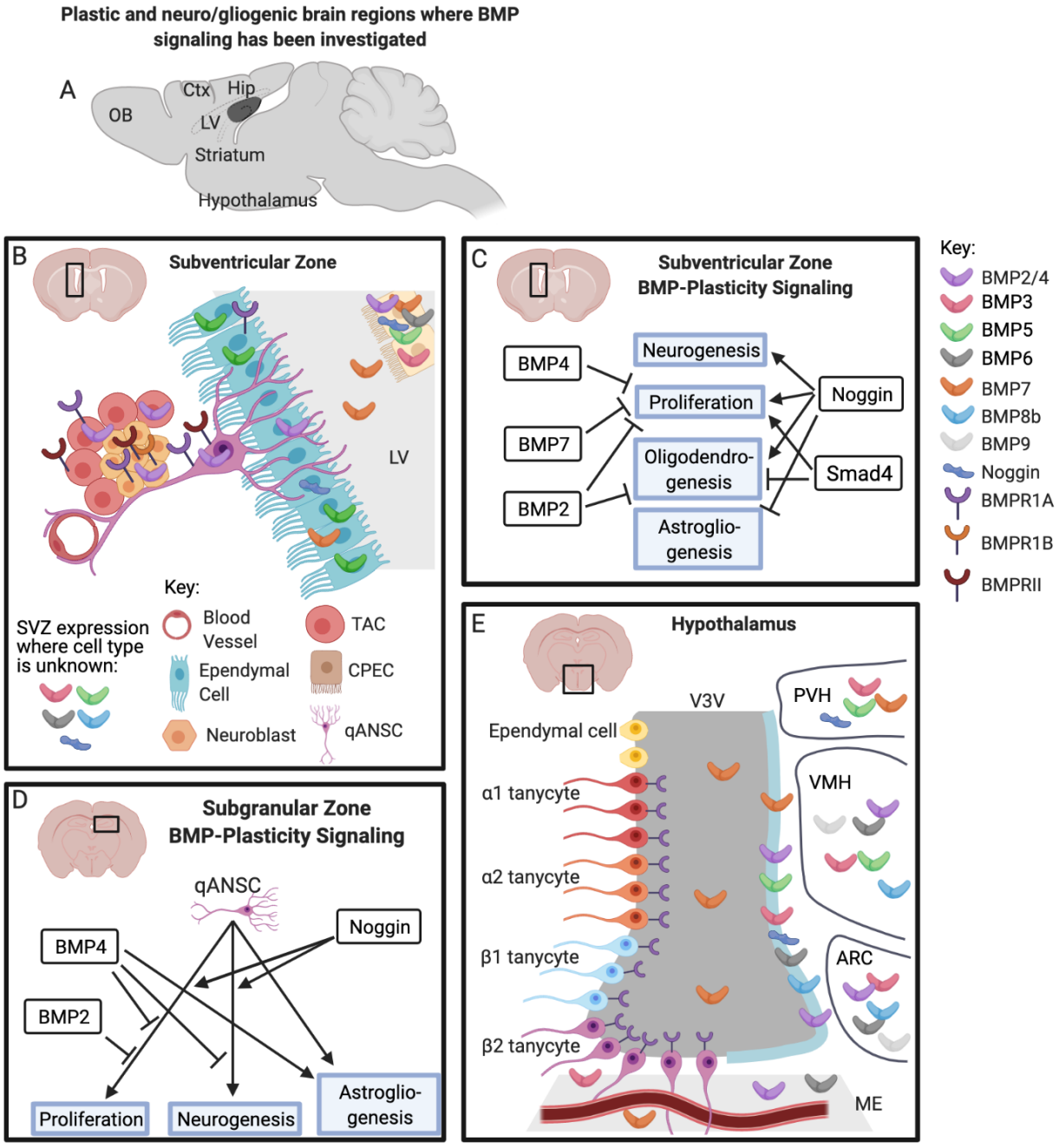

Figure A1: The role of BMP signaling on neuro/gliogenesis in the adult brain. BMPs play a role in regulation of adult neuro/gliogenesis and proliferation in various neuro/gliogenic niches of the adult brain. A) Sagittal view of an adult mouse brain showing known plastic, or neuro/gliogenic areas where BMP ligands have been studied, B) BMP ligands, receptors, and inhibitors are differentially expressed throughout the lateral ventricles, with differing expression within the SVZ, ependymal cell layer, and choroid plexus. BMPs 3, 4, 5, 9, and Noggin are known to be expressed within the SVZ, but the cell types that express them are currently unknown. Noggin is expressed

by ependymal cells as well as unknown SVZ cell types. C) BMP2, BMP4, and BMP7 halt proliferation and turnover, while Noggin and Smad4 balance adult neurogenesis and gliogenesis in the SVZ. D) Hippocampal BMP signaling affects proliferation of NSCs, neurogenesis, and astrogliogenesis. Here, BMP4 signaling plays a major role in proliferation and neurogenesis, while Noggin counters these effects. E) In the hypothalamus, various BMPs are found throughout the CSF, ventricular wall, PVH, VMH, ARC, ME, and more (dorsal/ventral location of BMPs along the wall in this figure are not indicative of dorsal/ventral location in the adult brain). Tanycytes, a proposed population of hypothalamic stem cells, express BMPR1A and are hypothesized to play a role in ventricular BMP signaling. However, the effects of BMPs and downstream signaling in this niche remain unstudied. (OB: Olfactory bulb, Ctx: Cortex, LV: Lateral Ventricle, Hip: Hippocampus, qANSC: quiescent adult neural stem cell, TAC: Transit amplifying cell, CPEC: choroid plexus epithelial cell)

4. Adult Neuron and Glial Cell Maintenance

In the adult brain, neuro/gliogenesis is at least in part regulated by local and CSF-derived BMPs and antagonists, as well as BMP receptor expression. In the SVZ and SGZ, BMP-SMAD signaling holds stem cells in quiescence, downregulating neurogenesis and proliferation (Table A2). Gliogenic studies of BMP-SMAD signaling implicate BMPs in inducing astrogliogenesis while decreasing oligodendrogenesis (Table A2). Furthermore, BMPs play a major role in synaptic and dendritic plasticity in the brain. Their role in repair after injury and aging also indicate an important role in stem cell manipulation. Presently, the function of specific BMPs have been understudied compared to downstream SMAD signaling, making it hard to identify the role of specific BMPs throughout all neuro/gliogenic regions of the brain. However, it is clear that BMPs play a major role in maintenance of the adult brain, and further elucidation of these pathways will be important in generating a complete understanding of adult neuro/gliogenesis and plasticity. Finally, while BMP-SMAD signaling has been functionally studied in the SVZ and hippocampus, the presence of BMPs and their receptors in various other neuro/gliogenic and plastic brain regions hints at undiscovered BMP-regulated functions in the adult brain (Appendix Fig A1A, Table A1).

4.1 Adult Gliogenesis

In the adult mouse SVZ, BMP signaling inhibits oligodendrogenesis [496]. Data using a conditional Glial High Affinity Glutamate Transporter (GLAST)-mediated SMAD4 knockout (KO) model showed that ablation of SMAD signaling in NSCs and glia of adult mice increased oligodendrogenesis in the SVZ *in vivo* [496] (Appendix Fig A1C). Infusion of the BMP inhibitor Noggin also resulted in increased oligodendrocyte numbers [496] (Appendix Fig A1C). Adult mice administered with BMP2 via intracerebroventricular injections into the lateral ventricles showed decreased SVZ Oligodendrocyte Transcription Factor 2 (Olig2)-positive oligodendrocytes [522] (Appendix Fig A1C). Postnatal BMPR1A knockout in Olig1+ oligodendrocyte precursor cells resulted in significantly higher numbers of oligodendrocytes than WT mice, which was likely due to reduced cell cycle length of progenitor cells, due to a loss of BMP signaling [523].

While BMP signaling appears to typically inhibit oligodendrogenesis, it promotes astrogliogenesis throughout the brain [523, 524]. Transgenic neuron-specific enolase (NSE) BMP4 overexpression mice, which overexpress BMP4 in neurons postnatally, had a 40% increase in astrocytic density in multiple adult brain regions [524]. Adenoviral overexpression of Noggin by ependyma decreased astrogliogenesis in the SVZ of adult rats [525]. When cultured with neural precursor cells (NPCs) *in vitro*, NSE-BMP4 neurons derived from the hippocampus increased astrocytic lineage commitment by the NPCs unless blocked via Noggin [524] (Appendix Fig A1D). Astrogliogenesis also results from BMP signaling in neural stem/progenitor cells from both the hippocampus as well as the SVZ respond to fibrinogen via BMP signaling-induced astrogliogenesis, which is accompanied by neuronal differentiation [526].

Experiments on cells derived from embryonic striatum treated with various BMPs resulted in cultures with higher numbers of cells expressing the astroglial protein glial fibrillary acidic protein (GFAP) [504]. BMP2 treatment also resulted in decreased proliferation, indicating differentiation of NSCs is driving the increased number of astrocytes, rather than astrocyte mitosis

[504]. In this study BMP2-induced astrogliogenesis was also correlated with decreased oligodendrogenesis, supporting the astrogliogenic and anti-oligodendrogenic actions of BMPs [504]. Overexpression of a dominant negative BMPR1A in adult-derived hippocampal progenitor cells also resulted in increased astroglial differentiation, but there was no change in oligodendrogenesis [527] (Appendix Fig A1D). Interestingly, oligodendrogenesis was significantly increased following overexpression of a dominant negative BMPR1B in hippocampal derived NSCs, while astrogliogenesis was decreased [527]. Noggin treatment mimicked these effects in these cells [527]. Additionally, in SVZ-derived cells Noggin inhibited astrocyte differentiation [497]. This is clearly contrasted by the finding that BMP5-induced SMAD1/5/8 signaling limited the proliferation of astrocytes while promoting mature astrocyte differentiation from immature astrocytes *in vitro*, supporting the evidence above that BMPs may be increasing astrocyte differentiation rather than proliferation [528].

Taken together, BMP signaling works to reduce oligodendrocytic differentiation of NSCs in the SVZ and increase astrogliogenesis throughout multiple brain regions. Currently, it is hypothesized that BMPs hold NSCs in quiescence, and that a lack of BMP signaling leads to unrestricted differentiation, resulting in decreased NSC levels. However, if BMPs can also act to induce astrogliogenesis, it may be through a different mechanism. Additionally, it is important to note that GFAP, a common marker used to measure astrocytes and measure astrogliogenesis, is also a marker of NSCs in the SVZ and SGZ. Therefore, it is possible that GFAP+ cell numbers, often used to measure astrogliogenesis, may be confounding data regarding astrocyte quantification.

4.2 Adult Neurogenesis

Development of the CNS occurs through an orchestrated combination of cell proliferation, precursor differentiation, and maintenance of the stem cell pool. In the adult mammalian brain, NSCs reside within neurogenic niches and give rise to newborn neurons [529]. By adulthood, the

number of dividing and proliferating cells decreases drastically in rodents and humans [179, 530]. There are a few areas of the brain that are known to maintain the ability to divide and replenish the stem/progenitor cell niche [531]. Those areas include the SGZ [11, 532], the SVZ [19], and the hypothalamus [58, 59, 384]. The hypothalamic niche is a more recently discovered neurogenic niche, where tanycytes are hypothesized as one population capable of giving rise to adult-born hypothalamic neurons or support local stem cell differentiation [129].

To allow for long-term plasticity within the neurogenic niches, NSCs require controlled levels of proliferation, as increased proliferation and neurogenesis could result in depletion of the NSC pool. This process is regulated in the adult brain by BMP signaling, as BMPs hold NSCs in a quiescent, non-proliferative state, and BMP inhibition results in neurogenesis [352, 496, 497, 506, 533, 534]. In the adult SVZ, overexpression of BMP7 inhibits proliferation of precursor cells (Appendix Fig A1C). BMP2 and BMP4 regulate adult neurogenesis as well, as treatment of SVZ-derived cells with BMP2 or BMP4 reduces neurogenesis *in vitro* [497]. Decreased neurogenesis was also observed after viral expression of constitutively active BMPR1A and BMPR1B receptors in SVZ-derived cells [497]. The downstream SMAD pathway also regulates these processes, as SMAD4 KO from astrocytes and NSCs in the same niche impeded the transition of NSCs to progenitor cells [496] (Appendix Fig A1C). SVZ BMP signaling leads to expression of the quiescence marker Cyclin Dependent Kinase 4 Inhibitor D, indicating that BMP signaling may promote cell cycle arrest [535]. Reduced BMP4 clearance in the SVZ resulting from LRP2 deficiency decreased proliferative capacity of NSCs in the SVZ *in vivo* [536]. SVZ-derived neurospheres treated with BMP2 decreased neurosphere numbers, indicating impaired proliferation *in vitro* [522]. Additionally, adherent cultures of neurosphere-generated TACs showed reduced cell cycle marker expression after BMP2 treatment [522]. These examples demonstrate the neurogenic regulatory capacities that BMPs have *in vitro* using SVZ cells, and *in*

vivo within the niche, to hold cells in a quiescent and non-proliferative state. BMPs have a similar regulatory role in other neurogenic niches.

In the hippocampus, BMPs also act to decrease proliferation and decrease the number of NSCs in the cell cycle. Treatment with BMP4 in this niche reduced cycling NSCs, neuroblasts, and EdU-labeled cells, but not the number of NPCs, indicating the cells were being held in a non-proliferative state [534] (Appendix Fig A1D). NSE-BMP4 mice, which overexpress BMP4 in adult neurons, have significantly greater numbers of slowly dividing stem-like cells in the DG [533]. Slowly cycling hippocampal cells are far reduced in NSE-Noggin mice compared to both wild-type and NSE-BMP4 mice [533]. Further studies showed that in the adult mouse Noggin acted to accelerate NPC activation and increased the number of proliferating precursor cells and neuroblasts [352, 534] (Appendix Fig A1D). However, the long-term effects of Noggin on the hippocampus were decreased proliferation and fewer label retaining NSCs, indicating a reduction in the stem cell pool or loss of proliferative abilities of SGZ NSCs [352]. Increased proliferation followed by a reduction in NSC division and newborn precursors was also found in mice with a conditional BMPR1A ablation in hippocampal NSCs or SMAD4 KO mice [352] (Appendix Fig A1D). *In vitro*, treatment of Noggin on neurospheres generated from adult mouse hippocampus resulted in increased numbers of neurospheres, as well as larger neurospheres, indicating higher levels of proliferation with the BMP inhibitor [533].

Proliferation and activation of NSCs leads to the production of NPCs, which migrate and differentiate into adult-born neurons. Studies examining neurogenesis in the SVZ reveal that overexpression of BMP7 prevents the repopulation of NPCs in the SVZ following the loss of proliferative progenitors [497]. Noggin expression in NSCs in the SVZ increased proliferation, as well as the number of NPCs, but at the expense of quiescent NSCs [537]. Noggin overexpression in the striatum also promoted neuronal differentiation of transplanted SVZ cells [497]. These

findings are potentially due to BMPs holding NSCs in a non-committed state and preventing differentiation to NPCs.

The anti-neurogenic role of BMPs also impacts cognition in the adult hippocampus. Interventions known to improve cognition (which included exercise, environmental enrichment, and maze training) increased neurogenesis and improved cognition, apparently working through the BMP-Noggin axis, as these interventions reduced BMP signaling and increased Noggin expression in this region [506, 538]. When mice were exposed to Morris water maze testing, they had an increase in expression of Noggin mRNA in the DG, thus demonstrating that a decrease in BMP signaling could lead to cognitive improvements [506]. Elective exercise in the form of wheel running also increased Noggin expression and decreased BMP expression [538]. Exercise resulted in increased cellular turnover, and heightened numbers of NPCs and neuroblasts [538]. Improved cognition and increased neurogenesis were mirrored in NSE-Noggin mice and antagonized in NSE-BMP4 animals [538]. Importantly, the cognitive advancements in NSE-Noggin mice required neurogenesis and cell proliferation, as treatment with the mitotic inhibitor 1-β-d-Arabinofuranosyl-cytosine (Ara-C) reversed cognitive improvements in these mice [538]. BMPs are likely inhibited in states of adult neural plasticity.

In vitro studies examining the neurogenic impacts of BMP signaling in adult hippocampal cells show a similar trend. Treatment of adult hippocampal NSCs with BMP2 or BMP4 resulted in decreased proliferation, which was reversible with Noggin treatment [352] (Appendix Fig A1D). Intriguingly, rat adult hippocampal NSCs treated with BMP2 or BMP4 were found to increase neurogenesis in a WNT-dependent manner *in vitro* [539]. In SVZ-derived NPCs, these BMPs reduced the number of newborn neurons in culture [497], while Noggin treatment promoted differentiation of neurons from neurospheres [537]. Investigation of BMP signaling in neuronal progenitor cells from the olfactory epithelium revealed that BMPs reduce neuronal colonies in culture and inhibit proliferation in olfactory epithelium explants [540]. Taken together, BMPs

clearly impede neurogenesis and the BMP inhibitor Noggin can increase proliferation and neurogenesis.

Appendix Table A2 - Impact of BMPs on Adult Neural Plasticity *(neurogenesis, gliogenesis)*

Animal model	Treatment(s)	Brain Area	Findings	Citation
Wildtype mice	Ara-C treatment followed by Adenoviral overexpression of BMP7	Subventricular zone (SVZ)	BMP7 overexpression inhibited proliferation and type A cell production.	Lim, 2000 [497]
Wildtype mice	BMP2, BMP4; constitutively active BMPR1A/B	SVZ-derived cells	BMP treatment or signaling upregulation inhibits neurogenesis.	
NSE-Noggin mice *(overexpression in hippocampal neurons)*	-	Subgranular Zone (SGZ)	Noggin overexpression in the SGZ increased GFAP+ cell populations at the expense of other precursors *in vivo*.	Bonaguidi, 2008 [533]
C57BL/6 mice	Noggin	Hippocampus-derived neurospheres	Noggin treatment increases proliferative and self-renewal ability of NSCs and allows for multipotential differentiation into neurons and glia.	
GLAST:CreERT2/ Smad4f/fl mice *(Smad4 KO in NSCs and glia)*	-	SVZ	Smad4 deletion in glia and ANSCs increased oligodendrocyte precursor numbers and impaired neurogenesis via BMP-mediated signaling.	Colak, 2008 [496]

Table A2 continued

NSE-BMP4 mice and NSE-Noggin mice *(overexpression of BMP4 or Noggin in hippocampal neurons)*	-	Hippocampus	BMP4 overexpression decreased proliferation (CldU+ or IdU+ cells), neurogenesis (Sox2+ or DCX+ cells), and cognition. Noggin overexpression increased proliferation, neurogenesis, and proliferation-mediated cognition.	Gobeske, 2009 [538]
GLAST:CreERT2/ Smad4fl/fl mice *(Smad4 KO in NSCs and glia)*	-	Hippocampus	Noggin treatment causes NSCs to enter the cell cycle and increases neurogenesis *in vivo*.	Mira, 2010 [352]
CD-1 mice	*i.c.v.* Noggin	Hippocampus	Short-term Noggin treatment increases proliferation of NSCs and neuroblast number, while chronic exposure decreases proliferative ability of NSCs.	
Wildtype mice	Lentiviral BMP4, Lentiviral Noggin	Hippocampus	Overexpression of BMP4 in the hippocampus caused NPC cycle exit and reduced neurogenesis. Overexpression of Noggin led to accelerated neurogenesis.	Bond, 2014 [534]
hGFAP-CreER^{T2} x BMPRII^{flx}; Rosa^{zsG} mice *(Deletion of BMPRII from activated ANSCs)*	-	Hippocampus	BMPRII ablation in NSCs accelerated maturation.	
FVB/N x pBi-Noggin-EGFP *(Conditional Noggin expression in NSCs)*	-	SVZ	Noggin expression in Nestin+ NSCs lead to increased proliferation, increased neuroblasts and oligodendrocyte progenitors, and decreased numbers of quiescent NCSs.	Morell, 2015 [537]
C57BL/7 mice	BMP2	SVZ-derived neurospheres	BMP treatment limits EGF-induced proliferation of TACs, while inhibition of BMP-SMAD signaling promotes activation of quiescent NSCs.	Joppé, 2015 [522]

Table A2 continued

Crl:CD1 mice	BMP2, BMP4	Adult hippocampal NSCs	Exposure to BMP2 and BMP4 ligands OR overexpression of BMPR1A increases neurogenesis while decreasing oligodendrogenesis.	Armenteros, 2018 [539]

6. The role of BMPs in the neural control of energy balance

Single nucleotide polymorphisms (SNPs) in BMP2 and BMPR1A are associated with human obesity and BMPR1A SNPs are implicated in obesity-related traits such as plasma leptin and plasma glucose, but their actions in the regulation of energy balance are still being investigated [157, 158]. The two major types of adipose tissue are white adipose tissue (WAT), which is made up of white adipocytes that store fuel, and brown adipose tissue (BAT) that can produce heat via non-shivering thermogenesis, in response to norepinephrine released by sympathetic nerves after cold stimulation. Our work, as well as the work of others, has demonstrated that BMPs and their receptors are important for the regulation of energy balance both by acting in the CNS to regulate appetite and by stimulating sympathetic activity in BAT, as well as promoting the development and production of heat producing (thermogenic), calorie-burning brown adipocytes [6, 9, 10].

6.1 Hypothalamic Neurogenesis

Whether BMPs are also involved in these processes in the hypothalamus remains unknown. However, it is clear that other factors, including BDNF and CNTF are able to modulate metabolic function through a hypothalamic pathway that incorporates neurogenesis. As previous work has uncovered the expression of BMP2, BMP3, BMP4, BMP5, BMP6, BMP7, BMP8b and

BMPR1A in the V3V ependymal/ tanycytic layer, ME, ARC, VHM, and PVH, and because BMPs affect neurogenesis in both the SVZ and SGZ, it is possible that within the hypothalamus, hypothalamic neurogenesis could also be controlled by BMP signaling. Indeed, the presence of BMP-rich CSF and a leaky BBB within the ME indicates a clear possibility for the complex coordination of hypothalamic neurogenesis by both BMPs and their antagonists.

Tanycytes are known to respond to dietary changes via the creation of newborn neurons within the hypothalamus [97, 100, 162]. After high fat diet, young adult mice showed reductions in neurogenesis in the ARC, and female mice also had increased neurogenesis in the ME [163]. These newborn neurons within the ME were determined to be progeny of tanycytes in proximity to the ME. In addition, irradiation of the median eminence attenuated weight gain in female mice fed an HFD, resulting in significantly lower weight gain than their HFD-sham counterparts, providing evidence that adult-born neurons in the median eminence respond to HFD with increased body weight [163]. Interestingly, this effect was not seen in male mice, indicating that adult hypothalamic neurogenesis may be a sexually dimorphic method of body weight regulation and energy storage. This process may be regulated by BMP signaling, although the specific pathways involved are unknown.

6.2 Appetite Regulation

The role of BMP pathways in regulating appetite can be traced back to D. melanogaster and C. elegans. In C. elegans, the TGF-β family ligand DAF-7, signals through the canonical SMAD signaling pathway, and is upregulated during refeeding after fasting [164, 165]. Additionally, mutations in daf-7 and the TGF-β receptor homologs daf-1 and daf-4 play a role in quiescence after fasting and refeeding, indicating a role for the TGF-β-SMAD signaling pathway in satiety [164, 165]. This signaling pathway is highly similar to the BMP-SMAD signaling pathway as they

both utilize canonical SMAD signaling, and points to a shared evolutionary role for appetite regulation. In drosophila larvae, reduced glass bottom boat (Gbb)/BMP signaling affects metabolism of fat body cells [166]. Additionally, the phosphorylated Smad1/5 protein homologue, pMad, which normally accumulates in the nuclei of wild-type fat bodies, is reduced after nutrient-deprivation in larvae [166]. These studies indicate an evolutionary role of BMP-SMAD signaling in regulating and responding to appetite and fuel storage.

BMP signaling regulates appetite in mice as well. Following HFD in adult mice housed at 23°C, Bmp8b expression increased 4-fold in BAT [6]. Changes were also seen in the expression of transcripts of BMP8b, BMP2, BMP4, BMP5, and BMP6 in BAT after fasting and re-feeding [6]. BMP8b knockout mice consumed less energy on chow and HFD, yet still gained more weight than their wild-type counterparts (Fig 2D). This phenotype may have occurred through a CNS appetite axis, as neuropeptides AgRP, NPY, POMC, and cocaine and amphetamine regulated transcript (CART) mRNA levels were all decreased in BMP8b-/- mouse hypothalami [6]. This change in appetite may have been directly correlated with BMP and hypothalamic signaling, and the significantly reduced metabolic rate of BMP8b-/- mice was paired with impaired thermogenesis, which potentially also may have had a CNS origin if hypothalamic control over adipose sympathetic drive was also affected by BMPs [6].

A study performed by our group demonstrated that systemic BMP7 treatment reduced appetite, increased metabolic rate, and promoted weight loss in C57BL/6 mice with diet-induced obesity [10] (Fig A2A). This weight loss resulted from decreased fat mass, not lean mass. In the same study, systemic BMP7 treatment of leptin-deficient (ob/ob) mice resulted in weight loss associated with decreased food intake, indicating that the decreased appetite and weight loss seen in both mouse lines were found to be mediated via a leptin-independent rapamycin-sensitive mTOR-p-p70S6K pathway [10] (Fig A2A). This study also examined the effects of BMP7 administered i.c.v. The results showed a 44.4% decrease in food intake in C57BL/6 mice, which was mirrored in

ob/ob mice [10] (Fig A2B). When analyzing hypothalamic neuronal activity, central BMP7 administration was associated with increased c-Fos-immunoreactive neurons in the ARC, which houses neurons that affect food intake and energy expenditure. Additionally, hypothalamic POMC expression (an anorexigenic neuropeptide) was increased in C57BL/6 mice that received BMP7, supporting the relationship between BMPs and hypothalamic appetite reduction. Interestingly, targeted knockdown of BMPRII in the brain before treatment with centrally administered BMP7 led to no reduction in food intake [10]. These data support the idea that BMPs act through the hypothalamus to reduce appetite in a leptin-independent manner, likely via type 1 receptors.

Intriguingly, another study showed that BMP7 treatment resulted in a dose dependent increase in food intake in C57Bl6/J mice held in subthermoneutrality. Here, BMP7 effects appeared to have opposite effects as the prior study, but there are major differences in the mice and treatments between these two studies. In this study where BMP7 treatment led to increased appetite, 4-wk old male C57BL/6J mice were treated for 4 weeks with BMP7 while on a 45% HFD, which itself can increase hyperphagia. Here, food intake was measured over 1 week during the last week of BMP7 treatment. These mice were also housed in subthermoneutral conditions. The previous study utilized adenoviral expression of BMP7 in C57BL/6 mice after 12 weeks of 45% HFD when analyzing systemic BMP7 treatment in obese animals, and measured food intake over 12 days to determine if BMP7 could reverse (and not prevent as in the prior study) weight gain. These large differences between methodology may have resulted in the opposite effects on appetite. However, BMP7 treatment in both studies led to improved metabolic phenotype and caused changes in appetite, leading us to conclude that BMP7 plays a role in appetite and hypothalamic signaling in the adult mouse brain.

To identify the mechanism by which BMP7 in the hypothalamus physiologically regulates appetite, we showed that selective knockout of BMPR1A (a BMP7 receptor) in POMC neurons of adult mice resulted in hyperphagia as anticipated, but with a striking lack of obesity even on a 45%

HFD for up to 24wks [9] (Fig A2C). This resistance to obesity was associated with increased sympathetic activation and thermogenic ability of the brown adipose tissue in these animals. There was also a compensatory increase in BMPR1A throughout the hypothalamic regions of the VMH and ARC after the knockout, highlighting the importance of BMP signaling in regulating energy balance, given this re-establishment of energy balance after a BMP receptor KO in the hypothalamus was likely due to neural plasticity in the hypothalamus.

6.3 BMPs and Thermogenesis

The role of BMPs in the process of BAT thermogenesis has been linked to both input from the CNS as well as local signals and endocrine factors. BAT, a multilocular, highly thermogenic organ that exhibits high numbers of mitochondria uniquely expressing uncoupling protein 1 (UCP-1) to produce heat, is controlled by BMP signaling in both development and adult maintenance [167-169]. Studies in orexin-null mice showed that BMP-SMAD signaling is required for orexin-directed brown adipogenic action and thermogenesis [170]. This process of orexin-directed brown adipogenic action and thermogenesis was dependent on BMPR1A-Smad1/5 signaling in vitro [170]. It is unclear if the orexin pathways involve the nervous system in activating BAT. Additionally, BMP8b administered centrally i.c.v. improved global energy balance by increasing body short-term body temperature and lead to the activation of thermogenic gene expression in BAT [6]. These improvements were coordinated with sympathetic nerve activation to BAT [6], similar to the POMC-BMPR1A KO model described above.

Much is known about the role of BMP signaling in non-CNS driven adipose thermogenesis, including brown adipogenesis, browning of white fat, and activation of mitochondrial activity in BAT. Neural innervation of adipose tissue also allows for the regulation of lipolysis, adipogenesis, and browning. Our lab has previously characterized large nerves in the mouse inguinal

subcutaneous depot and is currently working to identify the possibility of true synaptic connections within this tissue, as well as characterizing the products that these nerves may be releasing into adipose depots. Perhaps the nerve-adipose axis may also include local BMP regulation of neural plasticity within adipose tissues [171-173]. Indeed, BMP8b regulated neuro-vascular remodeling has been identified and shown to promote synaptic plasticity [174]. In this study, BMP8b, which is secreted locally by adipose tissues, upregulated local neuregulin-4 expression and enhanced browning and thermogenic capacity when overexpressed, leading to increased sympathetic innervation in vivo as well as sympathetic axon growth and branching in vitro. Since BMPs in adipose tissue development and function have been reviewed elsewhere, we will focus on the role of BMPs in the central nervous system on the regulation of energy balance.

6.4 BMPs and Obesity

Obesity is a complex disease that involves increased mass of WAT due to energy imbalance, which can lead to chronic inflammation, peripheral neuropathy, cardiometabolic diseases, and type 2 diabetes mellitus. In mice, BMPs have been found to play a role in 'browning' of WAT, where WAT changes to more resemble the more energetically favorable BAT with UCP1 expression and thermogenic capacity. This change has also been associated with healthier adipose phenotypes and weight loss. BMPs also regulate obesity and body weight throughout the adult human body. The specific ligands involved in body weight and obesity include BMP2, BMP3, BMP3b, BMP4, BMP7, BMP8B, and BMP14 (Reviewed in [175]), but it is unclear if more than BMP7 and BMP8B have actions in the brain. BMP2 and BMP4 expression are increased in overweight and obese individuals [176, 177]. BMP2 and BMP4 can form heterodimers with BMP7 [178], but it is unknown if they synergize to impact energy balance. Importantly, due to the fact that BMP heterodimers exhibit magnified effects compared to their homodimers in inducing osteoblastogenesis and bone formation, it is possible that BMP2/7 and BMP4/7 heterodimers

could more potently mediate browning and be used as a potential therapy to boost energy expenditure in obese individuals [179].

BMP3b, which is increased during obesity in mouse mesenteric adipose tissue [180], protects against HFD-induced obesity when overexpressed in adipose tissues [181]. BMP2 and BMP4 enhance white adipogenesis [182, 183], while BMP7 causes differentiation of brown preadipocytes and commits mesenchymal progenitor cells to a brown adipocyte lineage [169]. BMP7 treatment also increased BAT weight and BAT Ucp1 expression at the subthermoneutral temperature of 21°C in C57BL6/J mice [184]. This treatment was associated with decreased WAT mass and upregulation of intracellular lipolysis genes, followed by browning of WAT [184]. However, except for browning, these effects were only seen at 21°C, as housing at 28°C reduced these effects [184]. BMP7 KO eliminated brown fat and UCP-1 expression in embryos [169]. Moreover, growth of E9 rat embryo mesoderm within the BMP7-rich kidney capsule resulted in differentiation into brown fat [185]. These results implicate sympathetic activation of BAT as a requirement for BMP7 to induce browning and improved metabolic health. Intriguingly, BMPR1A KO of POMC neurons in the hypothalamus leads to sympathetic activity of BAT, resulting obesity resistance via increased energy expenditure, thermogenesis, and browning of WAT in adult mice, highlighting the importance of BMPs in the central regulation of obesity [9].

The role of BMPs and their association with the obesity-related factors leptin and insulin have also been studied extensively in adipose. While the relationship between BMPs and insulin within the brain have not been studied, it is understood that insulin acts centrally by regulating POMC+ neuron activity within the hypothalamus [186]. As BMPR1A activity in POMC neurons affects whole-body energy balance and metabolism, there is a chance that there is an insulin-BMP axis in the CNS. Outside of the CNS, BMP-SMAD signaling enhances insulin-mediated glucose uptake in both insulin-sensitive and insulin-insensitive adipocytes [187]. Additionally, plasma insulin levels were elevated in BMP6-treated leptin-resistant ob/ob mice [188]. Recent evidence

indicates that insulin resistance can be induced after loss of the bone morphogenetic protein-binding endothelial regulator (BMPER), which adapts endothelial cells to inflammatory stress [189]. Inducible KO of BMPER in endothelial cells or globally led to increased insulin levels, glucose intolerance, and insulin resistance [189]. Fitting with this, in assessments of metabolic syndrome patients, circulating levels of BMP9 reduced progressively with an increasing number of metabolic syndrome components, and BMP9 was specifically negatively associated with fasting blood glucose, the hemoglobin subunit alpha Hba1c, and a 2-hour oral glucose tolerance test – all signs of insulin resistance [190]. Loss of BMP3b also leads to metabolic syndrome and increased adipogenesis [191].

The relationship between leptin and BMP signaling is more completely understood. When administered systemically, BMP7 was found to act independent of leptin, as decreased food intake and weight loss in response to BMP7 were observed in both diet-induced obesity and ob/ob animals [10]. C57BL/6 and ob/ob mice administered BMP7 centrally via i.c.v. reduced food intake [10]. Central BMP7 treatment also induced c-Fos and alpha-melanocyte stimulating hormone (α-MSH) expression and downregulated expression of NPY and AgRP in the ARC, supporting the central mechanism of BMP7 appetite suppression. Knockdown of BMPRII via i.c.v. lentivirus inhibited the anorexigenic effects of BMP7. [10]. The leptin-BMP axis can be seen in the brain, as leptin-treated ARH explants show increased neurite outgrowth, which decreases to normal levels with Noggin administration [192]. Leptin treatment of control vs. BMPR1A KO ARH explants also showed that BMP signaling is essential for neurite outgrowth in the hypothalamus [192]. Leptin injection induced pSMAD1/5/8 activation in AgRP+ neurons in postnatal mice in vivo [193]. Additionally, BMP8b and leptin both have been found to act on the VMH of the hypothalamus to induce SNS-directed BAT thermogenesis [194]. Overall, BMPs act to improve metabolic health via both systemic and central pathways. Although there appear to be BMP-leptin interactions within the hypothalamus, the ability of certain BMPs to bypass leptin signaling to regulate food

intake and weight loss indicates that BMPs may serve as a potential therapeutic for leptin-resistant obese patients. Currently, however, these pathways and their relationship to known metabolic pathways requires further investigation.

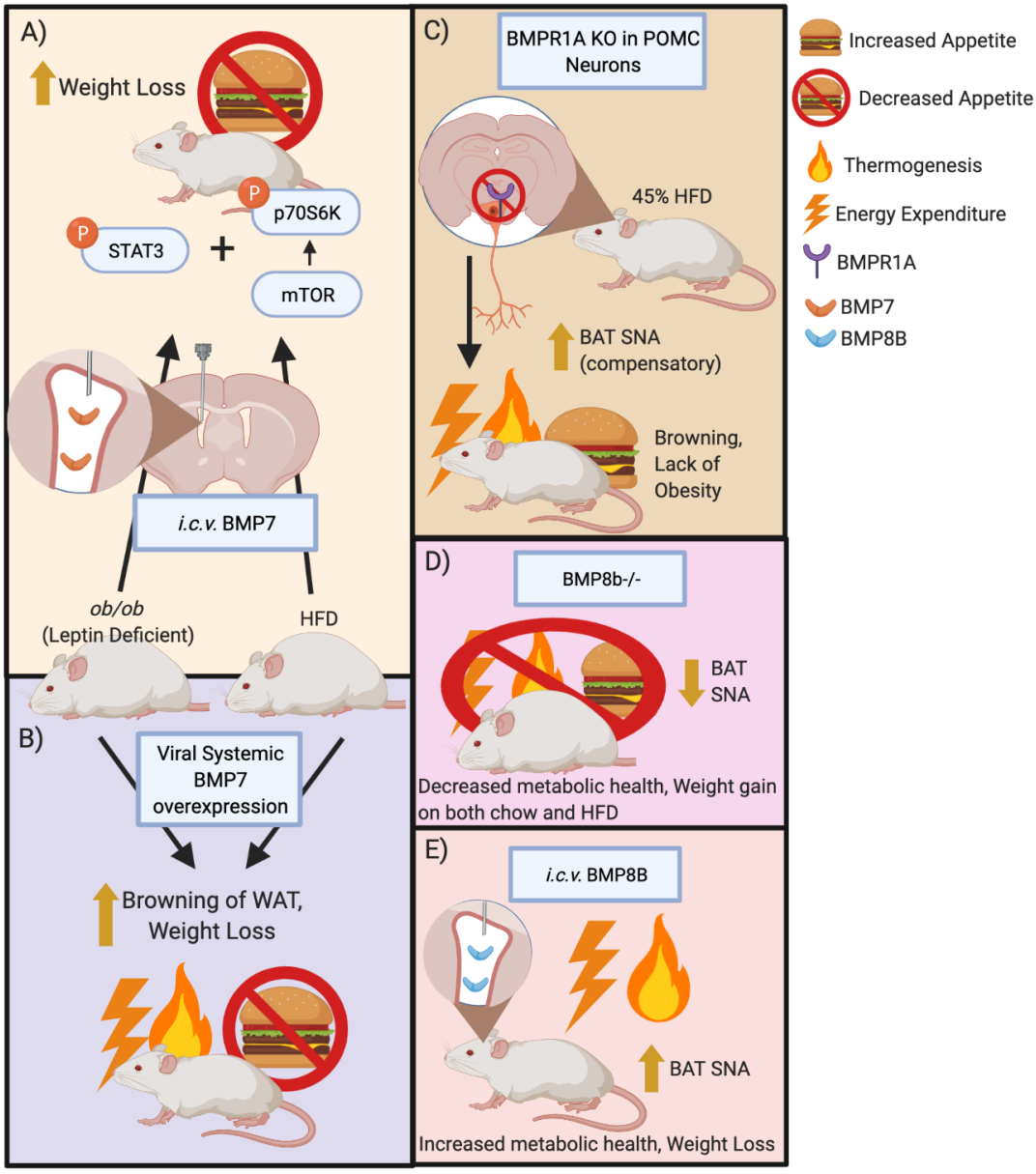

Figure A2. BMPs affect both arms of energy balance through actions in the nervous system. A) BMP administered i.c.v. led to decreased food intake and increased thermogenesis in obese adult mice via a leptin-independent pathway [10]. B) Systemic viral BMP7

overexpression reduced appetite while increasing thermogenesis and energy expenditure in metabolic cages [10]. C) BMPR1A KO in POMC neurons in mice fed HFD increased sympathetic activity of BAT and resulted in increased appetite, thermogenesis, and energy expenditure in metabolic cages, as well as a lack of obesity and browning. Here, these improvements may have resulted from a compensatory increase in BMPR1A expression [9]. D) BMP8b KO mice are metabolically unhealthy and show increased weight gain with reduced energy expenditure, thermogenesis, and appetite [6]. E) In contrast, i.c.v. treatment with BMP8b resulted in increased sympathetic activity, thermogenesis, and energy expenditure, indicating improved metabolic health [6].

APPENDIX B

LINEAGE TRACING OF INDUCIBLE FLUORESCENTLY-LABELED STEM CELLS IN THE ADULT MOUSE BRAIN

Published in J Vis Exp. (JoVE) 2022 May 20; (183)

DOI: 10.3791/63998

Authors: Gabriel S. Jensen, Jake W. Willows, David T. Breault, Kristy L. Townsend

Sections, figures, and tables in this dissertation are GJ contributions

Summary

The ability to permanently mark stem cells and their progeny with a fluorophore using an inducible transgenic lineage tracing mouse line allows for spatial and temporal analysis of activation, proliferation, migration, and/or differentiation *in vivo*. Lineage tracing can reveal novel information about lineage commitment, response to intervention(s), and multipotency.

Abstract

A telomerase reverse transcriptase (Tert) lineage-tracing mouse line was developed to investigate the behavior and fate of adult tissue stem cells, by crossing the 'Tet-On' system oTet-Cre mouse with a novel reverse tetracycline transactivator (rtTA) transgene linked to the Tert promoter [287]. This is one example of a transgenic mouse approach to lineage tracing adult brain stem cells. When a tetracycline derivative, doxycycline, is administered to the mouse this indelibly marks a population of cells that express a 4.4kb fragment of the promoter region of the gene Tert, which we have demonstrated to mark a novel population of adult brain stem cells. When using the Rosa-mTmG reporter mated to the mTert-rtTA::oTet-Cre double-positive mice, expression of

membrane tdTomato (mTomato) is replaced with membrane EGFP (mGFP) in cells that also express the rtTA, upon induction with doxycycline. The triple-transgenic mTert-rtTA::oTet-Cre::Rosa-mTmG mice are given doxycycline (the "pulse" period during which TERT expressing cells are marked), followed by observation of the indelibly marked mGFP+ cells that can be tracked for any desirable amount of time after doxycycline removal (the "chase" period), even if Tert expression is subsequently lost. Brains are then perfusion-fixed and processed for immunofluorescence and other downstream applications, in order to interpret changes to stem cell activation, proliferation, lineage commitment, migration to various brain niches, and differentiation to mature cell types. Using this system, any rtTA mouse can be mated to oTet-Cre and a Rosa reporter to conduct doxycycline-inducible "pulse-chase" lineage tracing experiments using markers of stem cells.

Introduction

Value of a lineage tracing mouse line

Analysis of stem cells *in vivo* can be difficult since many assays that examine such cells only focus on characterizing these cells at the time of death of the animal, which represents a terminal snapshot in time. To better understand the processes of proliferation, differentiation, and migration of progenitor, intermediate/transition cell types, and mature cells over time, a longitudinal analysis approach is required. This can be achieved with lineage tracing studies whereby stem/progenitor cells are marked indelibly and can be followed for any length of time after this.

In the adult mammalian brain, the process of neurogenesis by which adult-born neurons are created from stem and progenitor cells was first analyzed via label retention with thymidine-H3 [4, 5, 543] or 5-bromo-2'-deoxyuridine (BrdU) [10, 11, 40, 544]. In these studies, proliferative cells were marked with the thymine analog, which was incorporated into the cells' DNA during replication and cell division/proliferation. The marked cell, as well as their progeny, therefore

contained this analog, which were then identified post-mortem. However, while thymidine-H3 and BrdU allowed for the marking of proliferative cells and their progeny in brain regions where stem cells were poorly understood, these studies were hindered by the downsides of these tools. Thymidine-H3 induces cell-cycle arrest, apoptosis, and dose-dependent DNA synthesis inhibition [12], while BrdU marks cells at varying levels depending on the route of administration [13] and is taken up by cells during repair or apoptosis, as well as during cell division [14]. More efficient labeling methods have been utilized recently, such as labeling with 5-ethynyl-2'-deoxyuridine (EdU), but many of the same issues as BrdU still remain [15]. These approaches are also limiting in that they mark any proliferative cell, not just stem cells, and thus interpretation of results can be confounded. In the neurogenic lineage, all stem and progenitor cells retain mitotic capacity, and only terminal/mature neurons are not proliferative. For astrocytes and microglia, but not oligodendrocytes, proliferation is maintained indefinitely [545-547].

Transgenic mice used to lineage trace only cells that express a protein of interest, such as one confirmed to identify adult stem cells as we use here, have therefore become more common when investigating stem cells and their progeny. While difficult to generate through mouse transgenic approaches, lineage-tracing mouse lines allow for the tracing of specifically marked cells in the brain, and do not rely on proliferation alone. In Tet-On transgenic mouse system, administration of tetracycline or doxycycline (a tetracycline derivative) induces Cre-recombinase expression in cells that have been engineered with a reverse tetracycline transactivator (rtTA), which is transcribed by a promoter of interest. The Tet-inducible Cre-driven recombination will then activate the expression of an indelible fluorescent or luminescent protein in the cells of interest, depending on the Rosa-reporter mouse employed. These indelibly marked cells continue to express this reporter after division, differentiation, or migration, allowing the tracking of these cells and their progeny over time or after different interventions [548]. Advantages of transgenic lineage-tracing approaches include: 1) specificity of tracing to a particular cell lineage or progenitor/stem cell marked by the rtTA, 2) indelible expression of the

fluorescent or luminescent protein despite cell turnover or differentiation, 3) low toxicity, 4) conditional activation during any point in the animal's life cycle, and 5) ease of use with common assays, including immunostaining/immunofluorescence [548].

Other methods of temporally inducible reporter tools in mice include the use of Cre-ERT2 mice, which can be paired with ROSA-GFP, ROSA-mTmG, or other fluorescent reporter transgenes. In these animals, a cell-specific regulatory element, such as a promoter or enhancer region of interest, drives the production of Cre recombinase, which can only be activated via the administration of tamoxifen. While Cre-ERT2 mouse lines allow for the induction of Cre in specific cell lines, there is a wealth of knowledge detailing the effects of tamoxifen on adult neurogenesis [549, 550]. Additionally, there exist many ROSA-driven fluorescent reporter genes that can be utilized instead of GFP or mTmG, including YFP or CFP, which would allow for alternate fluorescent labeling in other fluorescent wavelengths. These fluorescent reporter genes can be used with Tet-On or Cre-ERT2 systems.

Telomerase reverse transcriptase (TERT) is the rate-limiting component of the holoenzyme telomerase, which works to extend telomeres after they are shortened during cell division [258, 259]. TERT has been identified as a marker of adult tissue stem cells in the intestine [284, 285], bone marrow [284], liver [286], adipose [551], endometrium [283, 344] and bone [287]. Whether TERT expression in these adult stem cells is solely for telomerase-extending activity or to perform non-canonical TERT roles [313] is still unknown. TERT-expressing quiescent adult stem cells (qASCs) have been identified and traced throughout the body with transgenic lineage tracing mice to study the multipotency and self-renewal ability of these stem cells, as well as their potential to activate, proliferate, differentiate, and migrate [285-288]. The creation of the Tert-rtTA transgene has been performed previously [287]. In this paper, we will describe the use of a lineage tracing TERT mouse line to study TERT+ qASCs which we have identified as a novel ASC population in the adult mouse brain.

Generation of a transgenic lineage tracing mouse line

To generate a lineage-tracing mouse line using the Tet-On system, three transgenes must be combined within a single animal through mouse mating. The first is a rtTA, expressed under the control of the promoter of the gene of interest (ours is TERT-rtTA). In a cell that expresses this gene of interest, the rtTA will therefore be expressed. The second is an oTet-Cre gene, which contains a tetracycline response element (TRE) that will allow for the transcription of Cre recombinase in the presence of both a rtTA fusion transcript and tetracycline or doxycycline. Tetracycline or doxycycline can be administered to an animal via drinking water or chow [552]. Finally, there must be a gene that will be activated by Cre recombinase cleavage. In this manuscript, the labeling gene we will describe is the Rosa26-mTmG gene, which until Cre recombination will ubiquitously transcribe mTomato (membrane red fluorescence in all cells). However, if a cell expresses the rtTA transcript and contains tetracycline or doxycycline, Cre recombination of a set of lox P sites between the mTomato and mGFP sites will change the R26 site and cause the cell to produce membrane EGFP (mGFP, or membrane green fluorescence) instead of membrane tomato. The indelible nature of this mGFP signal will allow for *in vivo* labeling and tracing of cells as they proliferate, migrate, and differentiate. Following the trace, cells can be analyzed for expression of GFP via immunofluorescence in standard cryosections or thicker optically cleared brains.

In this paper, we will describe the use of the specific mouse line, mTert-rtTA::oTet-Cre::Rosa-mTmG. To create this triple transgenic mouse line, we first mated oTet-Cre animals (The Jackson Lab strain #006234) to Rosa-mTmG animals (The Jackson Lab strain #007676) to create oTet-Cre::Rosa-mTmG double transgenic mice. These animals were genotyped with primers and PCR templates indicated in Supplementary Tables 1-2. mTert-rtTA mice (created by David Breault [287]) were mated to oTet-Cre::Rosa-mTmG animals to create mTert-rtTA::oTet-Cre::Rosa-mTmG mice (Figure A3A) [287, 553]. The mechanism of action of the

mTert-rtTA::oTet-Cre::Rosa-mTmG mouse line is illustrated in Figure A3B.

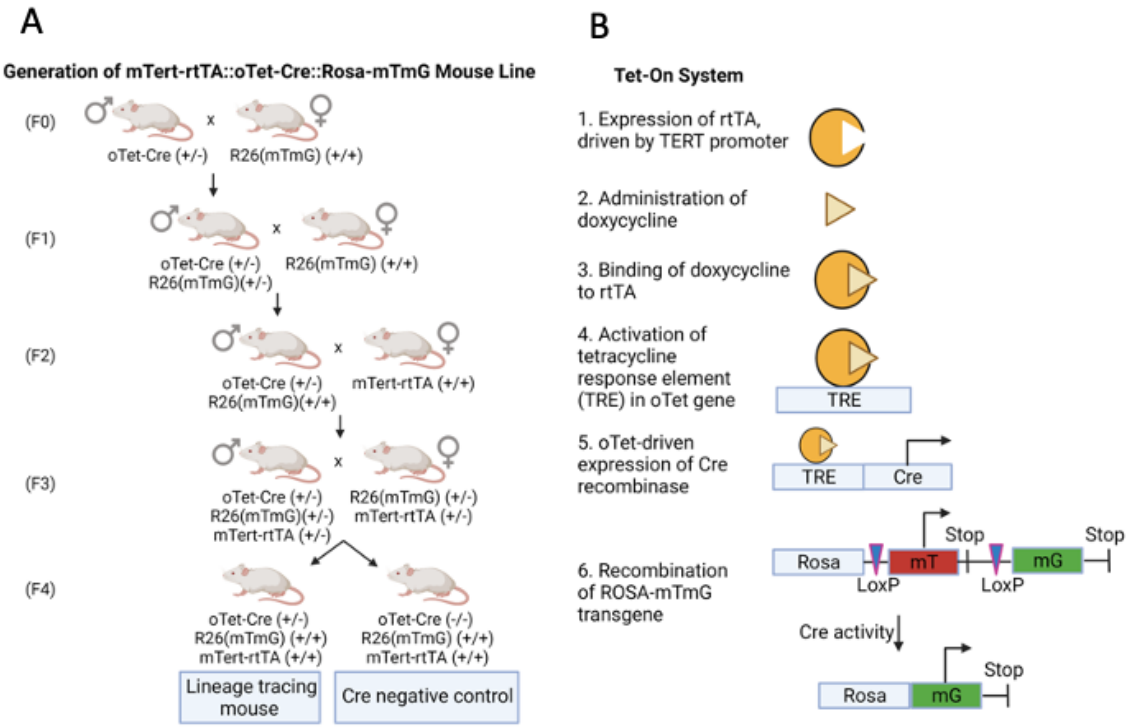

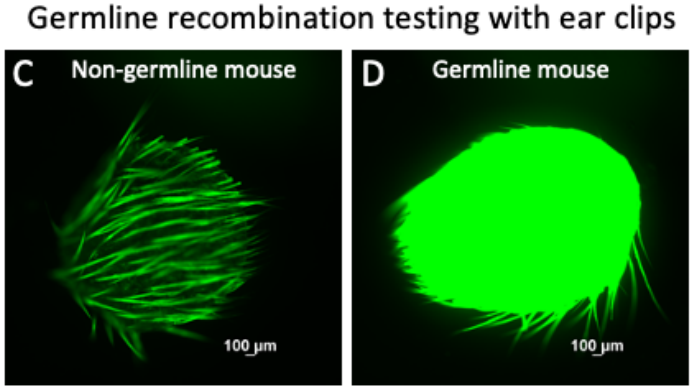

Figure A3. Generation of a Tet-On mouse line.

A) Outline of the breeding scheme for the creation of mTert-rtTA::oTet-Cre::Rosa-mTmG mice from individual mouse lines.

B) Schematic of the Tet-On system in the mTert-rtTA::oTet-Cre::Rosa-mTmG mouse line.

C-D) Representative images of ear clips imaged with FITC channel of an epifluorescent microscope from non-germline (C) and germline (D) mTert-rtTA::oTet-Cre::Rosa-mTmG mice.

Doxycycline induction and pulse-chase design

When planning experiments, it is important to consider several factors that will affect the outcome of lineage tracing experiments, including the age of the animal at doxycycline induction, the length of doxycycline administration (the "pulse" period), the length of time after doxycycline removal before tissue collection (the "chase" period), and the timing of any interventions during these processes. These study design considerations are essential for understanding the labeled cells and their progeny at the conclusion of the experiment. The first step in the process is to identify the age of interest of the animal and the length of the doxycycline administration. Longer pulse periods will allow for the potential for more cells to express the rtTA-linked promoter to be expressed and more cells of interest to be indelibly marked. A cell type that exhibits transient expression of the gene of interest may require a longer pulse period than cells that continuously express the gene of interest. However, if the goal of the study is to understand short-term effects of the cell of interest or an acute intervention, the pulse period cannot be too long, as once a cell is marked, it will be traced through any number of changes during the remainder of the pulse period. In some of our studies, a 2-day pulse with no chase period was used to more closely mimic a direct-reporter for TERT. This is because the minimum length of time for recombination of the Rosa-mTmG gene is 2 days [359].

The next essential period in a pulse-chase experiment is the length between removal of doxycycline and perfusion of the animal, also known as the 'chase'. The half-life of doxycycline in

mice is approximately 170 minutes regardless of administration route, allowing for the conclusion that doxycycline induction is likely no longer occurring several hours after removal [554]. However, it is important to note that doxycycline metabolism is slowed in aged mice, which may lead to longer effective ‘pulse’ periods than young animals [555].

During the chase period, labeled cells will continue to be labeled, even after proliferation, differentiation, or migration. The progeny of these cells will also be labeled. The goal of the study will shape the length of the pulse-chase paradigm. Perhaps the goal of the study is to understand the regeneration of a tissue over a long period of time with the cells of interest. In this case, a long chase period may be required. Finally, the timing of any interventions or treatments must be decided. Administration during the pulse period will affect the cells expressing the gene of interest as well as any progeny created during this time, whereas administration during the chase period may affect mostly progeny of the cells of interest, although this will depend on how quickly the labeled cells divide or differentiate. Examples of pulse-chase experimental designs we have utilized are outlined in Figure A4A.

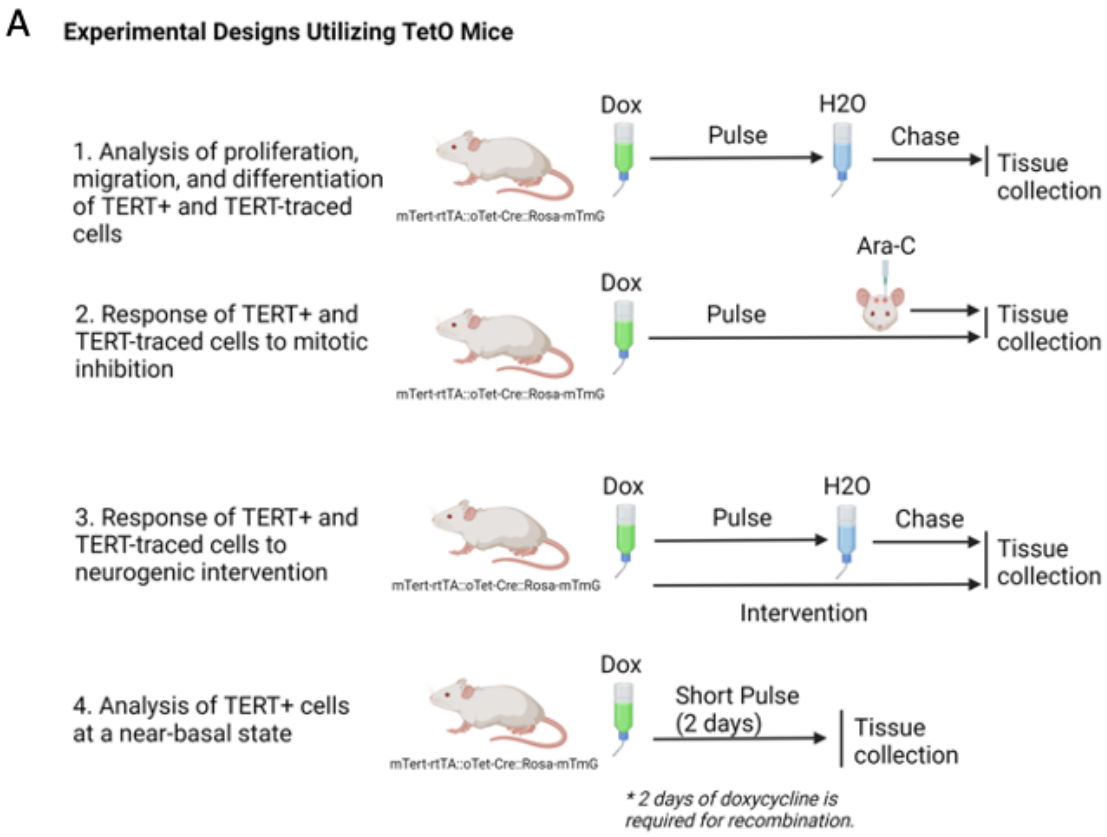

Figure A4. Experimental designs with lineage tracing Tet-On mice.

A) Illustrations of experiments possible with Tet-On mice from basal proliferation, migration, and differentiation (1) to treatments during dox pulse with no chase for regeneration or re-equilibration (2), interventions during pulse with an opportunity to visualize long-term effects (3). A short pulse of 2 days with no subsequent chase will provide insight into a near-basal state of TERT+ cells, as these cells will have little time to activate, proliferate, migrate, or differentiate (4).

It is also important to be aware of the possibility of background GFP signal due to leaky expression. Leaky expression occurs as a result of inherent binding potential between rtTA and the Otet sequences in the absence of doxycycline, and residual activity of the Otet transgene in the absence of rtTA (reviewed in [556]). Leaky expression represents one weakness of the Tet systems, and although the leak is often an acceptable downside to the system, situations where

the leaky expression can lead to toxicity and mortality, such as with diptheria toxin (DTA) in Otet-DTA animals can limit the use of these systems [557].

Brain processing, sectioning, and immunofluorescence of thin sections for microscopy

To analyze the brains of mice after a lineage tracing experiment, mice must first be perfused via transcardial perfusion to remove blood and CSF that can lead to high autofluorescence in the brain. There are two commonly used fixatives that the animal may be perfused with; Histochoice Tissue Fixative, a glyoxal fixative (GF) or 4% paraformaldehyde (PFA). Glyoxal fixatives allow for a relatively gentle fixation process with less cross-linking than PFA. This reduces tissue stiffness, reduces the need for antigen retrieval, and allows for less concentrated antibody solutions during immunostaining. However, if they contain methanol this may serve to increase autofluorescence [558]. On the other hand, PFA will often allow for a more robust fixation and while antigen retrieval will be required during immunostaining, there are antibodies that will only work with PFA-fixed tissues, and perfusion with 4% PFA is required for the optical clearing technique described later.

Following perfusion is a post-fixation step, in which brains are immersed in the same type of fixative utilized during the perfusion overnight. This allows for any brain regions that may not have been fully fixed during the perfusion to continue to fix. Next, brains will be incubated in sucrose in phosphate buffered saline (PBS) to remove as much water as possible before the freezing step to prevent ice formation within the tissue ("cryo-preservation"). Brains may then be cut into any number of sagittal, coronal, or transverse tissue sections for processing. For both precision and reproducibility, calibrated brain blocks need to be used in a way that ensures consistent bregma cuts between animals. The most important factor that can affect how brains are sectioned is the brain region(s) of interest. For example, while a sagittal cut may allow for more brain regions to be analyzed in one tissue section, this cut will not allow analysis of neuro/gliogenic regions of the ventricular-subventricular zone (V-SVZ) as the lateral and medial

sides of the lateral ventricle will be impossible to discern in that dimension and are better observed in the coronal plane. This can be an important distinction to make in adult neurogenesis studies, as the lateral side of the lateral ventricle contains the neurogenic V-SVZ, while the medial wall of the lateral ventricle is a more gliogenic niche [93].

After tissues have been divided into coronal, sagittal, or transverse sections, they will be frozen into blocks using Optimal Cooling Temperature (OCT) embedding solution. Here, brains are frozen within this embedding material, with the use of a mixture of dry ice and ethanol. If thin section analysis is required, blocks will be sliced on a cryostat and depending on the downstream analysis required can be adhered to positively charged glass slides as thin sections (<20μm). Glass slides that are not charged can also be used, but the use of uncharged slides may result in tissues becoming unstuck from the slides [559]. If medium-thickness free-floating tissue sections (>20μm) are required, tissues will be collected as free-floating sections. If thick sections (0.5-4mm) are required, slicing non-frozen brain sections with a vibratome is required. It is important to note the storage differences between sections on slides, which require freezing at -20 to -80 degrees Celsius and free-floating sections, which will be stored at 4 degrees Celsius.

Protocol

1. Creation of a lineage tracing Tet-On mouse line, breeding strategies, and genotyping for experimental cohort mice - Here, we outline creation of Tet-On mouse system with Rosa-mTmG as the fluorescent reporter gene that undergoes Cre recombination, however various other Cre-recombination-driven reporter lines can be utilized with the Tet-On system as well.

1.1. Set up a mating cage of 1 oTet-Cre (+/-) male with 1 or more R26(mTmG) (+/+) females. See Figure 3 for an overview of the experimental mouse mating setup.

1.2. Resulting pups (F1) will be oTet-Cre (+/-) or oTet-Cre (-/-) and R26(mTmG) (+/-). Perform genotyping according to the primers in Supplemental Table 1 and protocols in Supplementary Table 2.

1.3. At weaning, perform germline testing by taking an ear punch from each weanling. Examine the ear punch under an epifluorescent microscope in the GFP/FITC spectrum to determine whether the animal had undergone germline recombination in development. If so, the animal will express GFP in every cell, and the ear punch will fluoresce with mGFP signal. These animals cannot be used for matings or experiments.

1.3.1. NOTE: Ear clips from mice that are not germline show only endogenous fluorescence under the microscope (Figure A3C), while germline animals show a bright GFP signal (Figure A3D). Control ears can be from mice that do not contain fluorescent transgenes. As a note, ear hairs have high endogenous fluorescence and must not be used as a determining factor (Figure A3C). Additionally, differences in endogenous fluorescence are observed between mice of white vs. black coat color, and controls from mice of the same coat color as mice being tested will need to be used in this analysis.

1.4. Mate 1 male oTet-Cre (+/-) x R26(mTmG) (+/-) with 1 or more female oTet-Cre (-/-) x R26(mTmG) mice.

1.5. The resulting generation (F2) will be ¼ R26(mTmG) (+/+) and ½ Cre (+/-). These animals will then be crossed with mTert-rtTA (+/+) animals by mating 1 oTet-Cre (+/-) x R26(mTmG) (+/+) with 1 or more mTert-rtTA (+/+) animals.

1.5.1. Note: We used mTert-rtTA (+/+) animals, but this process can be performed with any rtTA mouse line [553].

1.6. For experimental animals, set up breedings to generate mTert-rtTA (+/+) or (+/-) x oTet-Cre (+/-) x R26(mTmG) (+/+) or (+/-).

2. Doxycycline induction of Cre and pulse-chase design

2.1. When animals are at the correct age for the study to begin, replace their drinking water with dox water: drinking water containing 5% sucrose and 2mg/ml doxycycline hyclate. Cre-negative animals that receive the same doxycycline pulse-chase as experimental animals will be used as a control group for the resulting fluorescent expression patterns.

2.1.1. NOTE: After preparation, dox water must be stored at 4°C for up to 1 month. See Solution Composition Table for more information. Dox water may be administered to animals in drinking bottles for up to 5 days before being changed out, as fungal growth can occur if dox water is left out at room temperature for longer periods of time.

2.1.2. NOTE: A doxycycline pulse of at least 2 days is required for induction of mGFP signal when utilizing the mTmG transgene (initial mTmG paper).

2.1.3. NOTE: We have not tested doxycycline concentrations other than 2mg/ml. Previous literature has identified that this concentration has the highest effects when administered through

drinking water [552]. The amount of doxycycline delivered may differ depending on the amount of drinking done by each animal. Doxycycline injection or gavage may also be done in order to be consistent between animals [560].

2.2. After the pulse period has ended, dox water is to be removed from the cages and replaced with normal drinking water. The animals will now be in the 'chase' period until death.

3. Transcardial perfusion and brain dissection

3.1. Remove a mouse from its cage and restrain the animal using your left thumb and forefinger. Inject the animal via intraperitoneal (*i.p.*) injection with a solution of 100mg/ml ketamine and 20mg/ml Xylazine in 0.9% sterile saline for a final concentration of 200 mg/kg ketamine and 20 mg/kg xylazine. See Solution Composition Table for more information.

3.2. Caution: The protocols for anesthesia may differ depending on the country. Additionally, there are effects of anesthetics on the brain including changes in microglial morphology and action and corticosterone levels that must be understood when performing perfusions for the purpose of brain collection and analysis [561, 562].

3.3. After approximately 1-2 minutes the animal will lose its righting reflex. To test this, simply roll the animal on its back and if it cannot roll back onto its feet it has lost the righting reflex.

3.4. After approximately 5-10 minutes the animal will lose its pedal reflex. To check the pedal reflex, use your thumb and forefinger to pinch each of the animal's feet. If there is no response, in the form of a jump or muscle spasm, use the nails of your thumb and forefinger to pinch each of the animal's feet. If there is no response, the animal has lost the pedal reflex.

3.4.1. NOTE: If the animal responds to the pedal reflex for greater than 15 minutes after injection, an additional injection of ½ of the initial ketamine/xylazine injection may be required. Age, sex, genotype, phenotype, and treatment may affect the response of the animal to this drug cocktail.

3.5. After the righting and pedal reflexes are lost, test the ocular reflex by lightly contacting the mouse eyeball with a gloved finger. A lack of response indicates that the ocular reflex has been lost.

3.6. Secure the mouse in a supine position with paws pinned to a pinnable work surface.

3.7. Make an incision through the skin with surgical scissors along the thoracic midline approximately 1-2cm below the xiphoid process. Cut superior until at the xiphoid process.

3.8. Grasp the cartilage of the xiphoid process with forceps. Insert scissors and cut through the musculature and ribcage diagonally along the mouses right side to the level of the clavicles. Raise the thoracic musculature with forceps and slice through the diaphragm until you can visualize the heart. Then make an identical diagonal cut along the mouse's left side, making sure

to prevent any contact with the heart. Use a hemostat to keep the thoracic musculature away from the cavity.

3.8.1. NOTE: At this point, the mouse will not be able to breathe any longer, so work quickly to prevent death prior to the next steps.

3.9. Secure the beating heart with blunt forceps and insert a dispensing needle into the left ventricle through the base of the aortic arch.

3.10. Clamp the needle base to the left ventricle just above the insertion site.

3.11. Make an incision in the right atrium, and at the first sign of blood flow, begin perfusing the animal with 20ml 1X PBS at 8.11 ml/minute.

3.12. After the 1X PBS has perfused the body, switch to the appropriate fixative for your downstream application and perfuse the mouse with 20 ml of fixative.

3.12.1. NOTE: For frozen sectioning and immunostaining, perfuse animal with the glyoxal fixative for brain clearing, perfuse animal with 4% PFA in 1X PBS (pH 7.4).

3.12.2. NOTE: Signs of a successful perfusion include animal stiffness (slight stiffness with glyoxal, intense stiffness with PFA) and a lack of visible blood vessels throughout the tissues.

3.13. Decapitate the mouse and remove the brain by inserting scissors into the brainstem and cutting along the squamosal suture through to the frontomaxillary suture on each side. Then cut across the fontonasal suture to remove the skull cap, being careful not to damage the olfactory bulb. From there, turn the skull upside down, and use curve forceps to remove the brain, making sure to sever the optic nerve.

3.14. Place the perfused brain in a tissue cartridge and immerse in the fixative used to perfuse the animal overnight at 4°C.

4. Brain treatment, slicing, and immunostaining

4.1. <u>Brain Treatment and Slicing</u>

4.1.1. Remove brain cartridges from the glyoxal fixative and incubate in 15% sucrose in 1X PBS for 2 days at 4°C or until brains sink.

4.1.2. Remove brain cartridges from 15% sucrose and incubate in 30% sucrose in 1X PBS for 2 days at 4°C or until brains sink.

4.1.2.1. NOTE: See Solution Composition Table for more information.

4.1.3. Remove brains from 30% sucrose in 1X PBS and separate brain into various ‘blocks’ using a coronal brain block or sagittal brain block.

4.1.4. Embed coronal or sagittal brain sections in OCT compound by placing brain sections on a mixture of dry ice and ethanol (EtOH). After OCT has turned white and become solid, remove from dry ice-EtOH mixture and store wrapped in parafilm, inside an air-tight bag at -20°C.

4.1.5. Remove frozen blocks from the freezer and place inside a cryostat with an internal temperature set to -20°C. Use OCT to attach the block to a metal chuck so that the tissue is solidly attached. Allow ~5 minutes for the tissue to freeze to the chuck. Slice the tissue at 7um, placing each tissue slice on a charged glass slide.

4.1.6. Allow for slides to bake overnight at 37°C, then place at -20°C until used for immunostaining.

4.2. Immunostaining

4.2.1. Warm slides to room temperature (RT) and post-fix with ice-cold acetone (Fisher Scientific) for 15 minutes.

4.2.2. Wash slides for 5 minutes in 1X IHC Select TBS Rinse Buffer (rinse buffer) shaking at 60 rpm at RT between each step.

4.2.3. Permeabilize for staining of nuclear antigens with 0.3% Triton X-100 for 10 minutes at RT. Permeabilize for staining of cytoplasmic antigens with 0.3% Tween-20 for 10 minutes at RT.

4.2.4. Perform antigen retrieval by microwaving slides in 50-100mL 1X DAKO Antigen Retrieval Solution on low for 10 minutes, twice. Then rinse with rinse buffer 5m at RT.

4.2.5. Incubate slides in 0.3% Typogen Black in 70% EtOH for 20 minutes at RT then wash with Rinse Buffer.

4.2.6. Block for 20 minutes at 37°C with Millipore Blocking Reagent, and incubate with primary antibody diluted in antibody diluent overnight at 4°C.

4.2.7. The next day, incubate sections in Alexa Fluor secondary antibodies for 10 minutes at RT, then wash slides in rinse Buffer.

4.2.8. Cover brain sections in 100uL of 1:500 anti-GFP antibody conjugated to AlexaFluor 488 and incubate overnight at 4°C.

4.2.9. The next day, wash with rinse Buffer 2x, then wash in running DI water for 5 minutes.

4.2.10. Counterstain with 100ng/mL 4′,6-diamidino-2-phenylindole (DAPI) for 5 minutes, then wash in running DI water for 5 minutes.

4.2.11. Add a drop of mounting medium on top of the tissue and seal with a 22 x 22mm coverslip. Imaging is recommended on the day of mounting to ensure optimal signal.

5. iDISCO brain clearing (adapted from [563])

5.1. Fixation and Sectioning

5.1.1. Post-fix brains in 4% PFA overnight at 4°C and then again for 1 hour at RT.

5.1.2. Wash brains in 1X PBS for an hour, twice, at RT and then cut into 1mm thick sections using the necessary brain block and place into 5mL microcentrifuge tubes containing 1X PBS.

5.2. Methanol Pre-treatment (with methanol)

5.2.1. NOTE: Due to the possibility of methanol impacting immunostaining of certain proteins, the authors would like to point the reader to Renier et al., 2014 for a protocol to a methanol free iDISCO protocol alternative [563]

5.2.2. NOTE: See Solution Composition Table for more information regarding the following solutions in this section.

5.2.3. Wash with 1X PBS for 1 hour twice (shaking) at RT.

5.2.4. Wash in 50% methanol (Fisher; in PBS) for 1 hour (shaking) at RT.

5.2.5. Wash in 80% methanol for 1 hour (shaking) at RT.

5.2.6. Wash in 100% methanol for 1 hour twice (shaking) at RT.

5.2.7. Bleach samples with 5% hydrogen peroxide (H2O2) in 20% dimethyl sulfoxide (DMSO)/methanol (1 volume 30%H2O2/1 volume DMSO/4 volume methanol, ice cold) at 4oC overnight (shaking).

5.2.8. After bleaching, wash samples in methanol for 1 hour twice (shaking) at RT.

5.2.9. Wash in 20% DMSO/methanol for 1 hour twice (shaking) at RT.

5.2.10. Wash in 80% methanol for 1 hour (shaking) at RT.

5.2.11. Wash in 50% methanol for 1 hour (shaking) at RT.

5.2.12. Wash in PBS for 1 hour twice (shaking) at RT.

5.2.13. Wash in PBS/0.2% Triton X-100 for 1 hour twice (shaking) at RT.

5.3. Immunostaining of clearing brains

5.3.1. Incubate samples in 1X PBS/0.2% Triton X-100 /20% DMSO/0.3M glycine at 37°C overnight on an orbital shaker.

5.3.2. Block in 1X PBS/0.2% Triton X-100/10% DMSO/6% goat serum at 37°C for 3 days on an orbital shaker.

5.3.3. Wash samples in 1X PBS/0.2% Tween-20/10 µg/ml heparin sodium salt from porcine mucosa for 1 hour twice at 37°C and then incubate in 1X PBS/0.2% Tween-20 /10µg/ml heparin /5% DMSO/ 3% goat serum containing 1:500 concentration of rabbit anti-GFP AlexaFluor 488 at 37°C on an orbital shaker for 2 days.

5.3.4. Wash samples in 1X PBS /0.2% Tween-20 with 10 µg/ml heparin for 1 hour at 37°C on orbital shaker, 3 times, and then once a day for 2 days.

5.3.5. Incubate samples overnight in 10mL of 50% v/v Tetrahydrofuran (THF)/H2O in a 15mL conical tube.

5.3.6. Incubate samples for 1 hour in 10mL of 80% THF/H2O.

5.3.7. Incubate samples twice for 1 hour in 100% THF.

5.3.8. Dry samples with a sterile wipe and incubate in dichloromethane until they sink to the bottom of the vial (approximately 40min). Do not incubate >60min.

5.3.8.1. NOTE: Be sure to handle dichloromethane under a fume hood.

5.3.9. Incubate samples in 18mL of Dibenzyl Ether (DBE) until clear (>2hrs)

5.3.10. Store samples in DBE at RT until ready to image.

5.3.10.1. NOTE: For best results, it is important to image samples as soon as possible after clearing is complete.

Representative Results

While the fluorescent signal resulting from a Tet-On system with a fluorescent reporter will vary depending on the promoter of interest and fluorophore(s) used, we will describe how findings were analyzed with mTert-rtTA::oTet-Cre::Rosa-mTmG animals. Analysis of adult brains after a pulse-chase resulted in membrane GFP-expressing cells throughout various anatomical niches. The difference in fluorescent intensity between various cell types must be noted. One variable regarding fluorescent intensity is the size of the cell membrane. For instance, choroid epithelial cells (CPECs) in the choroid plexus have a thick cell membrane and strong fluorescent signal that was easily distinguished from the surrounding cells (Fig. A5A, B). However, other smaller and currently unidentified cell types in the choroid plexus stroma had a weaker GFP signal (Fig A5C). In the cerebellum, Bergmann glial cells expressed higher levels of mGFP than basket cells, and variation in mGFP expression even existed between individual basket cells (Fig A5D). Olfactory sensory neuron axons within the glomerular layer of the olfactory bulb also expressed high levels of mGFP (Fig. A5A, E). To ensure that all mGFP+ cells are identified, it is therefore important to identify both bright and dim GFP+ cells throughout the brains of mTmG animals. In mTert-

rtTA::oTet-Cre::Rosa-mTmG animals, we observed low background mGFP expression across brain regions including the cerebral cortex (Fig. A5A). Interestingly, the cerebellum and brainstem showed lower background mGFP expression in this manner (Fig. A5A).

During analysis of brain tissue after a lineage trace there will be differences in mGFP and mTomato expression patterns across both brain regions and cell types. Olfactory sensory neuron axons that fill the glomerular layer of the olfactory bulb expressed high levels of membrane tomato when compared to most other brain regions, even when the same neurons are mGFP+, indicating that some cells appeared to lose mTomato signal more slowly (Fig. A5D). In contrast, in the choroid plexus mGFP+ cells expressed low mTomato (Fig. A5B, C). In most other brain regions tomato signal is spread evenly between cell types with endothelial cells being some of the only cells whose fluorescent signal was bright enough to stand out from the red fluorescent background (Fig. A5B). The activation of mGFP expression and cleavage of mTomato from the genome during recombination results in a loss of mTomato expression, but the mTomato fluorophores that are expressed on the membrane are retained until they degrade. For this reason, mGFP+ cells will often express variable mTomato signal which will depend on the recency of the recombination, the cell type, and size of the cell membrane. Therefore, it is important to analyze cells based on the expression of mGFP and to not exclude them from analysis if they express both mGFP and mTomato.

Alternative reporters may also be utilized in conjunction with the Tet-On system. Cre recombination may act to induce expression of GFP or RFP in cells that will not normally not express any fluorescent tag in Rosa-GFP or Rosa-RFP animals. Here, analysis of GFP or RFP will indicate the expression of the promoter of interest and no fluorophore signal will be removed such as with mTmG animals. Single-fluorophore reporters allow for immunostaining with more fluorescent antibody combinations, as the membrane tomato in mTmG animals prevents staining in the red wavelength.

Cleared brain of mTert-mTmG mouse after a doxycycline pulse-chase

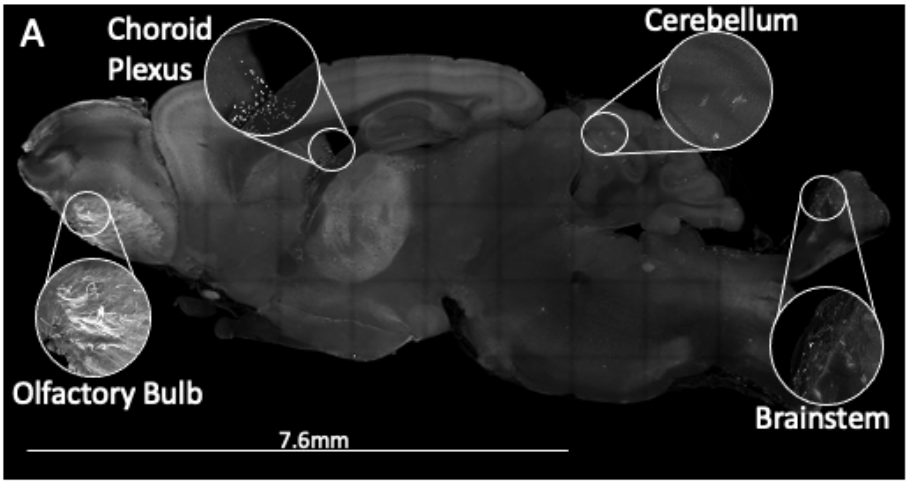

Fixed-frozen slides of mTert-rtTA::oTet-Cre::Rosa-mTmG mouse after a doxycycline pulse-chase

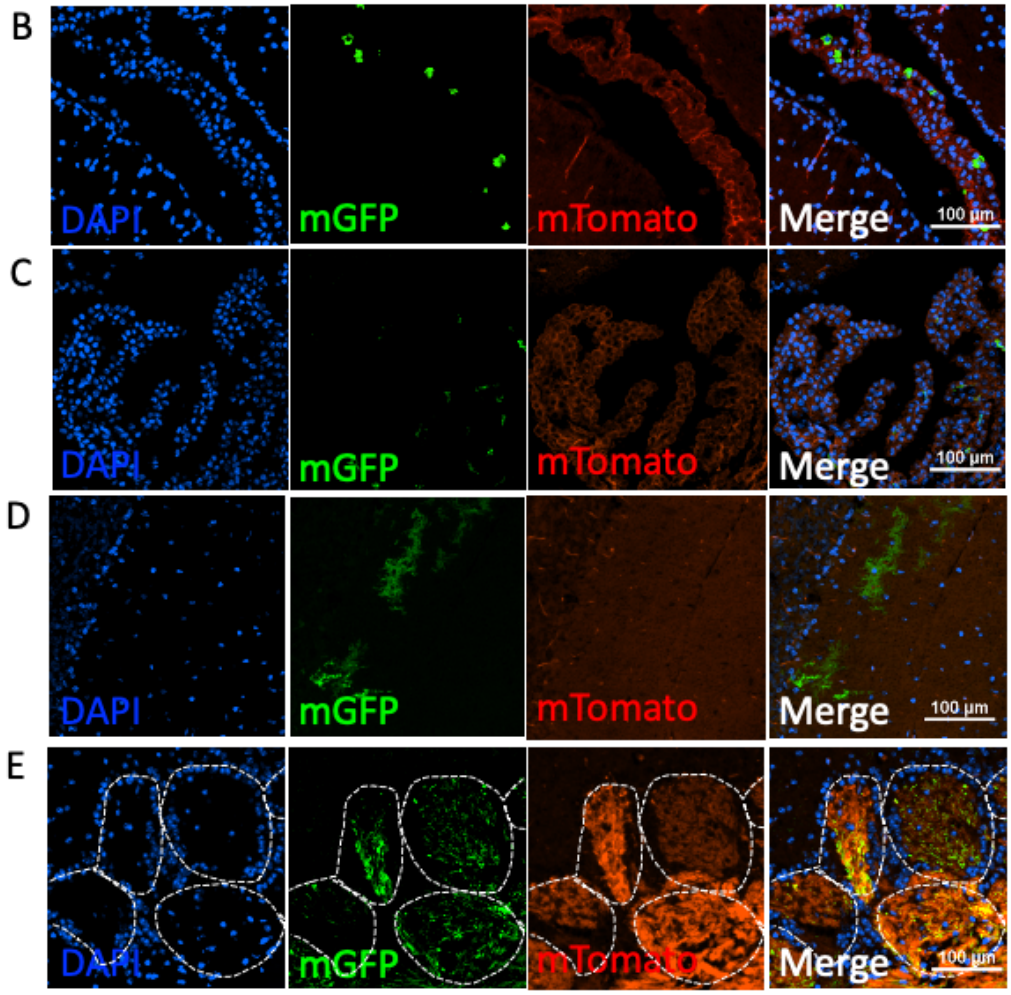

Figure A5. Lineage tracing of adult mTert-rtTA::oTet-Cre::Rosa-mTmG mouse brains after a 3-week pulse and 11-day chase.

A) Cleared brain section of adult mTert-rtTA::oTet-Cre::Rosa-mTmG mouse with specific areas of mGFP signal shown with insets (N=3 male mice).

B-C) Representative image of mTert-rtTA::oTet-Cre::Rosa-mTmG choroid plexus identifying mGFP+ CPECs (B) and smaller, fainter mGFP+ cell types (C; N=4 males, N=6 females)

D) Representative image of mTert-rtTA::oTet-Cre::Rosa-mTmG cerebellar Bergmann glia (bright) and basket cells in the molecular layer of the cerebellum (dim; N=4 males, N=6 females).

E) Representative image of the olfactory glomerular layer of mTert-rtTA::oTet-Cre::Rosa-mTmG brains. Dotted lines indicate glomerular compartments (N=4 males, N=6 females).

Scale bars are 100μm.

Discussion

A method for the creation, utilization, and analysis of a triple transgenic lineage tracing mouse line marking stem cells within the adult mouse brain *in vivo* is described. When combined with immunostaining or brain clearing, the identification and characterization of traced fluorescent cells across the brain can be accomplished. This technique offers the ability to understand the plastic/regenerative/remodeling potential of labeled stem cells as they activate, migrate, differentiate, or proliferate. While previous data obtained via label retention with thymidineH3 and BrdU concluded that the V-SVZ, olfactory bulb, and subgranular zone of the dentate gyrus were the only neurogenic brain regions in adult mammals [4, 5, 10, 11, 40, 543, 544, 564], it is now understood that adult neurogenesis also occurs in the cortex [73], hypothalamus [58, 565], and striatum [566-568], as well as potentially other novel niches that have not been well-studied. Adult gliogenesis, the process by which glial precursor cells create newborn astrocytes and oligodendrocytes, occurs throughout the brain as well [93], and glia and neurons are hypothesized to derive from the same multipotent stem cell. For these reasons, lineage tracing studies have been integral in understanding the role of various stem cell types that contribute to replenishing and regenerating neurons and glia in the adult mammalian brain (reviewed in [569]).

For studies in adult brain plasticity, the optimal age is 12 weeks of age, when the murine brain has completed development [570]. When planning the length of the doxycycline pulse and subsequent chase, an understanding of the process of interest is crucial, so that the pulse-chase timing is long enough to allow for the processes of interest to occur. For example, the creation of newborn neurons in the olfactory bulb from adult neural stem cells (ANSCs) in the V-SVZ is approximately 4 weeks, as determined by previous lineage tracing studies [340]. A pulse-chase study that will label the ANSCs in the V-SVZ must therefore be within that timeframe to allow for the ANSCs in the V-SVZ to divide, for these ANSCs to differentiate into intermediate cell types, and for these intermediate cell types to migrate to the olfactory bulb and differentiate into adult-born neurons. The length of the chase will determine the amount of time that labeled cells and their progeny must continue their migration and differentiation, although these processes will occur during the pulse as well. Taken together it is important to understand the processes involved, as the timeline of each lineage tracing experiment must allow for the proper processes to occur.

While this manuscript details the Tet-On system, other lineage tracing transgenes exist that may be utilized. The CreERT2 transgene allows for the expression of a Cre recombinase that is only active in the presence of tamoxifen or 4-OHT, a tamoxifen derivative. When this Cre is regulated by a promoter of interest, 4-OHT or tamoxifen administration will only produce Cre recombination in cells that express that promoter. When paired with a reporter gene such as Rosa-LSL-GFP or Rosa-mTmG, Cre-lox recombination will indelibly mark the cells that express Cre during tamoxifen administration. One downside of this system is the use of tamoxifen, which has long-lasting adverse effects on neurogenesis in both prenatal and adult brains [549]. For this reason, lineage tracing studies with CreERT2 lines will need to consider the caveats involved.

Lineage tracing studies in the adult brain are often performed with markers of stem cells such as Nestin or markers of glial precursor cells including NG2 [571, 572]. While resulting data indicates the turnover and differentiation of these cells into newborn mature cell types, the

expression of these markers by various other cell types in the adult brain can be confounding. For example, Nestin, an intermediate filament protein involved in mitosis [573] is also expressed by mature neurons [574] and meningeal cell types [154]. Other stem cell markers include glial fibrillary acidic protein (GFAP) [18, 19], and glutamate aspartate transporter 1 (GLAST) [575] are also expressed by astrocytes throughout the adult brain [576]. For this reason, lineage tracing studies with additional markers are needed. As we learn more about the broad impact of adult plasticity in the brain, the characterization and analysis of the cells that play a role in these processes and their progeny remain vitally important to our understanding of neurogenic and gliogenic pathways involved in neurodegenerative health and more.

BIOGRAPHY OF THE AUTHOR

Gabriel Jensen is a human. The brain and body that create the consciousness that calls itself Gabriel is one of 8 billion on the planet Earth. ‘Gabriel’ often thinks about what it means to be alive. The ridiculous nature of the struggle for survival in tandem with the fleeting nature of humanity prevents the brain that governs ‘Gabriel’ from attaching significant value to anything except his family, friends, dogs, and loving wife - all of which are also human except for the dogs. His dog is named Miranda. His childhood dog that lives with his parents is named Shorty. Gabriel also dearly loves the following dogs: Shasta, Greta, Finn, Yogi, Bella, Bubba, Cleo, Lola, Luma, Nala, Taramac, Everett, Poco, Mattie, Brinley, and Max. Gabriel is a candidate for a Doctor of Philosophy degree in Biomedical Science from the University of Maine in August 2022.